Tampere University

MARKUS OJANEN

Reverse Genetics to Study Immunity against Mycobacteria in Zebrafish (*Danio rerio*)

Tampere University Dissertations 11

Tampere University Dissertations 11

MARKUS OJANEN

Reverse Genetics to Study Immunity against Mycobacteria in Zebrafish (*Danio rerio*)

ACADEMIC DISSERTATION
To be presented, with the permission of
the Faculty Council of the Faculty of Medicine and Life Sciences
of the University of Tampere,
for public discussion in the auditorium F115
of the Arvo building, Arvo Ylpön katu 34, 33520 Tampere,
on 15.2.2019, at 12 o'clock.

ACADEMIC DISSERTATION

Tampere University, Faculty of Medicine and Health Technology
Finland

Responsible supervisor and Custos	Professor Mika Rämet University of Tampere Finland	
Supervisor	Professor Marko Pesu University of Tampere Finland	
Pre-examiner(s)	Associate professor Susanna Fagerholm University of Helsinki Finland	Docent Pia Rantakari University of Turku Finland
Opponent	Professor Outi Vaarala University of Helsinki Finland	

The originality of this thesis has been checked using the Turnitin OriginalityCheck service.

Cover design: Roihu Inc.

ISBN 978-952-03-0994-7 (print)
ISBN 978-952-03-0995-4 (pdf)
ISSN 2489-9860 (print)
ISSN 2490-0028 (pdf)
http://urn.fi/URN:ISBN:978-952-03-0995-4

PunaMusta Oy
Tampere 2019

TABLE OF CONTENTS

LIST OF ORIGINAL COMMUNICATIONS

This thesis is based on the following original communications, which are referred in the text by their Roman numerals (I-III):

I **Ojanen MJT**, Turpeinen H, Cordova ZM, Hammarén MM, Harjula SK, Parikka M, Rämet M, Pesu M. The Proprotein Convertase Subtilisin/Kexin FurinA Regulates Zebrafish Host Response against *Mycobacterium marinum*. *Infection and Immunity*. (2015) 83:1431–1442.[1]

II Aspatwar A, Tolvanen ME[3], **Ojanen MJT**[3]**,** Barker HR, Saralahti AK, Bäuerlein CA, Ortutay C, Pan P, Kuuslahti M, Parikka M, Rämet M, Parkkila S. Inactivation of *ca10a* and *ca10b* Genes Leads to Abnormal Embryonic Development and Alters Movement Pattern in Zebrafish. *PLoS ONE* (2015) 28;10(7):e0134263.[2]

III **Ojanen MJT**, Uusi-Mäkelä M, Saralahti AK, Harjula S-KE, Oksanen KE, Kähkönen N, Määttä JAE, Hytönen VP, Pesu M, Rämet M. Intelectin 3 is dispensable for resistance against a mycobacterial infection in zebrafish (*Danio rerio*). *Accepted for publication in Scientific Reports.*

[1]) The original communication I was in part used in the doctoral thesis of Zuzet Cordova (University of Tampere, 2017)
[2]) The original communication II was in part used in the doctoral thesis of Ashok Aspatwar (University of Tampere, 2014)
[3]) Equal contribution

ABBREVIATIONS

ASO	Anti-sense oligonucleotide
BCG	Bacillus Calmette–Guérin
Cas	CRISPR-associated
CA	Carbonic anhydrase
CD	Cluster of differentiation
CFU	Colony forming unit
CRISPR	Clustered regularly interspaced short palindromic repeats
DC	Dendritic cell
DSB	Double-stranded break
EDTA	Ethylenediaminetetraacetic acid
EGFP	Enhanced green fluorescent protein
EZRC	European Zebrafish Resource Center
foxp	Forkhead box P
gRNA	Guide RNA
HDR	Homology-directed repair
HIV	Human immunodeficiency virus
IFNG	Interferon gamma
IGRA	Interferon gamma release assay
IL	Interleukin
ITLN	Intelectin
MDR	Multi-drug-resistant
MHC	Major histocompatibility complex
NHEJ	Non-homologous end joining
NK	Natural killer cell
PAM	Protospacer adjacent motif
PCR	Polymerase chain reaction
PCSK	Proprotein convertase subtilisin/kexin
PRR	Pathogen recognition receptors
qPCR	Quantitative PCR
RC	Random control morpholino
RORC	Retinoic acid receptor-related orphan receptor C

RT	Room temperature
SDS	Sodium dodecyl sulfate
siRNA	Small interfering RNA
TAE	Tris-acetate-EDTA
TALEN	Transcription activator-like effector nuclease
TB	Tuberculosis
TBX	T-box
TGFB	Transforming growth factor beta
Th	T helper cell
TLR	Toll-like receptor
TNF	Tumor necrosis factor
Treg	Regulatory T cell
TST	Tuberculin skin test
T7EI	T7-endonuclease I
WHO	World Health Organization
WT	Wild type
ZFIN	Zebrafish Information Network
ZFN	Zinc-finger nuclease
ZIRC	Zebrafish International Resource Center

ABSTRACT

Tuberculosis (TB) causes over a million mortalities annually. The disease is caused by the intracellular bacterial species *Mycobacterium tuberculosis*, and currently no completely preventive vaccination against the infection exists. Additionally, since the drug-sensitive TB is challenging to cure and the amount of drug-resistant *M. tuberculosis* strains is increasing, novel drug candidates against the disease need to be developed. The influence of the genetic variation of the host on the susceptibility against TB is well-established. Therefore, screening for novel candidate genes in a mycobacterial infection and studying them systemically in an appropriate model organism provides a powerful starting point for drug development.

With the advent of commercially available mutant zebrafish lines as well as efficient genome modification tools, such as the clustered regularly interspaced short palindromic repeats (CRISPR)/CRISPR-associated 9 (Cas9) system, the zebrafish provides an interesting genetically controllable alternative for studying gene specific effects *in vivo*. Furthermore, the zebrafish *Mycobacterium marinum* infection recapitulates several aspects of human TB, providing a safe and a cost-efficient model for studying mycobacterial pathogenesis. This study examined the genetic component of TB susceptibility using the zebrafish *M. marinum* infection model. Specifically, the aims were: to set up an in-house CRISPR/Cas9 mutagenesis method in the zebrafish, and to verify that this system can be efficiently used to create targeted genomic mutations, as well as to study the roles of an important regulator of T cell function FURIN, and of microbial recognition proteins, Intelectins (ITLNs), *in vivo* in the zebrafish host response against mycobacteria.

Using a commercially available *furinA*^{td204e} zebrafish line, it was found that the expression levels of the T helper (Th) cell subtype specific transcription factors *tbx21*, *gata3* and *foxp3a* were elevated in the *furinA*$^{td204e/+}$ mutant fish in steady state compared to the wild type (WT) fish. In addition, it was observed that the *furinA*$^{td204e/+}$ mutants had reduced *furinA* mRNA levels compared to the WT controls and that *furinA* expression was induced upon a mycobacterial challenge. Finally, we demonstrated that the *furinA*$^{td204e/+}$ mutant fish had an infection-inducible proinflammatory phenotype, characterized by the increased expression of

tnfa, *lta* and *il17a/f3*, which was associated with a reduced mycobacterial burden in a chronic *M. marinum* infection.

Demonstrating that the CRISPR/Cas9 mutagenesis system is feasible in our hands, an *enhanced green fluorescent protein* gene (*egfp*) was efficiently mutated in a transgenic tg(*fli1a:egfp*) zebrafish line. Moreover, also the endogenous *ca10a* and *ca10b* genes could be modified in the zebrafish embryos using the CRISPR/Cas9 technology.

Based on a genome-wide gene expression analysis, *intelectin 3* (*itln3*) was identified as one of the most up-regulated zebrafish genes in a *M. marinum* infection. Consequently, the CRISPR/Cas9 system was utilized to create *itln3*^{uta145} and *itln3*^{uta148} mutant zebrafish lines, and to characterize the effects of *itln3* deficiency in a mycobacterial infection. Despite its strongly induced expression during an infection, *itln3* was found dispensable for the protective immune response against *M. marinum* as was suggested by the comparable mycobacterial burden and survival of *itln3* mutants and WT controls. Further studies are warranted to assess if FURIN and ITLN levels could be used as novel diagnostic measures in TB, and whether FURIN-inhibitors have the potential to be used as anti-mycobacterial drugs.

TIIVISTELMÄ

Tuberkuloosi aiheuttaa vuosittain yli miljoona kuolonuhria. Taudin aiheuttaja on solunsisäinen bakteeri *Mycobacterium tuberculosis*, eikä sen aiheuttamaa infektiota vastaan ole täysin estävää rokotetta. Koska tuberkuloosi-infektio on hankala parantaa nykyisillä lääkkeillä ja lääkeresistenssien *M. tuberculosis* -kantojen määrä on kasvussa, uusien tuberkuloosihoitojen kehittäminen on tarpeellista. Ihmisen geneettiset tekijät vaikuttavat tuberkuloosialttiuteen, minkä vuoksi uusien mykobakteeri-infektioon vaikuttavien geenien seulominen sekä niiden tutkiminen systeemisesti sopivissa malliorganismeissa toimii hyvänä lähtökohtana lääkekehitykselle.

Saatavilla olevien kaupallisten mutanttikalalinjojen ja tehokkaiden genominmuokkaustyökalujen, kuten clustered regularly interspaced short palindromic repeats (CRISPR)/CRISPR-associated 9 (Cas9) -systeemin, vuoksi seeprakala (*Danio rerio*) on geneettisesti muokattavissa oleva vaihtoehto geenikohtaisten vaikutusten tutkimiseksi eliötasolla. Tämän lisäksi seeprakalan *Mycobacterium marinum* -infektio mallintaa useita piirteitä ihmisen tuberkuloosi-infektiosta, tarjoten turvallisen ja taloudellisen mallin mykobakteeripatogeneesin tutkimiseksi. Tässä tutkimuksessa selvitettiin tuberkuloosialttiuteen vaikuttavia geenejä käyttäen seeprakalan *M. marinum* -infektiomallia. Tutkimuksen tavoitteina oli pystyttää tiedekunnan sisäinen seeprakalan CRISPR/Cas9-mutageneesimenetelmä ja varmentaa, että menetelmällä voidaan tehokkaasti luoda kohdennettuja mutaatioita seeprakalan genomiin, sekä tutkia T-solujen toiminnalle tärkeää FURIN-säätelyproteiinia ja mikrobien tunnistusproteiineja, Intelektiinejä, seeprakalan mykobakteeri-immuniteetissä.

Käyttämällä kaupallisesti saatavilla olevaa *furinA*^{td204e} -seeprakalalinjaa, *furinA*$^{td204e/+}$ -mutanteilla osoitettiin olevan normaaliolosuhteissa yli-ilmentyneet auttaja-T-soluille tyypilliset transkriptiotekijät *tbx21*, *gata3* ja *foxp3a* verrattuna villityypin kaloihin. Sen lisäksi *furinA*$^{td204e/+}$ mutanteilla havaittiin olevan alentuneet *furinA*-lähetti-RNA-tasot ja *furinA*-geenin olevan indusoitunut *M. marinum* -infektiossa. Osoitimme myös, että *furinA*$^{td204e/+}$ -mutanttikaloilla oli infektiossa lisääntynyt tulehdusvaste, jota kuvasti kasvaneet *tnfa*, *lta* ja *il17a/f3* ilmentymistasot, ja joka assosioitui matalampiin mykobakteerimääriin kroonisessa infektiossa.

CRISPR/Cas9-menetelmän toimivuuden osoitimme mutatoimalla *enhanced green fluorescent protein* –geenin transgeenisessä tg(*fli1a:egfp*) seeprakalalinjassa. Tämän lisäksi onnistuimme CRISPR/Cas9-teknologian avulla muokkaamaan endogeeniset *ca10a* ja *ca10b* geenit seeprakalan alkioissa.

Pohjautuen genominlaajuiseen ilmentymisanalyysiin *itln3*-geenin havaittiin olevan eräs korkeimmin ilmentyneistä seeprakalan geeneistä *M. marinum* -infektiossa. Tästä johtuen CRISPR/Cas9-menetelmää käytettiin *itln3*^{uta145} ja *itln3*^{uta148} -mutanttiseeprakalalinjojen tuottamiseksi ja *itln3*-puutoksen vaikutuksen selvittämiseksi mykobakteeri-infektiossa. Huolimatta selkeästi kohonneesta ilmentymistasosta, *itln3*-geenin havaittiin olevan merkityksetön immuunivasteessa *M. marinum*ia vastaan, sillä homotsygooteilla *itln3*-mutanteilla oli infektiossa verrattavissa olevat mykobakteerimäärät sekä selviytyminen villityypin kontrollikaloihin nähden. Lisätutkimuksia tarvitaan arvioimaan voitaisiinko FURIN- ja ITLN-proteiinitasoja käyttää uusina diagnostisina mittareina tuberkuloosissa ja olisiko FURIN-inhibiittoreita mahdollista käyttää mykobakteerilääkkeinä.

1 INTRODUCTION

Despite the availability of effective antibiotics since the 1940´s, tuberculosis (TB) persists as one of the deadliest human infectious diseases leading to more than a million casualties annually. Making matters even worse, there are no completely preventive vaccines against TB and the relative amount of antibiotic resistant *M. tuberculosis* strains is increasing. While environmental factors, as well as *M. tuberculosis* virulence can affect immunity against mycobacteria, also host genetics have proven important in determining mycobacterial host-pathogen interactions. In fact, new insights into how genetics influence the mycobacterial host response can promote the development of novel diagnostic methods as well as drugs against TB. To this end, genetically tractable animal models are required.

The zebrafish (*Danio rerio*) is a versatile model organism for studying biological processes such as immunity. The zebrafish immune system has cellular and humoral components comparable to those of humans, and both zebrafish embryos as well as adult fish can be used in experimental immunological research, making zebrafish a versatile tool for answering scientific questions. Also, commercial mutant zebrafish lines and the recently developed CRISPR/Cas9 genome modification system provide the means to create knockout zebrafish for studying individual genes at a whole organism level. Importantly, the zebrafish *M. marinum* infection model provides a safe non-mammalian alternative for TB research.

FURIN is a prototypical member of the proprotein convertase subtilisin/kexin (PCSK) enzyme family, and it converts immature proproteins into their active forms by proteolytic cleavage. FURIN has been identified in vertebrates and in invertebrates, and numerous substrate proteins for this PCSK have been recognized so far. In fact, FURIN has been shown to regulate T cell function and inflammation. However, not much is known about its functions in the host response against infections. Furthermore, since FURIN controls the differentiation of T helper (Th) type 1 cells, a T cell subtype crucial for the immune response against TB, *FURIN* is an interesting candidate gene in mycobacterial immunity.

Intelectins (ITLNs) are a family of the sugar-binding lectin proteins. Several *in vitro* studies have suggested that ITLNs function in the innate immune response by directly binding to carbohydrates of the surface of bacteria and thus acting as

microbial recognition proteins. In addition, the infection-inducible expression of *ITLN* genes as well as their protective role in parasitic infections have been demonstrated *in vivo*. However, the phenotype of *ITLN* knockout animal models have not been previously reported in mycobacterial infections.

This thesis was aimed at understanding the role of the *furinA* and *itln3* genes in the immune response against mycobacteria. To this end, the zebrafish *M. marinum* infection model was used together with the *furinA* and *itln3* mutant zebrafish lines. While the *furinA*^{td204e} mutant line was commercially available, we initially needed to set up our own zebrafish CRISPR/Cas9 mutagenesis to mutate *itln3*. For this purpose, the methodology was initially tested with an exogenous *egfp* gene in our transgenic tg(*fli1a:egfp*) zebrafish, and further validated by mutating endogenous *ca10a* and *ca10b* genes in wild type (WT) fish. Subsequently the CRISPR/Cas9 system was used to create *itln3* mutant zebrafish.

2 REVIEW OF THE LITERATURE

2.1 Tuberculosis

2.1.1 Epidemiology

Tuberculosis (TB) is an epidemic infectious disease caused by the mycobacterial species *Mycobacterium tuberculosis*. It has been proposed that one-third of the entire human population is infected with *M. tuberculosis* (Dye et al. 1999). Predominantly, a *M. tuberculosis* infection remains in a non-transmissible and asymptomatic form called the latent disease, and only a fraction of the infected individuals develop active TB (Rangaka et al. 2015). Nonetheless, in the latest report of the World Health Organization (WHO) it was estimated that more than 10 million people are affected by TB and that approximately 1.7 million deaths were caused by the disease in 2016 (Global Tuberculosis Report, 2017).

As it is a multifactorial disease, several risk factors have been associated with TB susceptibility, including poverty and malnutrition (Dheda, Barry & Maartens 2016; Fogel 2015; Lawn & Zumla 2011). Accordingly, the highest TB incidence rates are found in Sub-Saharan Africa as well as in South-East Asia in low-income countries such as the Democratic Republic of the Congo, South Africa, the Philippines and Myanmar (Figure 1). Furthermore, a high TB incidence is directly linked to the high prevalence of the human immunodeficiency virus (HIV), putting HIV-infected people at substantially higher risk of developing TB than the healthy individuals (Figure 2) (Global Tuberculosis Report, 2017). In fact, of the TB infected individuals circa 10% are simultaneously co-infected with HIV. Other risk factors associated with a higher susceptibility for TB include immunosuppressive treatment, diabetes, alcohol usage, smoking as well as indoor air pollution (Dheda, Barry & Maartens 2016). In addition, genetic polymorphisms are known to affect TB susceptibility (See chapter 2.1.4.) (Lerner, Borel & Gutierrez 2015; Meyer & Thye 2014; Sørensen et al. 1988).

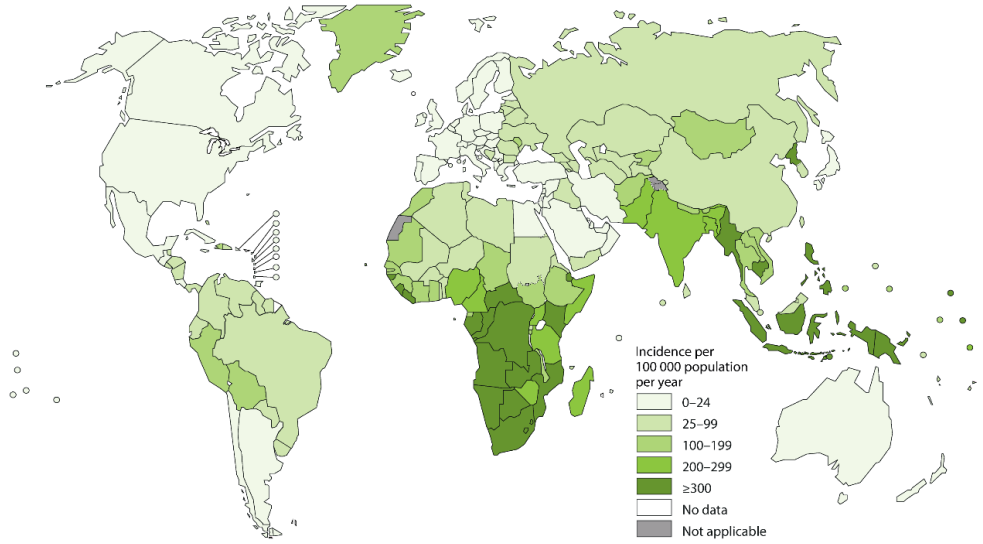

Figure 1. Global TB incidence rates in 2016. TB incidence per 100,000 people per year is depicted separately in each country with the shades of green. Figure is reprinted from the Global Tuberculosis Report, 2017, World Health Organization, Page 31, Copyright (2017). Translated with the permission of the publisher from http://gamapserver.who.int/mapLibrary/Files/Maps/gho_tb_incidence_2016.png (17th of August, 2018).

Although in most cases TB is treatable with a standard anti-tubercular regimen, the numbers of drug- and multi-drug-resistant (MDR) *M. tuberculosis* infections are increasing with approximately 600,000 new MDR cases annually (Global Tuberculosis Report, 2017). Most of the MDR *M. tuberculosis* infections are reported in the Russian federation (63,000), India (147,000) and China (73,000) accounting for a total of 47% of the cases world-wide (Global Tuberculosis Report, 2017; Lawn & Zumla 2011). Moreover, for example in Russia, the fraction of MDR cases compared to the total amount of reported cases is increasing and was noticeable high (27%) in 2016. Taken together the high prevalence of *M. tuberculosis* infected latent individuals, the high susceptibility of active TB in HIV-patients as well as the increased incidence of MDR bacterial infections, makes the battle against TB far from being over. Especially, since completely preventive vaccines against the disease are yet to be developed.

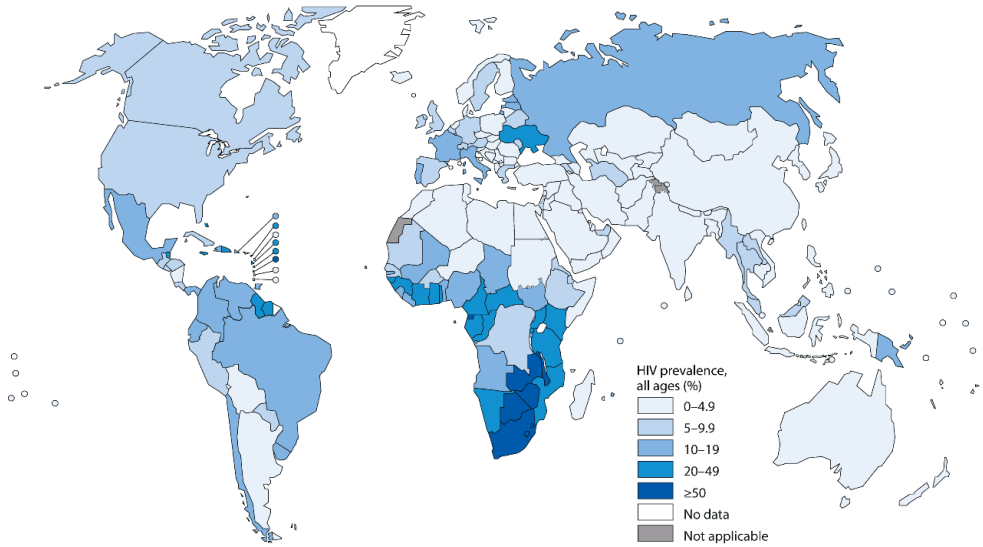

Figure 2. Global HIV prevalence in TB patients in 2016. HIV prevalence (%) among the TB patients is depicted separately in each country with the shades of blue. Figure is reprinted from the Global Tuberculosis Report, 2017, World Health Organization, Page 32, Copyright (2017). Translated with the permission of the publisher from http://gamapserver.who.int/mapLibrary/Files/Maps/Global_HIVprevalence_NewRelapseTB cases_2016.png (17th of August, 2018).

2.1.2 Diagnosis, treatment and prevention

The complex nature of a *M. tuberculosis* infection, with its latent and active diseases, the large proportion of HIV-co-infected individuals and drug resistance, make it challenging to diagnose, treat and prevent TB. Active pulmonary TB is usually diagnosed by lung radiography and/or sputum smear microscopy and culture (Table 1) (Dheda, Barry & Maartens 2016; Eddabra & Ait Benhassou 2018; Lawn & Zumla 2011; Zumla et al. 2013). Furthermore, nucleic acid amplification tests such as the Gene Xpert MTB/RIF as well as the loop-mediated isothermal amplification (LAMP) assay are expanding the methodology for pulmonary TB diagnostics, and similarly to culture based diagnostics, they provide additional means to screen for drug resistance (Dheda, Barry & Maartens 2016; Eddabra & Ait Benhassou 2018). While the aforementioned tests can be used to detect the pulmonary disease, computer tomography (CT) and magnetic resonance imaging (MRI) have proven important in identifying extra-pulmonary TB e.g. in the bones and in the central nervous system, respectively (Skoura, Zumla & Bomanji 2015).

Common diagnostic tests used to detect a latent *M. tuberculosis* infection include the tuberculin skin test (TST) and the interferon gamma release assay (IGRA) (Table 1). While both TST and IGRA reveal the presence of memory T cells against tuberculous antigens by measuring the extent of the host´s T cell response, these tests are not able to distinguish between the latent and active stages of the disease (Chee et al. 2013; Dheda, Barry & Maartens 2016). For the same reason, they fail to distinguish between eradicated bacilli and bacteria still present in the host. Moreover, both of these diagnostic measures can result in false negative results in immunocompromised individuals e.g. in HIV-infected people (Dheda, Barry & Maartens 2016) Overall, simple diagnostic tests that could differentiate between healthy people, latently infected individuals and active TB patients would be important for choosing the correct treatment strategy. To this end, at least gene expression profiling (Lee et al. 2016; Roe et al. 2016) and fluorescence activated cell sorting (FACS) (Pollock et al. 2013; Yang et al. 2015) from patient blood samples, as well as comparative screening of secreted *M. tuberculosis* proteins (Zhang et al. 2014) have provided new diagnostic possibilities.

Table 1. Diagnostic possibilities in human *M. tuberculosis* infection.

Diagnostic measure	Tissue specificity of the diagnosis	Diagnostic sample	Clinical use in diagnosis (Active TB vs. latent disease)
Radiography	Lungs	–	Active TB
Microscopy	Lungs	Sputum smear	Active TB
Bacterial culture	Lungs	Sputum smear	Active TB
Nucleic acid amplification tests	Lungs	Sputum smear	Active TB
Computer tomography (CT)	Bones	–	Active TB
Magnetic resonance imaging (MRI)	Central nervous system	–	Active TB
Tuberculin skin test (TST)	Unspecific	Skin reactivity	Latent disease (unspecific)
Interferon gamma release assay (IGRA)	Unspecific	Blood	Latent disease (unspecific)
Gene expression profiling	Unspecific	Blood	Active TB and latent disease
Fluorescence activated cell sorting (FACS)	Unspecific	Blood	Active TB and latent disease
M. tuberculosis protein screening	Unspecific	Blood	Active TB and latent disease

The mortality rates of an active, untreated TB infection can be as high as 90% (Chiang et al. 2009). Fortunately however, active drug-susceptible TB can be treated with a drug combination of isoniazid, rifampin, pyrazinamide, and either ethambutol

or streptomycin (Global Tuberculosis Report, 2017; Fogel 2015). Nonetheless, the long duration of the regimen (at least six months) causes a large proportion (18.7%-49.3%) of the patients to stop the treatment as soon as they feel better, already before the end of 2 months (Kruk, Schwalbe & Aguiar 2008). This in turn has led to treatment success rates of only 85%, and to the accelerated development of drug-resistant TB (Kruk, Schwalbe & Aguiar 2008).

Compared to the standard anti-tuberculosis regimen, the MDR TB medication has a lower success rate of 54% and it requires a prolonged treatment time of up to 9-12 months (Global Tuberculosis Report, 2017). Additionally, the cost of treating MDR TB is approximately 25 times higher compared to the drug-sensitive infection (Global Tuberculosis Report, 2017). In fact, the low success rates in treating the MDR disease, the high cost of medication as well as the emergence of totally drug-resistant bacteria substantiate the need for new and efficient short-term TB drugs. To this end, the WHO reported that in 2017 there were more than a dozen new TB drugs in clinical trials that will hopefully prove efficient in the fight against the TB epidemic. Moreover, in order to reduce the development of drug-resistance in the first place, drug susceptibility testing is important in choosing the correct regimen in treating *M. tuberculosis* infections (Global Tuberculosis Report, 2017; Kim 2005).

While active TB always requires treatment, a latent *M. tuberculosis* infection can remain asymptomatic and harmless for decades (Fogel 2015). Consequently, a latent infection is diagnosed and treated only in individuals with a high risk of disease reactivation (e.g. HIV-patients), in children under five years with active household TB contacts or in people that have lived in high-prevalence countries and have later settled elsewhere in a place with a lower TB prevalence (Zumla et al. 2013). The recommended treatment for a latent infection is a 9-month period of isoniazid administration, an interval that can be extended to ensure efficient treatment (Zumla et al. 2013).

Although the Bacillus Calmette–Guérin (BCG) vaccine is efficient in preventing severe disseminated TB (Rodrigues, Diwan & Wheeler 1993; Trunz, Fine & Dye 2006), no completely preventive vaccine against TB exists. In fact, efficient vaccination strategies against TB would be highly important for the preventive measures against TB. The development of new TB vaccines is however problematic. While the high cost of clinical studies limits the amount of novel vaccine candidates from ever entering the developmental "pipeline", the high disease burden and the different infection outcomes complicate the study design by making the proper control individuals difficult to choose (Voss et al. 2018). Moreover, comprehensive knowledge about the host immune response against *M. tuberculosis* is required in order

to induce a selective and an efficient TB immunity upon vaccination. Nevertheless, several new vaccines are in clinical trials and their efficacy remains to be proven (Global Tuberculosis Report, 2017). Overall, the factors contributing to the disease onset and its pathogenesis need to be understood in more detail in order to develop more efficient remedies against TB.

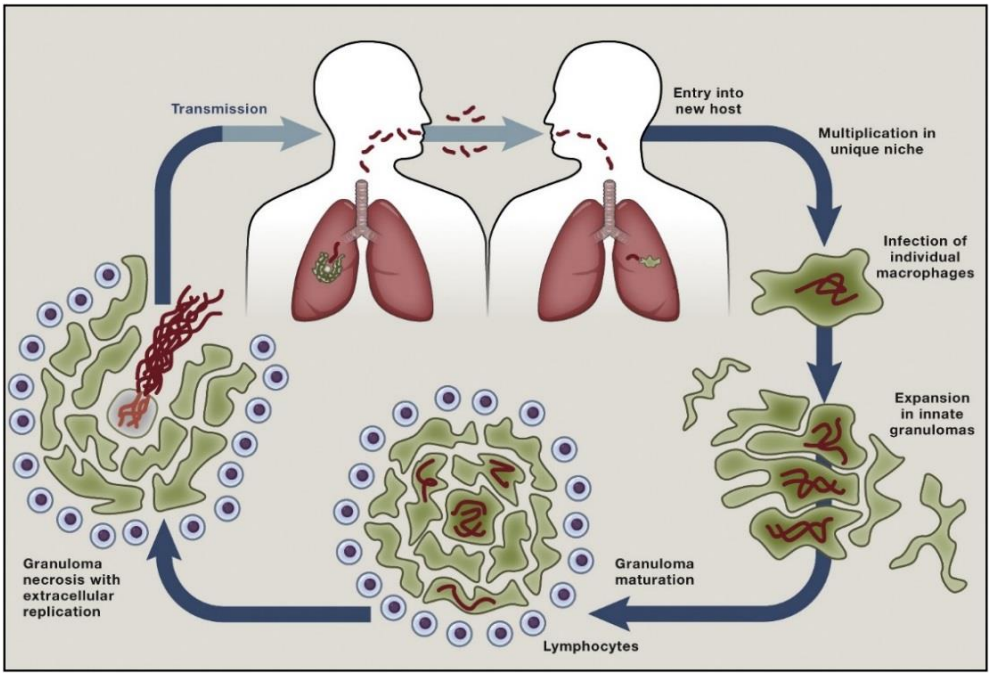

Figure 3. Immunological life cycle of TB. *M. tuberculosis* is transmitted from an active disease carrier to a new host through inhaled aerosol droplets. If the mycobacterium is not destroyed it uses macrophages to multiply and spreads in the immunoprivileged niche of the alveoli. After the initiation of the adaptive immune response, lymphocytes traffick to the lungs, leading to granuloma maturation and often to containment of the infection (latency). If the host immune response fails to achieve latency or the disease is reactivated e.g. in a HIV co-infection, *M. tuberculosis* can disseminate from the granulomas, continue its replication and cause transmissive active TB. Figure is reprinted from Cell, Volume 159, Issue 7, December 18, 2014 (doi: 10.1016/j.cell.2014.11.024), Cambier CJ, Falkow S, & Ramakrishnan L, Host Evasion and Exploitation Schemes of *Mycobacterium tuberculosis*, Pages No. 1497-1509, Copyright (2014), with permission from Elsevier.

2.1.3 Immune response against *Mycobacterium tuberculosis*

Referred to as the immunological life cycle of TB by Ernst (2012), the different stages of a *M. tuberculosis* infection in humans include mycobacterial entry, primary

disease, immunological equilibrium (latency), reactivation and transmission to new hosts (Figure 3). In addition, also immediate bacterial elimination has been suggested as a possible outcome of an infection (Ernst 2012; Meermeier & Lewinsohn 2018; Weiss & Schaible 2015). Collectively, the complex host immune response against the intracellular *M. tuberculosis* bacterium dictates the final infection outcome ranging from bacterial sterilization to latent and active TB.

2.1.3.1 Innate immune response

A *M. tuberculosis* infection is conferred from an infected individual to its new host through inhaled aerosol droplets (Figure 3) (Cambier, Falkow & Ramakrishnan 2014; Ernst 2012; Philips & Ernst 2012). Therefore, it has been proposed that the first cells to react to and mount an immune response against the bacterium are the alveolar macrophages (Philips & Ernst 2012). Albeit macrophages are able to recognize mycobacterial antigens directly through their pattern recognition receptors (PRRs) such as C-type lectin-, scavenger- or toll-like receptors (TLRs) (Figure 4) (Brightbill et al. 1999; Means et al. 1999; Mortaz et al. 2015; Stamm, Collins & Shiloh 2015; Zimmerli, Edwards & Ernst 1996), also an opsonin-mediated interaction has been shown to contribute to mycobacterial recognition (Hirsch et al. 1994; Stamm, Collins & Shiloh 2015). In addition, cytoplasmic PRRs i.e. STING (or transmembrane protein 173, TMEM173) can recognize cytosolic mycobacterial DNA, further contributing to the repertoire of *M. tuberculosis* recognition receptors (Watson, Manzanillo & Cox 2012). Collectively, the stimulation of the PRRs dictates the following steps in the macrophage response against mycobacteria in the host. Noteworthy, also other professional phagocytes of the lungs, such as neutrophils, monocyte-derived macrophages and dendritic cells (DCs) play an important role in the innate immune response against *M. tuberculosis* (Kimmey et al. 2015; Weiss & Schaible 2015; Wolf et al. 2008).

Lectins are proteins capable of binding carbohydrate moieties in different cellular and extracellular spaces (Sharon & Lis 2004). Consequently, lectins act as recognition proteins that function in homeostasis (e.g. iron transfer) as well as in the immune response. In fact, the C-type lectin receptor Cluster of differentiation 209 (CD209 or DC-SIGN) has been identified as an essential protein in the DC-mediated binding of *M. tuberculosis* and the subsequent uptake of mycobacteria into these cells (Tailleux et al. 2003). Intelectins (ITLNs) are an evolutionarily conserved lectin sub-family identified at least in mammals, fish and ascidians (Yan et al. 2013). Although several different biological functions have been suggested for ITLNs, an increasing

amount of studies have provided evidence for their role in the innate immunity. Consequently, ITLNs have been shown to bind and agglutinate a number of bacterial species (Chen et al. 2016; Ding et al. 2017; Nagata 2018; Wesener et al. 2015) as well as to aid in mycobacterial phagocytosis (Tsuji et al. 2009).

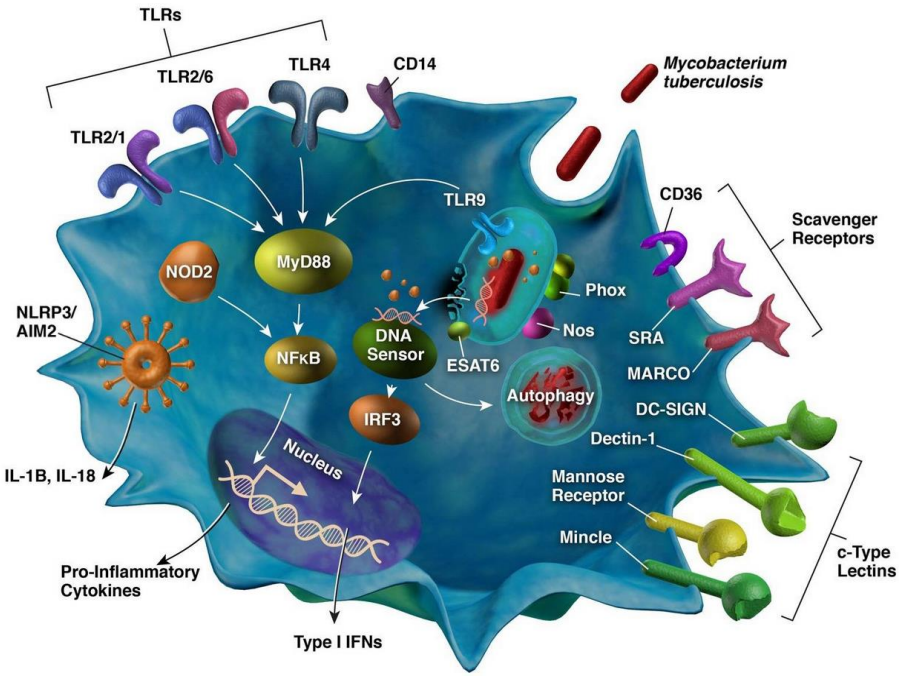

Figure 4. Pattern recognition receptors (PRRs) involved in the recognition of *M. tuberculosis*. C-type lectin-, scavenger and toll-like receptors (TLRs) can bind to mycobacterial surface structures on macrophages. While bacterial recognition through the Mannose receptor can lead to bacterial engulfment and to intracellular killing mechanisms in the phago-lysosomal compartments (e.g. production of nitric oxide, NO, by the Nitric oxide synthase, NOS), TLR-mediated mycobacterial binding activates the MYD88/NFKB pathway and the production of pro-inflammatory cytokines. Figure is re-printed from Immunological Reviews, Volume 264, Issue 1, Pages No. 204–219, Stamm et al., (2015), Sensing of *Mycobacterium tuberculosis* and consequences to both host and bacillus, (doi: 10.1111/imr.12263), Copyright (2015), with permission from John Wiley & Sons A/S.

As mentioned, the C-type lectin- and scavenger receptor mediated recognition or opsonization can lead to bacterial engulfment by phagocytosis. The main cell surface receptors that initiate phagocytosis of *M. tuberculosis* are the mannose receptors of the C-type lectin family (Stamm, Collins & Shiloh 2015). In addition, other C-type lectin receptors such as the C-type lectin domain containing 7A (CLEC7A or DECTIN-1) and CLEC4E (or MINCLE) as well as scavenger

receptors such as CD36 and MARCO are known to bind to *M. tuberculosis* (Stamm, Collins & Shiloh 2015). In contrast, following a TLR-mediated recognition of mycobacteria an intracellular signaling cascade through Myeloid differentiation primary response 88 (MYD88) leads to the activation of the nuclear factor kappa B (NFKB) and to production of immunological mediators such as cytokines and small lipid mediators by the macrophages (Philips & Ernst 2012; van Crevel, Ottenhoff & van der Meer 2003; Weiss & Schaible 2015). To date, at least TLR2, TLR4 and TLR9 have been reported to recognize mycobacterial surface structures (Mortaz et al. 2015; Stamm, Collins & Shiloh 2015).

Collectively, the activation of the PRRs can direct neutrophils to the site of infection, leading to the subsequent secretion of chemokines and the attraction of monocyte-derived macrophages (Weiss & Schaible 2015). Altogether, these three phagocyte populations produce proinflammatory cytokines including Tumor necrosis factor (TNF), IL1B, IL6 and IL12, which are important for macrophage activation and mycobacterial killing mechanisms, but also for the activation of natural killer (NK) cells and the adaptive immune system (Philips & Ernst 2012; Weiss & Schaible 2015). In fact, the activation of macrophages is classically thought to require stimulation from TNF, but also from Interferon gamma (IFNG), that can be produced by NK cells and T helper type 1 (Th1) cells (Mosser & Edwards 2008). As a result, macrophage activation leads to the production of nitric oxide (NO) and reactive oxygen species (ROS), and consequently can result in the oxidative destruction of engulfed mycobacteria inside the phago-lysosomal compartments (Nathan & Hibbs 1991; Roca & Ramakrishnan 2013; Weiss & Schaible 2015).

Although the activation of phagocytes can lead to bacterial destruction (Weiss & Schaible 2015), virulent mycobacteria can also actively avoid lysis by escaping from the phago-lysosomes (McDonough, Kress & Bloom 1993) as well as by inhibiting phagosome-lysosome fusion (Malik, Denning & Kusner 2000). More specifically, mycobacterial effectors such as ESAT6 and CFP-10 (or ESAT-6-like protein, EsxB) encoded by the Esx-1 loci have been found to cause damage to the phagosomal membrane and to promote the relocation of *M. tuberculosis* to the macrophage or DC cytosol (van der Wel et al. 2007). Additionally, inhibition of calcium-ion (Ca^{2+}) signaling by mycobacteria was demonstrated to prevent the fusion of the lysosome with the phagosomal compartment (Malik, Denning & Kusner 2000). *M. tuberculosis* also uses other mechanisms to avoid destruction by macrophages, including the translocation of bacteria-derived cyclic adenosine monophosphate (cAMP) into the macrophage cytoplasm (Agarwal et al. 2009) as well as masking their pathogen-associated molecular patterns (PAMPs) with membrane lipids (Cambier et al. 2014).

Overall, processes promoted by virulent mycobacterial strains increase the intracellular replication of bacteria and the death of host cells, as well as contribute to bacterial spread, survival and pathogenesis. Furthermore, not only bacterial virulence factors and immunodeficiency can cause mycobacterial outgrowth, but also excessive TNF production has been demonstrated to lead to macrophage necrosis and to increase the spread of extracellular mycobacteria (Roca & Ramakrishnan 2013; Tobin, David M et al. 2012), exemplifying the complexity of the host immunity against mycobacteria.

2.1.3.2 Adaptive immune response

Following the innate immune response, DCs present the mycobacterial antigens to naïve lymphocytes in the lymph nodes (Cooper 2009). In fact, already in the 1970´s T cells were shown to be important in the defense against TB infection (Lefford 1975; North 1973; Orme & Collins 1983). Later, both CD8+ (Canaday et al. 1999; Lin & Flynn 2015) and CD4+ T cells (Lyadova & Panteleev 2015) have been suggested to play an indispensable role in the human *M. tuberculosis* infection. Although the function of CD8+ T cells in TB immunity can be directly mediated by target cell killing mechanisms through cytotoxin production (e.g. perforin and granulysin) also the production of cytokines such as IFNG and TNF, similarly to CD4+ T cells, has been suggested to play a role (Lin & Flynn 2015). However, while the significance of CD8+ T cells in TB is still somewhat elusive, the role of the T helper (Th) type 1 cell response (a subtype of the CD4+ T cells) has been demonstrated to be crucial for the immune response against *M. tuberculosis* in human patients (Onwubalili, Scott & Robinson 1985; Zhang et al. 1994) and in experimental studies using *Il12* and *Ifng* knockout mice (Cooper et al. 1993; Cooper et al. 1997; Flynn et al. 1993; Flynn et al. 1995). Mechanistically, it has been suggested that the importance of Th1 cells stems from the important role of IFNG in the activation of macrophages (Weiss & Schaible 2015).

Nevertheless, not all of the regulators of the Th1 type immune response are well characterized. As an example, Th1 differentiation studies using mouse and human T cell microarrays, identified a proprotein convertase subtilisin/kexin (PCSK) family member *FURIN* as one of the genes regulated by the IL12/STAT4 signaling pathway (Lund et al. 2004; Pesu et al. 2006). Moreover, FURIN has been shown to enhance the secretion of IFNG from Th1 cells (Pesu et al. 2006), and to favor Th1 cell development by the inhibition of the expression of the IL-4 receptor alpha chain and the IL4/STAT6 signaling required for Th2 cell polarization

(Oksanen et al. 2014). In fact, the role of these Th1 type immunity regulators, like that of FURIN, in the host response to TB, requires further studies. In addition to Th1 cells, also other Th cell subtypes such as Th17 cells can confer protection against *M. tuberculosis* (Gallegos et al. 2011; Gopal et al. 2014; Khader et al. 2005), whereas regulatory T (Treg) cells can suppress the mycobacterial host response (Kursar et al. 2007; Quinn et al. 2006; Scott-Browne et al. 2007).

Although the induction of the adaptive immune response is similar to many other human pathogens, the initiation of the response is significantly delayed in a *M. tuberculosis* infection. In fact, mouse studies demonstrated that it took 9-11 days before T cell proliferation could be measured and a total of 15-17 days before effector T cells trafficked back to the lungs (Reiley et al. 2008; Wolf et al. 2008). Furthermore, in humans it has been reported that it can take as long as 42 days until a measurable T cell response against TB can be detected (Ernst 2012). Contributing to the delay of the adaptive response and the failure of the host to eliminate bacteria, *M. tuberculosis* has been shown to actively inhibit the expression of *major histocompatibility complex II* (*MHCII*) and the presentation of MHCII-mediated antigens to CD4+ T cells (Noss, Harding & Boom 2000), and it has been shown to disrupt IFNG-responses (Ting et al. 1999). It has also been suggested that the immune-privileged nature of the initial recognition-site of *M. tuberculosis*, the alveoli, delays the DC mediated antigen transport (Cambier, Falkow & Ramakrishnan 2014; Cooper 2009). Consequently, as hypothesized by Wolf et al. (2008), it is likely that this delayed induction of the adaptive immune response contributes to the inability of the host to eradicate the bacteria.

B cell responses in a *M. tuberculosis* infection have not been studied as extensively as the immune function of T lymphocytes. Nevertheless, it has been experimentally demonstrated that the lack of functional B cells increases infection susceptibility in mice (Maglione, Xu & Chan 2007; Vordermeier et al. 1996), and that immunoglobulins confer protection against TB (Achkar, Chan & Casadevall 2015; Balu et al. 2011; Lu et al. 2016; Maglione et al. 2008). Collectively, in most *M. tuberculosis* infections both the initial innate response and the subsequent activation of the adaptive immunity lead to bacterial containment and to the development of the hallmark signs of a mycobacterial infection - the granulomas.

2.1.3.3 The role of the mycobacterial granulomas in the immune response

Tuberculous granulomas are organized structures of several immune cell sub-types that encapsulate mycobacteria at their central core (Figure 3 and Figure 5)

(Ramakrishnan 2012). Studies performed in zebrafish embryos using the *M. marinum* model of TB have shown that granulomas initially form as macrophage aggregates in the absence of the adaptive immunity (Davis et al. 2002). However, at later stages of the infection also other immune cells such as NK cells, DCs and neutrophils as well as B and T lymphocytes are found at the granuloma site (Ramakrishnan 2012).

Although a long-held dogma was that the granulomas benefit the host by restricting bacterial spread, relatively new research has shown that the granulomas are dynamic structures that support also the proliferation and dissemination of mycobacteria (Ramakrishnan 2012). A host-protective view of the granuloma is supported by the impaired granuloma formation and consequent increase in the incidence of TB in HIV-infected people (Lawn, Butera & Shinnick 2002) as well as by experimental studies using *M. tuberculosis* infected *Ifng* and *Tnf* knockout mouse models with disrupted tuberculous granulomas and increased infection susceptibility (Bean et al. 1999; Cooper et al. 1993). Conversely, using the zebrafish *M. marinum* model it has later been demonstrated that mycobacteria exploit the granuloma macrophages in order to multiply and spread to novel sites in the host (Davis & Ramakrishnan 2009), and that this is mediated by mycobacterial virulence factors encoded by the *region of difference 1* (*RD1*) locus (Volkman et al. 2004). All in all, although the interplay between the innate and adaptive immunity enables the host to either eradicate or to isolate the mycobacteria inside the granulomas, the granuloma can also serve as a niche that benefits bacterial outgrowth. Furthermore, the host immune response is affected by several bacterial virulence factors but it is also largely dependent on the genetic composition of the host.

2.1.4 Genetic association of infection susceptibility

Similarly to other infectious diseases, the importance of host genetics in TB susceptibility is nowadays well-established. To this end, the genetic component in TB has been demonstrated with twin studies, by studying families with Mendelian susceptibility to mycobacterial diseases but also with human candidate gene and genome wide association studies (GWAS) (Barreiro et al. 2012; Bustamante et al. 2014; Meyer & Thye 2014). In addition, transcriptomic studies of blood samples from human TB patients have identified new gene candidates with a possible biomarker potential and association with mycobacterial immunity (Joosten, Fletcher & Ottenhoff 2013; Walzl et al. 2014).

Table 2. Genes associated with *M. tuberculosis* susceptibility.

Gene name	Gene symbol	Reference (reviewed in)
C-C motif chemokine ligand 2	CCL2	Möller et al., 2010
C-C motif chemokine ligand 5	CCL5 (RANTES)	Azad et al., 2012
CD14 molecule	CD14	Azad et al., 2012
CD209 molecule	CD209	Möller et al., 2010
complement C3b/C4b receptor 1	CR1	Azad et al., 2012
C-type lectin domain containing 7A	CLEC7A (Dectin-1)	Azad et al., 2012
C-X-C motif chemokine ligand 10	CXCL10	Azad et al., 2012
interferon gamma	IFNG	Möller et al., 2010
interleukin 1 beta	IL1B	Azad et al., 2012
interleukin 12	IL12	Azad et al., 2012
interleukin 6	IL6	Azad et al., 2012
interleukin 8	IL8	Azad et al., 2012
mannose binding lectin 2	MBL2	Möller et al., 2010
nitric oxide synthase 2	NOS2A	Möller et al., 2010
nucleotide binding oligomerization domain containing 1	NOD1	Azad et al., 2012
nucleotide binding oligomerization domain containing 2	NOD2	Azad et al., 2012
purinergic receptor P2X 7	P2RX7	Azad et al., 2012
solute carrier family 11 member 1	SLC11A1	Möller et al., 2010
SP110 nuclear body protein	SP110	Möller et al., 2010
surfactant protein A1	SFTPA1 (SP-A1)	Azad et al., 2012
surfactant protein A2	SFTPA2 (SP-A2)	Azad et al., 2012
TIR domain containing adaptor protein	TIRAP	Azad et al., 2012
toll like receptor 1	TLR1	Möller et al., 2010
toll like receptor 2	TLR2	Möller et al., 2010
toll like receptor 4	TLR4	Möller et al., 2010
toll like receptor 8	TLR8	Möller et al., 2010
toll like receptor 9	TLR9	Azad et al., 2012
tumor necrosis factor	TNF	Azad et al., 2012
vitamin D receptor	VDR	Möller et al., 2010

While observations made in human twins gave strong general evidence for the genetic association to TB susceptibility (Comstock 1978), later studies have identified specific genes such as the aforementioned *IFNG* (Onwubalili, Scott & Robinson 1985; Shimokata et al. 1982) and *IL12* (Zhang et al. 1994), that are important for TB immunity. The list of genes associated with the immune response against TB has later expanded substantially (Lerner, Borel & Gutierrez 2015; Meyer & Thye 2014; Möller, de Wit & Hoal 2010), and a large amount of gene polymorphisms have been linked to host susceptibility against *M. tuberculosis* i.e. in *TNF, TLR, complement receptor 1* (*CR1*) as well as *mannan-binding lectin* (*MBL*) genes (Azad, Sadee & Schlesinger 2012; Meyer & Thye 2014; Möller, de Wit & Hoal 2010; Selvaraj, Narayanan & Reetha 1999). Collectively, a thorough understanding of the host genetics in the immune response against mycobacteria can lead to personalized TB therapies and the development of new drugs and vaccines against *M. tuberculosis,* and it can also support the identification of new biomarkers for TB diagnostics. Nonetheless, experimental

models are invaluable in harnessing the knowledge about genetic susceptibility to the development of novel therapies and diagnosis methods. Table 2 lists some of the human genes associated with TB susceptibility.

2.2 Experimental models for TB

2.2.1 *In vitro* models

As described earlier, mycobacteria-macrophage interactions are crucial in the initial stages of granuloma formation (Davis et al. 2002) as well as in the pathogenesis of a mycobacterial infection (Davis & Ramakrishnan 2009). Not surprisingly, several *in vitro* models used in TB research are based either on cultures of immortalized monocytes, such as the leukemic THP-1 cell line, or on freshly derived peripheral blood mononuclear cells, that can be stimulated to differentiate into macrophages (Fonseca et al. 2017). Additionally, as described by Fonseca et al., (2017) several co-culture and three-dimensional tissue models have emerged in order to recapitulate cell-cell interactions in a mycobacterial infection as well as to mimic tuberculous granulomas. In fact, the *in vitro* models can provide the means for cost-effective TB studies, but they can also decrease the use of experimental animals. Nonetheless, animal models are required for studying the complex host-pathogen interactions in a mycobacterial infection and to test new TB regimens prior to clinical trials.

2.2.2 Animal models

2.2.2.1 Mammalian models

Common mammalian animal species used in modeling TB include mouse, guinea pig, rabbit, cattle and non-human primates (Dharmadhikari & Nardell 2008; Flynn 2006; Myllymäki et al. 2015). Of these animal models, the non-human primates offer major advantages to TB research such as the anatomical and physiological similarities between primates and humans, comparable clinical manifestations to human TB, comparable disease progression and pathology as well as the possibility to use human TB diagnostics in evaluating the outcome of an infection (Peña & Ho 2015). However, ethical concerns and high costs limit the usefulness of the non-human

primate models (Myllymäki et al. 2015). In fact, other mammalian TB models can also recapitulate important aspects of the human disease with both advantages and limitations to the research. While the mouse model is relatively affordable and a lot of tools are available for its genetic manipulation, *M. tuberculosis* is not a natural mouse pathogen and for example spontaneous latency does not occur in mice (Cooper 2014). On the other hand, although guinea pig, rabbit and cattle models have proven their feasibility in TB research and for example guinea pigs and cattle have been highly useful in vaccine development, the high cost, size as well as the lack of reagents and genetic tools limits the practicality of their use (Dharmadhikari & Nardell 2008; Flynn 2006; Myllymäki et al. 2015).

2.2.2.2 The zebrafish model

Mycobacterium marinum is a natural fish pathogen that normally causes a chronic progressive disease in its host (Stamm & Brown 2004). Together with *Mycobacterium ulcerans*, *M. marinum* is the closest genetic relative of *M. tuberculosis* outside the *M. tuberculosis* complex (Tønjum et al. 1998). In fact, *M. marinum* shares most of its virulence determinants with *M. tuberculosis* (Stamm & Brown 2004; Tobin, David & Ramakrishnan 2008) and genetic material from *M. tuberculosis* has been demonstrated to complement the lack of corresponding genomic regions in *M. marinum* (Gao et al. 2003a; Gao et al. 2003b; Gao et al. 2004). Importantly, the pathology of *M. marinum in vitro*, as well as in animal models, is similar compared to human TB. Accordingly, *M. marinum* is able to modulate the phago-lysosomal fusion of host macrophages (Barker et al. 1997) and to use them for its survival and replication (El-Etr, Yan & Cirillo 2001). In addition, human TB-like histopathological features have been reported in different *M. marinum* susceptible hosts, including frogs (Ramakrishnan et al. 1997), goldfish (Talaat et al. 1998) and zebrafish (Myllymäki, Bäuerlein & Rämet 2016; Parikka et al. 2012).

Zebrafish (*Danio rerio*) is a small fresh-water teleost that has been used in developmental biology research since the 1970´s (Sullivan & Kim 2008). Among other things, the applicability of the zebrafish as a model organism can be attributed to its small size, high fecundity, ex-utero development, the optical transparency of the embryos as well as to the ease of its genetic manipulation and vast genetic resources (Renshaw & Trede 2012; Yoder et al. 2002). Relatively recently, the zebrafish has also gained popularity as an immunological model organism with immune cell populations and humoral effectors comparable to those in humans (Renshaw & Trede 2012). Of the traditional human innate immune cells, at least

macrophages and neutrophils (Lieschke et al. 2001), DCs (Lugo-Villarino et al. 2010; Tanne et al. 2009), NK cells (Wei et al. 2007), mast cell-like cells (Dobson et al. 2008) and eosinophils (Balla et al. 2010) have been identified and characterized also in zebrafish. Furthermore, gamma-delta (γδ) T cells (Wan et al. 2016), T cells (Yoon et al. 2015) as well as B cells (Danilova & Steiner 2002) exist in the zebrafish, and more specifically comparable populations of Th2- and Treg cells (Dee et al. 2016; Kasheta et al. 2017) as well as the expression of Th subtype specific transcription factors (Hammaren et al. 2014; Mitra et al. 2010) have been reported. It is also noteworthy that effectors of the humoral immunity including complement components (Seeger, Mayer & Klein 1996) and immunoglobulins (Danilova et al. 2005; Lam et al. 2004) function in zebrafish. Moreover, anatomical similarities of the zebrafish immune system to that of humans include the lymphatic vasculature (Küchler et al. 2006; Yaniv et al. 2006) as well as the thymus (primary lymphoid organ for T cell development) and the spleen (secondary lymphoid organ) (Renshaw & Trede 2012).

While many similarities of the human and zebrafish immune systems can be specified, some differences are also found. First of all, the zebrafish kidney serves as the primary lymphoid organ and the place for B cell and blood cell precursor development (equivalent of the mammalian bone marrow) (Renshaw & Trede 2012). In addition, lymph nodes have not been identified in zebrafish, and in fact it has been proposed that the antigenic presentation in zebrafish takes place in the spleen as well as in the Peyer´s patch- like structures of the intestine (Renshaw & Trede 2012). Lastly, the absence of the lungs needs to be reckoned while studying pulmonary diseases in zebrafish.

An experimental *M. marinum* infection can be used to model TB in both zebrafish embryos (Davis et al. 2002) as well as in adult fish (Prouty et al. 2003) (Figure 5). Since it can take as long as 4 weeks until an immunocompetent adaptive immunity is present in the zebrafish (Lam et al. 2004; Trede et al. 2004), the zebrafish embryos can be used to specifically study the innate immune response against mycobacteria. In fact, microinjecting *M. marinum* into zebrafish embryos leads to a progressive infection characterized by the initial engulfment of the bacteria by macrophages and, in collaboration with neutrophils, the formation of the early granulomas (Davis et al. 2002; Yang et al. 2012). Furthermore, the small size of the embryos and the high-throughput yolk sac infection possibilities enable the efficient screening of drugs against TB (Carvalho et al. 2011), whereas the transparency of the embryos provides numerous imaging possibilities including the use of transgenic-reporter fish and bacteria for the real-time visualization of the host-mycobacterial interactions (Davis et al. 2002; Meijer, van der Vaart & Spaink 2014). In addition,

bacterial microinjections into different locations in the embryos, enable the separation of localized and systemic infections and consequently studying the different forms of a mycobacterial infection (Meijer 2016). Naturally, the lack of an adaptive immunity in the embryos means that the embryonic model cannot be used in studying the adaptive immune response.

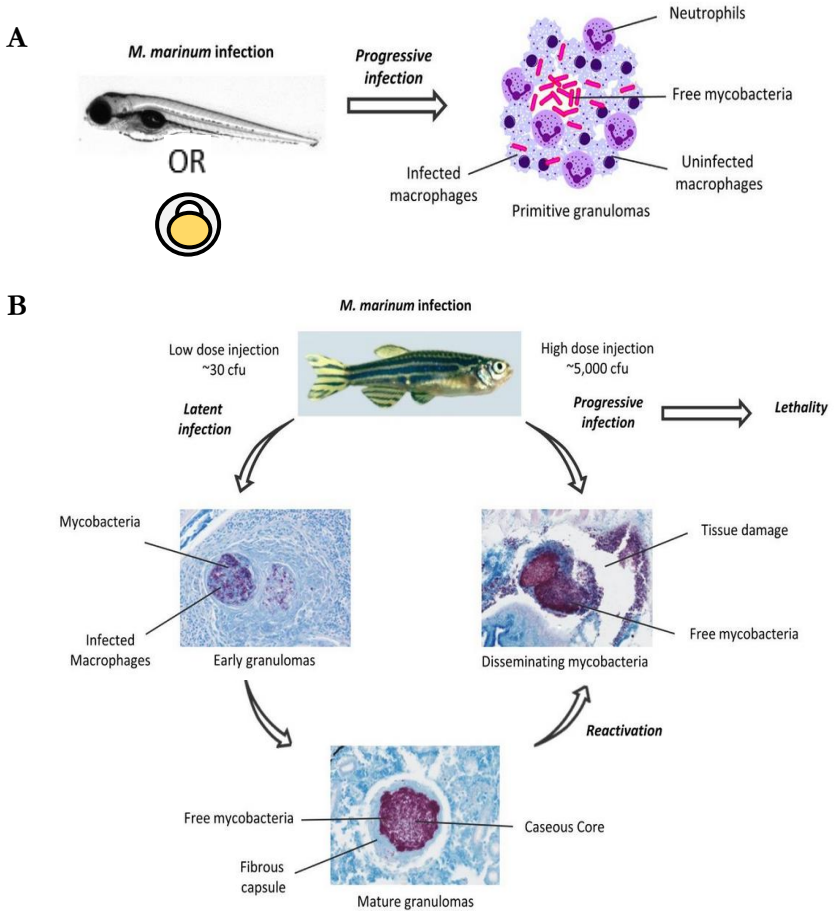

Figure 5. The zebrafish model for TB. A) Following a *M. marinum* infection, the embryos develop a progressive infection in which the early stages of granuloma formation can be studied in the presence of macrophages and neutrophils. B) Adult zebrafish can be used to model both latent and progressive mycobacterial infections as well as the reactivation of the infection. While a low-dose inoculate can cause well-organized granulomas and lead to bacterial containment, the reactivation of the latent disease and a high-dose infection cause unrestricted bacterial growth and a progressive disease leading to lethality. Figure is modified from Myllymäki et al., (2016), Frontiers in Immunology, Volume 7, Article 196, Copyright (2016), and reprinted under the terms of the Creative Commons Attribution license (https://creativecommons.org/licenses/by/4.0/legalcode).

An experimental *M. marinum* infection can be used to model TB in both zebrafish embryos (Davis et al. 2002) as well as in adult fish (Prouty et al. 2003) (Figure 5). Since it can take as long as 4 weeks until an immunocompetent adaptive immunity is present in the zebrafish (Lam et al. 2004; Trede et al. 2004), the zebrafish embryos can be used to specifically study the innate immune response against mycobacteria. In fact, microinjecting *M. marinum* into zebrafish embryos leads to a progressive infection characterized by the initial engulfment of the bacteria by macrophages and, in collaboration with neutrophils, the formation of the early granulomas (Davis et al. 2002; Yang et al. 2012). Furthermore, the small size of the embryos and the high-throughput yolk sac infection possibilities enable the efficient screening of drugs against TB (Carvalho et al. 2011), whereas the transparency of the embryos provides numerous imaging possibilities including the use of transgenic-reporter fish and bacteria for the real-time visualization of the host-mycobacterial interactions (Davis et al. 2002; Meijer, van der Vaart & Spaink 2014). In addition, bacterial microinjections into different locations in the embryos, enable the separation of localized and systemic infections and consequently studying the different forms of a mycobacterial infection (Meijer 2016). Naturally, the lack of an adaptive immunity in the embryos means that the embryonic model cannot be used in studying the adaptive immune response.

Unlike the zebrafish embryos, the adult zebrafish can be used to study the components of both the innate and the adaptive immune system in an infection. Normally an acute or a chronic progressive mycobacterial disease occurs in adult fish upon a *M. marinum* infection (van der Sar et al. 2009). However, as the final infection outcome depends on several host and bacterial specific factors, also a latent infection can be modeled by using a low-dose *M. marinum* inoculate of the *M. marinum* strain ATCC 927 (Parikka et al. 2012). While the acute and chronic infections can be used to determine differences in survival between e.g. knockout and WT fish or to study the transcriptomics of the host response, the latent model offers new possibilities to study latency/dormancy and reactivation (Myllymäki et al. 2018; Parikka et al. 2012). Additionally, the sequenced and assembled zebrafish genome (Howe et al. 2013) has not only made it possible to screen for the candidate genes of the adaptive immune response important for mycobacterial susceptibility, by performing transcriptomic analyses (e.g. Meijer et al. 2005), but it has also largely benefitted both the forward- (Tobin 2010) and the reverse genetic approaches (Clay, Volkman & Ramakrishnan 2008; van der Vaart et al. 2013). Conversely, while the embryos can be grown with relative ease on a petri dish in an incubator, the adult fish require costly maintenance in specific water circulation systems with constant monitoring of the water quality

and temperature. In addition, the relatively large size of the adult fish reduces the real-time imaging possibilities compared to the embryos.

2.3 Reverse genetics in zebrafish

The zebrafish genome sequencing project was initiated by the Wellcome Trust Sanger Institute (Cambridge, UK) in 2001, and the recent 11th assembly (GRCz11) provides invaluable information about the zebrafish genome to scientists (Howe et al. 2013). According to Howe et al. (2013), approximately 70% of all human genes have an orthologue in the zebrafish genome. However, complicating the direct comparison of the human and zebrafish genes, the teleost specific genome duplication event has led to duplicated orthologues (ohnologues) of human genes (Howe et al. 2013). Nevertheless, the large number of orthologous genes between human and zebrafish makes it possible to study numerous human disease-related genes in the zebrafish (Cronan & Tobin 2014).

2.3.1 Morpholino-mediated gene silencing

Anti-sense oligonucleotides are nowadays widely used in modulating gene expression in both *in vitro* as well as in *in vivo* applications. The two main approaches for the oligonucleotide specific silencing include RNA interference (RNAi) mediated knockdown and the administration of single-stranded oligos (Watts & Corey 2012). RNAi is based on the endogenous mechanism in which double-stranded small interfering RNA molecules (siRNAs) bind to the RNA-induced silencing complex (RISC) and subsequently degrade or repress the translation of the complementary mRNA translation (Watts & Corey 2012). Although this approach is widely applicable as well as efficient (Li & Cha 2007), the immunogenicity of siRNAs has raised concerns (Marques & Williams 2005). Conversely, single-stranded anti-sense oligonucleotides (ASOs) bind directly to their complementary RNA (Watts & Corey 2012). By doing so, they can block the initiation of mRNA translation, affect pre-mRNA splicing or block microRNA (miRNA) functionality (Watts & Corey 2012). In addition, as described by Watts & Corey (2012), initial problems such as a high nuclease degradation rate, significant off-target effects and low delivery efficiency have later been solved with chemical modifications to the oligonucleotide backbone.

Compared to natural single-stranded DNA and RNA molecules, the nucleic acid backbone in the morpholino ASOs has been modified with non-ionic

phosphorodiamidates that link adjacent morpholine moieties (Summerton & Weller 1997). With these modifications Summerton & Weller (1997) described nuclease-resistant, sequence-specific and highly efficient ASO that could be produced cost-efficiently compared to other DNA analogs of that time. Soon after their introduction, *in vivo* morpholino experiments were conducted in different model organisms including rat (Arora et al. 2000), mouse (Qin et al. 2000) and frog (*Xenopus laevis*) (Heasman, Kofron & Wylie 2000). In addition, at the same time Nascevisius & Ekker (2000) published the first article describing the use of morpholinos in zebrafish embryos by utilizing yolk sac microinjection. Not only were the morpholinos found to be efficient and target specific, the morphant phenotypes could also be recapitulated in the null-mutant embryos. Since then, morpholinos have been widely used in zebrafish embryos to perform gene knockdown by either blocking the translation or normal splicing of the mRNA (Table 3). Furthermore, the tissue specific use of morpholinos has been reported in adult zebrafish (Hyde, Godwin & Thummel 2012; Kizil et al. 2013; Thummel, Bailey & Hyde 2011). Here, only the embryonic use of morpholinos will be reviewed further.

From an immunological perspective, several genes important for the innate immune response have been studied using morpholino-mediated gene knockdown in zebrafish embryo infection models. To this end, van der Sar et al. (2006) knocked down the Tlr adaptor protein gene *myd88*, and demonstrated its importance in the zebrafish immune response. Similarly, Clay et al. (2008) blocked TNF signaling using a tumor necrosis factor receptor superfamily, member 1a (*tnfrsf1a*) morpholino, and demonstrated increased susceptibility of the morphants to a *M. marinum* infection as well as abnormal granuloma formation in these embryos. In addition, morpholino silencing has been used for the zebrafish orthologues of also other human genes such as *Wiskott-Aldrich syndrome* (*WAS*) (Rounioja et al. 2012), *macrophage receptor with collagenous structure* (*MARCO*) (Benard et al. 2014), *TNF receptor associated factor 6* (*TRAF6*) (Stockhammer et al. 2010) and *spi-1 proto-oncogene* (*SPI1*) (Rhodes et al. 2005).

Despite the widespread use of morpholinos, a relatively recent study revealed poor correlation between the phenotypes of morphants and mutant zebrafish, suggesting an under-estimated off-target prevalence in morpholino-mediated knockdown (Kok et al. 2015). In fact, the proper control of morpholino experiments is required to ensure the efficient and specific silencing of the gene of interest without unwanted effects such as *p53* activation mediated apoptosis (Eisen & Smith 2008; Robu et al. 2007; Stainier et al. 2017). These control methods include the use of multiple morpholinos for a given target gene, rescue experiments with the target

mRNA, random control (RC) morpholino usage as well as the generation of a dose response curve for the target morpholino. However, although appropriate control is necessary to prevent significant off-target effects, the lack of correlation between the morphant and mutant phenotypes can in some cases also be caused by compensatory mechanisms functioning in the null-mutants but not in the knockdown embryos (Rossi et al. 2015).

Table 3. Common gene silencing and mutagenesis methods in zebrafish.

Method	Silencing vs. Mutagenesis
Morpholino-oligonucleotides	Silencing
N-ethyl-N-nitrosourea (ENU) treatment	Mutagenesis
Zinc-finger nucleases (ZFNs)	Mutagenesis
Transcription activator-like effector nucleases (TALENs)	Mutagenesis
CRISPR/Cas9 technology	Mutagenesis

2.3.2 Knockout zebrafish lines

2.3.2.1 Commercial mutants

Initiated by the Wellcome Trust Sanger Institute, the Zebrafish mutation project aims to create and identify knockout alleles for all of the protein-coding genes in the zebrafish genome, and to make the produced mutant zebrafish lines commercially available (Kettleborough et al. 2013). To this end, a forward genetic screen using a combination of N-ethyl-N-nitrosourea (ENU) mutagenesis (Table 3) and high-throughput exome sequencing has been used, and currently null-mutations have been identified in approximately 60% of the zebrafish protein-coding genes, corresponding to a total of 37,624 knockout alleles (https://www.sanger.ac.uk/science/collaboration/zebrafish-mutation-project; 13th of August, 2018). Furthermore, the Zebrafish International Resource Center (ZIRC) as well as the European Zebrafish Resource Center (EZRC) have distributed the obtained mutant zebrafish lines to the research community. In fact, to date 17,882 fish lines containing knockout alleles are available from ZIRC or EZRC (13th of August, 2018). However, despite the impressive amount of commercial lines, mutant zebrafish are not yet available for all zebrafish genes. In addition, since the ENU mutagenesis causes random mutations into the zebrafish genome, off-target mutations do occur and they can co-segregate with the knockout allele of interest.

This in turn has to be controlled in the experiments, for example by using only siblings of the same parents or by performing exome sequencing.

2.3.2.2 Zinc-finger nucleases (ZFNs) and Transcription activator-like effector nucleases (TALENs)

Although a lot of attention has been recently given to the CRISPR/Cas9 system, Zinc-finger nucleases (ZFNs) and Transcription activator-like effector nucleases (TALENs) can be applied in the zebrafish to generate site-specific genetic modifications (Table 3) (Huang et al. 2012). Zinc-finger proteins were initially identified in *Xenopus laevis* oocytes and they were shown to bind DNA through their zinc-finger motifs (Miller, McLachlan & Klug 1985). Later, the fusion of these proteins to the catalytic domain of the FokI-endonuclease initiated the use of ZFNs in targeted and programmable genomic modifications (Kim, Cha & Chandrasegaran 1996). Similarly to the standard CRISPR/Cas9 system, ZFN induced double-stranded breaks (DSBs) in cellular DNA are repaired by endogenous non-homologous end joining (NHEJ) (Bibikova et al. 2002) and homology-directed repair (HDR) mechanisms (Porteus & Baltimore 2003). Subsequently, the DNA repair systems mutate the specified genomic target site. Several *in vitro* and *in vivo* studies using ZFNs have since been published (e.g. Bibikova et al. 2002; Lombardo et al. 2007), including the study by Meng et al. (2008) in which a zebrafish gene was mutated for the first time using ZFNs (Meng et al. 2008; Woods & Schier 2008).

Transcription activator-like (TAL) proteins are major virulence factors of pathogenic plant bacteria of the genus *Xanthomonas* (Bogdanove & Voytas 2011; Moscou & Bogdanove 2009). By localizing to the nucleus and binding to the host cell DNA, these proteins can alter the host´s gene expression signature for the benefit of the bacterium. Soon after the DNA binding strategy of the TAL proteins was determined, these proteins were engineered to target and modify genomic loci of interest *in vitro* in cell lines (Miller et al. 2011; Morbitzer et al. 2010). Furthermore, using the engineered TALs, or TALENs, described by Miller et al. (2011), *in vivo* genome modifications in the zebrafish were later reported (Sander et al. 2011).

2.3.2.3 CRISPR/Cas9 mutagenesis

The clustered regularly interspaced short palindromic repeats (CRISPR)/CRISPR-associated (Cas) system was initially identified as a bacterial and archaeal immune

response against viruses and phages (Bolotin et al. 2005; Mojica et al. 2005; Pourcel, Salvignol & Vergnaud 2005). In fact, in nature at least three types of CRISPR/Cas systems exists with their main function being to recognize and cleave foreign RNA or DNA by target specific RNAs (CRISPR RNA, crRNA; tracer RNA, tracrRNA) and Cas proteins with nuclease activity (Makarova et al. 2011). While the type I and type III systems require multi-protein complexes for their functionality, the type II system uses a single protein, Cas9, to generate target specific RNAs and to cleave target nucleic acids (Makarova et al. 2011). Importantly, the type II system was relatively recently engineered for scientific use as a two-component genome editing system with dual-tracrRNA:crRNA (or guide RNA, gRNA) and the Cas9-protein (Figure 6) (Jinek et al. 2012). More specifically, the site-specific gRNA molecule binds to the target DNA region through its complementary nucleic acid sequence, and directs the Cas9 endonuclease to the same site. For the Cas9-mediated cleavage an adjacent protospacer adjacent motif (PAM) downstream from the target site is additionally required. Consequently, Cas9 creates a double-stranded break that can be repaired with either the NHEJ or HDR system, leading to mutations at the target site (Ran et al. 2013). While NHEJ leads to insertion/deletion (indel) mutations and can result in the knockout of a gene, for example by disrupting the reading frame, the use of a repair template can lead to HDR and mediate the specific addition of genetic material (Ran et al. 2013). In fact, the CRISPR/Cas9 system can be used to knockout genes as well as to mediate DNA knock-in (Albadri, Del Bene & Revenu 2017; Hruscha et al. 2013) and gene knockdown (CRISPR interference) (Larson et al. 2013).

Not surprisingly, owing to its simplicity, effectivity and low cost, an enormous amount of both *in vitro* and *in vivo* systems have used CRISPR/Cas9 mutagenesis to create targeted genomic mutations. Importantly, this system has been used in the zebrafish in to create both bi-allelic mutations in F0-generation fish (Jao, Wente & Chen 2013) as well as knockout zebrafish lines (Table 3) (e.g. Cai et al. 2018; Hruscha et al. 2013; Sugimoto et al. 2017; Varshney et al. 2015). Still, as a relatively recent mutagenesis method the off-target effects of the CRISPR/Cas9 technology have raised concern. However, reports suggesting that the proper design of gRNAs can significantly reduce the off-target frequency (Cho et al. 2014) have later mitigated these worries. In addition, it has been demonstrated that the chromatin accessibility can influence the *in vivo* efficiency of the CRISPR/Cas9 system making some genes difficult to mutate (Uusi-Mäkelä et al. 2018).

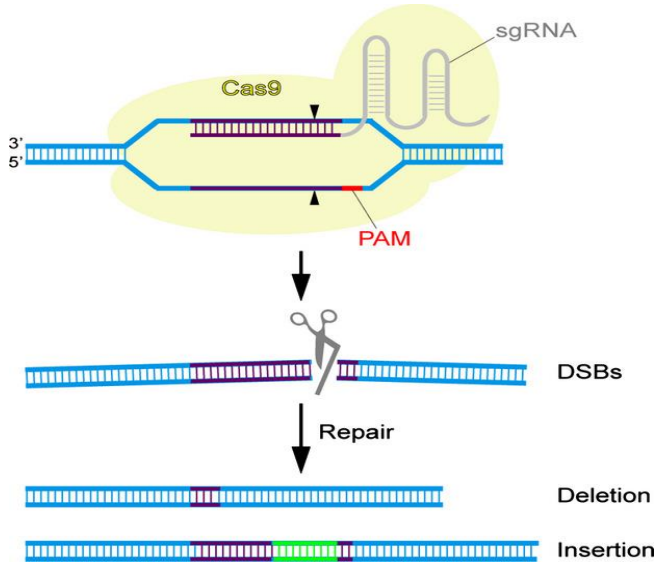

Figure 6. Overview of the engineered type II CRISPR/Cas9 mutagenesis. sgRNA targets the Cas9 protein to the target site by recognizing complementary genomic DNA. By recognizing the adjacent PAM sequence (NGG), Cas9 induces a double-stranded break (DSB) at the site. Finally, the endogenous DNA repair mechanisms repair the DSB, creating deletions or insertions in the corresponding genomic loci. Figure is re-printed from Peng et al., (2015), FEBS Journal, Volume 282, Issue 11, Pages No. 2089–2096, Copyright (2015) under the terms of the Creative Commons Attribution license (https://creativecommons.org/licenses/by/4.0/legalcode).

Together, the ZFN, TALEN and CRISPR/Cas9 systems have provided major advantages to the genetic tractability of the zebrafish genome, and efficient means of creating both somatic as well as germ-line transmitted indel-mutations. Importantly, these methods have made it possible to create mutant zebrafish lines in-house.

3 AIMS OF THE STUDY

The genetic influence on the susceptibility for TB is nowadays well-established. While the PCSK family member FURIN is known to regulate T cell function and activation, ITLNs have been shown to bind to different bacterial species *in vitro*. More precisely, human FURIN regulates the production of IFNG and the polarization of T helper (Th) type 1 cells, both of which are crucial for the immune response against TB, whereas ITLN1 can bind to carbohydrates on mycobacterial cell surface. However, not much is known about their *in vivo* role in infectious diseases or specifically in the host response against mycobacteria. The aims of this study were to set up an in-house CRISPR/Cas9 mutagenesis method in zebrafish, and to use *furinA*- and *itln3* -mutant zebrafish lines together with the zebrafish *M. marinum* model of TB in order to understand the significance of these genes for the mycobacterial immune response.

Specifically the aims can be divided as follows:

1) To study the role of FURIN in the immune response against mycobacteria by using commercially available *furinA*$^{td204e/+}$ mutant zebrafish.

2) To set up an in-house CRISPR/Cas9 mutagenesis system in zebrafish using exogenous *egfp* as well as endogenous *ca10a* and *ca10b* zebrafish gene targets.

3) To identify differentially expressed genes in the zebrafish *M. marinum* infection model, and to study the highly up-regulated *itln3* in the mycobacterial infection using self-produced *itln3* knockout zebrafish.

4 MATERIALS AND METHODS

4.1 Zebrafish maintenance

4.1.1 Ethical considerations (I, II, III)

The National Animal Experiment Board of Finland has approved the zebrafish housing, care and all of the experiments. In addition, experiments are in accordance with the EU-directive 2010/63/EU on the protection of animals used for scientific purposes and with the Finnish Act on Animal Experimentation (62/2006). Zebrafish were monitored daily and humane endpoint principles defined in the permits were applied. Permits: LSLH-2007-7254/Ym-23, ESAVI/10079/04.10.06/2015, ESAVI/6407/04.10.03/2012, ESAVI/733/04.10.07/2013, ESAVI/2267/04.10.03/2012, ESAVI/8125/04.10.07/2013, ESAVI/11133/04.10.07/2017, and ESAVI/2235/04.10.07/2015.

4.1.2 Fish lines and housing (I, II, III)

Zebrafish embryos were maintained in embryonic medium (E3, 5 mM NaCl, 0.17 mM KCl, 0.33 mM $CaCl_2$, 0.33 mM $MgSO_4$, 0.0003 g/l methylene blue) at 28.5°C until 7 days post fertilization. Media was changed completely at 2 dpf and half of it replaced at 4 dpf. From 5 dpf onwards the larvae were given SDS100 (Special Diets Services, Essex, UK) or GM75 (Skretting, Stavanger, Norway) food. In the experiments with adult zebrafish, three- to 16-month-old fish were used. Adult fish were maintained in a flowthrough system (Aquatic Habitats, Florida, USA or Aqua Schwarz, Göttingen, Germany) with an automatic cycle of 14 hours of light and 10 hours of dark and fed with SDS400 (Special Diets Services) or GM500 (Skretting) fish food. Zebrafish lines used in the thesis are shown in Table 4.

Table 4. Zebrafish lines used in the study.

Zebrafish line	ZFIN ID	Mutagenesis method	Used in	Reference
AB	ZDB-GENO-960809-7	–	I, II, III	–
TL	ZDB-GENO-990623-2	–	II, III	–
furinA ^{td204e}	ZDB-FISH-150901-26631	ENU	I	Walker et al., 2006
Tg(*fli1a*:*egfp*)	ZDB-TGCONSTRCT-070117-94	–	II	Lawson & Weinstein. 2012
itln3 ^{uta145}	–	CRISPR/Cas9	III	–
itln3 ^{uta148}	–	CRISPR/Cas9	III	–

4.2 Nucleic acid extraction

4.2.1 DNA extraction using ethanol precipitation (I, II, III)

Standard ethanol precipitation was used to isolate DNA from the adult zebrafish tailfins as well as from zebrafish embryos. For the tailfin isolation, the zebrafish were treated with 0.02% 3-amino benzoic acid ethyl ester (Sigma-Aldrich, Missouri, US) and a piece of their tailfin cut under anesthetic. Tissues/embryos were incubated overnight in 100 µl of buffer containing 10 mM Tris (pH 8.2), 10 mM ethylenediaminetetraacetic acid (EDTA), 200 mM NaCl, 0.5% Sodium dodecyl sulfate (SDS) and 200 µg/ml Proteinase K (Thermo Fischer Scientific) until homogenous lysate was obtained. The samples were centrifuged (16,000 g, 20 min, room temperature, RT) and the genomic DNA isolated using the following procedure. Briefly, 200 µl of 100% ethanol (twice the lysate volume) was mixed to the supernatant and the DNA precipitated in -20°C for at least 30 min. Precipitated DNA was pelleted by centrifugation (16,000 g, 10 min, RT), washed with 70% ethanol, centrifuged (16,000 g for 5 min, RT), air-dried and resuspended in 30µl (embryos) or 200 µl (tailfins) of ddH2O.

4.2.2 Rapid isolation of PCR-ready genomic DNA (III)

The method for PCR-ready genomic DNA isolation from zebrafish tissues published by Meeker et al. (2007) was used for genotyping of the adult zebrafish. Zebrafish were anesthetized and a piece of their tailfin cut as described above. Tailfin

tissue was placed in 50 µl of 50 mM NaOH, incubated for 30 min at 98°C, cooled down at +4°C and neutralized with 1 M Tris-HCl (pH 8.0). Tissue debris was removed by centrifugation (3000 g, 10 min, RT) and the DNA containing supernatant used directly to PCR.

4.2.3 RNA extractions (I, III)

RNeasy kits (Qiagen) were used for RNA isolations from the adult fish tissues as well as from the embryos. Prior the RNA extractions, zebrafish were euthanized in 0.04% 3-amino benzoic acid ethyl ester (Sigma-Aldrich, Missouri, USA) and samples kept in RNAlater (Qiagen) at +4°C, placed on dry ice and stored at -80°C or freshly suspended in RLT-lysis buffer (Qiagen). From the zebrafish embryos, simultaneous genomic DNA (gDNA) removal and RNA extraction were done using the RNeasy Mini Plus kit (Qiagen) according to the manufacturer´s instructions. RNA concentrations were measured using Nanodrop (ThermoFisher) and the RNA quality analyzed from randomly selected samples using the Fragment analyzer (Advanced Analytical). In order to simultaneously isolate DNA and RNA from the adult zebrafish organ blocks, Trireagent (Molecular research center, Ohio, USA) was used and the manufacturer´s instructions were followed.

4.3 Zebrafish genotyping

4.3.1 Sequencing (I, III)

Sanger sequencing was used to screen for *furinA*^{td204e}, *itln3*^{uta145} and *itln3*^{uta148} mutation carriers. To this end, genomic DNA was isolated from the zebrafish and the mutation site amplified by PCR. Primers used for mutation site amplification are shown in Table 5.

Table 5. Primers used for mutation site amplification by PCR.

Gene	Ensembl ID	Primer sequence 5´-3´	Product size (bp)	Used in
furinA	ENSDARG00000062909	F: ATCAGCAGCAGTACGCAAAA R: ATGAATTGGCTTGGCAGTTT	242	I
egfp	N/A (transgene)	F: CAAGGGCGAGGAGCTGTTCAC R: TCTTCTGCTTGTCGGCCATG	470	II
ca10a	ENSDARG00000052644	F: CTGCAAATCATCCCTTTGTG R: GTTCCTCGCATCAAAACACC	415	II
ca10b	ENSDARG00000009568	F: TCCACGACTCAGCCAACAG R: GCACTGCGTTATCAGCAAAAG	531	II
itln3	ENSDARG00000003523	F: GGAGCTGTCACTCCAAAGCC R: GTGGTTGATCAACCATTCAGCAC	212	III

4.3.2 Polymerase chain reaction (PCR) (III)

Genomic DNA was isolated from the *itln3* mutant zebrafish and two different PCR reactions for each sample were done with both the WT and the mutant target site specific PCR primers: *itln3*^{uta145} mutant F: ATGCTAGGTTGAGGAGCTCG, WT *itln3*^{uta145} F: ATGCTAGGTTGAGGAGCATC, *itln3*^{uta148} mutant R: CCGAGCTGATACTTACCTAGC, WT *itln3*^{uta148} F: CTAGGTTGAGGAGCATCGCT and the appropriate flanking primers (Table 5). PCR products were analyzed on 1.5% agarose Tris-acetate-EDTA (TAE) gel.

4.4 Reverse genetics

4.4.1 Gene knockdown using morpholino oligonucleotides (I, III)

All morpholino oligonucleotides were purchased from GeneTools (Oregon, USA) and microinjected into the yolk sac of the embryos prior to the 16-cell-stage. Whereas *furinA* and *furinB* morpholinos were designed to block the translation of the corresponding mRNAs, the *itln1* morpholino disrupted splicing of its cognate precursor mRNA. Morpholino injections were performed using borosilicate capillary needles (Sutter instrument Co., California, USA), a micromanipulator (Narishige International, London UK) and a PV830 Pneumatic PicoPump (World Precision Instruments, Florida, USA). Used morpholino concentrations are described in the original communications.

4.4.2 CRISPR/Cas9 mutagenesis (II, III)

4.4.2.1 gRNA design and production

Target site for *egfp* was obtained from Jao et al. (2013). gRNA target sites for *ca10a* and *ca10b* as well as *itln3* were designed using both the online CRISPR design tool (http://crispr.mit.edu/) as well as the sgRNA excel tool (Krebs 2014). Further evaluation of the specificity of the suggested target sites were done with the Basic Local Alignment Search Tool (BLAST) analysis (Altschul et al. 1997). The synthesis of the gRNAs was primarily based on a protocol by Hruscha and Schmid (2015). Briefly, DNA-oligos (containing the reverse complementary sequence of the gRNA) (Sigma-Adrich) were annealed to the T7-primers and the gRNAs synthetized using the MEGAshortscript T7 Transcription Kit (Ambion Life Technologies, USA). The quality and quantity of the gRNAs were evaluated using 1% agarose TAE gel electrophoresis and Nanodrop, respectively. Table 6 summarizes the gRNA target sites for the genes of interest.

Table 6. Genes and gRNA target sites for CRISPR/Cas9 mutagenesis.

Gene	Ensembl ID	Target site sequence 5´-3´	Targeted exon	Used in
egfp	N/A (transgene)	GGGCACGGGCAGCTTGCCGG	-	II
ca10a	ENSDARG00000052644	TCCACCCAAAATCCATGA	2	II
		TACAAAGAAGTTGTTCAG	2	II
		ACTGAGGCTCAACACTGG	3	II
ca10b	ENSDARG00000009568	AACGAACTCCCAAACGTG	1	II
		TTGGGAAGAGACAGTCGC	3	II
itln3	ENSDARG00000003523	AGGTTGAGGAGCATCGCT	2	III
		TGACATGACCACAGCCGG	3	III

4.4.2.2 gRNA and *Cas9* mRNA microinjections

Prior to the microinjections, the embryos were aligned on self-made 1.2% agarose E3-medium plates. For target site mutagenesis, 1.5 ng phenol red (Sigma), 270- 2000 pg gRNA and 330 pg Cas9 mRNA (Invitrogen, California, USA) were microinjected into one-cell-stage embryos in a 1 nl nuclease free water suspension. Whereas *egfp* was mutated from the transgenic tg(*fli1a:egfp*) zebrafish, both *ca10a* and *ca10b* as well as *itln3* were mutated from AB zebrafish. Previously described

microinjection equipment was used, and the injections were visualized under a SMZ645 microscope (Nikon, Tokio, Japan).

4.4.2.3 Target loci analysis using the T7 endonuclease I assay

The gRNA target sites were amplified by PCR using target site specific primers (Table 3) as well as Maxima Hot Start DNA polymerase (Thermo Scientific). 10 µl of the PCR product was denatured and annealed in 1x NEBuffer 2 (New England Biolabs, USA) and incubated with 0.5µl of T7 endonuclease I (T7EI, New England Biolabs) for 30 minutes at 37°C in a total reaction volume of 20 µl. Finally, the T7EI treated PCR products were analyzed by 2.5% agarose TAE gel electrophoresis.

4.4.2.4 Microscopical analysis of the CRISPR/Cas9 mutants

In report II, the phenotypes of the CRISPR/Cas9 mutated zebrafish were evaluated by microscopy. Enhanced green fluorescent protein (*EGFP*) mutagenesis was analyzed from 2-day-old tg(*fli1a:egfp*) zebrafish using fluorescence microscopy. Phenotypic consequences of the *ca10a* and *ca10b* mutations were assessed and imaged using a Lumar V12 microscope (Zeiss, Oberkochen, Germany) 1-5 dpf.

4.5 Experimental infections

4.5.1 Bacterial culture (I, III)

M. marinum strain ATCC 927 was used in all of the mycobacterial infection studies. Mycobacteria was cultured in the dark at a constant temperature of 28°C as described previously (Parikka et al. 2012). Bacterial amounts for the infection experiments were estimated from the 7H9 liquid cultures using a spectrophotometer and the optical density (OD) value at 600 nm as well as with a previously determined growth curve (Parikka et al. 2012).

4.5.2 Bacterial preparation and inoculation (I,III)

In the embryonic *M. marinum* infections both yolk sac method (0 dpf) and a blood island inoculate (2 dpf) were used. The yolk sac infection was also used in the *M. marinum* and morpholino coinjections. Whereas the general 1-2 nl injection suspension contained 2% polyvinylpyrrolidone (PVP) (Sigma-Aldrich) and 0.3 mg/ml phenol red in a PBS carrier solution, 7 mg/ml rhodamine dextran tracer was used in the morpholino and *M. marinum* co-injections. 2dpf zebrafish embryos were anesthetized with 0.02% 3-amino benzoic acid ethyl ester (Sigma-Aldrich) prior to injections. For the adult zebrafish *M. marinum* infections, zebrafish were anesthetized as above and mycobacteria injected into the abdominal cavity of the fish using a 30 G insulin needle. PBS solution with 0.3 mg/ml phenol red was used in the adult infections as a mycobacterial carrier solution. Bacterial dose in all of the experimental *M. marinum* infections was verified by plating on 7H10 agar plates.

4.6 Analyzing the outcome of the infection

4.6.1 Flow cytometry (I, III)

Zebrafish were first euthanized with 0.04% 3-amino benzoic acid ethyl ester, followed by isolation and suspension of the kidneys in a PBS solution with 0.5% fetal bovine serum (Sigma-Aldrich/Gibco). Before flow cytometry, the kidney cell suspensions were filtered using cell strainer caps with a 35 μm mesh (Corning/Thermo Fisher Scientific). Kidney cell samples were kept on ice prior to the runs. Flow cytometry was perfomed using FACSCanto II (Becton, Dickinson, New Jersey, USA) and the data analyzed with the FlowJo program (v7.5; Tree Star, Inc, Oregon, USA). Gating for the blood cell populations was based on previously published research articles (Langenau et al. 2004; Traver et al. 2003). Of note, steady state fish were analyzed by flow cytometry in report I whereas both steady state and *M. marinum* infected fish were analyzed in report III.

4.6.2 Ziehl-Neelsen staining (I)

Histological examination using Ziehl-Neelsen stain of tissue sections was used to verify mycobacterial presence in the adult *furinA*^{td204} zebrafish. To this end,

euthanized zebrafish were prepared using a previously described protocol (Parikka et al. 2012). In brief, fish were fixed in 10% phosphate buffered formalin (pH 7.0) for 5 days and de-calcified in 20% EDTA-citrate (pH 7.2) for 7 days. For dehydration and clearing, the fish were sequentially incubated in rising ethanol series from 70% to 100% followed by xylene, respectively. After tissue preparations, the zebrafish were embedded in paraffin, cut into 5 μm longitudinal sections and placed on microscopy slides. A basic Ziehl-Neelsen staining procedure utilizing carbolfuchsin, acid alcohol and methylene blue was used. Visualization of the stained tissues were performed either with an Olympus BX51 microscope together with an Olympus ColorView IIIu camera or with an automated Objective Imaging Surveyor virtual slide scanner (Objective Imaging, Cambridge, United Kingdom). Scanned slides were digitized at a resolution of 0.4 μm per pixel using a 20x Plan Apochromatic microscope objective. Scanned data were converted to JPEG2000 format as described previously (Tuominen & Isola 2009).

4.6.3 Gene expression microarray (III)

RNA from the zebrafish organ blocks was extracted with TRIreagent (Molecular Research Center, Ohio, USA) following the manufacturer's instructions. Zebrafish (V3) Gene Expression Microarray, 4x44K (Agilent Technologies, California, USA) was conducted by the Turku Centre for Biotechnology at the Finnish Microarray and Sequencing Centre. 100 ng of RNA was prepared with the RNA Spike-In Kit, One-Color (Agilent) and Low Input Quick Amp Labeling Kit, One-Color (Agilent) and analyzed using the 2100 bioanalyzer RNA 6000 Nano kit (Agilent). RNA labelling and hybridization were performed in a Microarray Hybridization Chamber (Agilent) using GE Hybridization Kit (Agilent). Agilent scanner G2565CA and AgilentHD_GX_1Color profile were used in scanning the arrays and a Feature Extraction Software v. 10.7.3 (Agilent) to obtain numerical data.

4.6.4 Quantitative PCR (I, III)

4.6.4.1 Expression analysis

RNA for qPCR analysis was extracted and analyzed as described above. cDNA synthesis was done with iScript Select cDNA synthesis kit (Bio-Rad, California,

USA) or SensiFAST™ cDNA synthesis kit (BioLine, London, UK). qPCR was done with Maxima SYBR green qPCR master mix (Fermentas, Burlington, Canada) or PowerUp™ SYBR® master mix (Thermo Fischer Scientific) and the CFX96™ PCR system (Bio-Rad Laboratories, In., California, USA). Data was obtained using Bio-Rad CFX Manager software. 2-deltaCt method was used to normalize the target gene expression to the expression of *eukaryotic translation elongation factor 1 alpha 1, like 1* (*eef1a1l1* or *ef1a*) (Tang et al. 2007). No-template controls as well as No-RT controls were included in the qPCRs. Melt curve analysis and agarose TAE gel electrophoresis were performed in order to confirm correct size of the qPCR products. Primers used in the qPCR analysis are depicted in Table 7.

4.6.4.2 *M. marinum* quantification

To determine the mycobacterial burden in *M. marinum* infected zebrafish, the total DNA was isolated from the zebrafish with previously described methods. In order to amplify *M. marinum* specific DNA, a previously described protocol utilizing *M. marinum* internal transcribed spacer (MMITS) –primers; F: CACCACGAGAAACACTCCAA and R: ACATCCCGAAACCAACAGAG were used (Parikka et al. 2012). SensiFAST™ SYBR® No-ROX kit and a CFX96 qPCR (Bio-Rad) machine was utilized in the qPCR. The results were normalized to previously determined *M. marinum* count controls and analyzed using the Bio-Rad CFX Manager software (Bio-Rad).

4.6.5 Immunosuppression by dexamethasone (III)

A mixture of 25mg dexamethasone (Sigma-Aldrich) and gelatin (Sigma-Aldrich) was used to coat 10 g of SDS400 food, and a daily food dose of 4 mg (10 µg dexamethasone)/fish was administered for a total duration of 5 weeks. The method for the dexamethasone food preparation has been previously reported (Myllymäki et al. 2018).

4.6.6 Statistical analysis (I, III)

Prism v. 5.02 (GraphPad Software, California, USA) was used in the statistical analyses. Whereas a log-rank (Mantel-Cox) test was used in the survival experiments,

the flow cytometry and qPCR results were analyzed using nonparametric one- or two-tailed Mann-Whitney. P values of < 0.05 were considered statistically significant.

Table 7. Primers used in the qPCR analyses.

Gene	Primer sequence 5´-3´	Used in
furinA	F: CCAAAGAGGCTTTCCAACGC	I
	R: CGTACTGCTGCTGATGGACAG	I
pcsk1	F CGGGAAAAGGAGTGGTCAT	I
	R GGTGGAGTCGTATCTGGG	I
pcsk2	F CGGATCTGTATGGAAACTGC	I
	R GCCGGACTGTATTTTATGAAT	I
furinB	F CCAAGGCATCTACATCAACAC	I
	R ACACCTCTGTGCTGGAAA	I
pcsk5a	F GGAGTTTCAATGACCCCAA	I
	R ACCACAACTCCTTTCCCA	I
pcsk5b	F TGTTCCTCGACCCTTACCAC	I
	R ATCTCGCCATGTCAGGAAAG	I
pcsk7	F AGAGTGTTGGACGGG	I
	R TGCCTAATGGATGCGGT	I
cd247 (cd3zeta)	F CATCACCGGCTTCTTTGTGC	I
	R CCCCAGTTTATCAATGGCCTGA	I
tbx21(T-bet)	F GGCCTACCAGAATGCAGACA	I
	R GGTGCGTACAGCGTGTCATA	I
gata3	F GGATGGCACCGGTCACTATT	I
	R CAGCAGACAGCCTCCGTTT	I
foxp3a	F CAAAAGCAGAGTGCCAGTGG	I
	R CGCATAAGCACCGATTCTGC	I
rorca	F GAAGGCTGCAAGGGCTTCTT	I
	R TGCAGTTCCTCTGCCTTGAG	I
tnfa	F GGGCAATCAACAAGATGGAAG	I
	R GCAGCTGATGTGCAAAGACAC	I
il1b	F TGGACTTCGCAGCACAAAATG	I
	R GTTCACTTCACGCTCTTGGATG	I
lta	F CCACAGTTCAGCAGGACCTC	I
	R TTTCCTGCGTGCTCTCATGTC	I
ifng1-1	F AAATGGTGCTACTCTGTGGAC	I
	R TTCCAACCCAATCCTTTG	I
il22 (ifnphi6)	F TCAGACGAGCACACAGATATG	I
	R GATGGCTGGAGTAGTCGTG	I
il17a/f3	F GGCTCTCACGGGTTTTCAG	I
	R ACACTTCTTCACACCAGAACATC	I
il10	F GCTCTGCTCACGCTTCTTC	I
	R TGGTTCCAAGTCATCGTTG	I
tgfb1a	F TCGTCTTCCAGCAAGCTCAG	I
	R TTGGAGACAAAGCGAGTTCC	I
itln1	F GACGACTACAAGAACCCTGG	III
	R ATCGTTGCATGTACCTATGCC	III
itln2	F TATGGGAATGGCTGCCTTTC	III
	R TTTCAAGCTCATGGTTGCTG	III
itln2-like	F ACTGTTCAAGAAATTCCCTGTG	III
	R ATGCCCAGTTGGTTTAGTGC	III
itln3	F GTGCAACACAGGATGGCATG	III
	R TTCTGCACTGCCAAACGTAG	III
eef1a1l1 (ef1a)	F CTGGAGGCCAGCTCAAACAT	I, III
	R ATCAAGAAGAGTAGTACCGCTAGCATTAC	I, III

4.7 The bacterial binding assay

4.7.1 Recombinant *itln3* gene construct and protein purification (III)

Zebrafish *itln3* gene was synthetized and cloned into a Gateway donor vector; pDONR™221 (Thermo Scientific) by GeneArt (Invitrogen). Subsequently, *itln3* was amplified by PCR using the following primers: F: GGGGACAAGTTTGTACAAAAAAGCAGGCTTCACCATGCTGCGCTGCC TGTTTGTCTTCG and R: GGGGACCACTTTGTACAAGAAAGCTGGGTTTTATTAACGATAAAACA GCAGAACTGCGCTC, and Gateway cloned into the pVBboostFGII+Wpre-VSV-G expression vector (Heikura et al. 2012). Freestyle 293-F cells (Thermo Fisher Scientific) were transfected with 10 μg of expression vector using FreeStyle™ MAX Reagent (Thermo Fisher Scientific) and the cells cultured for 7 days. Strep-Tactin®XT resin (IBA Lifesciences, Göttingen, Germany) was used for affinity chromatography together with automated ÄKTA pure protein purification system (GE Healthcare Life Sciences, UK), Strep-Tactin®/Strep-Tactin®XT wash buffer (IBA Lifesciences) and Strep-Tactin®XT elution buffer with biotin (IBA Lifesciences). Itln3-Strep-Tag®II was detected with 2.5 μg of Streptactin Oyster 645 conjugate (IBA Life Sciences) in 0.05% Tween TBS for 1 h at RT. Imaging was done with the Odyssey® CLx (LI-COR Biosciences, Nebraska, USA) and analyzed with the Image Studio Lite (v.5.2; LI-COR Biosciences).

4.7.2 Bacterial binding assay (III)

M. marinum (ATCC927) was cultured as described above and *S. pneumoniae* (serotypes T4 and S1) as described previously (Rounioja et al. 2012). *E. coli* was cultured overnight in LB-media at 37°C with constant shaking (200 rpm). Prior the binding experiments bacteria were pelleted by centrifugation, washed once with 1x PBS and incubated for two hours with 7.5 μg of Itln3-Strep-Tag®II or GFP-Strep-tag®II (Iba Lifesciences) in 500 μl of buffer containing 20 mM HEPES (pH 7.4), 150 mM NaCl, 10 mM $CaCl_2$, 0.1% BSA and 0.05% Tween-20 or in a similar buffer with 10 mM EDTA instead of $CaCl_2$ at +4°C. Subsequently, bacteria were re-pelleted and washed once with 1x PBS. Detection of the Strep-tagged proteins were done as described above.

5 SUMMARY OF THE RESULTS

5.1 FurinA regulates the zebrafish host response against *M. marinum* (I)

It is well known that both the innate and adaptive immunity are required for TB immunity and the containment of the bacteria in the mycobacterial granulomas. While aberrations in TNF signaling can lead to increased bacterial spread and dissemination (Roca & Ramakrishnan 2013; Tobin et al. 2012), a deficient Th1 cell function can reduce the efficiency of the macrophage-mediated killing of the mycobacteria (Lyadova & Panteleev 2015; Weiss & Schaible 2015). The proprotein convertase subtilisin/kexins (PCSKs) are a nine-membered enzyme family of serine endoproteases that function by activating immature pro-proteins through proteolytic cleavage (Seidah & Prat 2012). FURIN is a PCSK family member with a broad range of substrate proteins ranging from growth factors to bacterial toxins to immunological mediators (Thomas 2002). Consequently, FURIN regulates a wide variety of biological processes from embryogenesis to T cell function. More specifically, FURIN has been shown to regulate IFNG production and subsequently Th1 cell polarization (Pesu et al. 2006). In this study, we used the zebrafish *M. marinum* model of TB together with the commercially available *furinA*^{td204e} mutant zebrafish (Walker et al. 2006); Zebrafish Information Network (ZFIN) ID: ZDB-GENO-080606-310 in order to understand the role of FURIN in the host immune response against a mycobacterial infection.

5.1.1 Decreased *furinA* expression in *furinA*$^{td204e/+}$ mutant zebrafish affects granulocyte development as well as the expression of Th subtype transcription factors

furinA^{td204e} mutant zebrafish carry a splice site mutation that leads to the exclusion of exon 9 from the mature mRNA (Walker et al. 2006). Consequently, this results in the loss of a catalytic asparagine-residue (Asn295) and in a non-functional FurinA protein (I, Suppl. Fig. 1). Moreover, the exonic exclusion in the *furinA*^{td204e} mutant

zebrafish allows the specific quantification of the WT *furinA* mRNA molecules by qPCR. Due to the observed and published developmental lethality of homozygous *furinA* mutant zebrafish (Walker et al. 2006), the experiments were performed using heterozygous *furinA*$^{td204e/+}$ mutants as well as their WT siblings. In order to compare *furinA* expression in both *furinA*$^{td204e/+}$ mutants and in WT fish, the relative levels of *furinA* mRNA were measured by qPCR in steady state and *M. marinum* infected (34 CFU, SD 10 CFU) zebrafish 4 and 9 weeks post infection (wpi) (I, Fig. 1A). In line with the previous *in vitro* studies that have demonstrated induced *FURIN* expression in the activated immune cells of both the myeloid (Meissner et al. 2013) and lymphoid lineages (Lund et al. 2004; Pesu et al. 2006), *furinA* was significantly up-regulated in both *furinA*$^{td204e/+}$ mutants and in WT zebrafish upon a mycobacterial infection (I, Fig. 1A). Additionally, confirming the expression of zebrafish *furin* in both the innate and adaptive immune cells, *furinA* was expressed in FACS sorted zebrafish granulocytes and lymphocytes isolated from the fish kidneys (I, Fig. 2A). Importantly, decreased *furinA* levels were observed in the heterozygous *furinA*^{td204e} mutants compared to WT fish, validating the feasibility of using the *furinA*$^{td204e/+}$ zebrafish in our experiments.

Next, we characterized whether decreased *furinA* expression in *furinA*$^{td204e/+}$ zebrafish affects hematopoiesis. To this end, we studied the blood cell populations of steady state zebrafish kidneys by flow cytometry (I, Fig. 1B-C). Although blood cell precursor, erythrocyte and lymphocyte populations did not reveal any differences between *furinA*$^{td204e/+}$ mutants and WT fish, significantly lower granulocyte amounts were observed in *furinA*$^{td204e/+}$ zebrafish compared to the WT ones.

The significance of FURIN for T cell function has been studied with conditional T cell *FURIN* knockout mice (CD4cre-fur$^{f/f}$). Although thymocyte development is unaffected in the CD4cre-fur$^{f/f}$ mice, these animals have altered effector T cell populations as well as abnormalities in the production of Th subtype specific cytokines (e.g. IFNG, IL4)(Pesu et al. 2008). Moreover, activated Furin-deficient T cells produce significantly less transforming growth factor beta-1 (TGFB1) (Pesu et al. 2008), a cytokine that is crucial for the development of Treg cells and consequently for peripheral tolerance through inducing the expression of *Foxp3* (Andersson et al. 2008; Chen et al. 2003). Therefore, we next quantified the expression of the Th cell subtype specific transcription factors *T-box 21* (*tbx21*, Th1 marker), *gata3* (Th2 marker), *forkhead box P3a* (*foxp3a*, Treg marker), *retinoic acid receptor-related orphan receptor C a* (*rorca*, Th17 marker) as well as *tgfb1a* in *furinA*$^{td204e/+}$ mutants and in WT fish by qPCR (I, Fig. 1D). A transcriptional analysis indicated

significantly higher expression levels of *tbx21*, *gata3* as well as *foxp3a* in *furinA*$^{td204e/+}$ fish compared to WT controls. These results are in line with the increased Foxp3-positive T cell amounts as well as with the extensive Th1- and Th2 type cytokine production in CD4cre-fur$^{f/f}$ mice (Pesu et al. 2008), indicating a conserved role for FURIN in T cell activation. Additionally, the up-regulation of *tgfb1a* mRNA associated with the decreased expression of *furinA* in *furinA*$^{td204e/+}$ zebrafish, a result possibly arising from the compensatory transcriptional mechanisms complementing the deficient maturation of the TGFB1 protein in the mutants.

Since conventional PCSK family enzymes (PCSK1-7), including FURIN (also known as PCSK3), have an identical consensus cleavage site; (K/R)-(X)n-(K/R) (n= 0, 2, 4 or 6 and X= any amino acid), PCSKs can have redundant functions and shared substrate proteins (Turpeinen, Ortutay & Pesu 2013). To study whether reduced *furinA* expression influences the transcript levels of other *pcsk* family members in *furinA*$^{td204e/+}$ mutant zebrafish, we quantified the relative mRNA levels of *pcsk1*, *pcsk2*, *furinB*, *pcsk5a*, *pcsk5b* and *pcsk7* in steady state fish (I, Fig. 2B). Suggesting a possible transcriptional compensation mechanism, *pcsk1* and *pcsk2* expressions were significantly up-regulated in *furinA*$^{td204e/+}$ mutants compared to the WT controls. However, no differences were observed in the expression of *furinB*, *pcsk5a*, *pcsk5b* and *pcsk7*.

5.1.2 Silencing *furin* in zebrafish embryos decreases their survival in a mycobacterial infection

A *M. marinum* (ATCC-927) injection into the abdominal cavity of adult zebrafish (Parikka et al. 2012) as well as a yolk sac microinjection into the embryos (Carvalho et al. 2011) can be used to model TB pathogenesis. In order to study the immune defense against *M. marinum* in our *furinA* mutant fish, we first infected adult *furinA*$^{td204e/+}$ and WT zebrafish with a high-dose of *M. marinum* (8300 CFU, SD 1800 CFU) and followed the survival of these fish until 11 wpi (I, Fig. 3A) as well as performed Ziehl-Neelsen staining to verify the presence of mycobacteria (I, Fig. 3B). Although our histological analysis confirmed the presence of both mycobacteria and well-organized mycobacterial granulomas in the infected zebrafish at 3 and 11 wpi, respectively, we could not detect statistically significant differences in the infection-induced mortality between the adult *furinA*$^{td204e/+}$ mutants (ca. 80% mortality) and the WT controls (ca.70% mortality) during the 11-week follow-up.

While the adult zebrafish possess the components of the innate and adaptive immune system, the zebrafish embryos can be used to specifically study the innate immunity alone (Renshaw & Trede 2012; Sullivan & Kim 2008). To this end, we silenced *furinA* and *furinB* with morpholinos and simultaneously infected the same embryos with *M. marinum* (131 CFU, SD 125 CFU). After following their survival until 7 dpf (I, Fig. 3C), a significant difference was observed between the *furinA*/*furinB* morphants and the RC-morpholino injected control embryos with end-point mortalities of 100% and 93%, respectively.

5.1.3 Zebrafish *furinA*$^{td204e/+}$ mutants have an enhanced expression of proinflammatory cytokine genes and a decreased mycobacterial burden in a mycobacterial infection

To better understand the *furinA*-mediated modulation of the innate immune response in our experimental TB model, we infected adult *furinA*$^{td204e/+}$ mutants and WT zebrafish with a high-dose of *M. marinum* (10,300 CFU, SD 3,300 CFU) and quantified the expression of both proinflammatory (*tnfa*, *il1b*, *lta*, *ifng1-1*, *il22*, *il17a/f3*) as well as anti-inflammatory cytokine genes (*il10*, *tgfb1a*) between 1 and 12 dpi (I, Fig. 4A-I). In WT zebrafish, the early innate response at 1 and 6 dpi was characterized by an increase in the expression levels of *tnfa*, *lta*, *ifng1-1* and *il17a/f3* (I, Fig. 4A). Furthermore, while the expression levels of *tnfa*, *lta*, *ifng1-1* and *il17a/f3* had already decreased at 12 dpi, the expression of anti-inflammatory cytokine genes (*il10* and *tgfb1a*) were at their highest at 12 dpi. Interestingly, a comparison of the cytokine gene expression levels between *furinA*$^{td204e/+}$ mutants and WT controls revealed that the decrease in *furinA* expression was associated with the up-regulation of the proinflammatory cytokine genes *tnfa*, *lta* and *il17a/f3* at 1 dpi (I, Fig. 4B-I).

While a high-dose *M. marinum* infection leads to an acute, progressive disease with high mortality, a low-dose mycobacterial inoculate results in a different immune response and can lead to latency (Parikka et al. 2012). In order to see how the reduction in *furinA* mRNA levels affects the host response against a low-dose infection, we injected a low *M. marinum* dose (46 CFU, SD 8 CFU) into the abdominal cavity of *furinA*$^{td204e/+}$ zebrafish and their WT siblings and followed their survival for 9 weeks (I, Fig. 6A). Similarly to the high-dose infection (See I, Fig. 3A), we did not see a significant difference in the survival of the infected *furinA*$^{td204e/+}$ and WT zebrafish with end-point mortalities of ~75% and ~80%, respectively. Since the host immunity against an infectious agent is dependent on both tolerance as well

as host resistance, we next quantified the mycobacterial burden at 4 and 9 wpi (34 CFU, SD 10 CFU) (I, Fig. 6B). Interestingly, a *M. marinum* qPCR revealed a significantly reduced mycobacterial burden in *furinA*$^{td204e/+}$ mutants compared to the WT fish at 9 wpi, whereas the expression of Th subtype specific markers (*tbx21 gata3*, *foxp3a*, *rorca*) was unaltered at 4 and 9 wpi (I, Fig. 6C).

Collectively, our results imply that *furinA* regulates the development of zebrafish granulocytes in steady state, and that FURIN has an evolutionarily conserved function in regulating the differentiation of T cell subtypes. Moreover, in the context of a mycobacterial infection, *furinA* down-regulation can result in the enhanced expression of proinflammatory cytokine genes, which is associated with a lower mycobacterial burden in a chronic infection.

5.2 CRISPR/Cas9 mutagenesis can be used to efficiently mutate target loci in the zebrafish embryos (II)

Ever since the off-target effects of morpholins were reported (Kok et al. 2015; Robu et al. 2007), concerns about the use of morpholino-mediated gene silencing in zebrafish embryos have risen. Silencing *carbonic anhydrase 10 a* (*ca10a*) and *ca10b* in zebrafish embryos using morpholinos results in a dose-dependent mortality of the morphants characterized by severe phenotypic defects, including a curved body, small head and extensive neural apoptosis (II, Fig. 7A-C). In order to validate the phenotypic consequences seen in the *ca10a* and *ca10b* morphants, we established an in-house CRISPR/Cas9 mutagenesis system using *egfp* producing transgenic tg(*fli1a:egfp*) fish and subsequently knocked out both *ca10a* and *ca10b* in zebrafish embryos.

5.2.1 Inactivation of *egfp* in the transgenic tg(*fli1a:egfp*) zebrafish

Previously, Hruscha & Schmid (2015) reported a simple CRISPR/Cas9 mutagenesis method utilizing *in vitro* transcribed gRNA and *Cas9* mRNA and the subsequent one-cell-stage embryo microinjection of the synthetized RNAs (Hruscha & Schmid 2015). Using this report as a method template, we tested if we could silence the *enhanced green fluorescent protein* gene (*egfp*) in our transgenic tg(*fli1a:egfp*) zebrafish line (ZFIN ID: ZDB-ALT-011017-8) (Lawson & Weinstein 2002). Since the tg(*fli1a:egfp*) zebrafish express *egfp* under a blood vessel marker *fli1* promoter site (Lawson &

Weinstein 2002), the fluorescence intensity in the vasculature of the embryos can be used to directly visualize the success of mutagenesis. As a proof of concept, injection of a previously described *egfp* gRNA (Jao, Wente & Chen 2013) and *Cas9* mRNA into the zebrafish embryos, could reduce the Egfp fluorescence compared to the uninjected and gRNA injected controls at 2 dpf (II, Suppl. Fig. 2A).

As described previously, targeted mutagenesis in the CRISPR/Cas9-system is based on the endogenous NHEJ pathway that repairs the experimentally induced cuts at the target loci and creates random indel mutations at this site (Ran et al. 2013). In order to quantify the mutagenesis efficiency at the *egfp* target site, we used the T7EI assay (Krebs 2014). In the *egfp* gRNA and *Cas9* mRNA injected tg(*fli1a:egfp*) embryos, the expected PCR cleavage products of ~150bp and ~320bp were observed after the T7EI treatment, whereas only a single 470bp WT PCR product was detected in the control embryos (II, Suppl. Fig. 2B). Furthermore, an average of a 50% cleavage rate of the WT *egfp* PCR was observed with the comparison of the band intensities using the Image Lab™ Software (Bio-Rad). Taken together, our in-house CRISPR/Cas9 mutagenesis method can efficiently create mutations at the gRNA specified target loci in the zebrafish embryos.

5.2.2 *ca10a* and *ca10b* mutagenesis in zebrafish embryos leads to high mortality and developmental defects

The zebrafish CRISPR/Cas9 system can be used to create null-like phenotypes already in the parental F0-generation embryos (Figure 7) (Jao, Wente & Chen 2013). To this end, we initially designed and produced three gRNAs for *ca10a* as well as two for *ca10b* (II, Fig. 7B-C), and tested their *in vivo* functionality. Of these gRNAs, we found gRNAs for both *ca10a* and *ca10b* with as high as 86% and 97% PCR product cleavage rates corresponding to a 63% and 83% mutagenesis efficiency, respectively (II, Fig. 7F) (Ran et al. 2013). In line with the morpholino knockdown results of zebrafish *ca10a*, the mutagenesis of *ca10a* resulted in a high mortality of the embryos already at 1 dpf. Moreover, comparable phenotypes including a curved body and pericardial effusion were seen in both the *ca10a* morphants and the F0-generation *ca10a* mutant embryos (II, Fig. 8A-H). In addition, similarly to the *ca10b* morphants, all of the *ca10b* mutants died after the first few days of development with severe phenotypic defects (II, Fig. 8A-H). In comparison, gRNA injected control embryos did not show signs of developmental defects up to 5 dpf, indicating that the injected RNA amounts were not toxic for the developing embryos.

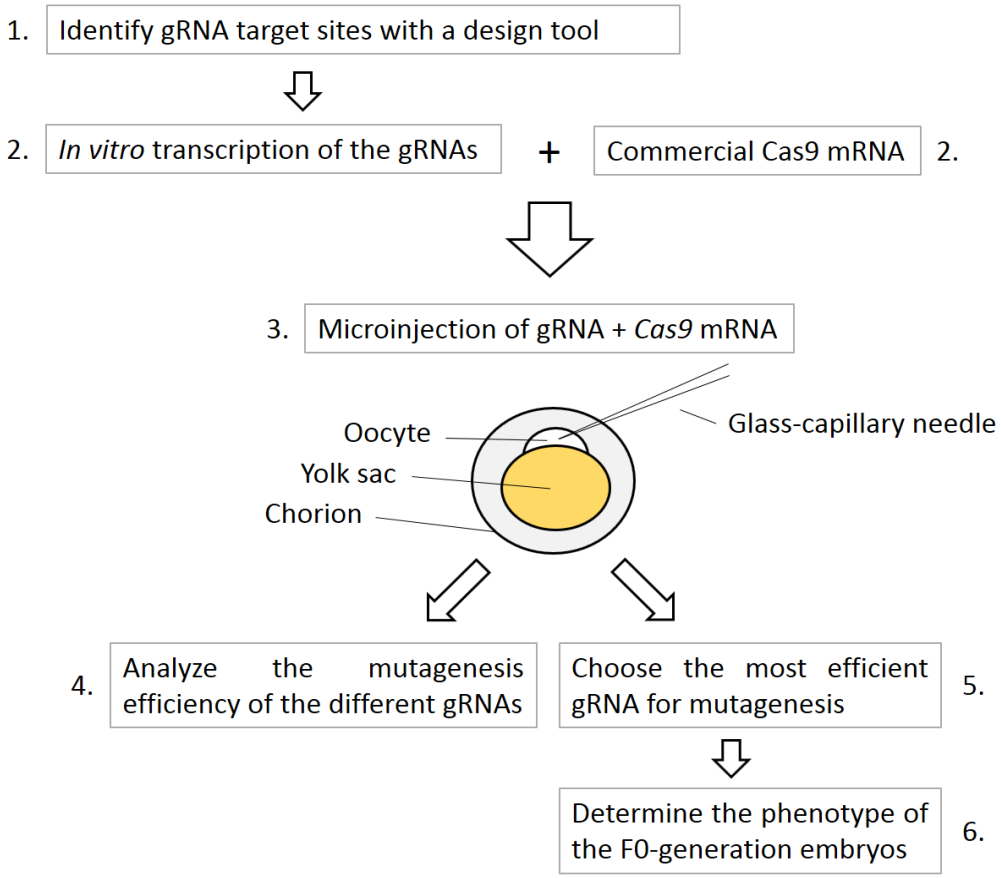

Figure 7. CRISPR/Cas9 mutagenesis in phenocopying null mutations in F0-generation zebrafish embryos. Possible target sites for mutagenesis are identified with a gRNA design tool. gRNAs are *in vitro* transcribed using a DNA template and microinjected into the oocyte with the *Cas9* mRNA. Mutagenesis efficiency is analyzed for all of the tested gRNAs (e.g. with T7EI assay) and the most efficient gRNA is chosen for the determination of the mutant phenotype in the embryos.

Altogether, our in-house CRISPR/Cas9 mutagenesis in zebrafish was proven efficient in modifying the target loci of both transgenic *egfp* as well as the endogenous *ca10a* and *ca10b* genes. Furthermore, similarly to Jao et al. (2013) this method could be used for creating null-like phenotypes in F0-generation mosaic embryos.

5.3 Intelectin 3 is not required for a protective immune response against mycobacteria in the zebrafish (III)

In order to screen for novel candidate genes important for mycobacterial immunity, we used the zebrafish *M. marinum* model together with a gene expression microarray analysis, and identified a lectin gene member *itln3* as one of the most highly up-regulated genes in a mycobacterial infection. To understand the function of ITLNs in the host defense against mycobacteria, we studied the *in vivo* significance of *itln3* in the zebrafish *M. marinum* infection model by creating two homozygous *itln3* mutant zebrafish lines using CRISPR/Cas9 mutagenesis, and tested the bacterial binding ability of recombinant Itln3.

5.3.1 Genome-wide expression analysis of genes induced by *M. marinum* in zebrafish

A limited number of genome-wide gene expression studies have been conducted in the zebrafish *M. marinum* TB model (Benard et al. 2016b; Hegedus et al. 2009; Kenyon et al. 2017; Meijer et al. 2005; Rougeot et al. 2014; van der Sar et al. 2009; van der Vaart, Spaink & Meijer 2012). To identify novel candidate genes in the mycobacterial host response, we infected adult zebrafish with a low-dose of *M. marinum* (20 CFU, SD 6 CFU) and studied their gene expression status using a microarray platform. While a large number of the induced genes such as *parvalbumin 1* (*pvalb1), tropomyosin* (*tpma*) and *troponin I, skeletal, fast 2b, tandem duplicate 2* (*tnni2b.2*) were related to muscle specific functions, also immunological genes e.g. *arachidonate 5-lipoxygenase b, tandem duplicate 3* (*alox5b.3*) and *CD59 molecule* (*cd59*) were up-regulated (log2 fold change $> |3|$) compared to the PBS injected controls (III, Fig. 1A). In contrast, some immunological genes, including *CD58 molecule* (*cd58*), *myeloid-specific peroxidase* (*mpx*) and *complement factor b-like* (*cfbl*), were down-regulated (III, Fig. 1A).

Previous studies in zebrafish (Lin et al. 2009), channel catfish (Peatman et al. 2007; Takano et al. 2008) and in Wuchang bream (Ding et al. 2017) have shown *itln* up-regulation upon a bacterial infection. In line with this, zebrafish *itln3* was induced (3.3-fold, log2 change) in our microarray data following a *M. marinum* infection (III, Fig. 1A). Conversely, the *itln2* and *itln2-like* genes were down-regulated (-3.5 and -3.2 -fold, respectively, log2 change) compared to the PBS-injected controls. Additional gene expression analyses of *itln1*, *itln2*, *itln2-like* and *itln3* in *M. marinum* infected (39 CFU; SD 47 CFU) adult zebrafish by qPCR confirmed the up-regulation of *itln3*

and the reduced *itln2* expression upon infection (III, Fig.1B-E). Interestingly, the expression of all of the studied four *itln* genes (*itln1*, *itln2*, *itln2-like*, *itln3*) in zebrafish embryos were significantly induced in a mycobacterial infection (III, Fig. 1F-I). While the expression of *itln1* and *itln3* was higher in the infected embryos already at 2 dpi, *itln2-like* and *itln2* were up-regulated later upon infection at 4 dpi and 7 dpi, respectively.

5.3.2 *itln3* mutant zebrafish in studying the host resistance against mycobacteria

Knowledge about the *in vivo* immune function of ITLNs in infectious diseases is scarce. While Pemberton et al. (2004) used the C57BL/10 mouse strain, in which the *Itln2* gene is naturally missing, and infected the mice with *Trichinella spiralis*, Voehringer et al. (2007) studied Itln1 and Itln2 over-expression in the mouse lungs against *Nippostrongylus brasiliensis* and *M. tuberculosis*. In these studies, the lack of Itln2 was associated with a higher susceptibility against *T. spiralis*, whereas no differences were seen in the resistance against *N. brasiliensis* or mycobacteria in the Itln transgenic mice. However, since Pemberton et al. (2004) did not perform further functional studies on the immunoprotective role of Itln2, they could only speculate that the increased susceptibility against the parasite was related to the dysfunctional innate immune response caused by the lack of Itln2.

In order to better understand the function of the infection-inducible zebrafish *itln3*, we used CRISPR/Cas9 mutagenesis to create *itln3* null mutant zebrafish. To this end, we tested three different gRNAs together with the *Cas9* mRNA and found one gRNA with an approximately 40% mutagenesis efficiency in the gRNA/*Cas9* mRNA injected F0-generation embryos (III, Fig. 3A-B). The target site for this gRNA was situated in the second exon of the *itln3* gene, leading to mutations early in the encoded regions of *itln3*. Following outcrosses of the adult F0-generation mutants with WT zebrafish, we identified two prominent out-of-frame and germ-line transmitted *itln3* mutations in the F1-generation fish (III, Fig. 3C), and annotated the mutation carrying zebrafish lines as *itln3*^{uta145} and *itln3*^{uta148}. In order to obtain F2-generation zebrafish for our experiments, we incrossed heterozygous F1-fish from both of the lines (*itln3*$^{uta145/+}$ and *itln3*$^{uta148/+}$) and used either the embryos or adult fish obtained from the spawnings.

5.3.2.1 Both *itln3* and *itln1* are dispensable for mycobacterial immunity in zebrafish embryos

Since both our observations of *itln3* up-regulation in a mycobacterial infection and the previous reports about the bacterial binding capability of ITLNs (Chen et al. 2016; Ding et al. 2017; Nagata 2018; Tsuji et al. 2009; Wesener et al. 2015) suggest a role for Itln3 in zebrafish immunity, we first tested if *itln3* mutant embryos are more susceptible than WT embryos to a *M. marinum* infection. In order to exclude possible variation in the immune response caused by the site of the mycobacterial microinjection (Meijer 2016), we infected *M. marinum* both into the yolk sac (40 CFU; SD 30 CFU) as well as into the blood circulation valley (46 CFU; SD 31 CFU) of zebrafish embryos at 0 dpf and 2 dpf, respectively. A survival analysis of the yolk sac injected *itln3*^{uta145} and *itln3*^{uta148} background embryos revealed average mortalities of 47 % and 48 %, respectively, but it did not reveal any statistically significant differences in the mortality of *itln3*$^{uta145/uta145}$ and *itln3*$^{uta148/uta148}$ mutants and their sibling controls prior to 7 dpi (III, Fig. 4A-B). In addition, the *M. marinum* burdens between the genotypes were comparable with the following bacterial copy number medians (log10) in 100ng of zebrafish DNA; 4.18 (WT *itln3*^{uta145}), 4.15 (WT *itln3*^{uta148}), 4.02 (*itln3*$^{uta145/+}$), 4.22 (*itln3*$^{uta148/+}$), 3.53 (*itln3*$^{uta145/uta145}$) and 4.25 (*itln3*$^{uta148/uta148}$) (III, Fig. 4C). In line with the injection site dependable infection outcome, the blood circulation valley *M. marinum* inoculate did not cause any mortality of the embryos before 5 dpi, although our qPCR analysis confirmed the presence of bacteria in these fish with bacterial burdens ranging from 3.61 to 3.83 (copy number medians (log10) in 100ng of zebrafish DNA) (III, Fig. 4D). However, no significant differences in the *M. marinum* burden were seen between the genotypes, suggesting that the injection site does not affect the *itln3* –dependent immune response against mycobacteria.

Genetic compensation is an evolutionarily important process that can restore an organism´s functionality in the case of a loss-of-function mutation (Tautz 1992). This can occur through additional mutations to the genome or by the increased expression of other complementing genes. As already mentioned, our gene expression analyses of *M. marinum* infected zebrafish embryos and PBS injected controls revealed induction of all of the studied *itln* gene family members (*itln1*, *itln2*, *itln2-like*, *itln3*) upon infection (III, Fig. 1F-I). However, only *itln1* and *itln3* had similar induction kinetics, suggesting a possible functional redundancy of these genes in the innate immune response. To see if *itln1* could compensate for the loss of *itln3*, we silenced *itln1* with a splice blocking (SB) morpholino in our mutant zebrafish lines *itln3*^{uta145} and *itln3*^{uta148} and simultaneously infected them with *M. marinum*

(20 CFU; SD 19 CFU). In our initial experiments, we could observe that the morpholino causes the exclusion of exon 2 from the final transcript, and we could measure the loss of WT *itln1* mRNA by qPCR. In fact, 82.9%, 78.2% and 66.1% reductions in the relative *itln1* mRNA amounts were observed in the SB morphants at 4 dpi, 5 dpi and 6 dpi, respectively (III, Fig. 5B). In the morpholino and *M. marinum* co-injections, we observed high genotype-independent mortality with both the RC and SB morpholinos ranging between 77.8% and 100% at 7 dpi (III, Fig. 5C-E). Nevertheless, we did not see any statistically significant differences between the *M. marinum* infected RC and SB morpholino injected groups (III, Fig. 5C) nor between the WT or *itln3* mutant zebrafish (III, Fig. 5D-E), suggesting that neither *itln1* nor *itln3* are required for the mycobacterial immune response in the embryos.

5.3.2.2 Survival and mycobacterial burden of adult *itln3*^{uta145} and *itln3*^{uta148} mutant zebrafish are similar to their WT siblings

A previous report in zebrafish showed that a low-dose *M. marinum* infection recapitulates a latent disease with well-defined granuloma structures and a constant bacterial burden (Parikka et al. 2012). Consequently, we infected adult *itln3*^{uta145} and *itln3*^{uta148} zebrafish with a similar dose of *M. marinum* (48 CFU; SD 5 CFU) and followed their survival for 24 weeks (III, Fig. 6A-B). At the end of this experiment, the following survival percentages were observed; 74% (WT *itln3*^{uta145}), 73% (*itln3*$^{uta145/+}$), 59% (*itln3*$^{uta145/uta145}$), 78% (WT *itln3*^{uta145}), 82% (*itln3*$^{uta148/+}$) and 84% (*itln3*$^{uta148/uta148}$). However, although a slight difference in the average end-point mortalities was observed between the *itln3*^{uta145} and *itln3*^{uta148} fish lines (30% and 20%, respectively), no statistically significant differences were detected between the different genotypes. In line with this, the mycobacterial burdens in *M. marinum* infected (422 CFU; SD 221 CFU) adult zebrafish were comparable between the WT fish and *itln3* mutants at 2 and 4 wpi (III, Fig. 6C-D).

Previously Myllymäki et al. (2018), introduced a dexamethasone mediated immunosuppression model in zebrafish in studying the reactivation of a mycobacterial infection. In this model, dexamethasone-containing feed could decrease the total lymphocyte amounts by 36% but it could also reduce the expression of the Th1 cell marker *tbx21* upon infection. For report III, we modified this model slightly by starting an immunosuppressive treatment one week prior to the infections, continued to the infections with *M. marinum* (47 CFU; SD 4 CFU) and followed the fish for another four weeks with daily dexamethasone administration (III, Fig. 7A). At 2 and 4 wpi, some of the fish were withdrawn from

the experiment and their blood cell composition and *M. marinum* burden were analyzed. In line with the study of Myllymäki et al. (2018), we observed a dexamethasone-mediated decrease in the lymphocyte populations of our *itln3*^{uta145} and *itln3*^{uta148} zebrafish lines (reduction between 23.7% and 40.5%, $P<0.01$ in all comparisons) (III, Fig. 7B-D), whereas the myeloid cell population was unaffected (III, Suppl. Fig. 6). In addition, homozygous *itln3* mutants (*itln3*$^{uta145/uta145}$ and *itln3*$^{uta148/uta148}$) and WT controls did not show any statistically significant differences in their cell amounts, suggesting that the decrease is independent of the *itln3* mutation. Nonetheless, no differences were seen in the *M. marinum* burden of *itln3*$^{uta145/uta145}$ fish and WT (*itln3*^{uta145}) controls or *itln3*$^{uta148/uta148}$ and WT (*itln3*^{uta148}) fish at 2 and 4 wpi (III, Fig. 7E-F). Here, the mycobacterial copy number medians of 2.60 and 2.65 in WT *itln3*^{uta145}, 2.55 and 3.10 in *itln3*$^{uta145/145}$, 2.87 and 2.43 in WT *itln3*^{uta148} and 2.25 and 2.91 in *itln3*$^{uta148/148}$ zebrafish were observed at 2 and 4 wpi, respectively (log10, in 100ng of zebrafish DNA).

Overall, our results demonstrated that *itln3* expression is highly up-regulated in a *M. marinum* infection in both adult zebrafish and zebrafish embryos. However, the lack of differences in our survival assays between *itln3* knockout fish and their WT siblings led us to conclude that *itln3* is dispensable for the zebrafish immune response against mycobacteria in our model. This conclusion was also supported by our mycobacterial binding experiment using recombinant Itln3 (III, Suppl. Fig. 7), in which we did not detect binding of Itln3 to the surface of *M. marinum*.

6 DISCUSSION

6.1 *Furin*, an important regulator of T cell function, as a candidate gene in TB immunity (I)

The activation of naïve T cells is largely dependent on the antigenic stimulation mediated by interactions between the T cell receptor (TCR) and the antigen-MHC complexes on antigen presenting cells (APCs) (Luckheeram et al. 2012). Eventually, the final differentiation into distinct CD4+ T helper cell subtypes (e.g. Th1, Th2, Th17 and Treg) is dependent on the additional interaction of a CD4 co-receptor with the MHC receptor (specifically MHC type II receptor) and on the present cytokine environment (Luckheeram et al. 2012). In fact, the central cytokines required for the differentiation of these subtypes are well known, and the cytokines produced by the differentiated Th cells can create positive feedback loops amplifying further polarization into the corresponding Th cell subtype and to suppress that of the other subtypes (Luckheeram et al. 2012). For example, the IL12-mediated production of IFNG can polarize naïve T cells into Th1 type cells by signaling via STAT4 and by inducing the expression of the *T-box transcription factor* (*T-bet*). T-bet can in turn induce the additional production of IFNG and thereby amplify its own expression via STAT1 and the additional differentiation of Th1 cells (Djuretic et al. 2007). Conversely, T-bet can inhibit the function of the GATA3 transcription factor and the consequent expression of IL4, a key cytokine in Th2 cell polarization (Djuretic et al. 2007). Interestingly, a conditional knockout of *Furin* (CD4cre-fur$^{f/f}$) in mouse T cells, leads to altered effector T cell populations as well as to abnormal production of Th subtype specific cytokines such as IFNG and IL4 (Pesu et al. 2008). In fact, it has also been demonstrated that *Furin* expression enhances secretion of IFNG, and that FURIN consequently controls the differentiation of Th1 cells (Pesu et al. 2006). Overall, FURIN is directly linked to the immunological function of T cells.

Since its discovery in the mid 1980´s (Roebroek et al. 1986), FURIN has been associated with a number of diseases (Thomas 2002; Turpeinen, Ortutay & Pesu 2013). While defective FURIN mediated pro-protein processing can lead to diseases such as X-linked hydrohidrotic ectodermal dysplasia and Alzheimer´s disease (Thomas 2002), *FURIN* overexpression has been associated with different types of

cancers (Thomas 2002), autoimmune diseases (Ranta et al. 2018; Valli et al. 2018) as well as atherosclerosis (Turpeinen et al. 2011). In addition, single nucleotide polymorphisms in the *FURIN* gene and its promoter site have been associated with the regulation of blood pressure and hypertension (Ganesh et al. 2013; Li et al. 2010; Turpeinen et al. 2015) as well as with HBV infections (Lei et al. 2009). Nevertheless, *FURIN* polymorphisms have not been linked to a susceptibility for bacterial infections. Moreover, complicating experimental research, a *Furin* knockout in mouse germline cells, leads to embryonic lethality between 10 and 12 days into development (Roebroek et al. 1998).

Zebrafish have two *FURIN* paralogs; *furinA* and *furinB* (Walker et al. 2006) with approximately 70% sequence similarity. However, of these PCSKs only FurinA is able to cleave zebrafish pro-Tgfb1a *in vitro* and to promote the translocation of mature Tgfb1a out of the cells into the cell culture supernatant (Turpeinen et al. 2013), which suggests that *furinA* is the true zebrafish ortholog of human *FURIN*. Consequently in report I, we used a commercially available *furinA*^{td204e} mutant zebrafish line (ZDB-FISH-150901-26631) to study the systemic role of FURIN in mycobacterial immunity *in vivo*. Previously, Walker et al. (2006) demonstrated the substantial lethality (more than 98%) of zebrafish lines carrying different homozygous non-sense *furinA* mutations. Corresponding with this observation as well as with the embryonic lethality of *Furin* null mice (Roebroek et al. 1998), we could not obtain adult homozygous *furinA* mutant (*furinA*$^{td204e/td204e}$) zebrafish. Nonetheless, since the heterozygous *furinA*$^{td204e/+}$ mutants were phenotypically normal and fertile and showed a measurable decrease in *furinA* expression, they could be used in our experiments.

The total numbers of splenocytes is reduced in myeloid cell specific *Furin* knockout mice (LysMCre-fur$^{f/f}$) compared to the corresponding WT controls, suggesting that FURIN affects the development of immune cells *in vivo* (Cordova et al. 2016). In line with this observation as well as with the normal thymocyte counts in CD4cre-fur$^{f/f}$ mice described by Pesu et al. (2008), the granulocyte amount was significantly lower in steady state *furinA*$^{td204e/+}$zebrafish, whereas the cell numbers in the lymphocyte gate were comparable between *furinA*$^{td204e/+}$ mutants and the WT controls. In order to provide a mechanistic explanation for the FurinA-mediated regulation of granulopoiesis, extensive proteomic analyses followed by functional studies would be required. Additionally, it can be speculated whether a more pronounced effect on granulopoiesis would have been seen with a complete *furinA* knock-out model.

CD4+ T cells, and more specifically the Th1 type immune response, are indispensable in a *M. tuberculosis* infection (Cooper et al. 1993; Cooper et al. 1997; Flynn et al. 1993; Flynn et al. 1995; Onwubalili, Scott & Robinson 1985; Zhang et al. 1994). To determine if also zebrafish *furinA* could regulate Th cell differentiation similarly to its mammalian counterparts, we analyzed the expression of different Th cell transcription factors in both *furinA*$^{td204e/+}$ fish and WT controls, and found increased levels of *tbx21*, *gata3* as well as *foxp3a* mRNAs in the *furinA*$^{td204e/+}$ mutants. Although the up-regulation of these transcription factors is likely to reflect the *furinA* mediated changes in the differentiation of Th cells in zebrafish, the quantification of the exact Th subtype cell amounts by e.g. a FACS analysis or semi-quantitative western blot would be required to confirm this. However, because of the shortage of commercial antibodies raised specifically against zebrafish proteins, the use of cross-reactive antibodies raised against other species, as in the study of Hammaren et al. (2014), would be required to study Th cell polarization in detail. Collectively, the mycobacteria dependent regulation of *FURIN* expression, association of *FURIN* polymorphisms and expression levels with a number of diseases as well as the direct effects of FURIN on the function of myeloid cells and T cells, make this PCSK family member an interesting candidate gene for studying the host response against a mycobacterial infection.

6.2 *furinA* regulates the zebrafish host response against mycobacteria (I)

The zebrafish *M. marinum* model can mimic several aspects of the pathogenesis of *M. tuberculosis*, such as the replication of bacteria in macrophages and the formation of granulomas, in a safe and cost-efficient manner. However, since the adult zebrafish *M. marinum* infection was introduced as a model for TB by Prouty et al. (2003), only a few articles have depicted the kinetics of the host cytokine response in adult zebrafish. Although genome-wide transcriptomic approaches have collectively studied several different timepoints post infection (Hegedus et al. 2009; Meijer et al. 2005; van der Sar et al. 2009; van der Vaart, Spaink & Meijer 2012), different mycobacterial strains used in these studies make the interpretation of the response kinetics from these studies demanding. In addition, while some qPCR-based expression data for genes such as *tnfa*, *il1b, il6*, *il12*, *nos2b* and *ifng1-2* in a *M. marinum* infection had been published prior to the publication of report I (Parikka et al. 2012), the information about the early cytokine response in this model was

incomplete. In order to fill this knowledge gap, we chose three different timepoints of 1, 6 and 12 dpi and a panel of eight common cytokine genes (*tnfa, il1b, lta, ifng1-1, il22, il17a/f3, il10* and *tgfb1a*) for our study. In line with observations from Parikka et al. (2012) and van der Vaart, Spaink & Meijer (2012), our *M. marinum* infection experiments could confirm the infection-inducible nature of genes such as *tnfa*, *il1b* and *il10*. Moreover, we were able to determine the timing for the resolution of their up-regulation. Most importantly, this data can benefit future research in the field of *M. marinum* infections in adult zebrafish by providing cytokine expression parameters for studying the innate response.

Previously, the lack of T cell expressed Furin in CD4cre-fur$^{f/f}$ mice was associated with an increase in the concentration of proinflammatory cytokine IL6 in the serum (Pesu et al. 2008), whereas the exogenous administration of Furin into mice with collagen-induced arthritis was shown to be able to reduce inflammation in mouse joints (Lin et al. 2012). To study the role of *furinA* in the early cytokine response and in inflammation upon infection, we used the previously described set of genes and time points and infected *furinA*$^{td204e/+}$ mutant zebrafish with *M. marinum*. Supporting the previously published data that indicated excess inflammation in CD4cre-fur$^{f/f}$ mice, the expression of the proinflammatory cytokines *tnfa*, *lta* and *il17a/f3* was increased in *furinA*$^{td204e/+}$ mutants in a mycobacterial infection. In addition, since this difference could only be seen at 1 dpi, it suggests a T cell independent role for *furinA* in regulating inflammation and the immune response against an infection. In fact, an immunogenic challenge in LysMcre-fur$^{f/f}$ mice, which have deficient Furin production in their myeloid cells, resulted in an increase in the levels of circulating proinflammatory cytokines such as Tnfa, suggesting that *furinA* deficient macrophages play a role in mediating the proinflammatory phenotype in zebrafish (Cordova et al. 2016). An outcross of *furinA*$^{td204e/+}$ mutants with transgenic Tg(*tnfa:eGFP-F*) zebrafish expressing eGFP under the *tnfa* promoter (Nguyen-Chi et al. 2015), could provide additional insights into the proinflammatory phenotype caused by FURIN deficiency both in steady state conditions and during an infection. Furthermore, it would be of great interest to determine, whether this phenotype is a consequence of the deficient FurinA-mediated cleavage of Tgfb1a and the resulting lack of peripheral immune tolerance (Pesu et al. 2008), or a result of abnormal proteolytic processing of other FURIN substrates.

The wide range of PCSK substrates functioning in different physiological processes offers a great deal of possibilities for developing PCSK-based drugs against different diseases (Artenstein & Opal 2011; Seidah & Prat 2012).

Consequently, while the exogenous administration of FURIN can reduce arthritis (Lin et al. 2012), FURIN inhibitors are considered potential drugs against infectious diseases. In fact, the inhibition of FURIN activity has been shown to prevent the activation of HIV (Hallenberger et al. 1992) and influenza viruses as well as bacterial toxins (Becker et al. 2012). Furthermore, FURIN inhibitors have been suggested as possible drug candidates also in cancer and atherosclerosis (Artenstein & Opal 2011; Seidah & Prat 2012; Turpeinen et al. 2011). Accordingly, our findings, which showed that *furinA* deficiency in *furinA*$^{td204e/+}$ mutant zebrafish can lead to a reduced mycobacterial burden in an infection, imply the possibility of using FURIN inhibitors also as anti-TB drugs by boosting the anti-mycobacterial host responses. However, the systemic administration of FURIN inhibitors could lead to severe side effects considering the role of FURIN in controlling inflammation (Cordova et al. 2016) and in maintaining peripheral tolerance (Pesu et al. 2008). Whether the inhibition of FURIN activity specifically in the lungs by, for example, the inhalation of small molecule inhibitors would prove safe and efficient in treating pulmonary TB remains to be studied. For this purpose, a conditional lung-specific Furin knockout mouse, together with the mouse TB models, could be useful.

As described previously, the most common diagnostic tests for latent TB, the TST and IGRA, can lead to false negative as well as false positive results. In fact, since both of these tests rely on the memory T cell response, genes or proteins chronically up-regulated in the presence of bacteria can provide additional diagnostic measures to diagnose the latent disease and to prevent false positive diagnoses. In report I, we found that the zebrafish *furinA* was up-regulated in a chronic mycobacterial infection at 4 and 9 wpi, making FURIN a possible biomarker candidate for latent TB. Although a comparable infection dose was shown to lead to a latent *M. marinum* infection (Parikka et al. 2012), further studies, such as the quantification of mycobacterial dormancy markers and the verification of the static bacterial burdens would be required to confirm latency-related *furinA* up-regulation.

6.3 CRISPR/Cas9 mutagenesis in studying gene-function relationships (II, III)

Commercial mutant lines have been invaluable in studying gene-function relationships in the zebrafish. Accordingly, since the beginning of the zebrafish mutation project, several zebrafish carrying knockout alleles have been identified, and subsequently made available at the zebrafish stock centers (EZRC and ZIRC).

Nevertheless, mutant lines are not yet commercially available for all protein coding zebrafish genes, and the off-target effects of ENU mutagenesis can potentially confound scientific findings. Relatively recent genome modification tools such as the ZFNs and TALENs, and most importantly the CRISPR/Cas9 system provide the means for the in-house production of mutant zebrafish by targeted mutagenesis (Hruscha et al. 2013; Jao, Wente & Chen 2013). As already described, targeting in the CRISPR/Cas9 method is mediated through the sequence specific binding of gRNA molecules and a so called PAM sequence (NGG) immediately downstream of the target site (Jinek et al. 2012; Ran et al. 2013). Since PAM sites are found frequently in DNA, it can be speculated that any gene of interest could be mutated by CRISPR/Cas9 mutagenesis. The dense array of PAM sequences also makes it possible to target the beginning of gene sequences, which in turn can lead to the early disruption of the reading frame upon translation and/or to the nonsense-mediated decay of transcribed mutant mRNAs (Nickless, Bailis & You 2017).

Although the *in vivo* efficiency of the CRISPR/Cas9 system can be affected by the chromatin accessibility or the nucleotide composition of the gRNA target site (Uusi-Mäkelä et al. 2018), several reports have published evidence for the relatively simple and highly efficient use of the CRISPR/Cas9-mediated mutagenesis in the zebrafish (e.g. Hruscha et al. 2013; Jao, Wente & Chen 2013). However, while even a low mutagenesis efficiency can result in the transmission of mutations to the germ-line cells of F0-generation fish (Hwang et al. 2013; Varshney et al. 2015), a substantially higher efficiency is required to study phenotypic effects already in the parental (F0-generation) mosaic fish (Jao, Wente & Chen 2013). Accordingly, approximately 20% rates for somatic mutation have been reported to function in creating mutant zebrafish lines (Hwang et al. 2013; Varshney et al. 2015), whereas Jao et al. (2013) concluded that with 75-99% mutagenesis rates most of the cells in the F0-embryos carried bi-allelic mutations. In this study, we were able to mutate both *ca10a* and *ca10b* with an average mutagenesis efficiency of 73% (II). In addition, suggesting that the functionality of these genes was lost already in the mosaic F0-embryos, CRISPR/Cas9 mutagenesis could phenocopy the severe developmental effects of the morpholino silencing. Conversely, in order to create *itln3* mutant zebrafish lines, an *itln3* mutagenesis efficiency of 40% was observed in the F0-generation embryos (III). Although the efficiency was substantially lower compared to the *ca10* mutagenesis, a significant proportion of the germ-line cells had a mutation in *itln3*. In fact, approximately 40% of the F1-generation fish (39/96) carried a mutant form of the *itln3* gene, and a total of three different indel-mutations were detected (Unpublished data) (Figure 8). Moreover, from a total of eight gRNAs

tested in reports II and III, a maximum of three were required to mutate the gene of interest in the F0-generation embryos. Overall, in line with previous literature, our experience with the CRISPR/Cas9 system in zebrafish supports the high mutagenesis rate as well as ease of mutagenesis.

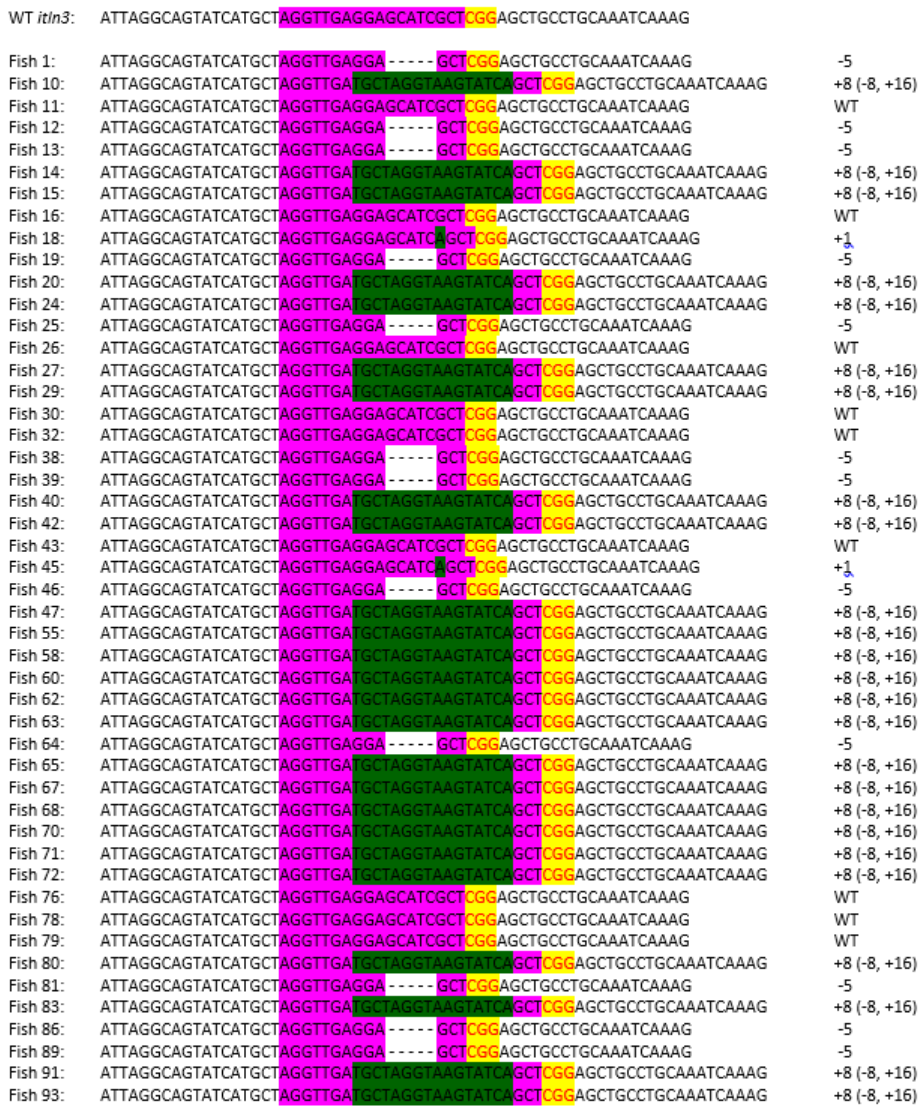

Figure 8. Alignment of the *itln3* mutation site sequence from F1-generation CRISPR/Cas9 mutants. After an outcross of F0-mutants with WT fish, the *itln3* target site loci was amplified by PCR, screened for mutations from 96 fish and sequenced from a total of 48 F1-mutant zebrafish. From these individuals, 39 zebrafish carried a mutant *itln3* allele with either an insertion or a deletion.

As with other mutagenesis or knockdown approaches, the off-target effects of CRISPR/Cas9 have raised concern regarding the use of the system for scientific research. While some of the early reports on using the CRIPSR/Cas9 method in human cells described a high frequency of off-target cleavage (Fu et al. 2013), it was later stated that the off-target cleavage properties of Cas9 are more limited compared to for example ZFNs and TALENs (Duan et al. 2014), and that he off-target activity can be abolished by the proper design of the gRNA target region (Cho et al. 2014). In fact, already at the gRNA design step, the design tools can recognize off-target binding sites and calculate the possibility for a given gRNA to mediate incorrect binding. Consequently, this information can be used in choosing a gRNA with a minimum off-target affinity but it can also later be used to assess whether off-target mutations have occurred after mutagenesis. In reports II and III, both the gRNA design tool from CRISPR.mit.edu as well as the sgRNA excel tool (Krebs 2014), were used to identify target-loci-specific gRNAs with minimal off-target site recognition. In addition, for further confirmation of the specificity of the gRNAs, a BLAST analysis was also utilized (Altschul et al. 1997). Since the comparable phenotypes of the *ca10a* and *ca10b* morphants and the CRISPR/Cas9 mutated embryos (II) as well as the unchanged resistance upon infection in two different *itln3* mutant zebrafish lines compared to the WT fish (III), off-target analyzes were not conducted in reports II or III.

6.4 Genome-wide gene expression analysis as a starting point for reverse genetics (III)

Since virulent *M. tuberculosis* strains are able to modify the host immune response upon infection to their own benefit, the immunity against TB is largely dependent on both the host as well as the bacterium. In order to better understand the complex host-pathogen interactions in mycobacterial infections, comprehensive analyses of this interplay are required. To this end, a large amount of studies have focused on studying blood samples from *M. tuberculosis* infected patients with genome-wide epigenetic, proteomic and transcriptomic approaches (Esterhuyse et al. 2015; Lee et al. 2016; Roe et al. 2016; Walzl et al. 2014; Zhang et al. 2014). In fact, based on these studies, several potential diagnostic biomarkers for TB have been identified for both the active and latent stages of the infection. Nevertheless, the blood samples derived form *M. tuberculosis* infected patients are inadequate for unraveling the mediators of the immediate systemic immune response upon infection or the spatio-temporal

expression of host response genes. For this purpose, proper animal models are required.

A few genome-wide transcriptomic studies have been so far published in the zebrafish *M. marinum* model (Benard et al. 2016b; Hegedus et al. 2009; Kenyon et al. 2017; Meijer et al. 2005; Rougeot et al. 2014; van der Sar et al. 2009; van der Vaart, Spaink & Meijer 2012). Moreover, since both zebrafish embryos as well as adult fish have been used in these studies, it has been possible to describe both the early and chronic stages of the infection in the context of the innate immunity (embryos) alone or with both innate and adaptive immune components (adult fish), respectively. However, since it is well-known that the virulence properties of different mycobacterial strains can also affect the immune response, we infected adult zebrafish with the *M. marinum* strain ATCC 927 that has been used previously in our experiments, and conducted a separate microarray gene expression analysis at 14 dpi (III). By using a low mycobacterial infection dose (20 CFU, SD 6 CFU), we found several muscle associated genes as well as immune function related transcripts such as *si:busm1-194e12.11* (*mhc2* family gene) and *CD59 molecule* (*cd59*) to be up-regulated compared to PBS controls. While the *si:busm1-194e12.11* induction could indicate the increased Mhc2-mediated antigen presentation from the APC´s and the initiation phase of the adaptive immune response, the increased *cd59* (membrane attack complex component gene) mRNA levels suggest the functionality of the complement system in the mycobacterial response. Overall, some of the differentially expressed immunological genes e.g. *myeloid specific peroxidase* (*mpx*) and *immunoresponsive gene 1, like* (*irg1l*) have previously also been described in the *M. marinum* infection of zebrafish (Benard et al. 2016a; Meijer et al. 2005; van der Sar et al. 2009; van der Vaart, Spaink & Meijer 2012). Importantly, we also detected one member of the *itln* gene family, *itln3*, whose expression was highly induced in an infection. In fact, although *itln* genes have been shown to be induced in parasite (Voehringer et al. 2007) and bacterial infections (Lin et al. 2009; Peatman et al. 2007; Takano et al. 2008; Ding et al. 2017), their infection-inducible expression has not previously been reported in a mycobacterial infection. Whether *itln* expression is of diagnostic relevance for TB, remains to be established. Overall, the previous transcriptomic studies as well as our microarray analysis demonstrate the feasibility of genome-wide gene expression studies in zebrafish in identifying novel candidate genes in the mycobacterial immune response.

6.5 *itln3* is not required for the zebrafish host response against *M. marinum* (III)

Taken together, the inducibility of *itln3* in a mycobacterial infection as well as previous *in vitro* findings about the bacterial binding ability of ITLNs, make *itln3* an interesting candidate gene for a role in the immunity against mycobacteria. Because there were no previous reports that would have addressed the role of *itln3* in the zebrafish immune response against mycobacteria, we used CRISPR/Cas9 mutagenesis to create two *itln3* knockout zebrafish lines and infected the fish with *M. marinum* in both the zebrafish embryos and the adult fish. All of our bacterial quantifications and survival analyses suggested that *itln3* is dispensable for mycobacterial resistance. Furthermore, our *in vitro* bacterial binding assays with recombinant zebrafish Itln3 proposed that Itln3 does not directly bind *M. marinum*. Although the dispensable role for Itln3 in the immunity can be directly explained by the lack of Itln3-mediated mycobacterial recognition in zebrafish, also other explanations can be hypothesized. In fact, perhaps the most striking difference between parasite and mycobacterial infections is the cellular localization of these pathogens. While e.g. *T. spiralis* is a large extracellular worm, *M. marinum* (like *M. tuberculosis*) is an intracellular bacterial species that exploits the host´s innate immune cells to replicate. In fact, the lack of *itln3* could hypothetically be beneficial to the host by restricting mycobacterial uptake by the myeloid cells. Conversely, to determine if Itln3 is important for the immunity against extracellular pathogens, we also infected *itln3*^{uta145} and *itln3*^{uta148} mutant embryos with two different *S. pneumoniae* serotypes and followed their survival up to 7 dpf (III, Suppl. Fig. 1B-E). Interestingly, comparably to the *M. marinum* infection, no differences were observed between the *itln3* mutant and the WT genotypes. The lack of observed survival differences with both intra- and extracellular bacteria also argues that zebrafish Itln3 may not act as an important receptor for other microbial recognition proteins such as lactoferrin either (Suzuki, Shin & Lönnerdal 2001).

Reactivation of latent TB is a significant contributor to the persistence of the TB epidemic (Rangaka et al. 2015). In humans, reactivation can occur because of environmental factors such as silica dust or as a result of immunosuppression e.g. in a HIV infection or upon immunosuppressive medication (Ai et al. 2016). Relatively recently, the zebrafish *M. marinum* infection model was engineered for studying the reactivation of a latent mycobacterial infection (Parikka et al. 2012; Myllymäki et al. 2018). While Parikka et al. (2012) used gamma irradiation for immunosuppression, Myllymäki et al. (2018) induced immunodeficiency through dexamethasone

administration. More specifically in Myllymäki et al. (2018), dexamethasone coated food was able to specifically decrease the zebrafish lymphocyte population, which consequently led to the reactivation of the latent infection. Although the initial purpose of the dexamethasone model was to reactivate an existing latent infection, we hypothesized that this model could also be re-purposed to highlight the importance of the innate mycobacterial immunity in our *itln3* mutation carrying zebrafish line. In fact, previously a somewhat similar approach for studying the innate immunity with homozygous *rag* mutant zebrafish has been suggested (Tokunaga et al. 2017). Consequently in report III, we used dexamethasone to reduce the lymphocyte pool prior to infecting homozygous *itn3* mutants (*itln3*$^{uta145/uta145}$ and *itln3*$^{uta148/uta148}$) as well as the corresponding WT zebrafish with *M. marinum*. Despite the similar bacterial burden in *itn3* mutant and WT zebrafish 2 and 4 wpi, future innate immunity studies in adult zebrafish are likely to benefit from the practicality of the described dexamethasone-mediated immunosuppression system. In addition, while some of the differentially expressed genes identified in our microarray analysis of *M. marinum* infected zebrafish can directly provide new candidate genes for upcoming research, it would also be of interest to study the broader role of the muscle tissue in a mycobacterial infection.

7 SUMMARY AND CONCLUSIONS

Tuberculosis (TB) is an infectious disease caused by the intracellular mycobacterial species *M. tuberculosis*. Although antibiotics against the drug-sensitive *M. tuberculosis* strains are available, the worldwide occurrence of the disease and the enormous amount of the latently infected *M. tuberculosis* carriers make the efforts to fight the disease difficult. Moreover, the increased fraction of antibiotic-resistant *M. tuberculosis* infections demands the development of new anti-tuberculous regimens. TB is a multifactorial disease with a strong genetic influence on its pathogenesis. In order to screen for novel genes affecting TB susceptibility and to understand their functional significance, genetically tractable animal models are required. Accordingly, the zebrafish *M. marinum* infection can be used as a safe TB model to provide new insights into the host-pathogen interactions in a mycobacterial infection.

The T helper (Th) type 1 immune response is of crucial importance in TB immunity. FURIN is an important regulator of T lymphocyte and macrophage function and it has been shown to control e.g. Th1 cell polarization. Our gene expression analysis of steady state heterozygous *furinA*$^{td204e/+}$ mutant zebrafish revealed an increase in the expression of Th-specific transcription factors *tbx21* (Th1 marker), *gata3* (Th2 marker) and *foxp3a* (Treg marker) in comparison to WT fish, suggesting a similar function for FurinA in T cell differentiation as its mammalian counterparts. Our findings also showed, for the first time, that *furinA*, the zebrafish ortholog of human *FURIN,* is upregulated in a mycobacterial infection. Furthermore, the decreased *furinA* mRNA levels in the *furinA*$^{td204e/+}$ mutants associated with a proinflammatory phenotype upon *M. marinum* infection, which was characterized by higher levels of *tnfa*, *lta* and *il17a/f3* expression, and with a decreased *M. marinum* burden in a chronic infection. Future studies using for example the zebrafish latency model would be required to assess whether *FURIN* expression or protein levels could be used as a diagnostic marker in latent TB. On the other hand, a conditional lung-specific deletion of *Furin* in a mouse TB model could help in evaluating the potential of inhaled FURIN-inhibitors as anti-TB drugs.

The relatively recently engineered CRISPR/Cas9 mutagenesis system has been demonstrated as an effective tool for creating genomic modifications also in model

organisms such as the zebrafish. To set up an in-house zebrafish CRISPR/Cas9 mutagenesis method an *egfp* transgene in the tg(*fli1a*:*egfp*) fish line as well as endogenous *ca10a* and *ca10b* genes in WT fish were targeted. Phenotypic and molecular analyses of the CRISPR/Cas9 mutated fish demonstrated both the applicability as well as the efficiency of our system in creating targeted genomic indel mutations *in vivo*. The described zebrafish CRISPR/Cas9 system can also be easily expanded to create knock-in animals as well as to knockdown genes of interest with the CRISPR interference approach.

In order to screen for novel candidate genes associated with a mycobacterial infection, a genome-wide gene expression microarray analysis of *M. marinum* infected zebrafish was conducted. Here, we found *itln3* to be one of the genes most induced during an infection. Consequently, the CRISPR/Cas9 system was used to create *itln3* mutant zebrafish lines, and to study ITLNs *in vivo* in the mycobacterial host response. However, despite our studies with both the *M. marinum* model of zebrafish embryos as well as the adult fish, we did not detect any differences in the survival or the mycobacterial burden of the *itln3* mutants compared to the WT controls. Understanding why Itln3 is dispensable for a *M. marinum* infection requires further studies, although, as suggested by our bacterial binding studies, the inability of Itln3 to bind to *M. marinum* provides one explanation for this. Collectively, our findings indicate that the zebrafish *M. marinum* infection model together with the genome-wide transcriptomic approaches enables screening for novel TB candidate genes, and that together with the mutant zebrafish they provide a powerful combination when studying the influence of the host´s genetics in a mycobacterial infection. Importantly, these studies can elucidate the detailed molecular mechanisms involved in the host response against mycobacteria, which is prerequisite for finding new diagnostic possibilities and therapeutic agents.

8 ACKNOWLEDGEMENTS

This PhD thesis was carried out in collaboration with the Research Groups of Immunoregulation and Experimental Immunology at the Faculty of Medicine and Life Sciences at the University of Tampere (Tampere, Finland) under the supervision of Professors Marko Pesu and Mika Rämet.

First, I wish to express my deepest gratitude to both of my supervisors, Marko and Mika, for providing me the opportunity to do scientific research in the fascinating field of immunology. I thank Marko for giving me the kick-off for my scientific career already as an undergraduate student doing my master´s thesis. Guiding and supporting me in these initial steps has been pivotal for nourishing my inner scientist. I am also ever grateful for Mika for taking me under your fins as a starting PhD student, and providing me the opportunity to tackle scientific questions in an invigorating environment during my thesis work. You have not only allowed me to do research independently, but at the same time you have provided the facilities for the experimental work as well as supported and guided me in the theoretical aspects. Thank you to both of you!

Next, I am grateful to all of the former and present people in the Research Groups of Immunoregulation and Experimental Immunology that I have been honored to work with during the past few years. Although all of you would deserve an individual part in this acknowledgement section, it would require another book to do so. Consequently, I have tried to equally list you here: Hannu Turpeinen, Zuzet Cordova, Saara Aittomäki, Anna Grönholm, Sanna Hämäläinen, Annemari Latvala, Zsuzsanna Ortutay, Dafne Jacome, Leena-Maija Vanha-aho, Susanna Valanne, Laura Vesala, Mirva Järvelä-Stölting, Carina Bäuerlein, Jenna Ilomäki, Kaisa Oksanen, Tuula Myllymäki, Mirja Niskanen, Henna Myllymäki, Leena Mäkinen, Hannaleena Piippo, Anni Saralahti, Meri Uusi-Mäkelä and Sanna-Kaisa Harjula. Without all of you this thesis would not have been possible.

A big thank you goes also to our collaborators Niklas Kähkönen, Juha Määttä, Vesa Hytönen, Milka Hammarén and Mataleena Parikka as well as to all of the other co-authors of my thesis work, including Ashok Aspatwar, Martti Tolvanen, Harlan Barker, Csaba Ortutay, Peiwen Pan, Marianne Kuuslahti and Seppo Parkkila. I wish to thank also Jukka Lehtiniemi, Latifeh Azizi, Jorma Isola, Henrik Hammarén, Lauri

Paulamäki, Hanna Luukinen, Bruno Luukinen and Juha Saarikettu that I have had the pleasure to work with during my work.

I would like to thank the pre-examiners, Assistant professor Susanna Fagerholm and Docent Pia Rantakari, for their valuable feedback and kind words related to my thesis. I would also like to acknowledge Professor Outi Vaarala for your consent to act as my opponent in the dissertation. Furthermore, I thank my PhD thesis follow-up group members Professor Dan Hultmark and Docent Ilkka Junttila for the important discussions during the past few years. Helen Cooper is greatly acknowledged for revising the language of my thesis work.

While I have found this line of work as more than exciting, it needs to be balanced by other things happening outside the Arvo-building. Consequently, I would like to express my sincerest gratitude to my family and friends: "Suuret kiitokset vanhemmilleni Makelle ja Jaanalle, siskoilleni Tarulle ja Maijulle, Tulosen serkkupojille Teemulle ja Miikalle sekä Arja-tädille ja Naimi-mummolle. Haluan myös esittää kiitokseni Iia-mammalle ja Tapsa-papalle kaikesta vuosien varrella saamastani tuesta. Erityiset kiitokset myös Jutan suvulle, perheelle sekä vanhemmille Helenalle ja Jyrkille kaikesta ystävällisyydestänne. Vilpittömin kiitos myös kaikille ystävilleni. Viimeisenä haluan kiittää mitä suurimmin puolisoani Juttaa sekä lapsiamme Emiliaa, Eeroa ja Oliveria. Varsinkin Jutalta saamani tuki sekä koti- että työasioissa on lopulta mahdollistanut tämän hetken. Sanat eivät riitä kuvaamaan tunteitani ja kiitollisuuttani teitä kohtaan."

The work was financially supported by the Orion Research Foundation, the Maud Kuistila Memorial Foundation, the Väinö and Laina Kivi Foundation, Tampere Tuberculosis Foundation, the Doctoral Programme in Biomedicine and Biotechnology at the University of Tampere and the Academy of Finland PROFI4-project at the University of Tampere. The book pressing costs of the thesis were in part financed by the City of Tampere. All of the financial supporters are greatly acknowledged.

Tampere, December 2018

Markus Ojanen

9 REFERENCES

Achkar, J.M., Chan, J. & Casadevall, A. 2015, "B cells and antibodies in the defense against Mycobacterium tuberculosis infection", *Immunological Reviews,* vol. 264, no. 1, pp. 167-181.

Agarwal, N., Lamichhane, G., Gupta, R., Nolan, S. & Bishai, W.R. 2009, "Cyclic AMP intoxication of macrophages by a Mycobacterium tuberculosis adenylate cyclase", *Nature,* vol. 460, no. 7251, pp. 98-102.

Ai, J., Ruan, Q., Liu, Q. & Zhang, W. 2016, "Updates on the risk factors for latent tuberculosis reactivation and their managements", *Emerging Microbes & Infections,* vol. 5, pp. e10.

Albadri, S., Del Bene, F. & Revenu, C. 2017, "Genome editing using CRISPR/Cas9-based knock-in approaches in zebrafish", *Methods (San Diego, Calif.),* vol. 121-122, pp. 77-85.

Altschul, S.F., Madden, T.L., Schäffer, A.A., Zhang, J., Zhang, Z., Miller, W. & Lipman, D.J. 1997, "Gapped BLAST and PSI-BLAST: a new generation of protein database search programs", *Nucleic acids research,* vol. 25, no. 17, pp. 3389-3402.

Andersson, J., Tran, D.Q., Pesu, M., Davidson, T.S., Ramsey, H., O'Shea, J.J. & Shevach, E.M. 2008, "CD4+ FoxP3+ regulatory T cells confer infectious tolerance in a TGF-beta-dependent manner", *The Journal of experimental medicine,* vol. 205, no. 9, pp. 1975-1981.

Arora, V., Knapp, D.C., Smith, B.L., Statdfield, M.L., Stein, D.A., Reddy, M.T., Weller, D.D. & Iversen, P.L. 2000, "c-Myc antisense limits rat liver regeneration and indicates role for c-Myc in regulating cytochrome P-450 3A activity", *The Journal of Pharmacology and Experimental Therapeutics,* vol. 292, no. 3, pp. 921-928.

Artenstein, A.W. & Opal, S.M. 2011, "Proprotein convertases in health and disease", *The New England Journal of Medicine,* vol. 365, no. 26, pp. 2507-2518.

Azad, A.K., Sadee, W. & Schlesinger, L.S. 2012, "Innate immune gene polymorphisms in tuberculosis", *Infection and Immunity,* vol. 80, no. 10, pp. 3343-3359.

Balla, K.M., Lugo-Villarino, G., Spitsbergen, J.M., Stachura, D.L., Hu, Y., Bañuelos, K., Romo-Fewell, O., Aroian, R.V. & Traver, D. 2010, "Eosinophils in the zebrafish: prospective isolation, characterization, and eosinophilia induction by helminth determinants", *Blood,* vol. 116, no. 19, pp. 3944-3954.

Balu, S., Reljic, R., Lewis, M.J., Pleass, R.J., McIntosh, R., van Kooten, C., van Egmond, M., Challacombe, S., Woof, J.M. & Ivanyi, J. 2011, "A novel human IgA monoclonal antibody protects against tuberculosis", *Journal of Immunology (Baltimore, Md.: 1950),* vol. 186, no. 5, pp. 3113-3119.

Barker, L.P., George, K.M., Falkow, S. & Small, P.L. 1997, "Differential trafficking of live and dead Mycobacterium marinum organisms in macrophages", *Infection and Immunity,* vol. 65, no. 4, pp. 1497-1504.

Barreiro, L.B., Tailleux, L., Pai, A.A., Gicquel, B., Marioni, J.C. & Gilad, Y. 2012, "Deciphering the genetic architecture of variation in the immune response to Mycobacterium tuberculosis infection", *Proceedings of the National Academy of Sciences of the United States of America,* vol. 109, no. 4, pp. 1204-1209.

Bean, A.G., Roach, D.R., Briscoe, H., France, M.P., Korner, H., Sedgwick, J.D. & Britton, W.J. 1999, "Structural deficiencies in granuloma formation in TNF gene-targeted mice underlie the heightened susceptibility to aerosol Mycobacterium tuberculosis infection, which is not compensated for by lymphotoxin", *Journal of Immunology (Baltimore, Md.: 1950),* vol. 162, no. 6, pp. 3504-3511.

Becker, G.L., Lu, Y., Hardes, K., Strehlow, B., Levesque, C., Lindberg, I., Sandvig, K., Bakowsky, U., Day, R., Garten, W. & Steinmetzer, T. 2012, "Highly potent inhibitors of proprotein convertase furin as potential drugs for treatment of infectious diseases", *The Journal of biological chemistry,* vol. 287, no. 26, pp. 21992-22003.

Benard, E.L., Rougeot, J., Racz, P.I., Spaink, H.P. & Meijer, A.H. 2016, "Transcriptomic Approaches in the Zebrafish Model for Tuberculosis-Insights Into Host- and Pathogen-specific Determinants of the Innate Immune Response", *Advances in Genetics,* vol. 95, pp. 217-251.

Benard, E.L., Roobol, S.J., Spaink, H.P. & Meijer, A.H. 2014, "Phagocytosis of mycobacteria by zebrafish macrophages is dependent on the scavenger receptor Marco, a key control factor of pro-inflammatory signalling", *Developmental and Comparative Immunology,* vol. 47, no. 2, pp. 223-233.

Bibikova, M., Golic, M., Golic, K.G. & Carroll, D. 2002, "Targeted chromosomal cleavage and mutagenesis in Drosophila using zinc-finger nucleases", *Genetics,* vol. 161, no. 3, pp. 1169-1175.

Bogdanove, A.J. & Voytas, D.F. 2011, "TAL effectors: customizable proteins for DNA targeting", *Science (New York, N.Y.),* vol. 333, no. 6051, pp. 1843-1846.

Bolotin, A., Quinquis, B., Sorokin, A. & Ehrlich, S.D. 2005, "Clustered regularly interspaced short palindrome repeats (CRISPRs) have spacers of extrachromosomal origin", *Microbiology (Reading, England),* vol. 151, no. Pt 8, pp. 2551-2561.

Brightbill, H.D., Libraty, D.H., Krutzik, S.R., Yang, R.B., Belisle, J.T., Bleharski, J.R., Maitland, M., Norgard, M.V., Plevy, S.E., Smale, S.T., Brennan, P.J., Bloom, B.R., Godowski, P.J. & Modlin, R.L. 1999, "Host defense mechanisms triggered by microbial lipoproteins through toll-like receptors", *Science (New York, N.Y.),* vol. 285, no. 5428, pp. 732-736.

Bustamante, J., Boisson-Dupuis, S., Abel, L. & Casanova, J. 2014, "Mendelian susceptibility to mycobacterial disease: genetic, immunological, and clinical features of inborn errors of IFN-γ immunity", *Seminars in Immunology,* vol. 26, no. 6, pp. 454-470.

Cai, S., Chen, Y., Shang, Y., Cui, J., Li, Z. & Li, Y. 2018, "Knockout of zebrafish interleukin 7 receptor (IL7R) by the CRISPR/Cas9 system delays retinal neurodevelopment", *Cell Death & Disease,* vol. 9, no. 3, pp. 273.

Cambier, C.J., Falkow, S. & Ramakrishnan, L. 2014, "Host evasion and exploitation schemes of Mycobacterium tuberculosis", *Cell,* vol. 159, no. 7, pp. 1497-1509.

Cambier, C.J., Takaki, K.K., Larson, R.P., Hernandez, R.E., Tobin, D.M., Urdahl, K.B., Cosma, C.L. & Ramakrishnan, L. 2014, "Mycobacteria manipulate macrophage recruitment through coordinated use of membrane lipids", *Nature,* vol. 505, no. 7482, pp. 218-222.

Canaday, D.H., Ziebold, C., Noss, E.H., Chervenak, K.A., Harding, C.V. & Boom, W.H. 1999, "Activation of human CD8+ alpha beta TCR+ cells by Mycobacterium tuberculosis via an alternate class I MHC antigen-processing pathway", *Journal of Immunology (Baltimore, Md.: 1950),* vol. 162, no. 1, pp. 372-379.

Carvalho, R., de Sonneville, J., Stockhammer, O.W., Savage, N.D., Veneman, W.J., Ottenhoff, T.H., Dirks, R.P., Meijer, A.H. & Spaink, H.P. 2011, "A high-throughput screen for tuberculosis progression", *PloS one,* vol. 6, no. 2, pp. e16779.

Chee, C.B., Sester, M., Zhang, W. & Lange, C. 2013, "Diagnosis and treatment of latent infection with Mycobacterium tuberculosis", *Respirology,* vol. 18, no. 2, pp. 205-216.

Chen, L., Yan, J., Sun, W., Zhang, Y., Sui, C., Qi, J., Du, Y. & Feng, L. 2016, "A zebrafish intelectin ortholog agglutinates both Gram-negative and Gram-positive bacteria with binding capacity to bacterial polysaccharide", *Fish & Shellfish Immunology,* vol. 55, pp. 729-736.

Chen, W., Jin, W., Hardegen, N., Lei, K., Li, L., Marinos, N., McGrady, G. & Wahl, S.M. 2003, "Conversion of peripheral CD4+CD25- naive T cells to CD4+CD25+ regulatory T cells by TGF-beta induction of transcription factor Foxp3", *The Journal of Experimental Medicine,* vol. 198, no. 12, pp. 1875-1886.

Chiang, C., Lee, J.-., Yu, M.-., Bai, K.-., Lin, T.-. & Luh, K.-. 2009, "Tuberculosis-related deaths without treatment", *The International Journal of Tuberculosis and Lung Disease: The Official Journal of the International Union Against Tuberculosis and Lung Disease,* vol. 13, no. 12, pp. 1563-1565.

Cho, S.W., Kim, S., Kim, Y., Kweon, J., Kim, H.S., Bae, S. & Kim, J. 2014, "Analysis of off-target effects of CRISPR/Cas-derived RNA-guided endonucleases and nickases", *Genome Research,* vol. 24, no. 1, pp. 132-141.

Clay, H., Volkman, H.E. & Ramakrishnan, L. 2008, "Tumor necrosis factor signaling mediates resistance to mycobacteria by inhibiting bacterial growth and macrophage death", *Immunity,* vol. 29, no. 2, pp. 283-294.

Comstock, G.W. 1978, "Tuberculosis in twins: a re-analysis of the Prophit survey", *The American Review of Respiratory Disease,* vol. 117, no. 4, pp. 621-624.

Cooper, A.M., Dalton, D.K., Stewart, T.A., Griffin, J.P., Russell, D.G. & Orme, I.M. 1993, "Disseminated tuberculosis in interferon gamma gene-disrupted mice", *The Journal of experimental medicine,* vol. 178, no. 6, pp. 2243-2247.

Cooper, A.M., Magram, J., Ferrante, J. & Orme, I.M. 1997a, "Interleukin 12 (IL-12) is crucial to the development of protective immunity in mice intravenously infected with mycobacterium tuberculosis", *The Journal of Experimental Medicine,* vol. 186, no. 1, pp. 39-45.

Cooper, A.M. 2014, "Mouse model of tuberculosis", *Cold Spring Harbor Perspectives in Medicine,* vol. 5, no. 2, pp. a018556.

Cooper, A.M. 2009, "Cell-mediated immune responses in tuberculosis", *Annual Review of Immunology,* vol. 27, pp. 393-422.

Cordova, Z.M., Grönholm, A., Kytölä, V., Taverniti, V., Hämäläinen, S., Aittomäki, S., Niininen, W., Junttila, I., Ylipää, A., Nykter, M. & Pesu, M. 2016, "Myeloid cell expressed proprotein convertase FURIN attenuates inflammation", *Oncotarget,* vol. 7, no. 34, pp. 54392-54404.

Cronan, M.R. & Tobin, D.M. 2014, "Fit for consumption: zebrafish as a model for tuberculosis", *Disease Models & Mechanisms,* vol. 7, no. 7, pp. 777-784.

Danilova, N., Bussmann, J., Jekosch, K. & Steiner, L.A. 2005, "The immunoglobulin heavy-chain locus in zebrafish: identification and expression of a previously unknown isotype, immunoglobulin Z", *Nature Immunology,* vol. 6, no. 3, pp. 295-302.

Danilova, N. & Steiner, L.A. 2002, "B cells develop in the zebrafish pancreas", *Proceedings of the National Academy of Sciences of the United States of America,* vol. 99, no. 21, pp. 13711-13716.

Davis, J.M., Clay, H., Lewis, J.L., Ghori, N., Herbomel, P. & Ramakrishnan, L. 2002, "Real-time visualization of mycobacterium-macrophage interactions leading to initiation of granuloma formation in zebrafish embryos", *Immunity,* vol. 17, no. 6, pp. 693-702.

Davis, J.M. & Ramakrishnan, L. 2009, "The role of the granuloma in expansion and dissemination of early tuberculous infection", *Cell,* vol. 136, no. 1, pp. 37-49.

Dee, C.T., Nagaraju, R.T., Athanasiadis, E.I., Gray, C., Fernandez Del Ama, L., Johnston, S.A., Secombes, C.J., Cvejic, A. & Hurlstone, A.F.L. 2016, "CD4-Transgenic Zebrafish Reveal Tissue-Resident Th2- and Regulatory T Cell-like Populations and Diverse Mononuclear Phagocytes", *Journal of Immunology (Baltimore, Md.: 1950),* vol. 197, no. 9, pp. 3520-3530.

Dharmadhikari, A.S. & Nardell, E.A. 2008, "What animal models teach humans about tuberculosis", *American Journal of Respiratory Cell and Molecular Biology,* vol. 39, no. 5, pp. 503-508.

Dheda, K., Barry, C.E. & Maartens, G. 2016, "Tuberculosis", *The Lancet,* vol. 387, no. 10024, pp. 1211-1226.

Ding, Z., Zhao, X., Zhan, Q., Cui, L., Sun, Q., Lin, L., Wang, W. & Liu, H. 2017, "Characterization and expression analysis of an intelectin gene from Megalobrama amblycephala with excellent bacterial binding and agglutination activity", *Fish & Shellfish Immunology,* vol. 61, pp. 100-110.

Djuretic, I.M., Levanon, D., Negreanu, V., Groner, Y., Rao, A. & Ansel, K.M. 2007, "Transcription factors T-bet and Runx3 cooperate to activate Ifng and silence Il4 in T helper type 1 cells", *Nature Immunology,* vol. 8, no. 2, pp. 145-153.

Dobson, J.T., Seibert, J., Teh, E.M., Da'as, S., Fraser, R.B., Paw, B.H., Lin, T. & Berman, J.N. 2008, "Carboxypeptidase A5 identifies a novel mast cell lineage in the zebrafish providing new insight into mast cell fate determination", *Blood,* vol. 112, no. 7, pp. 2969-2972.

Duan, J., Lu, G., Xie, Z., Lou, M., Luo, J., Guo, L. & Zhang, Y. 2014, "Genome-wide identification of CRISPR/Cas9 off-targets in human genome", *Cell Research,* vol. 24, no. 8, pp. 1009-1012.

Dye, C., Scheele, S., >Dolin, P., Pathania, V. & Raviglione, M.C. 1999, "Global Burden of Tuberculosis: Estimated Incidence, Prevalence, and Mortality by Country", *JAMA,* vol. 282, no. 7, pp. 677-686.

Eddabra, R. & Ait Benhassou, H. 2018, "Rapid molecular assays for detection of tuberculosis", *Pneumonia (Nathan Qld.),* vol. 10, pp. 4.

Eisen, J.S. & Smith, J.C. 2008, "Controlling morpholino experiments: don't stop making antisense", *Development (Cambridge, England),* vol. 135, no. 10, pp. 1735-1743.

El-Etr, S.H., Yan, L. & Cirillo, J.D. 2001, "Fish monocytes as a model for mycobacterial host-pathogen interactions", *Infection and Immunity,* vol. 69, no. 12, pp. 7310-7317.

Ernst, J.D. 2012, "The immunological life cycle of tuberculosis", *Nature Reviews Immunology,* vol. 12, no. 8, pp. 581-591.

Esterhuyse, M.M., Weiner, J., Caron, E., Loxton, A.G., Iannaccone, M., Wagman, C., Saikali, P., Stanley, K., Wolski, W.E., Mollenkopf, H., Schick, M., Aebersold, R., Linhart, H., Walzl, G. & Kaufmann, S.H.E. 2015, "Epigenetics and Proteomics Join Transcriptomics in the Quest for Tuberculosis Biomarkers", *mBio,* vol. 6, no. 5, pp. 1187.

Flynn, J.L., Chan, J., Triebold, K.J., Dalton, D.K., Stewart, T.A. & Bloom, B.R. 1993a, "An essential role for interferon gamma in resistance to Mycobacterium tuberculosis infection", *The Journal of experimental medicine,* vol. 178, no. 6, pp. 2249-2254.

Flynn, J.L., Goldstein, M.M., Triebold, K.J., Sypek, J., Wolf, S. & Bloom, B.R. 1995, "IL-12 increases resistance of BALB/c mice to Mycobacterium tuberculosis infection", *Journal of Immunology (Baltimore, Md.: 1950),* vol. 155, no. 5, pp. 2515-2524.

Flynn, J.L. 2006, "Lessons from experimental Mycobacterium tuberculosis infections.", *Microbes and infection,* vol. 8, no. 4, pp. 1179-1188.

Fogel, N. 2015, "Tuberculosis: a disease without boundaries", *Tuberculosis (Edinburgh, Scotland),* vol. 95, no. 5, pp. 527-531.

Fonseca, K.L., Rodrigues, P.N.S., Olsson, I.A.S. & Saraiva, M. 2017, "Experimental study of tuberculosis: From animal models to complex cell systems and organoids", *PLoS pathogens,* vol. 13, no. 8, pp. e1006421.

Fu, Y., Foden, J.A., Khayter, C., Maeder, M.L., Reyon, D., Joung, J.K. & Sander, J.D. 2013, "High-frequency off-target mutagenesis induced by CRISPR-Cas nucleases in human cells", *Nature Biotechnology,* vol. 31, no. 9, pp. 822-826.

Gallegos, A.M., van Heijst, Jeroen W. J., Samstein, M., Su, X., Pamer, E.G. & Glickman, M.S. 2011, "A gamma interferon independent mechanism of CD4 T cell mediated control of M. tuberculosis infection in vivo", *PLoS pathogens,* vol. 7, no. 5, pp. e1002052.

Ganesh, S.K., Tragante, V., Guo, W., Guo, Y., Lanktree, M.B., Smith, E.N., Johnson, T., Castillo, B.A., Barnard, J., Baumert, J., Chang, Y.C., Elbers, C.C., Farrall, M., Fischer, M.E., Franceschini, N., Gaunt, T.R., Gho, Johannes M. I. H., Gieger, C., Gong, Y., Isaacs, A., Kleber, M.E., Mateo Leach, I., McDonough, C.W., Meijs, M.F.L., Mellander, O., Molony, C.M., Nolte, I.M., Padmanabhan, S., Price, T.S., Rajagopalan, R., Shaffer, J., Shah, S., Shen, H., Soranzo, N., van der Most, Peter J., Van Iperen, Erik P. A., Van Setten, J., Van Setten, J.A., Vonk, J.M., Zhang, L., Beitelshees, A.L., Berenson, G.S., Bhatt, D.L., Boer, J.M.A., Boerwinkle, E., Burkley, B., Burt, A., Chakravarti, A., Chen, W., Cooper-Dehoff, R.M., Curtis, S.P., Dreisbach, A., Duggan, D., Ehret, G.B., Fabsitz, R.R., Fornage, M., Fox, E., Furlong, C.E., Gansevoort, R.T., Hofker, M.H., Hovingh, G.K., Kirkland, S.A., Kottke-Marchant, K., Kutlar, A., Lacroix, A.Z., Langaee, T.Y., Li, Y.R., Lin, H., Liu, K., Maiwald, S., Malik, R., Murugesan, G., Newton-Cheh, C., O'Connell, J.R., Onland-Moret, N.C., Ouwehand, W.H., Palmas, W., Penninx, B.W., Pepine, C.J., Pettinger, M., Polak, J.F., Ramachandran, V.S., Ranchalis, J., Redline, S., Ridker, P.M., Rose, L.M., Scharnag, H., Schork, N.J., Shimbo, D., Shuldiner, A.R., Srinivasan, S.R., Stolk, R.P., Taylor, H.A., Thorand, B., Trip, M.D., van Duijn, C.M., Verschuren, W.M., Wijmenga, C., Winkelmann, B.R., Wyatt, S., Young, J.H., Boehm, B.O., Caulfield, M.J., Chasman, D.I., Davidson, K.W., Doevendans, P.A., Fitzgerald, G.A., Gums, J.G., Hakonarson, H., Hillege, H.L., Illig, T., Jarvik, G.P., Johnson, J.A., Kastelein, J.J.P., Koenig, W., März, W., Mitchell, B.D., Murray, S.S., Oldehinkel, A.J., Rader, D.J., Reilly, M.P., Reiner, A.P., Schadt, E.E., Silverstein, R.L., Snieder, H., Stanton, A.V., Uitterlinden, A.G., van der Harst, P., van der Schouw, Yvonne T., Samani, N.J., Johnson, A.D., Munroe, P.B., de Bakker, Paul I. W., Zhu, X., Levy, D., Keating, B.J. & Asselbergs, F.W. 2013, "Loci influencing blood pressure identified using a cardiovascular gene-centric array", *Human Molecular Genetics,* vol. 22, no. 8, pp. 1663-1678.

Gao, L., Groger, R., Cox, J.S., Beverley, S.M., Lawson, E.H. & Brown, E.J. 2003a, "Transposon mutagenesis of Mycobacterium marinum identifies a locus linking pigmentation and intracellular survival", *Infection and Immunity,* vol. 71, no. 2, pp. 922-929.

Gao, L., Guo, S., McLaughlin, B., Morisaki, H., Engel, J.N. & Brown, E.J. 2004, "A mycobacterial virulence gene cluster extending RD1 is required for cytolysis, bacterial spreading and ESAT-6 secretion", *Molecular Microbiology,* vol. 53, no. 6, pp. 1677-1693.

Gao, L., Laval, F., Lawson, E.H., Groger, R.K., Woodruff, A., Morisaki, J.H., Cox, J.S., Daffe, M. & Brown, E.J. 2003b, "Requirement for kasB in Mycobacterium mycolic

acid biosynthesis, cell wall impermeability and intracellular survival: implications for therapy", *Molecular Microbiology,* vol. 49, no. 6, pp. 1547-1563.

Gopal, R., Monin, L., Slight, S., Uche, U., Blanchard, E., Fallert Junecko, B.A., Ramos-Payan, R., Stallings, C.L., Reinhart, T.A., Kolls, J.K., Kaushal, D., Nagarajan, U., Rangel-Moreno, J. & Khader, S.A. 2014, "Unexpected role for IL-17 in protective immunity against hypervirulent Mycobacterium tuberculosis HN878 infection", *PLoS pathogens,* vol. 10, no. 5, pp. e1004099.

Hallenberger, S., Bosch, V., Angliker, H., Shaw, E., Klenk, H.D. & Garten, W. 1992, "Inhibition of furin-mediated cleavage activation of HIV-1 glycoprotein gp160", *Nature,* vol. 360, no. 6402, pp. 358-361.

Hammaren, M.M., Oksanen, K.E., Nisula, H.M., Luukinen, B.V., Pesu, M., Ramet, M. & Parikka, M. 2014, "Adequate Th2-type response associates with restricted bacterial growth in latent mycobacterial infection of zebrafish", *PLoS pathogens,* vol. 10, no. 6, pp. e1004190.

Heasman, J., Kofron, M. & Wylie, C. 2000, "Beta-catenin signaling activity dissected in the early Xenopus embryo: a novel antisense approach", *Developmental Biology,* vol. 222, no. 1, pp. 124-134.

Hegedus, Z., Zakrzewska, A., Agoston, V.C., Ordas, A., Rácz, P., Mink, M., Spaink, H.P. & Meijer, A.H. 2009, "Deep sequencing of the zebrafish transcriptome response to mycobacterium infection", *Molecular Immunology,* vol. 46, no. 15, pp. 2918-2930.

Heikura, T., Nieminen, T., Roschier, M.M., Karvinen, H., Kaikkonen, M.U., Mähönen, A.J., Lesch, H.P., Rissanen, T.T., Laitinen, O.H., Airenne, K.J. & Ylä-Herttuala, S. 2012, "Baculovirus-mediated vascular endothelial growth factor-D(ΔNΔC) gene transfer induces angiogenesis in rabbit skeletal muscle", *The Journal of Gene Medicine,* vol. 14, no. 1, pp. 35-43.

Hirsch, C.S., Ellner, J.J., Russell, D.G. & Rich, E.A. 1994, "Complement receptor-mediated uptake and tumor necrosis factor-alpha-mediated growth inhibition of Mycobacterium tuberculosis by human alveolar macrophages", *Journal of Immunology (Baltimore, Md.: 1950),* vol. 152, no. 2, pp. 743-753.

Howe, K., Clark, M.D., Torroja, C.F., Torrance, J., Berthelot, C., Muffato, M., Collins, J.E., Humphray, S., McLaren, K., Matthews, L., McLaren, S., Sealy, I., Caccamo, M., Churcher, C., Scott, C., Barrett, J.C., Koch, R., Rauch, G.J., White, S., Chow, W., Kilian, B., Quintais, L.T., Guerra-Assuncao, J.A., Zhou, Y., Gu, Y., Yen, J., Vogel, J.H., Eyre, T., Redmond, S., Banerjee, R., Chi, J., Fu, B., Langley, E., Maguire, S.F., Laird, G.K., Lloyd, D., Kenyon, E., Donaldson, S., Sehra, H., Almeida-King, J., Loveland, J., Trevanion, S., Jones, M., Quail, M., Willey, D., Hunt, A., Burton, J., Sims, S., McLay, K., Plumb, B., Davis, J., Clee, C., Oliver, K., Clark, R., Riddle, C., Elliot, D., Threadgold, G., Harden, G., Ware, D., Mortimore, B., Kerry, G., Heath, P., Phillimore, B., Tracey, A., Corby, N., Dunn, M., Johnson, C., Wood, J., Clark, S., Pelan, S., Griffiths, G., Smith, M., Glithero, R., Howden, P., Barker, N., Stevens, C., Harley, J., Holt, K., Panagiotidis, G., Lovell, J., Beasley, H., Henderson, C., Gordon, D., Auger,

K., Wright, D., Collins, J., Raisen, C., Dyer, L., Leung, K., Robertson, L., Ambridge, K., Leongamornlert, D., McGuire, S., Gilderthorp, R., Griffiths, C., Manthravadi, D., Nichol, S., Barker, G., Whitehead, S., Kay, M. & ... 2013, "The zebrafish reference genome sequence and its relationship to the human genome", *Nature,* vol. 496, no. 7446, pp. 498-503.

Hruscha, A., Krawitz, P., Rechenberg, A., Heinrich, V., Hecht, J., Haass, C. & Schmid, B. 2013, "Efficient CRISPR/Cas9 genome editing with low off-target effects in zebrafish", *Development (Cambridge, England),* vol. 140, no. 24, pp. 4982-4987.

Hruscha, A. & Schmid, B. 2015, "Generation of zebrafish models by CRISPR /Cas9 genome editing", *Methods in Molecular Biology (Clifton, N.J.),* vol. 1254, pp. 341-350.

Huang, P., Zhu, Z., Lin, S. & Zhang, B. 2012, "Reverse genetic approaches in zebrafish", *Journal of Genetics and Genomics = Yi Chuan Xue Bao,* vol. 39, no. 9, pp. 421-433.

Hwang, W.Y., Fu, Y., Reyon, D., Maeder, M.L., Tsai, S.Q., Sander, J.D., Peterson, R.T., Yeh, J.-J. & Joung, J.K. 2013, "Efficient genome editing in zebrafish using a CRISPR-Cas system", *Nature Biotechnology,* vol. 31, no. 3, pp. 227-229.

Hyde, D.R., Godwin, A.R. & Thummel, R. 2012, "In vivo electroporation of morpholinos into the regenerating adult zebrafish tail fin", *Journal of Visualized Experiments: JoVE,* , no. 61.

Jao, L., Wente, S.R. & Chen, W. 2013, "Efficient multiplex biallelic zebrafish genome editing using a CRISPR nuclease system", *Proceedings of the National Academy of Sciences of the United States of America,* vol. 110, no. 34, pp. 13904-13909.

Jinek, M., Chylinski, K., Fonfara, I., Hauer, M., Doudna, J.A. & Charpentier, E. 2012, "A programmable dual-RNA-guided DNA endonuclease in adaptive bacterial immunity", *Science (New York, N.Y.),* vol. 337, no. 6096, pp. 816-821.

Joosten, S.A., Fletcher, H.A. & Ottenhoff, T.H.M. 2013, "A helicopter perspective on TB biomarkers: pathway and process based analysis of gene expression data provides new insight into TB pathogenesis", *PloS One,* vol. 8, no. 9, pp. e73230.

Kasheta, M., Painter, C.A., Moore, F.E., Lobbardi, R., Bryll, A., Freiman, E., Stachura, D., Rogers, A.B., Houvras, Y., Langenau, D.M. & Ceol, C.J. 2017, "Identification and characterization of T reg-like cells in zebrafish", *The Journal of Experimental Medicine,* vol. 214, no. 12, pp. 3519-3530.

Kenyon, A., Gavriouchkina, D., Zorman, J., Napolitani, G., Cerundolo, V. & Sauka-Spengler, T. 2017, "Active nuclear transcriptome analysis reveals inflammasome-dependent mechanism for early neutrophil response to Mycobacterium marinum", *Scientific Reports,* vol. 7, no. 1, pp. 6505.

Kettleborough, R.N.W., Busch-Nentwich, E.M., Harvey, S.A., Dooley, C.M., de Bruijn, E., van Eeden, F., Sealy, I., White, R.J., Herd, C., Nijman, I.J., Fényes, F., Mehroke, S., Scahill, C., Gibbons, R., Wali, N., Carruthers, S., Hall, A., Yen, J., Cuppen, E. & Stemple, D.L. 2013, "A systematic genome-wide analysis of zebrafish protein-coding gene function", *Nature,* vol. 496, no. 7446, pp. 494-497.

Khader, S.A., Pearl, J.E., Sakamoto, K., Gilmartin, L., Bell, G.K., Jelley-Gibbs, D.M., Ghilardi, N., deSauvage, F. & Cooper, A.M. 2005, "IL-23 compensates for the absence of IL-12p70 and is essential for the IL-17 response during tuberculosis but is dispensable for protection and antigen-specific IFN-gamma responses if IL-12p70 is available", *Journal of Immunology (Baltimore, Md.: 1950),* vol. 175, no. 2, pp. 788-795.

Kim, S.J. 2005, "Drug-susceptibility testing in tuberculosis: methods and reliability of results", *The European Respiratory Journal,* vol. 25, no. 3, pp. 564-569.

Kim, Y.G., Cha, J. & Chandrasegaran, S. 1996, "Hybrid restriction enzymes: zinc finger fusions to Fok I cleavage domain", *Proceedings of the National Academy of Sciences of the United States of America,* vol. 93, no. 3, pp. 1156-1160.

Kimmey, J.M., Huynh, J.P., Weiss, L.A., Park, S., Kambal, A., Debnath, J., Virgin, H.W. & Stallings, C.L. 2015, "Unique role for ATG5 in neutrophil-mediated immunopathology during M. tuberculosis infection", *Nature,* vol. 528, no. 7583, pp. 565-569.

Kizil, C., Iltzsche, A., Kaslin, J. & Brand, M. 2013, "Micromanipulation of gene expression in the adult zebrafish brain using cerebroventricular microinjection of morpholino oligonucleotides", *Journal of Visualized Experiments: JoVE,* , no. 75, pp. e50415.

Kok, F.O., Shin, M., Ni, C.-., Gupta, A., Grosse, A.S., van Impel, A., Kirchmaier, B.C., Peterson-Maduro, J., Kourkoulis, G., Male, I., DeSantis, D.F., Sheppard-Tindell, S., Ebarasi, L., Betsholtz, C., Schulte-Merker, S., Wolfe, S.A. & Lawson, N.D. 2015, "Reverse genetic screening reveals poor correlation between morpholino-induced and mutant phenotypes in zebrafish", *Developmental Cell,* vol. 32, no. 1, pp. 97-108.

Krebs, J. CRISPR design tool and protocol. 2015, Data retrieved: 07:16, May 19, 2015, GMT. https://figshare.com/articles/CRISPR_Design_Tool/1117899.

Kruk, M.E., Schwalbe, N.R. & Aguiar, C.A. 2008, "Timing of default from tuberculosis treatment: a systematic review", *Tropical medicine & international health: TM & IH,* vol. 13, no. 5, pp. 703-712.

Küchler, A.M., Gjini, E., Peterson-Maduro, J., Cancilla, B., Wolburg, H. & Schulte-Merker, S. 2006, "Development of the zebrafish lymphatic system requires VEGFC signaling", *Current biology: CB,* vol. 16, no. 12, pp. 1244-1248.

Kursar, M., Koch, M., Mittrücker, H., Nouailles, G., Bonhagen, K., Kamradt, T. & Kaufmann, S.H.E. 2007, "Cutting Edge: Regulatory T cells prevent efficient clearance of Mycobacterium tuberculosis", *Journal of Immunology (Baltimore, Md.: 1950),* vol. 178, no. 5, pp. 2661-2665.

Lam, S.H., Chua, H.L., Gong, Z., Lam, T.J. & Sin, Y.M. 2004, "Development and maturation of the immune system in zebrafish, Danio rerio: a gene expression profiling, in situ hybridization and immunological study", *Developmental and Comparative Immunology,* vol. 28, no. 1, pp. 9-28.

Langenau, D.M., Ferrando, A.A., Traver, D., Kutok, J.L., Hezel, J.P., Kanki, J.P., Zon, L.I., Look, A.T. & Trede, N.S. 2004, "In vivo tracking of T cell development, ablation, and engraftment in transgenic zebrafish", *Proceedings of the National Academy of Sciences of the United States of America,* vol. 101, no. 19, pp. 7369-7374.

Larson, M.H., Gilbert, L.A., Wang, X., Lim, W.A., Weissman, J.S. & Qi, L.S. 2013, "CRISPR interference (CRISPRi) for sequence-specific control of gene expression", *Nature Protocols,* vol. 8, no. 11, pp. 2180-2196.

Lawn, S.D., Butera, S.T. & Shinnick, T.M. 2002, "Tuberculosis unleashed: the impact of human immunodeficiency virus infection on the host granulomatous response to Mycobacterium tuberculosis", *Microbes and Infection,* vol. 4, no. 6, pp. 635-646.

Lawn, S.D. & Zumla, A.I. 2011, "Tuberculosis", *Lancet (London, England),* vol. 378, no. 9785, pp. 57-72.

Lawson, N.D. & Weinstein, B.M. 2002, "In vivo imaging of embryonic vascular development using transgenic zebrafish", *Developmental Biology,* vol. 248, no. 2, pp. 307-318.

Lee, S., Wu, L.S., Huang, G., Huang, K., Lee, T. & Weng, J.T. 2016, "Gene expression profiling identifies candidate biomarkers for active and latent tuberculosis", *BMC bioinformatics,* vol. 17 Suppl 1, pp. 3.

Lefford, M.J. 1975, "Transfer of adoptive immunity to tuberculosis in mice", *Infection and Immunity,* vol. 11, no. 6, pp. 1174-1181.

Lei, R.X., Shi, H., Peng, X.M., Zhu, Y.H., Cheng, J. & Chen, G.H. 2009, "Influence of a single nucleotide polymorphism in the P1 promoter of the furin gene on transcription activity and hepatitis B virus infection", *Hepatology (Baltimore, Md.),* vol. 50, no. 3, pp. 763-771.

Lerner, T.R., Borel, S. & Gutierrez, M.G. 2015a, "The innate immune response in human tuberculosis", *Cellular Microbiology,* vol. 17, no. 9, pp. 1277-1285.

Li, N., Luo, W., Juhong, Z., Yang, J., Wang, H., Zhou, L. & Chang, J. 2010, "Associations between genetic variations in the FURIN gene and hypertension", *BMC medical genetics,* vol. 11, pp. 124.

Li, W. & Cha, L. 2007, "Predicting siRNA efficiency", *Cellular and molecular life sciences: CMLS,* vol. 64, no. 14, pp. 1785-1792.

Lieschke, G.J., Oates, A.C., Crowhurst, M.O., Ward, A.C. & Layton, J.E. 2001, "Morphologic and functional characterization of granulocytes and macrophages in embryonic and adult zebrafish", *Blood,* vol. 98, no. 10, pp. 3087-3096.

Lin, B., Cao, Z., Su, P., Zhang, H., Li, M., Lin, Y., Zhao, D., Shen, Y., Jing, C., Chen, S. & Xu, A. 2009, "Characterization and comparative analyses of zebrafish intelectins: highly conserved sequences, diversified structures and functions", *Fish & Shellfish Immunology,* vol. 26, no. 3, pp. 396-405.

Lin, H., Ah Kioon, M., Lalou, C., Larghero, J., Launay, J., Khatib, A. & Cohen-Solal, M. 2012, "Protective role of systemic furin in immune response-induced arthritis", *Arthritis and Rheumatism,* vol. 64, no. 9, pp. 2878-2886.

Lin, P.L. & Flynn, J.L. 2015, "CD8 T cells and Mycobacterium tuberculosis infection", *Seminars in Immunopathology,* vol. 37, no. 3, pp. 239-249.

Lombardo, A., Genovese, P., Beausejour, C.M., Colleoni, S., Lee, Y.L., Kim, K.A., Ando, D., Urnov, F.D., Galli, C., Gregory, P.D., Holmes, M.C. & Naldini, L. 2007, "Gene

editing in human stem cells using zinc finger nucleases and integrase-defective lentiviral vector delivery", *Nature Biotechnology,* vol. 25, no. 11, pp. 1298-1306.

Lu, L.L., Chung, A.W., Rosebrock, T.R., Ghebremichael, M., Yu, W.H., Grace, P.S., Schoen, M.K., Tafesse, F., Martin, C., Leung, V., Mahan, A.E., Sips, M., Kumar, M.P., Tedesco, J., Robinson, H., Tkachenko, E., Draghi, M., Freedberg, K.J., Streeck, H., Suscovich, T.J., Lauffenburger, D.A., Restrepo, B.I., Day, C., Fortune, S.M. & Alter, G. 2016, "A Functional Role for Antibodies in Tuberculosis", *Cell,* vol. 167, no. 2, pp. 443.e14.

Luckheeram, R.V., Zhou, R., Verma, A.D. & Xia, B. 2012, "CD4+T Cells: Differentiation and Functions", *Clinical and Developmental Immunology,* vol. 2012, pp. 1-12.

Lugo-Villarino, G., Balla, K.M., Stachura, D.L., Bañuelos, K., Werneck, M.B.F. & Traver, D. 2010, "Identification of dendritic antigen-presenting cells in the zebrafish", *Proceedings of the National Academy of Sciences of the United States of America,* vol. 107, no. 36, pp. 15850-15855.

Lund, R.J., Chen, Z., Scheinin, J. & Lahesmaa, R. 2004, "Early target genes of IL-12 and STAT4 signaling in th cells", *Journal of immunology (Baltimore, Md.: 1950),* vol. 172, no. 11, pp. 6775-6782.

Lyadova, I.V. & Panteleev, A.V. 2015, "Th1 and Th17 Cells in Tuberculosis: Protection, Pathology, and Biomarkers", *Mediators of inflammation,* vol. 2015, pp. 854507.

Maglione, P.J., Xu, J., Casadevall, A. & Chan, J. 2008, "Fc gamma receptors regulate immune activation and susceptibility during Mycobacterium tuberculosis infection", *Journal of Immunology (Baltimore, Md.: 1950),* vol. 180, no. 5, pp. 3329-3338.

Maglione, P.J., Xu, J. & Chan, J. 2007, "B cells moderate inflammatory progression and enhance bacterial containment upon pulmonary challenge with Mycobacterium tuberculosis", *Journal of Immunology (Baltimore, Md.: 1950),* vol. 178, no. 11, pp. 7222-7234.

Makarova, K.S., Haft, D.H., Barrangou, R., Brouns, S.J.J., Charpentier, E., Horvath, P., Moineau, S., Mojica, F.J.M., Wolf, Y.I., Yakunin, A.F., van der Oost, J. & Koonin, E.V. 2011, "Evolution and classification of the CRISPR-Cas systems", *Nature Reviews. Microbiology,* vol. 9, no. 6, pp. 467-477.

Malik, Z.A., Denning, G.M. & Kusner, D.J. 2000, "Inhibition of Ca(2+) signaling by Mycobacterium tuberculosis is associated with reduced phagosome-lysosome fusion and increased survival within human macrophages", *The Journal of Experimental Medicine,* vol. 191, no. 2, pp. 287-302.

Marques, J.T. & Williams, B.R.G. 2005, "Activation of the mammalian immune system by siRNAs", *Nature Biotechnology,* vol. 23, no. 11, pp. 1399-1405.

McDonough, K.A., Kress, Y. & Bloom, B.R. 1993, "Pathogenesis of tuberculosis: interaction of Mycobacterium tuberculosis with macrophages", *Infection and Immunity,* vol. 61, no. 7, pp. 2763-2773.

Means, T.K., Wang, S., Lien, E., Yoshimura, A., Golenbock, D.T. & Fenton, M.J. 1999, "Human toll-like receptors mediate cellular activation by Mycobacterium tuberculosis", *Journal of Immunology (Baltimore, Md.: 1950),* vol. 163, no. 7, pp. 3920-3927.

Meeker, N.D., Hutchinson, S.A., Ho, L. & Trede, N.S. 2007, "Method for isolation of PCR-ready genomic DNA from zebrafish tissues", *BioTechniques,* vol. 43, no. 5, pp. 614.

Meermeier, E.W. & Lewinsohn, D.M. 2018, "Early clearance versus control: what is the meaning of a negative tuberculin skin test or interferon-gamma release assay following exposure to Mycobacterium tuberculosis?", *F1000Research,* vol. 7, pp. 664.

Meijer, A.H., Verbeek, F.J., Salas-Vidal, E., Corredor-Adamez, M., Bussman, J., van der Sar, A M, Otto, G.W., Geisler, R. & Spaink, H.P. 2005, "Transcriptome profiling of adult zebrafish at the late stage of chronic tuberculosis due to Mycobacterium marinum infection", *Molecular immunology,* vol. 42, no. 10, pp. 1185-1203.

Meijer, A.H. 2016, "Protection and pathology in TB: learning from the zebrafish model", *Seminars in Immunopathology,* vol. 38, no. 2, pp. 261-273.

Meijer, A.H., van der Vaart, M. & Spaink, H.P. 2014, "Real-time imaging and genetic dissection of host-microbe interactions in zebrafish", *Cellular Microbiology,* vol. 16, no. 1, pp. 39-49.

Meng, X., Noyes, M.B., Zhu, L.J., Lawson, N.D. & Wolfe, S.A. 2008, "Targeted gene inactivation in zebrafish using engineered zinc-finger nucleases", *Nature Biotechnology,* vol. 26, no. 6, pp. 695-701.

Meyer, C.G. & Thye, T. 2014, "Host genetic studies in adult pulmonary tuberculosis", *Seminars in Immunology,* vol. 26, no. 6, pp. 445-453.

Miller, J., McLachlan, A.D. & Klug, A. 1985, "Repetitive zinc-binding domains in the protein transcription factor IIIA from Xenopus oocytes", *The EMBO journal,* vol. 4, no. 6, pp. 1609-1614.

Miller, J.C., Tan, S., Qiao, G., Barlow, K.A., Wang, J., Xia, D.F., Meng, X., Paschon, D.E., Leung, E., Hinkley, S.J., Dulay, G.P., Hua, K.L., Ankoudinova, I., Cost, G.J., Urnov, F.D., Zhang, H.S., Holmes, M.C., Zhang, L., Gregory, P.D. & Rebar, E.J. 2011, "A TALE nuclease architecture for efficient genome editing", *Nature Biotechnology,* vol. 29, no. 2, pp. 143-148.

Mitra, S., Alnabulsi, A., Secombes, C.J. & Bird, S. 2010, "Identification and characterization of the transcription factors involved in T-cell development, t-bet, stat6 and foxp3, within the zebrafish, Danio rerio", *The FEBS journal,* vol. 277, no. 1, pp. 128-147.

Mojica, F.J.M., Díez-Villaseñor, C., García-Martínez, J. & Soria, E. 2005, "Intervening sequences of regularly spaced prokaryotic repeats derive from foreign genetic elements", *Journal of Molecular Evolution,* vol. 60, no. 2, pp. 174-182.

Möller, M., de Wit, E. & Hoal, E.G. 2010, "Past, present and future directions in human genetic susceptibility to tuberculosis", *FEMS immunology and medical microbiology,* vol. 58, no. 1, pp. 3-26.

Morbitzer, R., Römer, P., Boch, J. & Lahaye, T. 2010, "Regulation of selected genome loci using de novo-engineered transcription activator-like effector (TALE)-type transcription factors", *Proceedings of the National Academy of Sciences,* vol. 107, no. 50, pp. 21617-21622.

Mortaz, E., Adcock, I.M., Tabarsi, P., Masjedi, M.R., Mansouri, D., Velayati, A.A., Casanova, J. & Barnes, P.J. 2015, "Interaction of Pattern Recognition Receptors with Mycobacterium Tuberculosis", *Journal of Clinical Immunology,* vol. 35, no. 1, pp. 1-10.

Moscou, M.J. & Bogdanove, A.J. 2009, "A simple cipher governs DNA recognition by TAL effectors", *Science (New York, N.Y.),* vol. 326, no. 5959, pp. 1501.

Mosser, D.M. & Edwards, J.P. 2008, "Exploring the full spectrum of macrophage activation", *Nature Reviews Immunology,* vol. 8, no. 12, pp. 958-969.

Myllymäki, H., Bäuerlein, C.A. & Rämet, M. 2016, "The Zebrafish Breathes New Life into the Study of Tuberculosis", *Frontiers in Immunology,* vol. 7, pp. 196.

Myllymäki, H., Niskanen, M., Luukinen, H., Parikka, M. & Rämet, M. 2018, "Identification of protective postexposure mycobacterial vaccine antigens using an immunosuppression-based reactivation model in the zebrafish", *Disease Models & Mechanisms,* vol. 11, no. 3.

Myllymäki, H., Niskanen, M., Oksanen, K.E. & Rämet, M. 2015, "Animal models in tuberculosis research - where is the beef?", *Expert Opinion on Drug Discovery,* vol. 10, no. 8, pp. 871-883.

Nagata, S. 2018, "Xenopus laevis macrophage-like cells produce XCL-1, an intelectin family serum lectin that recognizes bacteria", *Immunology and Cell Biology,* .

Nasevicius, A. & Ekker, S.C. 2000, "Effective targeted gene 'knockdown' in zebrafish", *Nature genetics*, vol. 26, no. 2, pp. 216-220.

Nathan, C.F. & Hibbs, J.B. 1991, "Role of nitric oxide synthesis in macrophage antimicrobial activity", *Current Opinion in Immunology,* vol. 3, no. 1, pp. 65-70.

Nguyen-Chi, Mai, Béryl Laplace-Builhe, Jana Travnickova, Patricia Luz-Crawford, Gautier Tejedor, Quang Tien Phan, Isabelle Duroux-Richard, et al. 2015. "Identification of Polarized Macrophage Subsets in Zebrafish." *eLife* 4: e07288. doi:10.7554/eLife.07288.

Nickless, A., Bailis, J.M. & You, Z. 2017, "Control of gene expression through the nonsense-mediated RNA decay pathway", *Cell & Bioscience,* vol. 7, pp. 26.

North, R.J. 1973, "Importance of thymus-derived lymphocytes in cell-mediated immunity to infection", *Cellular Immunology,* vol. 7, no. 1, pp. 166-176.

Noss, E.H., Harding, C.V. & Boom, W.H. 2000, "Mycobacterium tuberculosis inhibits MHC class II antigen processing in murine bone marrow macrophages", *Cellular Immunology,* vol. 201, no. 1, pp. 63-74.

Oksanen, A., Aittomäki, S., Jankovic, D., Ortutay, Z., Pulkkinen, K., Hämäläinen, S., Rokka, A., Corthals, G.L., Watford, W.T., Junttila, I., O'Shea, J.J. & Pesu, M. 2014, "Proprotein convertase FURIN constrains Th2 differentiation and is critical for host resistance against Toxoplasma gondii", *Journal of Immunology (Baltimore, Md.: 1950),* vol. 193, no. 11, pp. 5470-5479.

Onwubalili, J.K., Scott, G.M. & Robinson, J.A. 1985, "Deficient immune interferon production in tuberculosis", *Clinical and Experimental Immunology,* vol. 59, no. 2, pp. 405-413.

Orme, I.M. & Collins, F.M. 1983, "Protection against Mycobacterium tuberculosis infection by adoptive immunotherapy. Requirement for T cell-deficient recipients", *The Journal of Experimental Medicine,* vol. 158, no. 1, pp. 74-83.

Parikka, M., Hammaren, M.M., Harjula, S.K., Halfpenny, N.J., Oksanen, K.E., Lahtinen, M.J., Pajula, E.T., Iivanainen, A., Pesu, M. & Ramet, M. 2012, "Mycobacterium marinum causes a latent infection that can be reactivated by gamma irradiation in adult zebrafish", *PLoS pathogens,* vol. 8, no. 9, pp. e1002944.

Peatman, E., Baoprasertkul, P., Terhune, J., Xu, P., Nandi, S., Kucuktas, H., Li, P., Wang, S., Somridhivej, B., Dunham, R. & Liu, Z. 2007, "Expression analysis of the acute phase response in channel catfish (Ictalurus punctatus) after infection with a Gram-negative bacterium", *Developmental and Comparative Immunology,* vol. 31, no. 11, pp. 1183-1196.

Pemberton, A.D., Knight, P.A., Gamble, J., Colledge, W.H., Lee, J., Pierce, M. & Miller, H.R.P. 2004, "Innate BALB/c enteric epithelial responses to Trichinella spiralis: inducible expression of a novel goblet cell lectin, intelectin-2, and its natural deletion in C57BL/10 mice", *Journal of Immunology (Baltimore, Md.: 1950),* vol. 173, no. 3, pp. 1894-1901.

Peña, J.C. & Ho, W. 2015, "Monkey models of tuberculosis: lessons learned", *Infection and Immunity,* vol. 83, no. 3, pp. 852-862.

Pesu, M., Muul, L., Kanno, Y. & O'Shea, J.J. 2006, "Proprotein convertase furin is preferentially expressed in T helper 1 cells and regulates interferon gamma", *Blood,* vol. 108, no. 3, pp. 983-985.

Pesu, M., Watford, W.T., Wei, L., Xu, L., Fuss, I., Strober, W., Andersson, J., Shevach, E.M., Quezado, M., Bouladoux, N., Roebroek, A., Belkaid, Y., Creemers, J. & O'Shea, J.J. 2008, "T-cell-expressed proprotein convertase furin is essential for maintenance of peripheral immune tolerance", *Nature,* vol. 455, no. 7210, pp. 246-250.

Philips, J.A. & Ernst, J.D. 2012, "Tuberculosis Pathogenesis and Immunity", *Annual Review of Pathology: Mechanisms of Disease, Vol 7,* vol. 7, pp. 353-384.

Pollock, K.M., Whitworth, H.S., Montamat-Sicotte, D.J., Grass, L., Cooke, G.S., Kapembwa, M.S., Kon, O.M., Sampson, R.D., Taylor, G.P. & Lalvani, A. 2013, "T-cell immunophenotyping distinguishes active from latent tuberculosis", *The Journal of Infectious Diseases,* vol. 208, no. 6, pp. 952-968.

Porteus, M.H. & Baltimore, D. 2003, "Chimeric nucleases stimulate gene targeting in human cells", *Science (New York, N.Y.),* vol. 300, no. 5620, pp. 763.

Pourcel, C., Salvignol, G. & Vergnaud, G. 2005, "CRISPR elements in Yersinia pestis acquire new repeats by preferential uptake of bacteriophage DNA, and provide additional tools for evolutionary studies", *Microbiology (Reading, England),* vol. 151, no. Pt 3, pp. 653-663.

Prouty, M.G., Correa, N.E., Barker, L.P., Jagadeeswaran, P. & Klose, K.E. 2003, "Zebrafish-Mycobacterium marinum model for mycobacterial pathogenesis", *FEMS microbiology letters,* vol. 225, no. 2, pp. 177-182.

Qin, G., Taylor, M., Ning, Y.Y., Iversen, P. & Kobzik, L. 2000, "In vivo evaluation of a morpholino antisense oligomer directed against tumor necrosis factor-alpha", *Antisense & Nucleic Acid Drug Development,* vol. 10, no. 1, pp. 11-16.

Quinn, K.M., McHugh, R.S., Rich, F.J., Goldsack, L.M., de Lisle, G.W., Buddle, B.M., Delahunt, B. & Kirman, J.R. 2006, "Inactivation of CD4+ CD25+ regulatory T cells during early mycobacterial infection increases cytokine production but does not affect pathogen load", *Immunology and Cell Biology,* vol. 84, no. 5, pp. 467-474.

Ramakrishnan, L., Valdivia, R.H., McKerrow, J.H. & Falkow, S. 1997, "Mycobacterium marinum causes both long-term subclinical infection and acute disease in the leopard frog (Rana pipiens)", *Infection and Immunity,* vol. 65, no. 2, pp. 767-773.

Ramakrishnan, L. 2012, "Revisiting the role of the granuloma in tuberculosis", *Nature Reviews. Immunology,* vol. 12, no. 5, pp. 352-366.

Ran, F.A., Hsu, P.D., Wright, J., Agarwala, V., Scott, D.A. & Zhang, F. 2013, "Genome engineering using the CRISPR-Cas9 system", *Nature Protocols,* vol. 8, no. 11, pp. 2281-2308.

Rangaka, M.X., Cavalcante, S.C., Marais, B.J., Thim, S., Martinson, N.A., Swaminathan, S. & Chaisson, R.E. 2015, "Controlling the seedbeds of tuberculosis: diagnosis and treatment of tuberculosis infection", *Lancet (London, England),* vol. 386, no. 10010, pp. 2344-2353.

Ranta, N., Valli, A., Grönholm, A., Silvennoinen, O., Isomäki, P., Pesu, M. & Pertovaara, M. 2018, "Proprotein convertase enzyme FURIN is upregulated in primary Sjögren's syndrome", *Clinical and Experimental Rheumatology,* vol. 36 Suppl 112, no. 3, pp. 47-50.

Reiley, W.W., Calayag, M.D., Wittmer, S.T., Huntington, J.L., Pearl, J.E., Fountain, J.J., Martino, C.A., Roberts, A.D., Cooper, A.M., Winslow, G.M. & Woodland, D.L. 2008, "ESAT-6-specific CD4 T cell responses to aerosol Mycobacterium tuberculosis infection are initiated in the mediastinal lymph nodes", *Proceedings of the National Academy of Sciences of the United States of America,* vol. 105, no. 31, pp. 10961-10966.

Renshaw, S.A. & Trede, N.S. 2012, "A model 450 million years in the making: zebrafish and vertebrate immunity", *Disease models & mechanisms,* vol. 5, no. 1, pp. 38-47.

Rhodes, J., Hagen, A., Hsu, K., Deng, M., Liu, T.X., Look, A.T. & Kanki, J.P. 2005, "Interplay of pu.1 and gata1 determines myelo-erythroid progenitor cell fate in zebrafish", *Developmental Cell,* vol. 8, no. 1, pp. 97-108.

Robu, M.E., Larson, J.D., Nasevicius, A., Beiraghi, S., Brenner, C., Farber, S.A. & Ekker, S.C. 2007, "p53 activation by knockdown technologies", *PLoS genetics,* vol. 3, no. 5, pp. e78.

Roca, F.J. & Ramakrishnan, L. 2013, "TNF dually mediates resistance and susceptibility to mycobacteria via mitochondrial reactive oxygen species", *Cell,* vol. 153, no. 3, pp. 521-534.

Rodrigues, L.C., Diwan, V.K. & Wheeler, J.G. 1993, "Protective effect of BCG against tuberculous meningitis and miliary tuberculosis: a meta-analysis", *International Journal of Epidemiology,* vol. 22, no. 6, pp. 1154-1158.

Roe, J.K., Thomas, N., Gil, E., Best, K., Tsaliki, E., Morris-Jones, S., Stafford, S., Simpson, N., Witt, K.D., Chain, B., Miller, R.F., Martineau, A. & Noursadeghi, M. 2016, "Blood transcriptomic diagnosis of pulmonary and extrapulmonary tuberculosis", *JCI insight,* vol. 1, no. 16, pp. e87238.

Roebroek, A.J., Umans, L., Pauli, I.G., Robertson, E.J., van Leuven, F., Van de Ven, W J & Constam, D.B. 1998, "Failure of ventral closure and axial rotation in embryos lacking the proprotein convertase Furin", *Development (Cambridge, England),* vol. 125, no. 24, pp. 4863-4876.

Roebroek, A.J., Schalken, J.A., Leunissen, J.A., Onnekink, C., Bloemers, H.P. & Van de Ven, W. J. 1986, "Evolutionary conserved close linkage of the c-fes/fps proto-oncogene and genetic sequences encoding a receptor-like protein", *The EMBO journal,* vol. 5, no. 9, pp. 2197-2202.

Rossi, A., Kontarakis, Z., Gerri, C., Nolte, H., Hölper, S., Krüger, M. & Stainier, D.Y.R. 2015, "Genetic compensation induced by deleterious mutations but not gene knockdowns", *Nature,* vol. 524, no. 7564, pp. 230-233.

Rougeot, J., Zakrzewska, A., Kanwal, Z., Jansen, H.J., Spaink, H.P. & Meijer, A.H. 2014, "RNA sequencing of FACS-sorted immune cell populations from zebrafish infection models to identify cell specific responses to intracellular pathogens", *Methods in Molecular Biology (Clifton, N.J.),* vol. 1197, pp. 261-274.

Rounioja, S., Saralahti, A., Rantala, L., Parikka, M., Henriques-Normark, B., Silvennoinen, O. & Rämet, M. 2012, "Defense of zebrafish embryos against Streptococcus pneumoniae infection is dependent on the phagocytic activity of leukocytes", *Developmental and Comparative Immunology,* vol. 36, no. 2, pp. 342-348.

Sander, J.D., Cade, L., Khayter, C., Reyon, D., Peterson, R.T., Joung, J.K. & Yeh, J.J. 2011, "Targeted gene disruption in somatic zebrafish cells using engineered TALENs", *Nature Biotechnology,* vol. 29, no. 8, pp. 697-698.

Scott-Browne, J.P., Shafiani, S., Tucker-Heard, G., Ishida-Tsubota, K., Fontenot, J.D., Rudensky, A.Y., Bevan, M.J. & Urdahl, K.B. 2007, "Expansion and function of Foxp3-expressing T regulatory cells during tuberculosis", *The Journal of experimental medicine,* vol. 204, no. 9, pp. 2159-2169.

Seeger, A., Mayer, W.E. & Klein, J. 1996, "A complement factor B-like cDNA clone from the zebrafish (Brachydanio rerio)", *Molecular Immunology,* vol. 33, no. 6, pp. 511-520.

Seidah, N.G. & Prat, A. 2012, "The biology and therapeutic targeting of the proprotein convertases", *Nature reviews.Drug discovery,* vol. 11, no. 5, pp. 367-383.

Selvaraj, P., Narayanan, P.R. & Reetha, A.M. 1999, "Association of functional mutant homozygotes of the mannose binding protein gene with susceptibility to pulmonary tuberculosis in India", *Tubercle and Lung Disease: The Official Journal of the International Union Against Tuberculosis and Lung Disease,* vol. 79, no. 4, pp. 221-227.

Sharon, N. & Lis, H. 2004, "History of lectins: from hemagglutinins to biological recognition molecules", *Glycobiology,* vol. 14, no. 11, pp. 62R.

Shimokata, K., Kawachi, H., Kishimoto, H., Maeda, F. & Ito, Y. 1982, "Local cellular immunity in tuberculous pleurisy", *The American Review of Respiratory Disease,* vol. 126, no. 5, pp. 822-824.

Skoura, E., Zumla, A. & Bomanji, J. 2015, "International journal of infectious diseases", *International journal of infectious diseases,* vol. 32, pp. 87-93.

Sørensen, T.I., Nielsen, G.G., Andersen, P.K. & Teasdale, T.W. 1988, "Genetic and environmental influences on premature death in adult adoptees", *The New England Journal of Medicine,* vol. 318, no. 12, pp. 727-732.

Stainier, D.Y.R., Raz, E., Lawson, N.D., Ekker, S.C., Burdine, R.D., Eisen, J.S., Ingham, P.W., Schulte-Merker, S., Yelon, D., Weinstein, B.M., Mullins, M.C., Wilson, S.W., Ramakrishnan, L., Amacher, S.L., Neuhauss, S.C.F., Meng, A., Mochizuki, N., Panula, P. & Moens, C.B. 2017, "Guidelines for morpholino use in zebrafish", *PLoS genetics,* vol. 13, no. 10, pp. e1007000.

Stamm, C.E., Collins, A.C. & Shiloh, M.U. 2015, "Sensing of Mycobacterium tuberculosis and consequences to both host and bacillus", *Immunological Reviews,* vol. 264, no. 1, pp. 204-219.

Stamm, L.M. & Brown, E.J. 2004, "Mycobacterium marinum: the generalization and specialization of a pathogenic mycobacterium", *Microbes and infection / Institut Pasteur,* vol. 6, no. 15, pp. 1418-1428.

Stockhammer, O.W., Rauwerda, H., Wittink, F.R., Breit, T.M., Meijer, A.H. & Spaink, H.P. 2010, "Transcriptome analysis of Traf6 function in the innate immune response of zebrafish embryos", *Molecular Immunology,* vol. 48, no. 1-3, pp. 179-190.

Sugimoto, K., Hui, S.P., Sheng, D.Z., Nakayama, M. & Kikuchi, K. 2017, "Zebrafish FOXP3 is required for the maintenance of immune tolerance", *Developmental and Comparative Immunology,* vol. 73, pp. 156-162.

Sullivan, C. & Kim, C.H. 2008, "Zebrafish as a model for infectious disease and immune function", *Fish & shellfish immunology,* vol. 25, no. 4, pp. 341-350.

Summerton, J. & Weller, D. 1997, "Morpholino antisense oligomers: design, preparation, and properties", *Antisense & Nucleic Acid Drug Development,* vol. 7, no. 3, pp. 187-195.

Suzuki, Y.A., Shin, K. & Lönnerdal, B. 2001, "Molecular cloning and functional expression of a human intestinal lactoferrin receptor", *Biochemistry,* vol. 40, no. 51, pp. 15771-15779.

Tailleux, L., Schwartz, O., Herrmann, J., Pivert, E., Jackson, M., Amara, A., Legres, L., Dreher, D., Nicod, L.P., Gluckman, J.C., Lagrange, P.H., Gicquel, B. & Neyrolles, O. 2003, "DC-SIGN is the major Mycobacterium tuberculosis receptor on human dendritic cells", *The Journal of Experimental Medicine,* vol. 197, no. 1, pp. 121-127.

Takano, T., Sha, Z., Peatman, E., Terhune, J., Liu, H., Kucuktas, H., Li, P., Edholm, E., Wilson, M. & Liu, Z. 2008, "The two channel catfish intelectin genes exhibit highly differential patterns of tissue expression and regulation after infection with Edwardsiella ictaluri", *Developmental and Comparative Immunology,* vol. 32, no. 6, pp. 693-705.

Talaat, A.M., Reimschuessel, R., Wasserman, S.S. & Trucksis, M. 1998, "Goldfish, Carassius auratus, a novel animal model for the study of Mycobacterium marinum pathogenesis", *Infection and Immunity,* vol. 66, no. 6, pp. 2938-2942.

Tang, R., Dodd, A., Lai, D., McNabb, W.C. & Love, D.R. 2007, "Validation of zebrafish (Danio rerio) reference genes for quantitative real-time RT-PCR normalization", *Acta Biochimica Et Biophysica Sinica,* vol. 39, no. 5, pp. 384-390.

Tanne, A., Ma, B., Boudou, F., Tailleux, L., Botella, H., Badell, E., Levillain, F., Taylor, M.E., Drickamer, K., Nigou, J., Dobos, K.M., Puzo, G., Vestweber, D., Wild, M.K., Marcinko, M., Sobieszczuk, P., Stewart, L., Lebus, D., Gicquel, B. & Neyrolles, O. 2009, "A murine DC-SIGN homologue contributes to early host defense against Mycobacterium tuberculosis", *The Journal of Experimental Medicine,* vol. 206, no. 10, pp. 2205-2220.

Tautz, D. 1992, "Problems and paradigms: Redundancies, development and the flow of information", *BioEssays,* vol. 14, no. 4, pp. 263-266.

Thomas, G. 2002, "Furin at the cutting edge: from protein traffic to embryogenesis and disease", *Nature Reviews. Molecular Cell Biology,* vol. 3, no. 10, pp. 753-766.

Thummel, R., Bailey, T.J. & Hyde, D.R. 2011, "In vivo electroporation of morpholinos into the adult zebrafish retina", *Journal of Visualized Experiments: JoVE,* , no. 58, pp. e3603.

Ting, L.M., Kim, A.C., Cattamanchi, A. & Ernst, J.D. 1999, "Mycobacterium tuberculosis inhibits IFN-gamma transcriptional responses without inhibiting activation of STAT1", *Journal of Immunology (Baltimore, Md.: 1950),* vol. 163, no. 7, pp. 3898-3906.

Tobin, D.M., Roca, F.J., Oh, S.F., McFarland, R., Vickery, T.W., Ray, J.P., Ko, D.C., Zou, Y., Bang, N.D., Chau, T.T., Vary, J.C., Hawn, T.R., Dunstan, S.J., Farrar, J.J., Thwaites, G.E., King, M.C., Serhan, C.N. & Ramakrishnan, L. 2012, "Host genotype-specific therapies can optimize the inflammatory response to mycobacterial infections", *Cell,* vol. 148, no. 3, pp. 434-446.

Tobin, D.M. & Ramakrishnan, L. 2008, "Comparative pathogenesis of Mycobacterium marinum and Mycobacterium tuberculosis", *Cellular Microbiology,* vol. 10, no. 5, pp. 1027-1039.

Tobin, D.M., Vary, J.C., Ray, J.P., Walsh, G.S., Dunstan, S.J., Bang, N.D., Hagge, D.A., Khadge, S., King, M., Hawn, T.R., Moens, C.B. & Ramakrishnan, L. 2010, "The lta4h locus modulates susceptibility to mycobacterial infection in zebrafish and humans", *Cell,* vol. 140, no. 5, pp. 717-730.

Tokunaga, Y., Shirouzu, M., Sugahara, R., Yoshiura, Y., Kiryu, I., Ototake, M., Nagasawa, T., Somamoto, T. & Nakao, M. 2017, "Comprehensive validation of T- and B-cell deficiency in rag1-null zebrafish: Implication for the robust innate defense mechanisms of teleosts", *Scientific Reports,* vol. 7, no. 1, pp. 7536.

Tønjum, T., Welty, D.B., Jantzen, E. & Small, P.L. 1998, "Differentiation of Mycobacterium ulcerans, M. marinum, and M. haemophilum: mapping of their relationships to M. tuberculosis by fatty acid profile analysis, DNA-DNA hybridization, and 16S rRNA gene sequence analysis", *Journal of Clinical Microbiology,* vol. 36, no. 4, pp. 918-925.

Traver, D., Paw, B.H., Poss, K.D., Penberthy, W.T., Lin, S. & Zon, L.I. 2003, "Transplantation and in vivo imaging of multilineage engraftment in zebrafish bloodless mutants", *Nature Immunology,* vol. 4, no. 12, pp. 1238-1246.

Trede, N.S., Langenau, D.M., Traver, D., Look, A.T. & Zon, L.I. 2004, "The use of zebrafish to understand immunity", *Immunity,* vol. 20, no. 4, pp. 367-379.

Trunz, B.B., Fine, P. & Dye, C. 2006, "Effect of BCG vaccination on childhood tuberculous meningitis and miliary tuberculosis worldwide: a meta-analysis and assessment of cost-effectiveness", *Lancet (London, England),* vol. 367, no. 9517, pp. 1173-1180.

Tsuji, S., Yamashita, M., Hoffman, D.R., Nishiyama, A., Shinohara, T., Ohtsu, T. & Shibata, Y. 2009, "Capture of heat-killed Mycobacterium bovis bacillus Calmette-Guérin by intelectin-1 deposited on cell surfaces", *Glycobiology,* vol. 19, no. 5, pp. 518-526.

Tuominen, V.J. & Isola, J. 2009, "The application of JPEG2000 in virtual microscopy", *Journal of Digital Imaging,* vol. 22, no. 3, pp. 250-258.

Turpeinen, H., Oksanen, A., Kivinen, V., Kukkurainen, S., Uusimaki, A., Ramet, M., Parikka, M., Hytonen, V.P., Nykter, M. & Pesu, M. 2013, "Proprotein Convertase Subtilisin/Kexin Type 7 (PCSK7) Is Essential for the Zebrafish Development and Bioavailability of Transforming Growth Factor beta1a (TGFbeta1a)", *The Journal of biological chemistry,* vol. 288, no. 51, pp. 36610-36623.

Turpeinen, H., Ortutay, Z. & Pesu, M. 2013, "Genetics of the first seven proprotein convertase enzymes in health and disease", *Current Genomics,* vol. 14, no. 7, pp. 453-467.

Turpeinen, H., Raitoharju, E., Oksanen, A., Oksala, N., Levula, M., Lyytikainen, L.P., Jarvinen, O., Creemers, J.W., Kahonen, M., Laaksonen, R., Pelto-Huikko, M., Lehtimaki, T. & Pesu, M. 2011, "Proprotein convertases in human atherosclerotic plaques: the overexpression of FURIN and its substrate cytokines BAFF and APRIL", *Atherosclerosis,* vol. 219, no. 2, pp. 799-806.

Turpeinen, H., Seppälä, I., Lyytikäinen, L., Raitoharju, E., Hutri-Kähönen, N., Levula, M., Oksala, N., Waldenberger, M., Klopp, N., Illig, T., Mononen, N., Laaksonen, R., Raitakari, O., Kähönen, M., Lehtimäki, T. & Pesu, M. 2015, "A genome-wide expression quantitative trait loci analysis of proprotein convertase subtilisin/kexin enzymes identifies a novel regulatory gene variant for FURIN expression and blood pressure", *Human Genetics,* vol. 134, no. 6, pp. 627-636.

Uusi-Mäkelä, M.I.E., Barker, H.R., Bäuerlein, C.A., Häkkinen, T., Nykter, M. & Rämet, M. 2018, "Chromatin accessibility is associated with CRISPR-Cas9 efficiency in the zebrafish (Danio rerio)", *PloS One,* vol. 13, no. 4, pp. e0196238.

Valli, A., Ranta, N., Grönholm, A., Silvennoinen, O., Pesu, M. & Isomäki, P. 2018, "Increased expression of the proprotein convertase enzyme FURIN in rheumatoid arthritis", *Scandinavian Journal of Rheumatology,* vol. 0, no. 0, pp. 1-5.

van Crevel, R., Ottenhoff, T. & Van Der Meer, J. 2003, "Innate immunity to Mycobacterium tuberculosis", *Tropical Diseases: from Molecule to Bedside,* vol. 531, pp. 241-247.

van der Sar, Astrid M., Stockhammer, O.W., van der Laan, C., Spaink, H.P., Bitter, W. & Meijer, A.H. 2006, "MyD88 innate immune function in a zebrafish embryo infection model", *Infection and Immunity,* vol. 74, no. 4, pp. 2436-2441.

van der Sar, Astrid M, Spaink, H.P., Zakrzewska, A., Bitter, W. & Meijer, A.H. 2009, "Specificity of the zebrafish host transcriptome response to acute and chronic mycobacterial infection and the role of innate and adaptive immune components", *Molecular Immunology,* vol. 46, no. 11-12, pp. 2317-2332.

van der Vaart, M., Spaink, H.P. & Meijer, A.H. 2012, "Pathogen recognition and activation of the innate immune response in zebrafish", *Advances in Hematology,* vol. 2012, pp. 159807.

van der Vaart, M., van Soest, J.J., Spaink, H.P. & Meijer, A.H. 2013, "Functional analysis of a zebrafish myd88 mutant identifies key transcriptional components of the innate immune system", *Disease Models & Mechanisms,* vol. 6, no. 3, pp. 841-854.

van der Wel, N., Hava, D., Houben, D., Fluitsma, D., van Zon, M., Pierson, J., Brenner, M. & Peters, P.J. 2007, "M. tuberculosis and M. leprae translocate from the phagolysosome to the cytosol in myeloid cells", *Cell,* vol. 129, no. 7, pp. 1287-1298.

Varshney, G.K., Pei, W., LaFave, M.C., Idol, J., Xu, L., Gallardo, V., Carrington, B., Bishop, K., Jones, M., Li, M., Harper, U., Huang, S.C., Prakash, A., Chen, W., Sood, R., Ledin, J. & Burgess, S.M. 2015, "High-throughput gene targeting and phenotyping in zebrafish using CRISPR/Cas9", *Genome Research,* vol. 25, no. 7, pp. 1030-1042.

Voehringer, D., Stanley, S.A., Cox, J.S., Completo, G.C., Lowary, T.L. & Locksley, R.M. 2007, "Nippostrongylus brasiliensis: identification of intelectin-1 and -2 as Stat6-dependent genes expressed in lung and intestine during infection", *Experimental Parasitology,* vol. 116, no. 4, pp. 458-466.

Volkman, H.E., Clay, H., Beery, D., Chang, J.C.W., Sherman, D.R. & Ramakrishnan, L. 2004, "Tuberculous granuloma formation is enhanced by a mycobacterium virulence determinant", *PLoS biology,* vol. 2, no. 11, pp. e367.

Vordermeier, H.M., Venkataprasad, N., Harris, D.P. & Ivanyi, J. 1996, "Increase of tuberculous infection in the organs of B cell-deficient mice", *Clinical and Experimental Immunology,* vol. 106, no. 2, pp. 312-316.

Voss, G., Casimiro, D., Neyrolles, O., Williams, A., Kaufmann, S.H.E., McShane, H., Hatherill, M. & Fletcher, H.A. 2018, "Progress and challenges in TB vaccine development", *F1000Research,* vol. 7, no. 199, pp. 199.

Walker, M.B., Miller, C.T., Coffin Talbot, J., Stock, D.W. & Kimmel, C.B. 2006, "Zebrafish furin mutants reveal intricacies in regulating Endothelin1 signaling in craniofacial patterning", *Developmental biology,* vol. 295, no. 1, pp. 194-205.

Walzl, G., Haks, M.C., Joosten, S.A., Kleynhans, L., Ronacher, K. & Ottenhoff, T.H.M. 2014, "Clinical immunology and multiplex biomarkers of human tuberculosis", *Cold Spring Harbor Perspectives in Medicine,* vol. 5, no. 4.

Wan, F., Hu, C., Ma, J., Gao, K., Xiang, L. & Shao, J. 2016, "Characterization of γδ T Cells from Zebrafish Provides Insights into Their Important Role in Adaptive Humoral Immunity", *Frontiers in Immunology,* vol. 7, pp. 675.

Watson, R.O., Manzanillo, P.S. & Cox, J.S. 2012, "Extracellular M. tuberculosis DNA targets bacteria for autophagy by activating the host DNA-sensing pathway", *Cell,* vol. 150, no. 4, pp. 803-815.

Watts, J.K. & Corey, D.R. 2012, "Silencing disease genes in the laboratory and the clinic", *The Journal of Pathology,* vol. 226, no. 2, pp. 365-379.

Wei, S., Zhou, J., Chen, X., Shah, R.N., Liu, J., Orcutt, T.M., Traver, D., Djeu, J.Y., Litman, G.W. & Yoder, J.A. 2007, "The zebrafish activating immune receptor Nitr9 signals via Dap12", *Immunogenetics,* vol. 59, no. 10, pp. 813-821.

Weiss, G. & Schaible, U.E. 2015, "Macrophage defense mechanisms against intracellular bacteria", *Immunological Reviews,* vol. 264, no. 1, pp. 182-203.

Wesener, D.A., Wangkanont, K., McBride, R., Song, X., Kraft, M.B., Hodges, H.L., Zarling, L.C., Splain, R.A., Smith, D.F., Cummings, R.D., Paulson, J.C., Forest, K.T. & Kiessling, L.L. 2015, "Recognition of microbial glycans by human intelectin-1", *Nature Structural & Molecular Biology,* vol. 22, no. 8, pp. 603-610.

Wolf, A.J., Desvignes, L., Linas, B., Banaiee, N., Tamura, T., Takatsu, K. & Ernst, J.D. 2008, "Initiation of the adaptive immune response to Mycobacterium tuberculosis depends on antigen production in the local lymph node, not the lungs", *The Journal of Experimental Medicine,* vol. 205, no. 1, pp. 105-115.

Woods, I.G. & Schier, A.F. 2008, "Targeted mutagenesis in zebrafish", *Nature Biotechnology,* vol. 26, no. 6, pp. 650-651.

World Health Organization. Global Tuberculosis Report. 2017. http://www.who.int/tb/publications/global_report/en/.

Yan, J., Xu, L., Zhang, Y., Zhang, C., Zhang, C., Zhao, F. & Feng, L. 2013, "Comparative genomic and phylogenetic analyses of the intelectin gene family: implications for their origin and evolution", *Developmental and Comparative Immunology,* vol. 41, no. 2, pp. 189-199.

Yang, C., Cambier, C.J., Davis, J.M., Hall, C.J., Crosier, P.S. & Ramakrishnan, L. 2012, "Neutrophils exert protection in the early tuberculous granuloma by oxidative killing of mycobacteria phagocytosed from infected macrophages", *Cell Host & Microbe,* vol. 12, no. 3, pp. 301-312.

Yang, Q., Xu, Q., Chen, Q., Li, J., Zhang, M., Cai, Y., Liu, H., Zhou, Y., Deng, G., Deng, Q., Zhou, B., Kornfeld, H. & Chen, X. 2015, "Discriminating Active Tuberculosis from Latent Tuberculosis Infection by flow cytometric measurement of CD161-expressing T cells", *Scientific Reports,* vol. 5, pp. 17918.

Yaniv, K., Isogai, S., Castranova, D., Dye, L., Hitomi, J. & Weinstein, B.M. 2006, "Live imaging of lymphatic development in the zebrafish", *Nature Medicine,* vol. 12, no. 6, pp. 711-716.

Yoder, J.A., Nielsen, M.E., Amemiya, C.T. & Litman, G.W. 2002, "Zebrafish as an immunological model system", *Microbes and Infection,* vol. 4, no. 14, pp. 1469-1478.

Yoon, S., Mitra, S., Wyse, C., Alnabulsi, A., Zou, J., Weerdenburg, E.M., van der Sar, Astrid M., Wang, D., Secombes, C.J. & Bird, S. 2015, "First Demonstration of Antigen Induced Cytokine Expression by CD4-1+ Lymphocytes in a Poikilotherm: Studies in Zebrafish (Danio rerio)", *PloS One,* vol. 10, no. 6, pp. e0126378.

Zhang, M., Gately, M.K., Wang, E., Gong, J., Wolf, S.F., Lu, S., Modlin, R.L. & Barnes, P.F. 1994, "Interleukin 12 at the site of disease in tuberculosis", *The Journal of Clinical Investigation,* vol. 93, no. 4, pp. 1733-1739.

Zhang, X., Liu, F., Li, Q., Jia, H., Pan, L., Xing, A., Xu, S. & Zhang, Z. 2014, "A proteomics approach to the identification of plasma biomarkers for latent tuberculosis infection", *Diagnostic Microbiology and Infectious Disease,* vol. 79, no. 4, pp. 432-437.

Zimmerli, S., Edwards, S. & Ernst, J.D. 1996, "Selective receptor blockade during phagocytosis does not alter the survival and growth of Mycobacterium tuberculosis in human macrophages", *American Journal of Respiratory Cell and Molecular Biology,* vol. 15, no. 6, pp. 760-770.

Zumla, A., Raviglione, M., Hafner, R. & von Reyn, C.F. 2013, "Tuberculosis", *The New England journal of medicine,* vol. 368, no. 8, pp. 745-755.

10 ORIGINAL COMMUNICATIONS

IAI Journals.ASM.org

The Proprotein Convertase Subtilisin/Kexin FurinA Regulates Zebrafish Host Response against *Mycobacterium marinum*

Markus J. T. Ojanen,[a] Hannu Turpeinen,[a] Zuzet M. Cordova,[a] Milka M. Hammarén,[a] Sanna-Kaisa E. Harjula,[a] Mataleena Parikka,[a] Mika Rämet,[a,b,c,d] Marko Pesu[a,e,f]

BioMediTech, University of Tampere, Tampere, Finland[a]; Department of Pediatrics, Tampere University Hospital, Tampere, Finland[b]; Department of Children and Adolescents, Oulu University Hospital, Oulu, Finland[c]; Department of Pediatrics, Medical Research Center Oulu, University of Oulu, Oulu, Finland[d]; Department of Dermatology, Tampere University Hospital, Tampere, Finland[e]; Fimlab Laboratories, Pirkanmaa Hospital District, Tampere, Finland[f]

Tuberculosis is a chronic bacterial disease with a complex pathogenesis. An effective immunity against *Mycobacterium tuberculosis* requires both the innate and adaptive immune responses, including proper T helper (Th) type 1 cell function. FURIN is a proprotein convertase subtilisin/kexin (PCSK) enzyme, which is highly expressed in Th1 type cells. *FURIN* expression in T cells is essential for maintaining peripheral immune tolerance, but its role in the innate immunity and infections has remained elusive. Here, we utilized *Mycobacterium marinum* infection models in zebrafish (*Danio rerio*) to investigate how *furin* regulates host responses against mycobacteria. In steady-state *furinA*$^{td204e/+}$ fish reduced *furinA* mRNA levels associated with low granulocyte counts and elevated Th cell transcription factor expressions. Silencing *furin* genes reduced the survival of *M. marinum*-infected zebrafish embryos. A mycobacterial infection upregulated *furinA* in adult zebrafish, and infected *furinA*$^{td204e/+}$ mutants exhibited a proinflammatory phenotype characterized by elevated *tumor necrosis factor a* (*tnfa*), *lymphotoxin alpha* (*lta*) and *interleukin 17a/f3* (*il17a/f3*) expression levels. The enhanced innate immune response in the *furinA*$^{td204e/+}$ mutants correlated with a significantly decreased bacterial burden in a chronic *M. marinum* infection model. Our data show that upregulated *furinA* expression can serve as a marker for mycobacterial disease, since it inhibits early host responses and consequently promotes bacterial growth in a chronic infection.

Tuberculosis (TB) is an epidemic infectious disease caused by the mycobacterial species *Mycobacterium tuberculosis* (1, 2). Circa 13% of the individuals with active TB were simultaneous carriers of the human immunodeficiency virus (HIV), and almost one-third of TB-associated deaths occurred among HIV$^+$ patients, demonstrating the critical role of cluster of differentiation 4 (CD4$^+$) T lymphocyte-mediated immunity in the control of *M. tuberculosis* infection (3, 4). More specifically, the adaptive immunity against TB is primarily mediated by T helper (Th) type 1 cells, as is suggested by the gene expression profile upon infection (5), as well as the infection-induced mortality of gamma interferon-deficient (6, 7) and interleukin-12 (IL-12)-deficient (8) mice.

The proprotein convertase subtilisin/kexin (PCSK) enzymes are a family of serine endoproteases with nine members in humans: PCSK1 and -2, FURIN, PCSK4 to -7, membrane-bound transcription factor peptidase site 1 (MBTPS1), and PCSK9 (9). Typically, PCSKs convert precursor proteins (proproteins) into their biologically active forms by cleaving them at specific target motifs made up of the basic amino acids lysine and arginine (9, 10). FURIN was the first identified mammalian PCSK and is present in vertebrates and many invertebrates (11, 12). A series of *in vitro* experiments have suggested a central role for FURIN in host defense because it proteolytically activates several immunoregulatory proproteins, such as membrane-inserted matrix metallopeptidase 14 (13) and integrins (9), as well as tumor necrosis factor (TNF) and transforming growth factor beta (TGFB) family cytokines (e.g., the TNF superfamily, member 13b, and TGFB1) (12). In addition, infectious agents, including bacterial toxins (anthrax) and viral proteins (HIV gp160), are processed by FURIN (12).

Previously, we and others have shown that *FURIN* is predominantly expressed in Th1 cells and that *FURIN* expression is induced in activated CD4$^+$ T lymphocytes and myeloid cells (14–17). Our functional analyses using mice with a tissue-specific deletion of *Furin* in T cells (CD4cre-fur$^{fl/fl}$) further demonstrated that FURIN is essential for the adequate maturation of proTGFB1 and for T regulatory (Treg) cell-mediated immune suppression *in vivo* (18). The breakage of peripheral immune tolerance in CD4cre-fur$^{fl/fl}$ mice resulted in an age-related progression of a systemic autoimmune disease characterized by excessive numbers of overtly activated CD4$^+$ and CD8$^+$ T cells and an increase in proinflammatory cytokine production. In line with the critical role of FURIN in immune suppression, the administration of exogenous recombinant FURIN can alleviate autoimmunity in an experimental arthritis model (19). Notably, as a germ line *Furin* gene knockout (KO) in mice is lethal during embryonic development (20), the systemic role of FURIN in immune regulation and infections is still poorly understood.

Zebrafish (*Danio rerio*) is a small nonmammalian vertebrate model organism, with humoral and cellular components of the

Received 30 December 2014 **Returned for modification** 12 January 2015
Accepted 19 January 2015

Accepted manuscript posted online 26 January 2015

Citation Ojanen MJT, Turpeinen H, Cordova ZM, Hammarén MM, Harjula S-KE, Parikka M, Rämet M, Pesu M. 2015. The proprotein convertase subtilisin/kexin FurinA regulates zebrafish host response against *Mycobacterium marinum*. Infect Immun 83:1431–1442. doi:10.1128/IAI.03135-14.

Editor: S. Ehrt

Address correspondence to Marko Pesu, marko.pesu@uta.fi.

Supplemental material for this article may be found at http://dx.doi.org/10.1128/IAI.03135-14.

doi:10.1128/IAI.03135-14

innate and adaptive immune systems similar to those of humans (21–24). *Mycobacterium marinum*, a close relative of *M. tuberculosis*, is a natural zebrafish pathogen and causes a mycobacterial disease, which shares the main pathological and histological features of human TB (25, 26). Consequently, an *M. marinum* infection in fish is considered a relevant, cost-effective and ethical tool for studying the human mycobacterial disease. Both embryo and adult zebrafish infection models are now well established; while embryos can be used to specifically investigate innate immune responses (27, 28), the adult model enables the study of a chronic progressive mycobacterial infection, as well as spontaneous latency (25, 29).

Genetic variation affects TB susceptibility in humans. To study mutant phenotypes of selected host genes, a large collection of mutant zebrafish strains is available (Zebrafish Mutation Project, Wellcome Trust Sanger Institute, Cambridge, United Kingdom). Zebrafish has two *FURIN* orthologs: *furinA* and *furinB*. *furinA*, like the mammalian *FURIN* gene, has a critical, nonredundant role in organism development (30). Here, we have silenced the expression of *furin* genes in developing fish and used a *furinA*$^{td204e/+}$ mutant zebrafish strain to study how FurinA regulates the development of adult zebrafish immune cells and the host response against mycobacteria.

MATERIALS AND METHODS

Zebrafish lines and maintenance. Nine- to 16-month-old zebrafish were used in the adult experiments. *furinA*^{td204e} mutation-bearing zebrafish in an AB genetic background (Zebrafish Information Network [ZFIN] ID: ZDB-GENO-080606-310) were purchased from the Zebrafish International Resource Center (Oregon). The genotypes of the *furinA*$^{td204e/+}$ mutant zebrafish and their wild-type (WT) siblings were confirmed by sequencing (30). The fish were kept in a standardized flowthrough system (Aquatic Habitats, Florida, USA) with a light/dark cycle of 14 h and 10 h and fed with SDS 400 food twice a day. Until 7 days postfertilization (dpf), embryos were grown according to standard protocols in embryo medium (E3) at 28.5°C. The zebrafish housing, care, and all experiments have been approved by the National Animal Experiment Board of Finland (permits LSLH-2007-7254/Ym-23, ESAVI/6407/04.10.03/2012, ESAVI/733/04.10.07/2013, ESAVI/2267/04.10.03/2012, and ESAVI/8125/04.10.07/2013).

Flow cytometry. Zebrafish were euthanized in a 0.04% 3-aminobenzoic acid ethyl ester anesthetic (pH 7.0; Sigma-Aldrich, Missouri, USA), and kidneys were isolated and homogenized into a single-cell suspension of phosphate-buffered saline with 0.5% fetal bovine serum (Gibco/Invitrogen, California, USA). Relative amounts of blood cell precursors, erythrocytes, granulocytes, and lymphocytes were determined by flow cytometry in steady-state (uninfected) *furinA*$^{td204e/+}$ mutants and WT controls by using a FACSCanto II (Becton Dickinson, New Jersey, USA). The data were analyzed with the FlowJo program (v7.5; Tree Star, Inc., Oregon, USA). Hematopoietic cell types were identified based on granularity (side scatter [SSC]) and particle size (forward scatter [FSC]) (31). Granulocytes and lymphocytes for *furinA* expression analyses were purified from WT AB zebrafish kidneys by using flow cytometric sorting with a FACSAria I apparatus (Becton Dickinson).

Experimental infections in adult zebrafish. *M. marinum* (ATCC 927 strain) was cultured and the inoculation performed as described previously (25). In brief, the zebrafish were anesthetized with 0.02% 3-aminobenzoic acid ethyl ester and various amounts of *M. marinum*, together with 0.3 mg/ml phenol red (Sigma-Aldrich), were injected intraperitoneally (i.p.) using an Omnican 100 (30-gauge) insulin needle (Braun, Melsungen, Germany). The *M. marinum* CFU used in the infections were verified by plating serial dilutions on 7H10 agar plates. Infected fish were tracked daily, and humane endpoint criteria of the national ethical board were monitored.

MO and *M. marinum* coinjections. Oligonucleotide sequences for *furinA* and *furinB* gene silencing morpholinos (MOs) and the injection protocol have been previously described (32). The injection volume was set to 2 nl, and 0.25 pmol of both *furinA* and *furinB* MOs or 0.5 pmol of RC MO was used. *M. marinum* was simultaneously coinjected into the yolk sac, and 2% polyvinylpyrrolidone was used as a carrier solution in the suspension (27, 33). Survival was analyzed daily with a visual inspection with an Olympus IX71 microscope.

Histology. The presence of *M. marinum* in infected adult zebrafish was verified with a histological analysis and Ziehl-Neelsen staining (25, 34). Uninfected controls were included to exclude background mycobacterial infection. Sections were visualized with an Olympus BX51 microscope and Olympus ColorView IIIu camera using a ×100 magnification or with a fully automated Objective Imaging Surveyor virtual slide scanner (Objective Imaging, Cambridge, United Kingdom). Digitization of scanned sample sections was done at a resolution of 0.4 μm per pixel using a 20× Plan Apochromatic microscope objective, and image data were converted to JPEG2000 format as described previously (35).

qRT-PCR. RNA and/or DNA was isolated from kidneys, lymphocytes, granulocytes, and the tissue homogenates of organs in the abdominal cavity using an RNeasy RNA purification kit (Qiagen, Hilden, Germany) or with an RNA-DNA coextraction method for TRIreagent (Molecular Research Center, Ohio, USA). The relative mRNA levels of target genes were quantified from cDNA with quantitative real-time PCR (qRT-PCR). The reverse transcription was done with an iScript Select cDNA synthesis kit (Bio-Rad, California, USA). Maxima SYBR green qPCR master mix (Fermentas, Burlington, Canada) and a CFX96 qPCR machine (Bio-Rad) were used. Primer sequences and ZFIN identification codes for the qRT-PCR-analyzed genes are listed in Table S1 in the supplemental material. The expression of target genes was normalized to the expression of *eukaryotic translation elongation factor 1 alpha 1, like 1* (*eef1a1l1* or *ef1a*) (36). Whenever the RNA-DNA coextraction method was used, the total DNA was isolated simultaneously with the RNA to quantify the *M. marinum* load in the fish with qRT-PCR (25). The results were analyzed with the Bio-Rad CFX Manager software v1.6 (Bio-Rad). No template control samples (H_2O) were included in all experiments to monitor contamination. Melting curve analyses, followed by 1.5% agarose (Bioline, London, United Kingdom) gel electrophoresis, were done to validate the qRT-PCR products of the target genes.

Statistical analysis. Statistical analyses were performed with the Prism v5.02 program (GraphPad Software, Inc., California, USA). A log-rank (Mantel-Cox) test was used in the survival experiments and a nonparametric Mann-Whitney analysis in the flow cytometry and qRT-PCR experiments. *P* values of <0.05 were considered significant.

RESULTS

***furinA* is upregulated in a mycobacterial infection and it controls granulopoiesis and Th cell transcription factor expression.** In the *furinA*^{td204e} mutant fish, a specific thymidine (T)-to-adenosine (A) splice site mutation results in a skipped exon 9 during the transcription of the *furinA* gene (see Fig. S1 in the supplemental material) (30). This leads to a loss-of-function FurinA mutant protein and enables the design of qRT-PCR primers, which can be used to specifically quantify native *furinA* mRNA molecules. In accordance with the developmental lethality of other homozygous *furinA* zebrafish mutants (>98% lethality of *furinA*$^{tg419/tg419}$ mutant) (30), no homozygous *furinA*$^{td204e/td204e}$ mutant fish could be obtained in our fish crosses (up to ~450 genotyped fish), suggesting that in homozygous form this allele is also lethal. In contrast, the heterozygous *furinA*$^{td204e/+}$ mutants were born in normal Mendelian ratios and did not show signs of developmental defects or spontaneous autoimmunity. First, to determine the effect of a heterozygous *furinA*^{td204e} mutation on mRNA levels, *furinA* expression in uninfected and *M. marinum*-infected adult fish (4 and

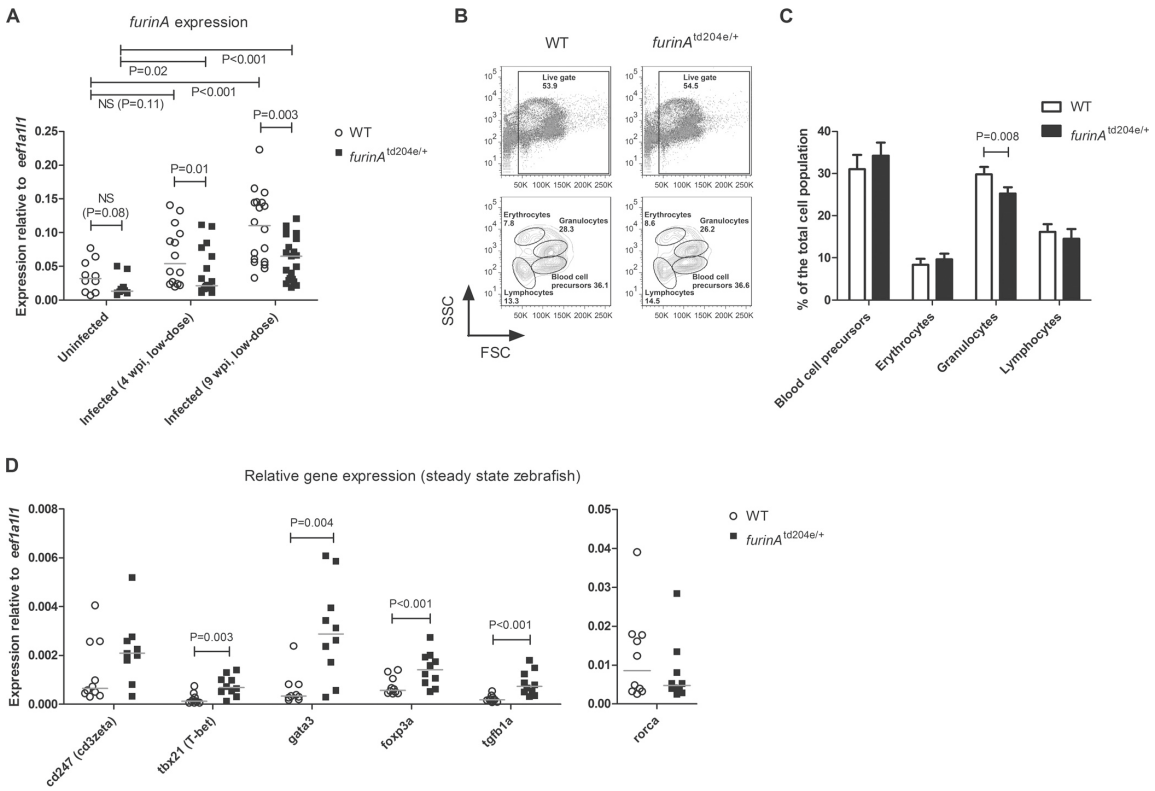

FIG 1 *furinA* expression is reduced in *furinA*$^{td204e/+}$ zebrafish and associates with decreased granulocyte counts, as well as altered T helper cell subtype transcription factor expression. (A) Relative *furinA* expression was measured in uninfected ($n = 10$) and *M. marinum*-infected (at 4 and 9 wpi, low-dose, $n = 13$ to 21) *furinA*$^{td204e/+}$ mutant adult zebrafish and WT controls with qRT-PCR. Samples were run as technical duplicates. (B and C) The relative percentages of blood cell precursors, erythrocytes, granulocytes, and lymphocytes were determined in the kidneys of steady-state (uninfected) *furinA*$^{td204e/+}$ mutants and WT zebrafish ($n = 5$ in both groups) with flow cytometry, based on granularity (SSC) and cell size (FSC). Representative flow cytometry plots are shown in panel B. Gated populations are outlined, and the cell counts inside the gates are given as the percentages of the total viable cell population. The average relative percentages of different hematopoietic cell populations in mutants and controls are plotted in panel C (error bars indicate the standard deviations). (D) Relative expressions of different Th cell-associated genes (*cd247*, *tbx21*, *gata3*, *foxp3a*, and *rorca*), as well as *tgfb1a*, were quantified in *furinA*$^{td204e/+}$ mutants and WT controls ($n = 10$ in both groups) with qRT-PCR. Gene expressions in panels A and D were normalized to *eef1a1l1* expression and represented as a scatter dot plot and median. In panel A, a one-tailed Mann-Whitney test was used in the statistical comparison of differences between *furinA*$^{td204e/+}$ zebrafish and WT controls, and a two-tailed Mann-Whitney test was used in panels C and D, as well as in the comparisons between uninfected and infected experimental groups in panel A.

9 weeks postinfection [wpi], low dose; 34 ± 10 CFU) was quantified with qRT-PCR (Fig. 1A). Previously, *in vitro* analyses have shown that *FURIN* expression is upregulated as a result of CD4$^+$ T cell activation and in lipopolysaccharide (LPS)-stimulated CD14$^+$ myeloid cells (14, 15). In accordance with this, the *M. marinum* infection caused an induction in *furinA* mRNA expression in both *furinA*$^{td204e/+}$ (1.6-fold at 4 wpi, $P = 0.02$, and 4.9-fold at 9 wpi, $P < 0.001$) and WT zebrafish (1.7-fold at 4 wpi, not significant [NS], $P = 0.11$; 3.4-fold at 9 wpi, $P < 0.001$) demonstrating that immune activation *in vivo* upregulates this convertase. Furthermore, in the infected groups, *furinA*$^{td204e/+}$ fish had on average 39% ($P = 0.01$) and 43% less ($P = 0.003$) *furinA* mRNA compared to WT controls at 4 and 9 wpi, respectively. A similar trend was also observed in uninfected zebrafish with a 44% decrease in *furinA* expression (NS, $P = 0.08$). Put together, the data indicate that *furinA* is upregulated in response to a mycobacterial infection, and that the *furinA*$^{td204e/+}$ zebrafish can be used to explore the functional role of this PCSK in a mycobacterial infection *in vivo*.

The development of hematopoietic cells in zebrafish is highly similar to that in humans (31, 37). To assess the effect of the reduced *furinA* expression on hematopoiesis in the *furinA*$^{td204e/+}$ fish, we studied their blood cell composition with flow cytometry (Fig. 1B and C) (31). The flow cytometric analysis revealed no marked differences in blood cell precursor, erythrocyte or lymphocyte populations in *furinA*$^{td204e/+}$ zebrafish compared to WT controls. However, the amount of granulocytes in *furinA*$^{td204e/+}$ fish was significantly decreased, by an average of 15.4% ($P = 0.008$), compared to controls, indicating a role for FurinA in granulopoiesis.

Previously, we showed that FURIN is critical for normal mammalian Th polarization and CD4$^+$ Treg cell function; CD4cre-fur$^{fl/fl}$ mice have abnormally large effector CD4$^+$ and Treg cell populations accompanied with an excessive production of Th1 and Th2 cytokines (15, 18). To address whether FurinA regulates the generation of Th subsets in zebrafish, we assessed the expression of different T cell markers (*CD247 antigen*; *cd247*, *T-box 21*;

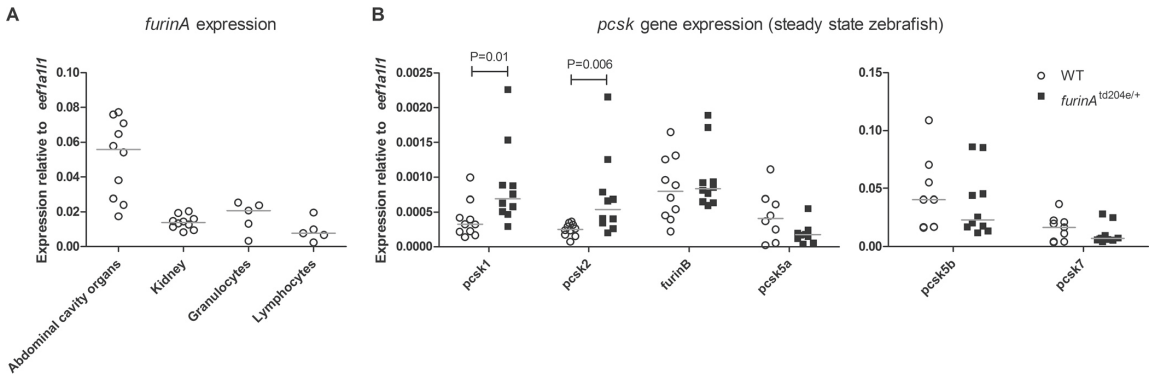

FIG 2 Expression of zebrafish *pcsk* genes in *furinA*$^{td204e/+}$ mutants and WT controls. (A) Relative *furinA* expression was measured with qRT-PCR in the tissue homogenates of organs in the abdominal cavity ($n = 10$) and kidney ($n = 10$) as well as in purified granulocytes ($n = 5$) and lymphocytes ($n = 5$) isolated from steady-state WT AB zebrafish. Samples were run as technical duplicates. (B) The relative expressions of zebrafish *pcsk* genes (*pcsk1*, *pcsk2*, *furinB*, *pcsk5a*, *pcsk5b*, and *pcsk7*) were quantified in the tissue homogenates of organs in the abdominal cavities of steady-state adult *furinA*$^{td204e/+}$ mutant ($n = 10$) and WT ($n = 8$ to 10) zebrafish by using qRT-PCR. Gene expressions were normalized to *eef1a1l1* expression and are represented as a scatter dot plot and median. A two-tailed Mann-Whitney test was used in the statistical comparison of differences.

tbx21, *gata3*, *forkhead box P3a*; *foxp3a*, *retinoic acid receptor-related orphan receptor C a*; *rorca*) in *furinA*$^{td204e/+}$ mutants and WT controls (Fig. 1D). As in T cell-specific FURIN conditional KO (cKO) mice, the mRNA levels of Th1, Th2, and the Treg cell markers *tbx21* (*T-bet*, $P = 0.003$), *gata3* ($P = 0.004$), and *foxp3a* ($P < 0.001$) were elevated in *furinA*$^{td204e/+}$ zebrafish. In contrast, there was no significant difference in the expression of the Th17 cell marker *rorca* between *furinA*$^{td204e/+}$ and WT zebrafish, which is in line with the normal IL-17 production previously observed in CD4cre-fur$^{fl/fl}$ mice (18).

TGFB1 directly induces *Furin* expression in rodents, which is a prerequisite for its functional maturation and anti-inflammatory function (18, 38). Consequently, the autoimmune phenotype of CD4cre-fur$^{fl/fl}$ mice can be chiefly attributed to a lack of bioavailable, T cell-produced TGFB1. In our present study, zebrafish FurinA was found to regulate *tgfb1a* expression *in vivo* (Fig. 1D), which could result from an attempt to compensate for the defective maturation of the Tgfb1a cytokine by increasing the efficiency of *tgfb1a* transcription.

The quantification of the *furinA* mRNA expression in WT zebrafish demonstrated that it is expressed in both innate and adaptive immune cells (Fig. 2A), which is in line with the previously reported ubiquitous expression pattern of *FURIN* orthologues in vertebrates (9, 32). In mammals, the first seven PCSK enzymes have been demonstrated to exhibit a significant functional redundancy and shared substrate molecules, which interferes with the interpretation of a PCSK specific phenotype (39). Therefore, we next addressed the expression of the zebrafish *pcsk* genes (*pcsk1*, *pcsk2*, *furinB*, *pcsk5a*, *pcsk5b*, and *pcsk7*) in *furinA*$^{td204e/+}$ mutants and WT controls (Fig. 2B). The *pcsk* genes *furinB*, *pcsk5a*, *pcsk5b*, and *pcsk7* showed comparable expression levels between *furinA*$^{td204e/+}$ and WT zebrafish, whereas *pcsk1* and *pcsk2* were significantly upregulated in the *furinA*$^{td204e/+}$ fish ($P = 0.01$ and $P = 0.006$, respectively), which theoretically could partially compensate for the effect of reduced *furinA* expression.

Furin regulates the survival of *M. marinum*-infected zebrafish embryos. Whereas upregulated T cell gene expression in *furinA*$^{td204e/+}$ zebrafish indicates enhanced immune responses, granulopenia can result in immunodeficiency. To study the net effect of FurinA on mycobacterial host defense in adult zebrafish, we infected *furinA*$^{td204e/+}$ and WT zebrafish with a high-dose of *M. marinum* (8,300 ± 1,800 CFU) and followed their survival for 11 weeks (Fig. 3A). WT fish exhibited ca. 60% mortality during the first 5 weeks and about one-third of them were alive at the study endpoint (Fig. 3A). *furinA*$^{td204e/+}$ mutants showed similar lethality, and no statistical difference in gross survival between mutant and WT fish could be detected. In addition, a histopathological examination revealed that the two fish groups had similarly organized granulomas at both 3 and 11 wpi, and there were no obvious differences in the numbers of granulomas (Fig. 3B). Uninfected WT and *furinA*$^{td204e/+}$ zebrafish controls did not show background mycobacteriosis in a Ziehl-Neelsen staining (data not shown).

Morpholino (MO)-based expression silencing in developing zebrafish embryos can be used to study a gene's function specifically in innate immune responses (22, 40). Since *furinA* regulated the granulopoiesis, we addressed its role in innate immunity by inhibiting the expressions of *furinA* and *furinB* in the embryonic *M. marinum* infection model (27, 32, 33). Infecting either control (random control MO injected [RC]) or the double *furin* gene knockdown embryos with *M. marinum* (131 ± 125 CFU) resulted in substantial lethality by 7 days postinfection (dpi; 93 and 100%, respectively, Fig. 3C). The survival of infected *furinA*+*B* morphants was, however, significantly reduced compared to controls (*furinA*+*B* versus RC, $P < 0.01$). Notably, as FurinA is essential for zebrafish development the increased lethality of *M. marinum*-infected *furin* morphant embryos could result from general developmental defects.

FurinA inhibits the early expression of proinflammatory cytokine genes in a mycobacterial infection. The containment of a mycobacterial disease is critically dependent on adaptive Th1 type responses but also on adequate innate immune responses. The significance of the innate immunity is perhaps best illustrated by an increased susceptibility to TB in patients receiving anti-TNF

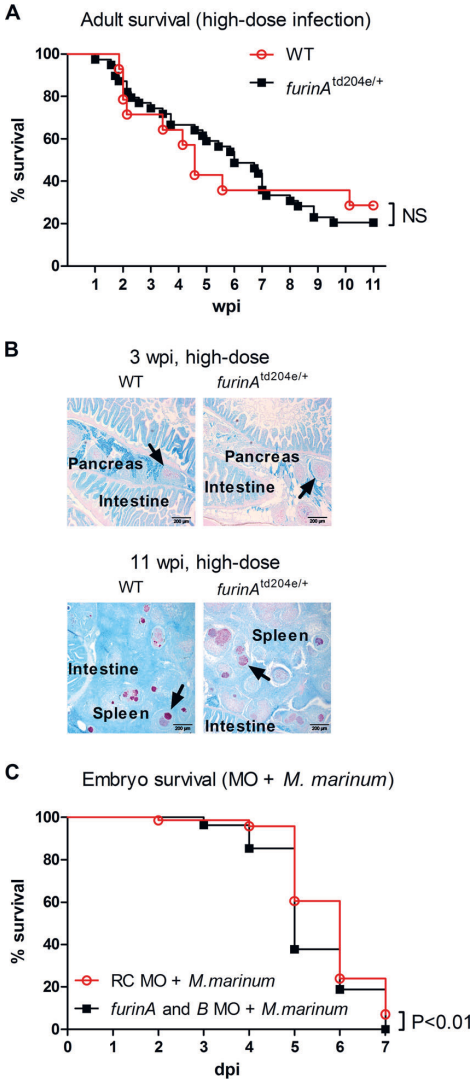

FIG 3 Role of *furin* in zebrafish survival during *M. marinum* infection. (A) The survival of adult *furinA*$^{td204e/+}$ ($n = 39$) and WT ($n = 14$) zebrafish was monitored for 11 weeks after an experimental high-dose *M. marinum* inoculate. The data were collected from a single experiment. (B) *M. marinum* granulomas in adult WT and *furinA*$^{td204e/+}$ zebrafish infected with a high-dose bacterial inoculate were identified with Ziehl-Neelsen staining at 3 wpi (17,300 ± 6,900 CFU) and 11 wpi (8,300 ± 1,800 CFU). Representative images from 4 to 10 individuals per group are shown. Typical granulomas are indicated with arrows. (C) Zebrafish embryos were microinjected before the four-cell stage with RC ($n = 71$) or both *furinA* and *furinB* MOs ($n = 82$) and *M. marinum* (131 ± 125 CFU). At 1 dpf, embryos were screened to identify successfully injected embryos, and survival was monitored up until 7 dpf. Collated data from two separate experiments with 30 and 41 embryos in the RC MO groups and 27 and 55 embryos in the *furinA* and *furinB* MO groups are shown. In panels A and C, a log-rank (Mantel-Cox) test was used for the statistical comparison of differences.

neutralizing antibodies and an association of human Toll-like receptor polymorphisms with an increased disease risk (4, 41, 42). FURIN can process target molecules that are important in innate immunity *in vitro* (e.g., TNF converting enzyme and Toll-like receptor 7) (43, 44), but whether it also regulates innate immune responses in infections *in vivo* has not been addressed. We next analyzed the early immune response against *M. marinum* by measuring the cytokine gene expression in *furinA*$^{td204e/+}$ fish and WT controls. Both *furinA*$^{td204e/+}$ and WT adult zebrafish were infected with a high dose of *M. marinum* (10,300 ± 3,300 CFU) and a qRT-PCR expression analysis of both proinflammatory (*tnfa*, *il1b*, *lta*, *ifng1-1*, *il22*, and *il17a/f3*) and anti-inflammatory (*il10* and *tgfb1a*) cytokine genes was performed at 1, 6, and 12 dpi (Fig. 4).

An analysis of the kinetics of the cytokine gene induction in WT fish (Fig. 4A) demonstrated that the expression levels of *tnfa*, *lta*, and *ifng1-1* were significantly upregulated upon *M. marinum* infection already at 1 dpi (15.1-, 5.5-, and 396.4-fold, respectively), with rising kinetics until 6 dpi (161.4-, 13.1-, and 478.8-fold, respectively). At 12 dpi, the induction of *tnfa* had declined to 110.3-fold, whereas *lta* and *ifng1-1* expressions had returned to their baseline levels. *il17a/f3* was also significantly induced at 1 dpi (18.0-fold), but its expression decreased during the following days (6 dpi, 7.7-fold; 12 dpi, baseline expression). In contrast, both *il1b* and *il22* showed a delayed expression pattern by peaking at 12 dpi (*il1b*, 2.3-fold; *il22*, 10.8-fold). The induction of the anti-inflammatory cytokine genes *il10* and *tgfb1a* was evident already by day 6 postinfection (*il10*, 2.4-fold; *tgfb1a*, 10.7-fold), and the expression of both genes was even more pronounced at 12 dpi (4.4- and 19.0-fold, respectively). In conclusion, an *M. marinum* infection in zebrafish results in an enhancement in the levels of various macrophage, natural killer cell, γδ T cell, and lymphoid tissue inducer cell-associated cytokines already during the first 12 days after infection, indicating an efficient activation of pro- and anti-inflammatory processes.

To determine how FurinA contributes to the early cytokine levels induced by *M. marinum*, we compared the expression of the aforementioned cytokine genes in infected *furinA*$^{td204e/+}$ and WT zebrafish (Fig. 4B to I). *furinA*$^{td204e/+}$ mutants showed a significantly higher relative expression of the proinflammatory cytokine genes *tnfa* ($P = 0.007$), *lta* ($P = 0.03$), and *il17a/f3* ($P = 0.002$) at 1 dpi compared to WT fish. Interestingly, the inherent relative upregulation of *tgfb1a* in *furinA*$^{td204e/+}$ mutants was completely abolished by the 12th postinfective day, and this was accompanied by a relative reduction in *il10* gene expression. The low *furinA* expression also associated with a sustained upregulation of the *il17a/f3* cytokine gene. Collectively, these results could indicate that inflammation-accelerating innate cytokine responses dominate in *M. marinum*-infected *furinA*$^{td204e/+}$ mutant fish. To demonstrate that FURIN attenuates proinflammatory responses specifically in innate immune cells, we used cultured macrophages from WT and LysMcre-fur$^{fl/fl}$ mice (Fig. 5) (45, 46). In these experiments we saw that in activated macrophages reduced *Furin* mRNA levels (77% decrease, $P = 0.004$) are associated with significantly upregulated transcription of the proinflammatory cytokine gene *Tnf* ($P = 0.03$).

***furinA*$^{td204e/+}$ mutants have decreased bacterial burden and *cd247* expression in a chronic *M. marinum* infection model.** We have recently established a model for studying a latent mycobacterial infection in adult zebrafish (25). A low-dose i.p. *M. mari-*

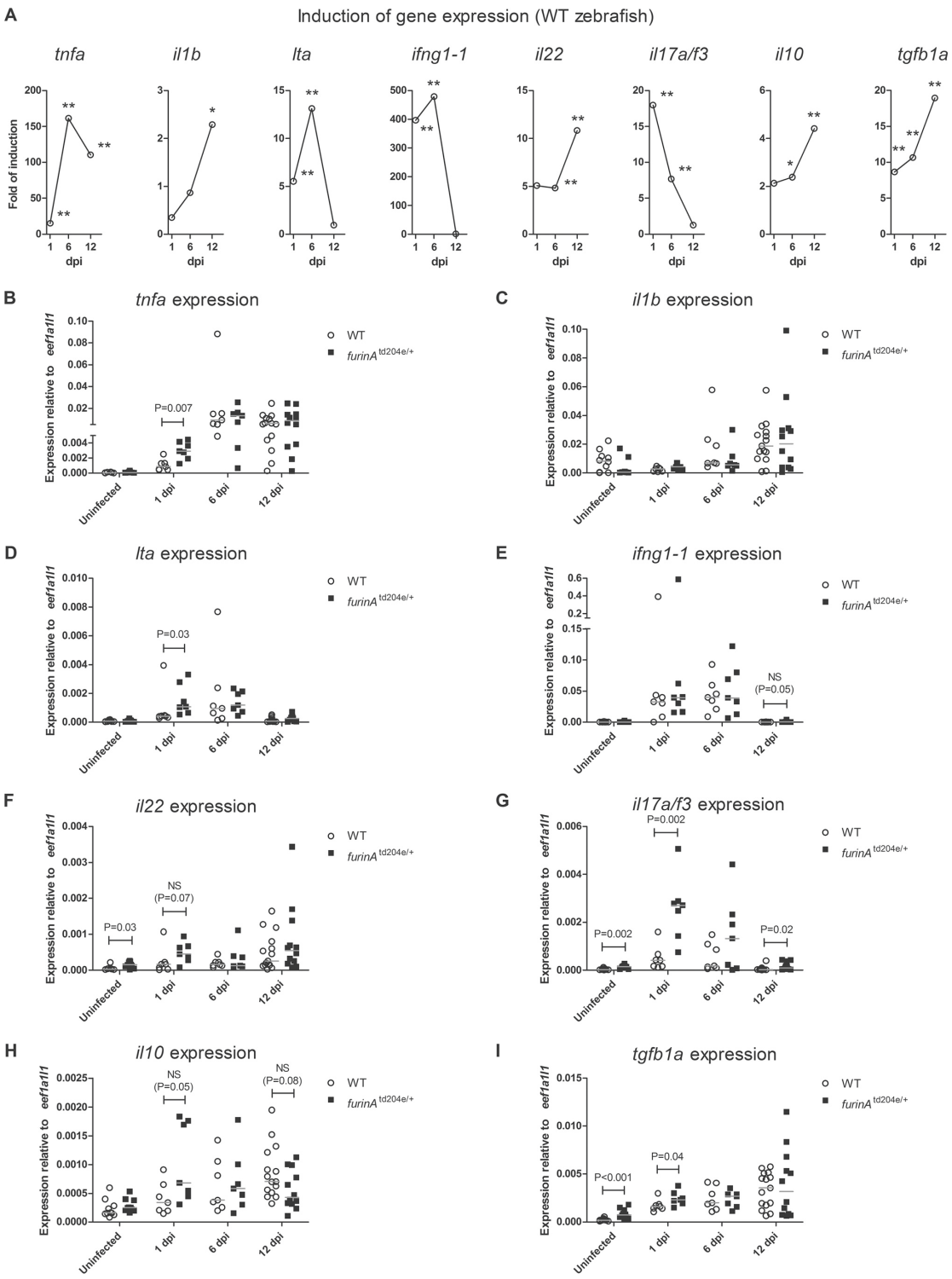

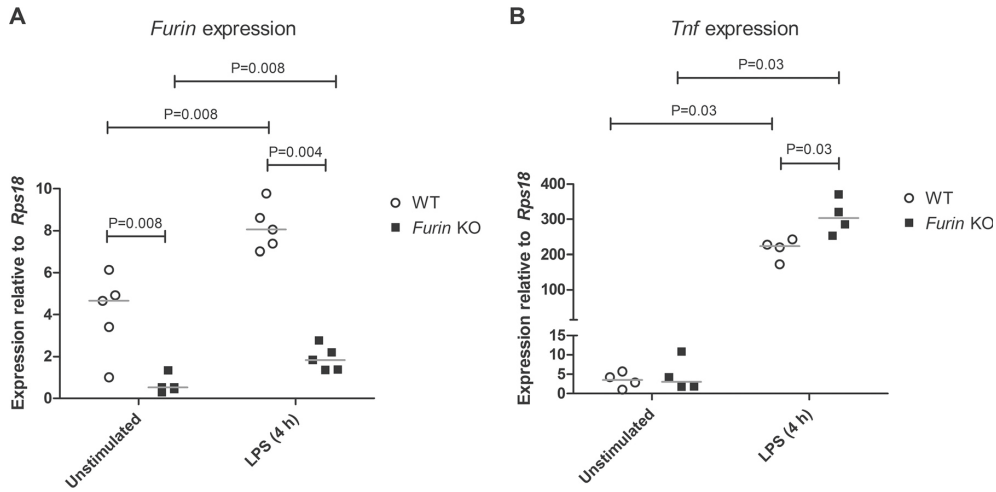

FIG 5 Reduced *Furin* expression is associated with an upregulated expression of *Tnf* in activated mouse macrophages. Bone marrow-derived macrophages were cultured from *Furin* KO (LysMcre-fur$^{fl/fl}$) and WT littermate mice ($n = 4$ to 5) as described previously (46). The relative expressions of *Furin* (Ensembl ID ENSMUSG00000030530) (A) and *Tnf* (Ensembl ID ENSMUSG00000024401) (B) were determined in unstimulated and LPS-stimulated (4 h) samples with qRT-PCR. Gene expressions were normalized to *ribosomal protein S18* (*Rps18*, Ensembl ID ENSMUSG00000008668) expression and are represented as a scatter dot plot and median. A two-tailed Mann-Whitney test was used in the statistical comparison of differences. The qRT-PCR primers used for the mouse genes were as follows: *Furin*, 5′-CAGAAGCATGGCTTCCACAAC-3′ and 5′-TGTCACTGCTCTGTGCCAGAA-3′; *Tnf*, 5′-CTTCTGTCTACTGAACTTCGGG-3′ and 5′-CAGGCTTGTCACTCGAATTTTG-3′; and *Rps18*, 5′-GTGATCCCTGAGAAGTTCCAG-3′ and 5′-TCGATGTCTGCTTTCCTCAAC-3′.

num inoculate (~35 CFU) results in static bacterial burdens, a constant number of granulomas, and low mortality. We thus utilized this model to investigate how FurinA contributes to the adaptive mycobacterial immunity and the development of mycobacterial latency. When *furinA*$^{td204e/+}$ mutant and WT control fish were infected with small amounts of *M. marinum* (46 ± 8 CFU) and survival was monitored for 9 weeks, statistically significant difference between the groups could not be observed (Fig. 6A). However, mycobacterial quantification revealed a trend of smaller bacterial amount in the *furinA*$^{td204e/+}$ mutants at 4 wpi (34 ± 10 CFU, NS) (Fig. 6B), but significantly reduced *M. marinum* copy numbers from the internal organ isolates of infected *furinA*$^{td204e/+}$ zebrafish compared to WT fish at 9 wpi (1.9-fold reduction, $P = 0.04$) (Fig. 6B). On average, bacterial copy number medians at 9 wpi were 11,000 (13 copies in 100 ng of zebrafish DNA) in *furinA*$^{td204e/+}$ mutants and 21,000 (50 copies in 100 ng of zebrafish DNA) in WT zebrafish, which suggests that *furinA* inhibits host responses in chronic mycobacterial infection.

The reduced mycobacterial load in latency could be a result of the upregulation of proinflammatory cytokines upon the *M. marinum* infection in *furinA*$^{td204e/+}$ mutant fish (Fig. 4B to G) but also a consequence of inherently accelerated T cell responses (Fig. 1D). To evaluate the T cell responses in latency, we quantified the relative expression of a general T cell marker *cd247* (*cd3zeta*) and Th cell subtype-associated transcription factors (*tbx21*, *gata3*, *foxp3a*, and *rorca*) in *furinA*$^{td204e/+}$ mutant and control fish at both 4 and 9 wpi (see Fig. S2 in the supplemental material and Fig. 6C). As expected, an infection-induced upregulation of these genes was seen in both WT and mutant zebrafish (at 4 wpi, 2.9- to 23.9-fold and 1.5- to 8.1-fold, respectively, and at 9 wpi, 4.2- to 19.0-fold and 2.5- to 8-fold, respectively), suggesting T cell activation. Interestingly, at 9 wpi, *cd247* expression was significantly lower in infected *furinA*$^{td204e/+}$ mutants compared to WT controls ($P = 0.03$), whereas the expression of the Th subset-associated transcription factors *tbx21*, *gata3*, *foxp3a*, and *rorca* did not differ between infected *furinA*$^{td204e/+}$ fish and controls. In addition, the expression levels of innate immunity cytokine genes (*tnfa*, *il1b*, *il10*, *tgfb1a*, *lta*, *ifng1-1*, and *il17a/f3*) were found to be similar between *furinA*$^{td204e/+}$ and WT fish (see Fig. S2 and S3 in the supplemental material), indicating that innate immune cell activity during a chronic *M. marinum* infection is FurinA independent.

Together, the reduced relative expression of *cd247* at 9 wpi and loss of upregulation of *tbx21*, *gata3*, and *foxp3a* in *furinA*$^{td204e/+}$ zebrafish compared to WT controls indicate that FurinA enhances T cell responses in a mycobacterial infection. However, *furinA*$^{td204e/+}$ mutants had lower *M. marinum* copy numbers,

FIG 4 FurinA attenuates the early expression of proinflammatory cytokine genes in an experimental high-dose mycobacterial infection. The relative expression of proinflammatory cytokine genes (*tnfa*, *il1b*, *lta*, *ifng1-1*, *il22*, and *il17a/f3*) and anti-inflammatory cytokine genes (*il10* and *tgfb1a*) was determined in adult *furinA*$^{td204e/+}$ ($n = 7$ to 12) and WT ($n = 7$ to 15) zebrafish with qRT-PCR after a high dose of an *M. marinum* inoculate at 1, 6, and 12 dpi. (A) Fold gene expression induction median shown for all of the aforementioned genes in infected WT zebrafish. The fold induction was normalized to the gene expression median in uninfected zebrafish. *, $P < 0.05$; **, $P < 0.01$. (B to I) Relative gene expression in *furinA*$^{td204e/+}$ and WT zebrafish represented as a scatter dot plot and median. Note the different scales of the *y* axes and the divided *y* axis in panels B and E. Gene expressions were normalized to *eef1a1l1* expression. At 1 and 6 dpi, samples were run as technical duplicates and uninfected, as well as 12-dpi, samples once. A two-tailed Mann-Whitney test was used in the statistical comparison of differences.

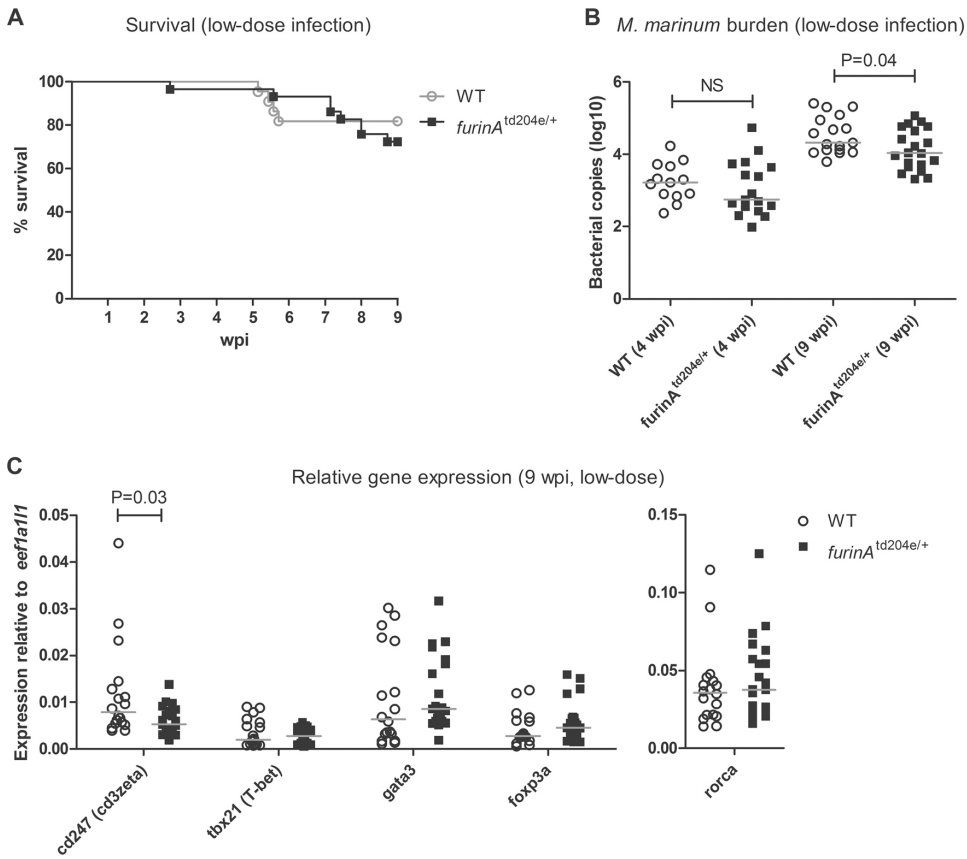

FIG 6 Downregulation of *furinA* expression decreases the *M. marinum* burden and the T cell marker *cd247* mRNA level in an experimental low-dose mycobacterial infection. A latent mycobacterial infection was induced with a low-dose *M. marinum* inoculate. (A) Survival of adult *furinA*$^{td204e/+}$ ($n = 29$) and WT ($n = 22$) zebrafish was monitored for 9 weeks. A log-rank (Mantel-Cox) test was used for the statistical comparison of differences. The data were collected from a single experiment. (B) The *M. marinum* burden of *furinA*$^{td204e/+}$ mutants ($n = 17$ to 20) and WT controls ($n = 13$ to 18) was quantified with DNA qRT-PCR at 4 and 9 wpi. Bacterial load is represented as the median of total bacterial copies ($\log_{10}$). *M. marinum* quantifications were run as technical duplicates. (C) The relative expression of Th cell markers (*cd247*, *tbx21*, *gata3*, *foxp3a*, and *rorca*) was quantified with qRT-PCR in *furinA*$^{td204e/+}$ mutants ($n = 18$ to 21) and WT controls ($n = 18$) at 9 wpi. Gene expressions were normalized to *eef1a1l1* expression and represented as a scatter dot plot and median. Expression analyses were run as technical duplicates. In panels B and C, a two-tailed Mann-Whitney test was used in the statistical comparison of differences.

which suggests that FurinA also inhibits antimycobacterial host responses.

DISCUSSION

Despite intensive studies, our understanding of the pathogenesis and host immunity of TB is still incomplete. We found that *furinA* expression is upregulated upon *M. marinum* infection and that inhibiting *furin* genes in developing zebrafish reduces the survival of infected embryos. An analysis of *furinA*$^{td204e/+}$ mutant adult zebrafish demonstrated that FurinA regulates the development of granulocytes and the expression of Th subset-associated genes in steady-state fish. When *furinA*$^{td204e/+}$ mutant fish were infected with a high dose of *M. marinum*, reduced *furinA* mRNA levels were found to correlate with an enhanced expression of the pro-inflammatory cytokine genes *tnfa*, *lta*, and *il17a/f3*. In contrast, experiments using a latent mycobacterial infection model showed that infected *furinA*$^{td204e/+}$ mutants have lowered expression levels of the T cell marker gene *cd247* (*cd3zeta*) compared to controls. The net effect of the reduced *furinA* expression in adult zebrafish was a significant decrease in *M. marinum* copy numbers in a low-dose infection model, suggesting that FurinA attenuates protective host responses against mycobacteria.

Through catalyzing the endoproteolytic cleavage of target molecules, PCSK enzymes regulate the maturation of host defense factors, as well as the activity of invading pathogens (9, 10). *In vitro* analyses have demonstrated that PCSK enzymes have significantly overlapping biochemical functions in substrate processing, and therefore genetic inactivation of PCSKs is instrumental for decoding their specific biological roles (9, 10, 47). We have previously characterized the expression of seven *pcsk* genes in developing embryos and multiple adult zebrafish tissues (32). Two orthologous genes of mammalian *FURIN*, *furinA* and *furinB* (30), were found to be ubiquitously expressed, and biochemical analyses

showed that FurinA, but not FurinB, is able to proteolytically process pro-Tgfb1a, suggesting that FurinA is the corresponding biological equivalent for human FURIN (32). Germ line *Furin* KO mice die on day 11 of embryogenesis due to severe developmental defects in ventral closure, as well as in heart tube fusion and looping (20). Accordingly, we could not identify any homozygous adult *furinA*$^{td204e/td204e}$ fish, indicating that FurinA has a specific, nonredundant function also during zebrafish development. Importantly, however, in its heterozygous form, the adult *furinA*^{td204e} allele did not interfere with normal development but reduced the levels of *furinA* mRNA. This in turn allowed the use of adult *furinA*$^{td204e/+}$ mutants in the experiments to assess how *furinA* expression regulates host responses. Interestingly, *furinA* downregulation in *furinA*$^{td204e/+}$ mutant zebrafish upregulated *pcsk1* and *pcsk2* expression, which implies an attempt to compensate for the reduced FurinA activity. In mammals, PCSK1 and PCSK2 have restricted gene expression patterns, function chiefly in neuroendocrine tissues, and are not able to compensate for FURIN during development (9, 10). However, the lack of PCSK1 was recently found to associate with a proinflammatory phenotype and increased lethality in LPS-induced septic shock in mice (48). Consequently, the elevated *pcsk1* expression in zebrafish could theoretically also attenuate inflammation in zebrafish and thus partially mask the specific immunoregulatory function of FurinA.

It is well established that protective immunity against TB is mediated by both innate and adaptive immune responses. As in mammals, the cells of the zebrafish immune system include lymphocytes, neutrophils, and macrophages (49), as well as dendritic cells (50), eosinophils (51, 52), human mast cell-like cells (53), and natural killer cells (54). Our flow cytometric analyses of *furinA*$^{td204e/+}$ mutant fish kidneys (the primary site of hematopoiesis in fish) showed normal numbers of lymphocytes, blood cell precursors, and erythrocytes, but low granulocyte counts, indicating that FurinA promotes granulopoiesis. Granulocyte maturation is regulated through a complex network of protein mediators (55), some of which are known substrates for PCSKs (12). For example, granulocyte development is disrupted in mice deficient in integrin alpha 9 (56). Also, functional NOTCH signaling promotes entry into granulopoiesis (57), whereas conditional inactivation of TNF converting enzyme increases granulopoiesis (58). Deciphering the detailed molecular mechanisms by which FurinA regulates granulocyte development, however, would require the spatiotemporal identification of its specific substrates using proteomics analyses, followed by characterizing the function of the substrates in zebrafish.

Although the Th1 type cell immune response is crucial in adaptive immunity against TB (5–8), other Th lymphocyte subsets, including Th2, Th17, and Treg cells, also regulate the magnitude of the host defense and survival (59–62). We have previously shown that FURIN is dispensable for T cell development in mice but that it plays a role in $CD4^+$ T cell activation and polarization (15, 18). When we characterized the expression of Th cell subtype transcription factors in steady-state zebrafish, we found that decreased *furinA* expression associated with the upregulation of *tbx21* (a Th1 cell marker), *gata3* (a Th2 cell marker), and *foxp3a* (a Treg cell marker) expression, suggesting an increase in Th1, Th2, and Treg cell counts in the *furinA*$^{td204e/+}$ mutants. These findings are in line with the previously reported hyperproduction of both Th1 and Th2 hallmark cytokines and increased Treg cell numbers in *FURIN* T cell cKO mice (18) but also indicate that reduced *FURIN* expression (and not only the lack of it) can accelerate Th1 and Th2 responses. In contrast, aging *furinA*$^{td204e/+}$ mutants did not develop overt autoimmunity, which demonstrates that the residual *furinA* expression, accompanied with elevated *tgfb1a* mRNA levels, is sufficient for maintaining adequate peripheral immune tolerance in steady state.

To assess how granulopenia and altered Th subtype gene expressions in *furinA*$^{td204e/+}$ mutants might contribute to the host defense against mycobacteria, adult zebrafish were infected i.p. with *M. marinum* inoculates. *furinA*$^{td204e/+}$ mutants exhibited similar gross survival, and statistically significant differences could not be observed. In contrast, inhibiting *furin* genes during development associated with significantly reduced survival of *M. marinum*-infected embryos. Albeit these findings could be indicative of either immunodeficiency or an unnecessarily strong host response in the lack of Furin, they need to be interpreted cautiously. The expression of *furinA* is critical for zebrafish development, and survival differences in *furinA*+*B* morphant fish could simply result from "failure to thrive." Therefore, we chose to use adult *furinA*$^{td204e/+}$ fish to address how *furinA* regulates the innate immune responses in *M. marinum* infection (30). After a high-dose mycobacterial infection, lower *furinA* mRNA expression levels resulted in a proinflammatory phenotype characterized by enhanced early expression of *tnfa*, *lta*, and *il17a/f3* but declining expression levels of the anti-inflammatory cytokine genes *il10* and *tgfb1a*. Previously, TNF and IL-17 have been linked to a protective, innate immunity against TB (61, 63), and an *LTA* polymorphism has been associated with susceptibility to the disease (64). The role of Tnfa appears, however, complicated; Roca and Ramakrishnan recently showed that either deficient or excess production of this cytokine accelerates TB pathogenesis through reduced microbicidal activity of macrophages or programmed necrosis of macrophages, respectively (65). Since *furinA* downregulation causes a proinflammatory phenotype, FurinA deficiency could be beneficial for protection by increasing the early microbicidal activity of innate cells through upregulated Tnfa levels. In addition, both *furinA*$^{td204e/+}$ mutants and controls showed well-organized granulomas and no free bacteria in Ziehl-Neelsen staining, which suggests relatively normal macrophage function also in controlling the high bacterial loads in the chronic phase.

We have previously shown that infecting zebrafish with a low *M. marinum* dose (~35 CFU) results in a nonprogressive mycobacterial disease that can be reactivated by gamma irradiation (25). In this model, the host survival and the latent state of infection both depend on functional adaptive immune responses and normal lymphocyte numbers. The determination of the mycobacterial burden in latency revealed that reduced *furinA* expression associated with significantly decreased *M. marinum* copy numbers, and this could not be explained by elevated T cell responses. Specifically, we noticed that *furinA*$^{td204e/+}$ mutant fish actually expressed lower levels of the general T cell marker gene *cd247* (*cd3zeta*) and that the overexpression of Th1/2, as well as Treg marker genes in steady-state mutants, was completely abolished in the chronically infected *furinA*$^{td204e/+}$ zebrafish. How *furinA* downregulation affects these responses is not clear but would require a careful kinetic analysis of marker gene expression levels. In summary, we can conclude that a reduction in systemic *furinA* expression associates with enhanced host responses to mycobacteria in zebrafish.

A challenge in TB diagnostics is to specifically identify the activation of latent infection. The present means, such as the tuberculin skin test, the interferon gamma release assay (IGRA), and a chest X-ray, can only reveal the presence of TB-associated memory cells and tissue damage, but there are no markers available for the detection of mycobacterial growth in the host in the clinic. Our data show that *furinA*/*FURIN* expression is upregulated in the host in response to a mycobacterial infection and the Th1 hallmark cytokine IL-12 (15). FURIN is also secreted from macrophages in response to LPS activation (14), and it can be measured from serum (66). Therefore, in the future it will be interesting to assess whether serum FURIN levels can be used as an infection biomarker to mirror mycobacterial growth and the activation of Th1 type immune responses. Furthermore, PCSK inhibitors have relatively recently been suggested as drugs for cancer and infectious diseases (9, 10, 67). Blocking FURIN also associates with accelerated immune responses, as shown by the spontaneous development of autoimmunity in T cell-specific *FURIN* cKO mice and by the prevention of experimental arthritis upon recombinant FURIN administration (18, 19). Our results here demonstrate that diminished *furinA* expression reduces mycobacterial loads in a latent infection model, which suggests that PCSK inhibitors could potentially be used to harness also TB. Adverse effects, such as autoimmunity and developmental defects in stem cells, may pose a significant clinical problem. Investigating the molecular mechanisms by which FURIN regulates mycobacterial immunity further may help us find specific target molecules for future drug development.

ACKNOWLEDGMENTS

This study was financially supported by the Jane and Aatos Erkko Foundation (M. Rämet), Academy of Finland (projects 128623 and 135980 [M. Pesu], 139225 [M. Rämet], and 121003 [M. Parikka]), a Marie Curie International Reintegration Grant within the 7th European Community Framework Programme (M. Pesu), the Emil Aaltonen Foundation (M. Pesu and S.-K. Harjula), the Sigrid Jusélius Foundation (M. Pesu and M. Rämet), The Tampere Tuberculosis Foundation (M. Pesu, M. Rämet, M. Parikka, S.-K. Harjula, and M. Hammarén), Competitive Research Funding of the Tampere University Hospital (grants 9M080, 9N056, and 9S051 [M. Pesu], 9M093 [M. Rämet], and 9NO52 [M. Parikka]), the Foundation of the Finnish Anti-Tuberculosis Association (S.-K. Harjula, M. Hammarén, and M. Parikka), the University of Tampere Doctoral Programme in Biomedicine and Biotechnology (M. Ojanen, M. Hammarén, and Z. Cordova), the City of Tampere (S.-K. Harjula), and the Orion-Farmos Research Foundation (M. Hammarén). The zebrafish work was carried out at the University of Tampere core facility supported by Biocenter Finland, the Tampere Tuberculosis Foundation, and the Emil Aaltonen Foundation. The authors declare no commercial or financial conflict of interest.

We thank Sanna Hämäläinen, Kaisa Oksanen, Leena Mäkinen, Hannaleena Piippo, Jenna Ilomäki, and Annemari Uusimäki for technical assistance and Jorma Isola for his help in performing virtual microscopy with the University of Tampere core facility equipment.

REFERENCES

1. **Butler D.** 2000. New fronts in an old war. Nature **406:**670–672. http://dx.doi.org/10.1038/35021291.
2. **Zumla A, Raviglione M, Hafner R, von Reyn CF.** 2013. Tuberculosis. N Engl J Med **368:**745–755. http://dx.doi.org/10.1056/NEJMra1200894.
3. **North R, Jung Y.** 2004. Immunity to tuberculosis. Annu Rev Immunol **22:**599–623. http://dx.doi.org/10.1146/annurev.immunol.22.012703.104635.
4. **Philips JA, Ernst JD.** 2012. Tuberculosis pathogenesis and immunity. Annu Rev Pathol **7:**353–384. http://dx.doi.org/10.1146/annurev-pathol-011811-132458.
5. **Cooper AM, Mayer-Barber KD, Sher A.** 2011. Role of innate cytokines in mycobacterial infection. Mucosal Immunol **4:**252–260. http://dx.doi.org/10.1038/mi.2011.13.
6. **Flynn JL, Chan J, Triebold KJ, Dalton DK, Stewart TA, Bloom BR.** 1993. An essential role for interferon gamma in resistance to *Mycobacterium tuberculosis* infection. J Exp Med **178:**2249–2254. http://dx.doi.org/10.1084/jem.178.6.2249.
7. **Cooper AM, Dalton DK, Stewart TA, Griffin JP, Russell DG, Orme IM.** 1993. Disseminated tuberculosis in interferon gamma gene-disrupted mice. J Exp Med **178:**2243–2247. http://dx.doi.org/10.1084/jem.178.6.2243.
8. **Cooper AM, Magram J, Ferrante J, Orme IM.** 1997. Interleukin 12 (IL-12) is crucial to the development of protective immunity in mice intravenously infected with *Mycobacterium tuberculosis*. J Exp Med **186:**39–45. http://dx.doi.org/10.1084/jem.186.1.39.
9. **Seidah NG, Prat A.** 2012. The biology and therapeutic targeting of the proprotein convertases. Nat Rev Drug Discov **11:**367–383. http://dx.doi.org/10.1038/nrd3699.
10. **Artenstein AW, Opal SM.** 2011. Proprotein convertases in health and disease. N Engl J Med **365:**2507–2518. http://dx.doi.org/10.1056/NEJMra1106700.
11. **Fuller RS, Brake AJ, Thorner J.** 1989. Intracellular targeting and structural conservation of a prohormone-processing endoprotease. Science **246:**482–486. http://dx.doi.org/10.1126/science.2683070.
12. **Thomas G.** 2002. Furin at the cutting edge: from protein traffic to embryogenesis and disease. Nat Rev Mol Cell Biol **3:**753–766. http://dx.doi.org/10.1038/nrm934.
13. **Remacle AG, Rozanov DV, Fugere M, Day R, Strongin AY.** 2006. Furin regulates the intracellular activation and the uptake rate of cell surface-associated MT1-MMP. Oncogene **25:**5648–5655. http://dx.doi.org/10.1038/sj.onc.1209572.
14. **Turpeinen H, Raitoharju E, Oksanen A, Oksala N, Levula M, Lyytikainen LP, Jarvinen O, Creemers JW, Kahonen M, Laaksonen R, Pelto-Huikko M, Lehtimaki T, Pesu M.** 2011. Proprotein convertases in human atherosclerotic plaques: the overexpression of FURIN and its substrate cytokines BAFF and APRIL. Atherosclerosis **219:**799–806. http://dx.doi.org/10.1016/j.atherosclerosis.2011.08.011.
15. **Pesu M, Muul L, Kanno Y, O'Shea JJ.** 2006. Proprotein convertase furin is preferentially expressed in T helper 1 cells and regulates interferon gamma. Blood **108:**983–985. http://dx.doi.org/10.1182/blood-2005-09-3824.
16. **Meissner F, Scheltema RA, Mollenkopf HJ, Mann M.** 2013. Direct proteomic quantification of the secretome of activated immune cells. Science **340:**475–478. http://dx.doi.org/10.1126/science.1232578.
17. **Lund RJ, Chen Z, Scheinin J, Lahesmaa R.** 2004. Early target genes of IL-12 and STAT4 signaling in th cells. J Immunol **172:**6775–6782. http://dx.doi.org/10.4049/jimmunol.172.11.6775.
18. **Pesu M, Watford WT, Wei L, Xu L, Fuss I, Strober W, Andersson J, Shevach EM, Quezado M, Bouladoux N, Roebroek A, Belkaid Y, Creemers J, O'Shea JJ.** 2008. T-cell-expressed proprotein convertase furin is essential for maintenance of peripheral immune tolerance. Nature **455:**246–250. http://dx.doi.org/10.1038/nature07210.
19. **Lin H, Ah Kioon MD, Lalou C, Larghero J, Launay JM, Khatib AM, Cohen-Solal M.** 2012. Protective role of systemic furin in immune response-induced arthritis. Arthritis Rheum **64:**2878–2886. http://dx.doi.org/10.1002/art.34523.
20. **Roebroek AJ, Umans L, Pauli IG, Robertson EJ, van Leuven F, Van de Ven WJ, Constam DB.** 1998. Failure of ventral closure and axial rotation in embryos lacking the proprotein convertase Furin. Development **125:**4863–4876.
21. **Meeker ND, Trede NS.** 2008. Immunology and zebrafish: spawning new models of human disease. Dev Comp Immunol **32:**745–757. http://dx.doi.org/10.1016/j.dci.2007.11.011.
22. **Sullivan C, Kim CH.** 2008. Zebrafish as a model for infectious disease and immune function. Fish Shellfish Immunol **25:**341–350. http://dx.doi.org/10.1016/j.fsi.2008.05.005.
23. **Lohi O, Parikka M, Ramet M.** 2013. The zebrafish as a model for paediatric diseases. Acta Paediatr **102:**104–110. http://dx.doi.org/10.1111/j.1651-2227.2012.02835.x.
24. **Zhu LY, Nie L, Zhu G, Xiang LX, Shao JZ.** 2013. Advances in research of fish immune-relevant genes: a comparative overview of innate and adaptive immunity in teleosts. Dev Comp Immunol **39:**39–62. http://dx.doi.org/10.1016/j.dci.2012.04.001.
25. **Parikka M, Hammaren MM, Harjula SK, Halfpenny NJ, Oksanen KE,**

Lahtinen MJ, Pajula ET, Iivanainen A, Pesu M, Ramet M. 2012. *Mycobacterium marinum* causes a latent infection that can be reactivated by gamma irradiation in adult zebrafish. PLoS Pathog **8:**e1002944. http://dx.doi.org/10.1371/journal.ppat.1002944.

26. **Stamm LM, Brown EJ.** 2004. *Mycobacterium marinum*: the generalization and specialization of a pathogenic *Mycobacterium*. Microbes Infect **6:**1418–1428. http://dx.doi.org/10.1016/j.micinf.2004.10.003.
27. **Carvalho R, de Sonneville J, Stockhammer OW, Savage ND, Veneman WJ, Ottenhoff TH, Dirks RP, Meijer AH, Spaink HP.** 2011. A high-throughput screen for tuberculosis progression. PLoS One **6:**e16779. http://dx.doi.org/10.1371/journal.pone.0016779.
28. **Davis JM, Clay H, Lewis JL, Ghori N, Herbomel P, Ramakrishnan L.** 2002. Real-time visualization of *Mycobacterium*-macrophage interactions leading to initiation of granuloma formation in zebrafish embryos. Immunity **17:**693–702. http://dx.doi.org/10.1016/S1074-7613(02)00475-2.
29. **Prouty MG, Correa NE, Barker LP, Jagadeeswaran P, Klose KE.** 2003. Zebrafish-*Mycobacterium marinum* model for mycobacterial pathogenesis. FEMS Microbiol Lett **225:**177–182. http://dx.doi.org/10.1016/S0378-1097(03)00446-4.
30. **Walker MB, Miller CT, Coffin Talbot J, Stock DW, Kimmel CB.** 2006. Zebrafish furin mutants reveal intricacies in regulating Endothelin1 signaling in craniofacial patterning. Dev Biol **295:**194–205. http://dx.doi.org/10.1016/j.ydbio.2006.03.028.
31. **Langenau DM, Ferrando AA, Traver D, Kutok JL, Hezel JP, Kanki JP, Zon LI, Look AT, Trede NS.** 2004. In vivo tracking of T cell development, ablation, and engraftment in transgenic zebrafish. Proc Natl Acad Sci U S A **101:**7369–7374. http://dx.doi.org/10.1073/pnas.0402248101.
32. **Turpeinen H, Oksanen A, Kivinen V, Kukkurainen S, Uusimaki A, Ramet M, Parikka M, Hytonen VP, Nykter M, Pesu M.** 2013. Proprotein convertase subtilisin/kexin type 7 (PCSK7) is essential for the zebrafish development and bioavailability of transforming growth factor β1a (TGFβ1a). J Biol Chem **288:**36610–36623. http://dx.doi.org/10.1074/jbc.M113.453183.
33. **Benard EL, van der Sar AM, Ellett F, Lieschke GJ, Spaink HP, Meijer AH.** 2012. Infection of zebrafish embryos with intracellular bacterial pathogens. J Vis Exp **61:**3781. http://dx.doi.org/10.3791/3781.
34. **Oksanen KE, Halfpenny NJ, Sherwood E, Harjula SK, Hammaren MM, Ahava MJ, Pajula ET, Lahtinen MJ, Parikka M, Ramet M.** 2013. An adult zebrafish model for preclinical tuberculosis vaccine development. Vaccine **31:**5202–5209. http://dx.doi.org/10.1016/j.vaccine.2013.08.093.
35. **Tuominen VJ, Isola J.** 2009. The application of JPEG2000 in virtual microscopy. J Digital Imaging **22:**250–258. http://dx.doi.org/10.1007/s10278-007-9090-z.
36. **Tang R, Dodd A, Lai D, McNabb WC, Love DR.** 2007. Validation of zebrafish (*Danio rerio*) reference genes for quantitative real-time RT-PCR normalization. Acta Biochim Biophys Sin **39:**384–390. http://dx.doi.org/10.1111/j.1745-7270.2007.00283.x.
37. **Ellett F, Lieschke GJ.** 2010. Zebrafish as a model for vertebrate hematopoiesis. Curr Opin Pharmacol **10:**563–570. http://dx.doi.org/10.1016/j.coph.2010.05.004.
38. **Dubois CM, Blanchette F, Laprise MH, Leduc R, Grondin F, Seidah NG.** 2001. Evidence that furin is an authentic transforming growth factor-beta1-converting enzyme. Am J Pathol **158:**305–316. http://dx.doi.org/10.1016/S0002-9440(10)63970-3.
39. **Seidah NG, Mayer G, Zaid A, Rousselet E, Nassoury N, Poirier S, Essalmani R, Prat A.** 2008. The activation and physiological functions of the proprotein convertases. Int J Biochem Cell Biol **40:**1111–1125. http://dx.doi.org/10.1016/j.biocel.2008.01.030.
40. **Nasevicius A, Ekker SC.** 2000. Effective targeted gene "knockdown" in zebrafish. Nat Genet **26:**216–220. http://dx.doi.org/10.1038/79951.
41. **Gupta A, Kaul A, Tsolaki AG, Kishore U, Bhakta S.** 2012. *Mycobacterium tuberculosis*: immune evasion, latency, and reactivation. Immunobiology **217:**363–374. http://dx.doi.org/10.1016/j.imbio.2011.07.008.
42. **Velez DR, Wejse C, Stryjewski ME, Abbate E, Hulme WF, Myers JL, Estevan R, Patillo SG, Olesen R, Tacconelli A, Sirugo G, Gilbert JR, Hamilton CD, Scott WK.** 2010. Variants in Toll-like receptors 2 and 9 influence susceptibility to pulmonary tuberculosis in Caucasians, African-Americans, and West Africans. Hum Genet **127:**65–73. http://dx.doi.org/10.1007/s00439-009-0741-7.
43. **Adrain C, Zettl M, Christova Y, Taylor N, Freeman M.** 2012. Tumor necrosis factor signaling requires iRhom2 to promote trafficking and activation of TACE. Science **335:**225–228. http://dx.doi.org/10.1126/science.1214400.
44. **Hipp M, Shepherd D, Gileadi U, Aichinger M, Kessler B, Edelmann M, Essalmani R, Seidah N, Reis e Sousa C, Cerundolo V.** 2013. Processing of human Toll-like receptor 7 by furin-like proprotein convertases is required for its accumulation and activity in endosomes. Immunity **39:**711–721. http://dx.doi.org/10.1016/j.immuni.2013.09.004.
45. **Clausen BE, Burkhardt C, Reith W, Renkawitz R, Forster I.** 1999. Conditional gene targeting in macrophages and granulocytes using LysMcre mice. Transgenic Res **8:**265–277. http://dx.doi.org/10.1023/A:1008942828960.
46. **Taverniti V, Stuknyte M, Minuzzo M, Arioli S, De Noni I, Scabiosi C, Cordova ZM, Junttila I, Hamalainen S, Turpeinen H, Mora D, Karp M, Pesu M, Guglielmetti S.** 2013. S-layer protein mediates the stimulatory effect of *Lactobacillus helveticus* MIMLh5 on innate immunity. Appl Environ Microbiol **79:**1221–1231. http://dx.doi.org/10.1128/AEM.03056-12.
47. **Turpeinen H, Ortutay Z, Pesu M.** 2013. Genetics of the first seven proprotein convertase enzymes in health and disease. Curr Genomics **14:**453–467. http://dx.doi.org/10.2174/1389202911314050010.
48. **Refaie S, Gagnon S, Gagnon H, Desjardins R, D'Anjou F, D'Orleans-Juste P, Zhu X, Steiner DF, Seidah NG, Lazure C, Salzet M, Day R.** 2012. Disruption of proprotein convertase 1/3 (PC1/3) expression in mice causes innate immune defects and uncontrolled cytokine secretion. J Biol Chem **287:**14703–14717. http://dx.doi.org/10.1074/jbc.M111.323220.
49. **Renshaw SA, Trede NS.** 2012. A model 450 million years in the making: zebrafish and vertebrate immunity. Dis Model Mech **5:**38–47. http://dx.doi.org/10.1242/dmm.007138.
50. **Lin AF, Xiang LX, Wang QL, Dong WR, Gong YF, Shao JZ.** 2009. The DC-SIGN of zebrafish: insights into the existence of a CD209 homologue in a lower vertebrate and its involvement in adaptive immunity. J Immunol **183:**7398–7410. http://dx.doi.org/10.4049/jimmunol.0803955.
51. **Bennett CM, Kanki JP, Rhodes J, Liu TX, Paw BH, Kieran MW, Langenau DM, Delahaye-Brown A, Zon LI, Fleming MD, Look AT.** 2001. Myelopoiesis in the zebrafish, *Danio rerio*. Blood **98:**643–651. http://dx.doi.org/10.1182/blood.V98.3.643.
52. **Balla KM, Lugo-Villarino G, Spitsbergen JM, Stachura DL, Hu Y, Banuelos K, Romo-Fewell O, Aroian RV, Traver D.** 2010. Eosinophils in the zebrafish: prospective isolation, characterization, and eosinophilia induction by helminth determinants. Blood **116:**3944–3954. http://dx.doi.org/10.1182/blood-2010-03-267419.
53. **Dobson JT, Seibert J, Teh EM, Da'as S, Fraser RB, Paw BH, Lin TJ, Berman JN.** 2008. Carboxypeptidase A5 identifies a novel mast cell lineage in the zebrafish providing new insight into mast cell fate determination. Blood **112:**2969–2972. http://dx.doi.org/10.1182/blood-2008-03-145011.
54. **Yoder JA, Turner PM, Wright PD, Wittamer V, Bertrand JY, Traver D, Litman GW.** 2010. Developmental and tissue-specific expression of NITRs. Immunogenetics **62:**117–122. http://dx.doi.org/10.1007/s00251-009-0416-5.
55. **Ward AC, Loeb DM, Soede-Bobok AA, Touw IP, Friedman AD.** 2000. Regulation of granulopoiesis by transcription factors and cytokine signals. Leukemia **14:**973–990. http://dx.doi.org/10.1038/sj.leu.2401808.
56. **Chen C, Huang X, Atakilit A, Zhu Q, Corey SJ, Sheppard D.** 2006. The integrin α9β1 contributes to granulopoiesis by enhancing granulocyte colony-stimulating factor receptor signaling. Immunity **25:**895–906. http://dx.doi.org/10.1016/j.immuni.2006.10.013.
57. **Tan-Pertel HT, Walker L, Browning D, Miyamoto A, Weinmaster G, Gasson JC.** 2000. Notch signaling enhances survival and alters differentiation of 32D myeloblasts. J Immunol **165:**4428–4436. http://dx.doi.org/10.4049/jimmunol.165.8.4428.
58. **Horiuchi K, Kimura T, Miyamoto T, Miyamoto K, Akiyama H, Takaishi H, Morioka H, Nakamura T, Okada Y, Blobel CP, Toyama Y.** 2009. Conditional inactivation of TACE by a Sox9 promoter leads to osteoporosis and increased granulopoiesis via dysregulation of IL-17 and G-CSF. J Immunol **182:**2093–2101. http://dx.doi.org/10.4049/jimmunol.0802491.
59. **Scott-Browne JP, Shafiani S, Tucker-Heard G, Ishida-Tsubota K, Fontenot JD, Rudensky AY, Bevan MJ, Urdahl KB.** 2007. Expansion and function of Foxp3-expressing T regulatory cells during tuberculosis. J Exp Med **204:**2159–2169. http://dx.doi.org/10.1084/jem.20062105.
60. **Chen X, Zhou B, Li M, Deng Q, Wu X, Le X, Wu C, Larmonier N, Zhang W, Zhang H, Wang H, Katsanis E.** 2007. $CD4^+$ $CD25^+$ $FoxP3^+$ regulatory T cells suppress *Mycobacterium tuberculosis* immunity in patients with active disease. Clin Immunol **123:**50–59. http://dx.doi.org/10.1016/j.clim.2006.11.009.

61. **Khader SA, Bell GK, Pearl JE, Fountain JJ, Rangel-Moreno J, Cilley GE, Shen F, Eaton SM, Gaffen SL, Swain SL, Locksley RM, Haynes L, Randall TD, Cooper AM.** 2007. IL-23 and IL-17 in the establishment of protective pulmonary $CD4^+$ T cell responses after vaccination and during *Mycobacterium tuberculosis* challenge. Nat Immunol **8:**369–377. http://dx.doi.org/10.1038/nrm2146.
62. **Hammaren MM, Oksanen KE, Nisula HM, Luukinen BV, Pesu M, Ramet M, Parikka M.** 2014. Adequate Th2-type response associates with restricted bacterial growth in latent mycobacterial infection of zebrafish. PLoS Pathog **10:**e1004190. http://dx.doi.org/10.1371/journal.ppat.1004190.
63. **Clay H, Volkman HE, Ramakrishnan L.** 2008. Tumor necrosis factor signaling mediates resistance to mycobacteria by inhibiting bacterial growth and macrophage death. Immunity **29:**283–294. http://dx.doi.org/10.1016/j.immuni.2008.06.011.
64. **Garcia-Elorriaga G, Carrillo-Montes G, Mendoza-Aguilar M, Gonzalez-Bonilla C.** 2010. Polymorphisms in tumor necrosis factor and lymphotoxin A in tuberculosis without and with response to treatment. Inflammation **33:**267–275. http://dx.doi.org/10.1007/s10753-010-9181-8.
65. **Roca FJ, Ramakrishnan L.** 2013. TNF dually mediates resistance and susceptibility to mycobacteria via mitochondrial reactive oxygen species. Cell **153:**521–534. http://dx.doi.org/10.1016/j.cell.2013.03.022.
66. **Kumar A, Singh S, Ahirwar SK, Nath G.** 2014. Proteomics-based identification of plasma proteins and their association with the host-pathogen interaction in chronic typhoid carriers. Int J Infect Dis **19:**59–66. http://dx.doi.org/10.1016/j.ijid.2013.10.008.
67. **Becker GL, Lu Y, Hardes K, Strehlow B, Levesque C, Lindberg I, Sandvig K, Bakowsky U, Day R, Garten W, Steinmetzer T.** 2012. Highly potent inhibitors of proprotein convertase furin as potential drugs for treatment of infectious diseases. J Biol Chem **287:**21992–22003. http://dx.doi.org/10.1074/jbc.M111.332643.

Supplemental Table 1. Primers used in the qRT-PCR analyses.

Gene	ZFIN ID	Human gene ortholog (HGNC)	Sequence 5´-3´	Reference
furinA	ZDB-GENE-040901-1	*FURIN*	F CCAAAGAGGCTTTCCAACGC R CGTACTGCTGCTGATGGACAG	-
pcsk1	ZDB-GENE-071009-1	*PCSK1*	F CGGGAAAAGGAGTGGTCAT R GGTGGAGTCGTATCTGGG	Turpeinen et al. 2013
pcsk2	ZDB-GENE-090608-1	*PCSK2*	F CGGATCTGTATGGAAACTGC R GCCGGACTGTATTTTATGAAT	Turpeinen et al. 2013
furinB	ZDB-GENE-040901-2	*FURIN*	F CCAAGGCATCTACATCAACAC R ACACCTCTGTGCTGGAAA	Turpeinen et al. 2013
pcsk5a	ZDB-GENE-060531-130	*PCSK5*	F GGAGTTTCAATGACCCCAA R ACCACAACTCCTTTCCCA	Turpeinen et al. 2013
pcsk5b	ZDB-GENE-070822-7	*PCSK5*	F TGTTCCTCGACCCTTACCAC R ATCTCGCCATGTCAGGAAAG	Turpeinen et al. 2013
pcsk7	ZDB-GENE-030131-7293	*PCSK7*	F AGAGTGTTGGACGGG R TGCCTAATGGATGCGGT	Turpeinen et al. 2013
cd247 (*cd3zeta*)	ZDB-GENE-061130-4	*CD247*	F CATCACCGGCTTCTTTGTGC R CCCCAGTTTATCAATGGCCTGA	Hammarén et al. 2014
tbx21(*T-bet*)	ZDB-GENE-080104-3	*TBX21*	F GGCCTACCAGAATGCAGACA R GGTGCGTACAGCGTGTCATA	Hammarén et al. 2014
gata3	ZDB-GENE-990415-82	*GATA3*	F GGATGGCACCGGTCACTATT R CAGCAGACAGCCTCCGTTT	Hammarén et al. 2014
foxp3a	ZDB-GENE-061116-2	*FOXP3*	F CAAAAGCAGAGTGCCAGTGG R CGCATAAGCACCGATTCTGC	Hammarén et al. 2014
rorca	ZDB-GENE-990415-250	*RORC*	F GAAGGCTGCAAGGGCTTCTT R TGCAGTTCCTCTGCCTTGAG	-
tnfa	ZDB-GENE-050317-1	*TNF*	F GGGCAATCAACAAGATGGAAG R GCAGCTGATGTGCAAAGACAC	Parikka et al. 2012
il1b	ZDB-GENE-040702-2	*IL1B*	F TGGACTTCGCAGCACAAAATG R GTTCACTTCACGCTCTTGGATG	Parikka et al. 2012
lta	ZDB-GENE-050601-3	*LTA*	F CCACAGTTCAGCAGGACCTC R TTTCCTGCGTGCTCTCATGTC	-
ifng1-1	ZDB-GENE-060210-1	*IFNG*	F AAATGGTGCTACTCTGTGGAC R TTCCAACCCAATCCTTTG	Oksanen et al. 2013
il22 (*ifnphi6*)	ZDB-GENE-060209-3	*IL22*	F TCAGACGAGCACACAGATATG R GATGGCTGGAGTAGTCGTG	-
il17a/f3	ZDB-GENE-041001-192	*IL17A* and *IL17F*	F GGCTCTCACGGGTTTTCAG R ACACTTCTTCACACCAGAACATC	-
il10	ZDB-GENE-051111-1	*IL10*	F GCTCTGCTCACGCTTCTTC R TGGTTCCAAGTCATCGTTG	-
tgfb1a	ZDB-GENE-030618-1	*TGFB1*	F TCGTCTTCCAGCAAGCTCAG R TTGGAGACAAAGCGAGTTCC	-
eef1a1l1 (*ef1a*)	ZDB-GENE-990415-52	*EEF1A1*	F CTGGAGGCCAGCTCAAACAT R ATCAAGAAGAGTAGTACCGCTAGCATTAC	Tang et al. 2007
mmits	-	-	F CACCACGAGAAACACTCCAA R ACATCCCGAAACCAACAGAG	Parikka et al. 2012

Zebrafish gene names and qRT-PCR primer sequences are listed accompanied with the ZFIN identification codes and the names of the orthologous genes in humans. HGNC, HUGO Gene Nomenclature Committee.

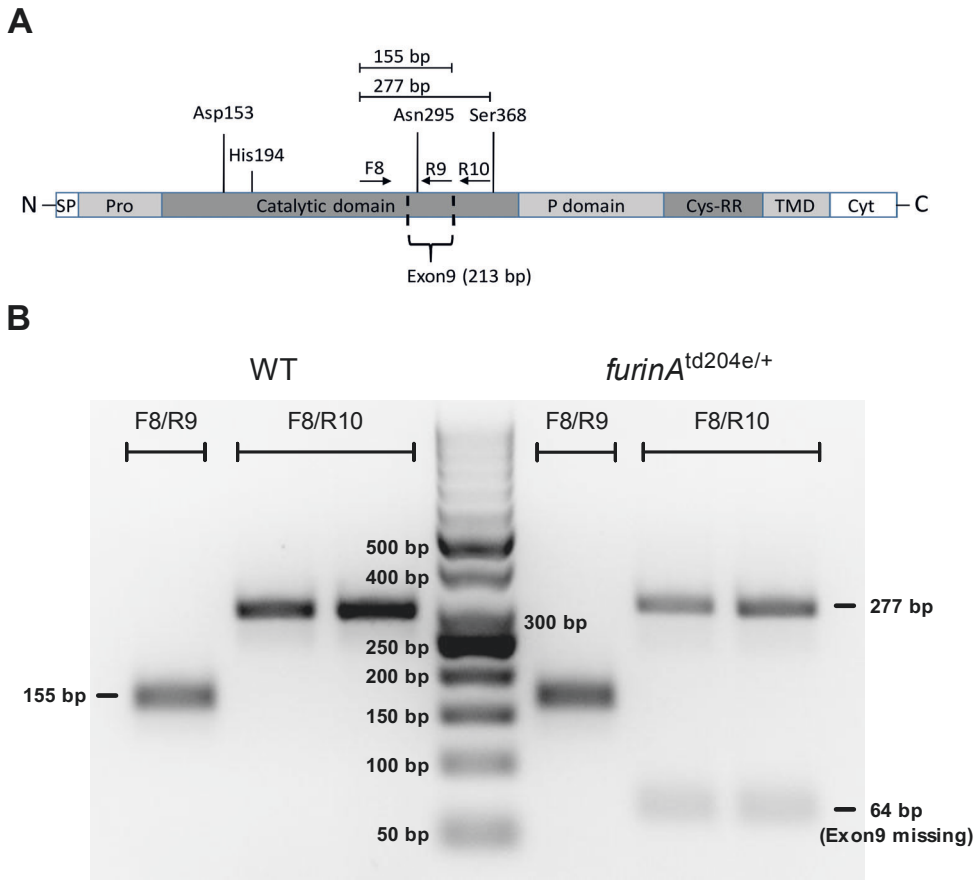

Supplemental Figure 1. *furinA*^{td204e} mutation disrupts the transcription of exon 9.

(A) A schematic presentation of the FURIN/FurinA domain structure and the catalytic amino acid residues (Asp153, His194, Asn295 and Ser 368), as well as the location of exon 9. **(B)** cDNA from both WT and *furinA*$^{td204e/+}$ mutant zebrafish was used as a template in a standard PCR reaction with different primer pairs (F8=Forward primer in exon 8, R9=Reverse primer in exon 9, R10=Reverse primer in exon 10). PCR products were analyzed with agarose gel electrophoresis, which demonstrates the presence of a 64 bp band only in reactions containing cDNA from *furinA*$^{td204e/+}$ mutants. The bands were excised and further verified by DNA sequencing (Data not shown).

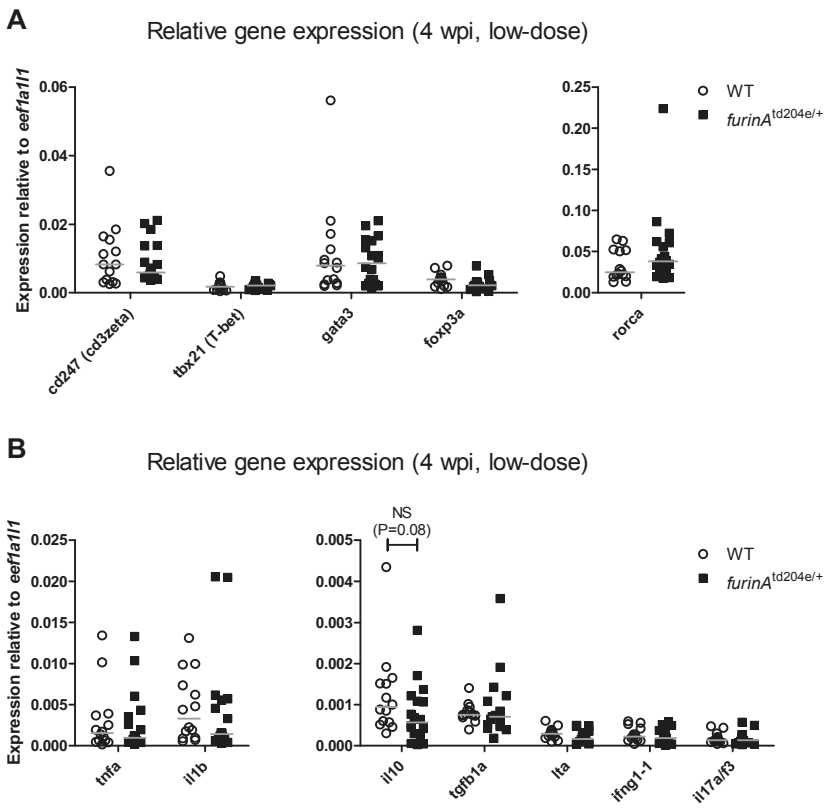

Supplemental Figure 2. Comparison of the T cell marker gene expression and the innate cytokine response in *furinA*$^{td204e/+}$ mutants and WT controls in an experimental low-dose mycobacterial infection at 4 wpi.

A latent mycobacterial infection was induced with a low-dose *M. marinum* inoculate. Relative expression of **(A)** Th cell marker genes (*cd247*, *tbx21*, *gata3*, *foxp3a*, *rorca*) as well as **(B)** pro-inflammatory cytokine genes (*tnfa*, *il1b*, *lta, ifng1-1, il17a/f3*) and anti-inflammatory cytokine genes (*il10*, *tgfb1a*) was determined in *furinA*$^{td204e/+}$ (n=13-14) and WT (n=16-18) zebrafish with qRT-PCR at 4 wpi. Gene expressions were normalized to *eef1a1l1* expression and represented as a scatter dot plot and median. A two-tailed Mann-Whitney was used in the statistical comparison of differences.

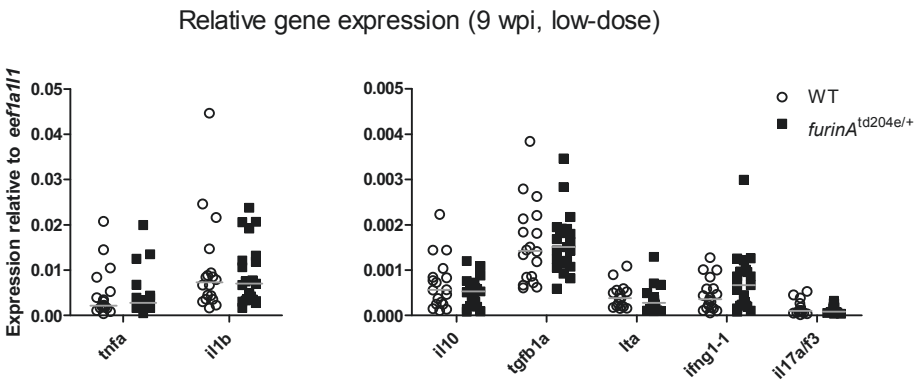

Supplemental Figure 3. Comparison of the innate cytokine response in *furinA*$^{td204e/+}$ mutants and WT controls in an experimental low-dose mycobacterial infection at 9 wpi.

A latent mycobacterial infection was induced with a low-dose *M. marinum* inoculate. Relative expression of pro-inflammatory cytokine genes (*tnfa*, *il1b*, *lta, ifng1-1, il17a/f3*) and anti-inflammatory cytokine genes (*il10*, *tgfb1a*) was determined in *furinA*$^{td204e/+}$ (n=18-21) and WT (n=16-18) zebrafish with qRT-PCR at 9 wpi. Gene expressions were normalized to *eef1a1l1* expression and represented as a scatter dot plot and median. A two-tailed Mann-Whitney was used in the statistical comparison of differences.

PLOS ONE

RESEARCH ARTICLE

Inactivation of *ca10a* and *ca10b* Genes Leads to Abnormal Embryonic Development and Alters Movement Pattern in Zebrafish

Ashok Aspatwar[1,2]*, Martti E. E. Tolvanen[1,3☯], Markus J. T. Ojanen[1☯], Harlan R. Barker[2], Anni K. Saralahti[1], Carina A. Bäuerlein[1], Csaba Ortutay[1], Peiwen Pan[2], Marianne Kuuslahti[2], Mataleena Parikka[1], Mika Rämet[1,4,5], Seppo Parkkila[2,6]

1 BioMediTech, University of Tampere, Tampere, Finland, **2** School of Medicine, University of Tampere, Tampere, Finland, **3** Department of Information Technology, University of Turku, Turku, Finland, **4** PEDEGO Research Center, and Medical Research Center Oulu, University of Oulu, Oulu, Finland, **5** Department of Children and Adolescents, Oulu University Hospital, Oulu, Finland, **6** Fimlab ltd and Tampere University Hospital, Tampere, Finland

☯ These authors contributed equally to this work.
* ashok.aspatwar@staff.uta.fi

Citation: Aspatwar A, Tolvanen MEE, Ojanen MJT, Barker HR, Saralahti AK, Bäuerlein CA, et al. (2015) Inactivation of *ca10a* and *ca10b* Genes Leads to Abnormal Embryonic Development and Alters Movement Pattern in Zebrafish. PLoS ONE 10(7): e0134263. doi:10.1371/journal.pone.0134263

Editor: Bruce B Riley, Texas A&M University, UNITED STATES

Received: January 23, 2015

Accepted: June 30, 2015

Published: July 28, 2015

Data Availability Statement: All relevant data are within the paper and its Supporting Information files.

Funding: This work was supported by the competitive Research Funding of the Tampere University Hospital and grants from the Jane and Aatos Erkko Foundation (SP, MR), Academy of Finland (SP, MR, MP), Finnish Cultural Foundation (HB), Sigrid Juselius Foundation (SP, MR), and Tampere Tuberculosis Foundation (SP, MR and MP). The zebrafish work was carried out at the Tampere Zebrafish Core Facility funded by the Biocenter Finland and Tampere Tuberculosis Foundation.

Abstract

Carbonic anhydrase related proteins (CARPs) X and XI are highly conserved across species and are predominantly expressed in neural tissues. The biological role of these proteins is still an enigma. Ray-finned fish have lost the *CA11* gene, but instead possess two co-orthologs of *CA10*. We analyzed the expression pattern of zebrafish *ca10a* and *ca10b* genes during embryonic development and in different adult tissues, and studied 61 CARP X/XI-like sequences to evaluate their phylogenetic relationship. Sequence analysis of zebrafish *ca10a* and *ca10b* reveals strongly predicted signal peptides, N-glycosylation sites, and a potential disulfide, all of which are conserved, suggesting that all of CARP X and XI are secretory proteins and potentially dimeric. RT-qPCR showed that zebrafish *ca10a* and *ca10b* genes are expressed in the brain and several other tissues throughout the development of zebrafish. Antisense morpholino mediated knockdown of *ca10a* and *ca10b* showed developmental delay with a high rate of mortality in larvae. Zebrafish morphants showed curved body, pericardial edema, and abnormalities in the head and eye, and there was increased apoptotic cell death in the brain region. Swim pattern showed abnormal movement in morphant zebrafish larvae compared to the wild type larvae. The developmental phenotypes of the *ca10a* and *ca10b* morphants were confirmed by inactivating these genes with the CRISPR/Cas9 system. In conclusion, we introduce a novel zebrafish model to investigate the mechanisms of CARP Xa and CARP Xb functions. Our data indicate that CARP Xa and CARP Xb have important roles in zebrafish development and suppression of *ca10a* and *ca10b* expression in zebrafish larvae leads to a movement disorder.

Competing Interests: The authors have declared that no competing interests exist.

Introduction

The α-carbonic anhydrases (α-CA) are zinc-containing metalloenzymes that catalyze the reversible hydration of carbon dioxide ($CO_2 + H_2O \leftrightarrow HCO_3^- + H^+$) [1–3]. In vertebrates there are 17 members in the α-CA gene family (*CA1-17*) which includes 14 catalytically active (CA I, II, III, IV, V, VI, VII, IX, XII, XIII, XIV, XV, XVI, XVII) and 3 inactive (CARP VIII, X, XI) forms [4]. The catalytic inactivity of CARP VIII, X, and XI is due to the lack of one, or more, of the three zinc atom binding histidine residues, which are essential for the classical catalytic activity of CAs [5]. Genes, which code for enzymatically inactive α-CAs, are found in seemingly all metazoan genomes, often in multiple copies. In previous studies of invertebrate CAs, two *CA10*-like genes have been detected in insect genomes [6–8], exemplified by CG32698 and CG1402 in *Drosophila melanogaster*, and two of the six α-CAs in the *Caenorhabditis elegans* genome (*cah-1* and *cah-2*) code for CARP X-like proteins. The *CA10*-like genes in invertebrates are more similar to their vertebrate homologs than are any enzymatically active *CA* genes compared to their vertebrate homologs [7,8].

The expression of *CA10* and *CA11*genes and their protein products has been analyzed in fetal and adult brain in humans, in developing mouse embryos, and in adult mouse tissues [9–12]. In humans the expression of *CA10* and *CA11* has been seen ubiquitously in the central nervous system (CNS), while weak, but significant, signals of the expression were seen in the fetal brain [9]. Similarly, expression studies at the mRNA and protein level showed that the proteins are expressed in all parts of the brain in the adult mouse [6,11]. Developmental expression profiling of *Ca10* and *Ca11* in the brain of mouse embryos showed that *Ca10* mRNA appeared in the middle phase of the gestation, whereas *Ca11* mRNA was seen during early gestational period [11]. In addition, recent studies show that *CA10* is highly expressed in the pineal gland during the nighttime, compared with the daytime, suggesting its involvement in sleep-wake patterns of humans [13].

Previous studies have shown that CARP X and CARP XI play a role in several human diseases such as certain tumors and neurological conditions. For example, human *CA10* sequence contains seven CCG repeats in the 5'-untranslated region followed by two CCG repeats 16 bp downstream of the sequence. The expansion of these trinucleotide repeats lead to various neuropsychiatric diseases in humans [14]. In addition, CARP XI is overexpressed in the gastrointestinal stromal tumors (GISTs), promoting their proliferation and invasion [15]. Finally, three recent expression analyses of *CA11* in transgenic mice with Machado-Joseph disease (MJD), a human patient with Spinocerebellar ataxia type 3 (SCA3), and in cultured neuronal cells producing mutant Ataxin 3 showed an upregulation of CARP XI, suggesting a role for the *CA11* gene in the development of ataxia in humans and mice [16].

The zebrafish has recently emerged as an attractive model organism for studying vertebrate development, as it uniquely combines the advantages of genetic tractability with biologic relevance [17]. Our previous studies showed that there is no *CA11* ortholog in ray-finned fish species, however the *CA10* gene has been duplicated, resulting in genes *ca10a* and *ca10b* [6]. Recently, we have developed an ataxic zebrafish model lacking the *ca8* gene product [18]. The phenotype of these zebrafish resembles that which is observed in human patients with a mutation in the *CA8* gene [18–20]. Our ultimate aim is to find the mechanisms of action and precise physiological roles of *CA10*-like genes, and their protein products, in the brain, especially during embryonic development.

The physiological roles of CARP X and CARP XI have been largely unknown. Furthermore, there have been no systematic studies on the expression pattern of *CA10* and *CA11* genes during embryonic development. Similarly, genetically modified model organisms have not been available to evaluate the function of *CA10* and *CA11* genes. To extend our understanding on

the function of the CARP family, we investigated the expression pattern of *ca10a* and *ca10b* genes during embryonic development in zebrafish. In addition, we studied the developmental roles of CARP X and CARP XI by silencing the *ca10a* and *ca10b* genes in zebrafish larvae.

Materials and Methods

Sequence analysis

Using an automated pipeline, a total of 83 *CA10* and 54 *CA11* protein sequences, and their corresponding coding regions, were retrieved from vertebrate genomes in the Ensembl database v. 74 and analyzed for completeness. Of these sequences, 46 were identified as complete and correct, and predictions using the Exonerate software package [21] were performed for the remaining incomplete sequences. As a result a total of 16 sequences were manually improved to completeness using the exonerate program. For each analysis, homologous sequences were used as queries to model the gene intron/exon boundaries with full genomes as the search space. Because no bird sequences for *CA11* were found, we performed full-genome scans with Exonerate on all available bird genomes in Ensembl v. 74 (*Ficedula albicollis*, *Gallus gallus*, *Meleagris gallopavo*, and *Taeniopygia guttata*) and one preliminary, unannotated Ensembl genome (*Anas platyrhynchos*). After seeing that the genome of the lamprey in Ensembl (*Petromyzon marinus*) only yielded short sequence fragments of *CA10*, we retrieved the genome of Japanese lamprey (*Lethenteron japonicum*) from the Institute of Molecular and Cell Biology at A*STAR, Singapore (http://jlampreygenome.imcb.a-star.edu.sg/) and performed a full-genome scan to find complete *CA10*-like genes of a jawless vertebrate. Because of the unique position of the jawless vertebrates in evolution, the two nearly complete *L. japonicum CA10*-like sequences were also included in further analyses, even though they lack initiation ATG/Met and are slightly shorter than the other sequences. Hence, a total of 57 vertebrate sequences were retrieved for analyses. For comparison purposes, we used two *D. melanogaster* CARPs and the cah-2 of *C. elegans* directly from the Ensembl and NCBI databases (CARP-A, CG1402: Ensembl FBGN0029962; CARP-B, CG32698: Ensembl FBGN0052698; cah-2: RefSeq NP_495567.3), whereas the existing predicted gene model coding for cah-1 of *C. elegans* was revised with the help of Exonerate and support from a fragment sequence FM247165. The full list of sequence names, as they appear in the phylogenetic tree, and their database codes are presented in S1 Table. All multiple sequence alignments were performed with Clustal Omega [22]. To calculate amino acid identity percentages, the number of conserved amino acid residues in each aligned sequence pair was divided by the length of the shorter sequence.

SignalP 4.1 [23] and TargetP 1.1. [24] were used to predict N-terminal secretion signal peptides in the protein sequences (http://www.cbs.dtu.dk/services/). The default cutoff values were used in SignalP (chosen to optimize performance), and predefined cutoffs for specificity >0.95 were used in TargetP. C-terminal glycosylphoshpatidylinositol anchor attachment sites were predicted in the Pred-GPI server [25] (http://gpcr.biocomp.unibo.it/predgpi/) with the general model and taking "Highly probable" and "Probable" predictions (99.5% specificity cutoff) as positive. Potential N-glycosylation sites were identified by the sequence motif (N—not P—S/T—not P).

Phylogenetics

For phylogenetic analysis, the 57 vertebrate CARP X/XI and Drosophila CARP-B (CG32698) protein sequences were aligned with Clustal Omega. The protein alignment was used as guide in generation of a codon-based coding DNA sequence (CDS) alignment with the Pal2Nal web server [26], with the remove gaps/internal stop codons option. MrBayes [27] was run first to estimate a reliable set of model parameters. To produce our final tree, MrBayes was run for 50,000

generations utilizing the GTR+I (+G) model, with all other parameters as optimized by MrBayes. A 50% majority rule consensus tree was created, rooted by Archaeopteryx [28], with the *Drosophila* sequence as an outgroup. Final trees were drawn aided by the R package Ape [29].

Protein model

Preliminary protein models of human CARP X were constructed using the I-TASSER server [30,31] at http://zhanglab.ccmb.med.umich.edu/I-TASSER/ by submitting the sequence of residues 22–328. UCSF Chimera 1.8.1 [32] was used for creating model visualizations.

Zebrafish maintenance and ethics statement

Wild-type zebrafish of the AB and TL strain were maintained at 28.5°C as described previously [33]. The larvae were grown at +28.5°C in embryonic medium (5 mM NaCl, 0.17 mM KCl, 0.33 mM $CaCl_2$, 0.33 mM $MgSO_4$, and 10–15% Methylene Blue (Sigma-Aldrich)). All the experiments using zebrafish were performed according to the Provincial Government of Western Finland, Province Social and Health Department Tampere Regional Service Unit protocol # LSLH-2007-7254/Ym-23. The care was taken to ameliorate suffering by euthanizing the zebrafish by prolonged immersion in a petridish containing 0.04% tricaine (Sigma-Aldrich).

Isolation of total RNA and synthesis of cDNA

Total RNA was isolated from whole larvae at different stages of development during 0–168 hpf (0–7 dpf) and from specific organs of the adult zebrafish using the RNeasy mini RNA extraction kit (Qiagen, Hilden, Germany) according to the manufacturer's instructions. The concentration and purity of total RNA were determined using a NanoDrop Spectrophotometer (NanoDrop 2000, Thermo Scientific). cDNA synthesis was performed using 0.1–5 μg of total RNA and the First Strand cDNA Synthesis kit (Applied Biosystems, Foster City, CA) with random primers and M-MuLV reverse transcriptase according to the protocol recommended by the manufacturer.

Cloning and sequencing of *ca10a* and *ca10b* genes

ca10a and *ca10b* cDNAs were amplified using the primers P1 and P2 (Table 1). The primer P2 adds restriction sites for BamHI and XhoI to the amplification products. The resulting PCR products and pcDNA 3.1 vector were then digested with BamHI and XhoI and ligated with T4 DNA ligase (Promega). The *ca10a* and *ca10b* constructs were then transformed into One Shot TOP10 competent cells (Invitrogen, Espoo, Finland), and the cells were spread on LB plates containing ampicillin (2500μg/ml). The overnight colonies were screened by colony PCR for the presence of the *ca10a* or *ca10b* insert. The pcDNA3.1 plasmid was isolated from the 3-ml overnight culture using Plasmid Maxi Kit (QIAGEN), and sequencing of *ca10a* and *ca10b* was carried out using P2 from the plasmid DNA. The sequences were aligned with ClustalW and compared with cDNA obtained from Ensembl database (Transcript IDs *ca10a* and *ca10b* are ENSDART00000074540 and, ENSDART00000055264 respectively).

Quantitative analysis of *ca10a* and *ca10b* genes

Real time quantitative PCR (RT-qPCR) primers were designed based on the complete cDNA sequences taken from Ensembl (Transcript IDs as above: using the program Primer Express Software v2.0 (Applied Biosystems)) (Table 1). The RT-qPCR was performed using a SYBR Green PCR Master Mix Kit in an ABI PRISM 7000 Detection System according to the manufacturer's instructions (Applied Biosystems). The PCR conditions consisted of an initial

Table 1. Primer sequences used in the present study.

Gene /Ensembl transcript-ID	Name of the Primer	Upstream primer (5'-3')	Downstream primer (5'-3')	Product size (bp)
ca10a/ ENSDART00000074540	*ca10a*-G-DNA	TCAGGGAAGCCACCCTTGAATGA	AGAGAAGGCCTGGCCATTGAGG	400
	ca10a-RT PCR (P1)	ATGGATATAATCTGGGAAATATTTATTATTC	CTATTTCAGCAGCCATTCGTTC	Full Length
	ca10a-RT PCR	TCTCTCGGGGCTAAACATTG	TTGACTTAGCAGTCGCATGG	100
	ca10a-RT-qPCR	GAAACCAGTCGCATGATTTTTG	TTGCGTTGCCCTGCATT	-
	ca10a-T7 (P2) promoter-insertion	TAATACGACTCACTATAGGGATGGATATAATCTGGGAAATATTT	AATCCACCCAAAATCCATGA	Full Length
ca10b /ENSDART00000055264	*ca10b* -G-DNA	TAGTGTAAACGGGGCCTTACATTTTA	GATTGTCCTCACTGCCAAAGTG	400
	ca10b -RT PCR (P1)	ATGCCGCACGTTTGGGAGTT	TTATTTCAGAAGCCATTCATTCACTC	Full Length
	ca10b -RT PCR	TGGGGCTGAATATTGAGGAG	GGCTGGTTTTGACTGAGGAG	100
	ca10b -RT-qPCR	CCTGACACCACTGAGGCTCAA	CGGCCGGTGTTGTACATTG	-
	ca10b -T7 (P2) promoter-insertion	TAATACGACTCACTATAGGGATGCCGCACGTTTGGGAG	ACGTTTGGGAGTTCGTTCTG	Full Length

doi:10.1371/journal.pone.0134263.t001

denaturation step at 95°C for 10 min followed by 40 cycles at 95°C for 15 sec (denaturation) and 60°C for 1 min (elongation). The data was analyzed using the ABI PRISM 7000 SDS software (Applied Biosystems). Each PCR reaction was performed in a total reaction volume of 15 μl containing 20ng of cDNA, 1 × Power SYBR green PCR Master Mix (Applied Biosystems, Foster City, CA, USA), and 0.5 μM of each primer. The relative expression of the genes between the studied samples, and internal control gene β-actin were calculated according to Pfaffl's equation [34].

Knockdown of *ca10a* and *ca10b* genes in zebrafish larvae using antisense morpholino oligonucleotides

To check for the possible polymorphism in genomes at the morpholino target site, we amplified the genomic target region of six adult zebrafish (Table 1) and sequenced the PCR products. The sequenced genomic regions were analyzed for the presence of polymorphism before designing the antisense morpholinos (MOs). Two independent MOs, translation-blocking and splice junction blocking, were designed for the *ca10a* gene, while two splice site blocking MOs, each one targeting a different exon, were designed for the *ca10b* gene. The MOs were designed by Gene Tools (GeneTools LLC, Philomath, OR, USA). As a control, random control (RC) MOs, which did not correspond to any gene in the zebrafish, and *p53*-MOs, which suppress the expression of *p53* mRNA, were used. The control MOs were also obtained from the Gene Tools (Table 2). 1–2 nl of antisense MOs in 0.2 M KCl, 10% phenol red and 10% Rhodamine B (Sigma-Aldrich) was injected into the yolks of one to two-cell stage larvae.

Phenotypic analysis of morphant and control larvae

The phenotype of the morphant and control embryos (0-5dpf) was analyzed under a light microscope. Approximately 10 to 15 *ca10a* and *ca10b* morphant larvae were screened per set of experiments, with a similar number of control larvae. For the imaging, the larvae were anesthetized using 0.02% Tricaine in embryonic medium and embedded in 17% high molecular weight methylcellulose in 15x30 mm transparent polypropylene Petri dish. The images were taken using a Lumar V1.12 fluorescence stereomicroscope attached to a camera with a 1.5X lens (Carl Zeiss MicroImaging GmbH, Göttingen, Germany). The images were analyzed with AxioVision software versions 4.7 and 4.8.

Rescue of *ca10a* and *ca10b* morphant zebrafish with mRNA injections

Capped mRNAs encoding full-length sequences of human *CA10* and *CA11* were used for the rescue of *ca10a* and *ca10b* morphant embryos. The human *CA10* and *CA11* clones (*CA10*: IMAGE Id 5276935, CA11: IMAGE Id 3613247) were purchased from the mammalian gene collection (MGC Geneservice Ltd, Cambridge, UK). The coding regions of *CA10* and *CA11*

Table 2. Morpholino sequences used for knockdown of *ca10a* and *ca10b* genes.

Gene Name	Name of Morpholinos	Morpholino oligonucleotide sequence
ca10a	MO1-Translation blocking	5'TGTCTTCATTCCAAGTCCATTGCGC3'
	MO2-Splice site blocking	5'CATCTGTAAGGACAAGCAGAGGTTT3'
ca10b	MO1-Splice site blocking	5'ACTGACCTGAAAAACACACCCAAAC3'
	MO2-Splice site blocking	5'GACTGCATCTATGGAAATTCATTAT3'
Radom control (RC)	Control MO	5'CCTCTTACCTCAGTTACAATTTATA3'
p53	*p53* MO	5' GCGCCATTGCTTTGCAAGAATTG 3'

doi:10.1371/journal.pone.0134263.t002

were PCR amplified using the same primers and protocol described previously (Table 1). The restriction sites were added into the PCR product using P2 primers (Table 1) and cloned into a pcDNA3.1 (+) vector. The vector containing the inserts was linearized using KpnI and the capped *CA10* and *CA11* mRNA was transcribed using the mMESSAGE mMACHINE T7 Kit (Ambion), according to the manufacturer's instructions. For the rescue experiments, two groups of embryos were injected with 300 μM of *CA10*/*CA11* MOs, 300 μM antisense MOs, and 80 pg/embryo of *CA10*/*CA11* capped mRNA.

Design and production of guide RNAs (gRNAs) for CRISPR/Cas9 mediated genome editing

Target sequences for the *ca10a* and the *ca10b* gRNAs were identified with the online based CRISPR design tool (http://crispr.mit.edu/) and validated with the sgRNA tool of the Casellas laboratory [35], (Retrieved 07:16, May 19, 2015 (GMT)) and BLAST analysis [36]. Initially, three target sequences for *ca10a* and two for *ca10b* were tested (Table 3). The target sequence for *egfp* gRNA was adopted from Jao et al. [37] and gRNAs were produced mostly as described previously [38]. In brief, gRNA oligo (Sigma-Aldrich) and T7 promoter site oligo (Sigma-Aldrich) were annealed and transcribed *in vitro* using the MEGAshortscript T7 Transcription Kit (Ambion Life Technologies, CA, USA). The integrity and size of the produced gRNAs was checked with a 1% agarose Tris-acetate-EDTA (TAE) gel electrophoresis. However, the gRNA design template was slightly modified with two additional guanine nucleotides in the 3′ end of the T7-promoter site (S1 Fig).

gRNA and *cas9* mRNA microinjection and genomic DNA extraction

The gRNAs and the *cas9* mRNA (Invitrogen, Life Technologies) were co-injected into one-cell stage zebrafish embryos with a micro injector (PV830 Pneumatic PicoPump, World Precision Instruments) under a Nikon microscope (SMZ645). The embryos were aligned on 1.2% agarose embryonic medium plates prior to the injection. For genome editing, injection solution of 1 nl contained 270 pg gRNA and 330 pg cas9 mRNA in nuclease-free water. 1.5 ng of phenol red tracer was added to the solution for visualization of the injections. The injection experiments were controlled with un-injected, and gRNA-injected (a mixture of different gRNAs for *ca10a* and *ca10b*, 1280 pg in an injection) embryos. Between 1 and 5 days post fertilization (dpf), zebrafish embryos were visually inspected and imaged with a Lumar V12 microscope (Zeiss, Germany). At 2 and 5 dpf, selected embryos were lysed and genomic DNA isolated from either a single or a pool of embryos (5–10 individuals).

Table 3. Gene targets and primers for CRISPR/Cas9 mediated knockout studies.

Gene	Targeted exon	Targeted sequence	Primer sequences
ca10a	2	TCCACCCAAAATCCATGA	F GAAGCTGTTTGCCAGAAATC
			R ATCCAACACCATCAAAGAAGTC
	2	TACAAAGAAGTTGTTCAG	F GAAGCTGTTTGCCAGAAATC
			R ATCCAACACCATCAAAGAAGTC
	3	ACTGAGGCTCAACACTGG	F CTGCAAATCATCCCTTTGTG
			R GTTCCTCGCATCAAAACACC
ca10b	1	AACGAACTCCCAAACGTG	F TCCACGACTCAGCCAACAG
			R GCACTGCGTTATCAGCAAAAG
	3	TTGGGAAGAGACAGTCGC	F CCGCTCTTCCAAACAGATC
			R GTGGATGATTGACAGGGCTC

doi:10.1371/journal.pone.0134263.t003

T7 Endonuclease mutation detection assay

Targeted loci were amplified from genomic zebrafish DNA by PCR using Maxima Hot Start DNA polymerase (Thermo Scientific) according to manufacturer's instructions. PCR primers (Table 3) were designed to anneal upstream and downstream of the expected cutting site. A previously described T7 endonuclease assay protocol with minor changes was used [35]: 1.5μg of PCR product was annealed in a 20μl reaction of 1x NEBuffer 2 (New England Biolabs, MA, USA) and the annealed sample was incubated with 0.5μl (6 units) of T7 endonuclease I (New England Biolabs) for 30 minutes at 37°C. Obtained products were separated with a 2.5% agarose TAE gel and the band sizes were compared to control samples.

Histochemical analysis and TUNEL assay

To study the tissue morphology of 5 dpf *ca10a* and *ca10b* morphant larvae a histochemical analysis was performed. Prior to the analysis the larvae were washed with PBS and fixed in 4% paraformaldehyde (PFA) in PBS for 3 hours at room temperature and the fixed larvae were transferred to 70% ethanol and stored at 4°C before being embedded in paraffin. The paraffin embedded samples were sectioned into 5 μm slices for the histochemical staining.

The fixed sections were deparaffinized in xylene, rehydrated in an alcohol series and histologically stained with Mayer's Hematoxylin and Eosin Y (both from Sigma-Aldrich). After dehydration, the slides were mounted with Entellan Neu (Merck; Darmstadt, Germany), examined and photographed using a Nikon Microphot microscope (Nikon Microphot-FXA, Japan).

To detect apoptotic cell death in the *ca10a* and *ca10b* morphants and the control larvae, a TdT-UTP nick end labeling (TUNEL) assay was performed for the prepared slides using the QIA39 FragEL DNA Fragmentation Detection Kit (Merck Chemicals Ltd., Nottingham United Kingdom). Briefly, the deparaffinized sections of the larvae were incubated with the TdT enzyme followed by incubation with anti-digoxigenin. Fluorescence staining was detected and photographed using a Nikon Microphot microscope (Nikon Microphot-FXA, Japan).

Swim pattern analysis

In order to analyze the minute body movements of the *ca10a* and *ca10b* morphant larvae the swimming pattern of the morphants, uninjected, and the RC MO injected larvae were observed under a microscope. For the analysis, 5 dpf larvae were placed on a Petri dish (5 larvae/dish) containing embryonic medium. The larvae were allowed to settle in the dish for 2 min. The video recording of the swim pattern was done using a Lumar V1.12 fluorescence stereomicroscope (Carl Zeiss MicroImaging GmbH) and AxioVision software versions 4.7 and 4.8. The swimming pattern study of the larvae was repeated a minimum of three times. In addition to these videos, a total of 457 5dpf zebrafish larvae from four groups (*ca10a* morphants, n = 127; *ca10b* morphants, n = 145; RC, n = 101; and uninjected, n = 80) were analyzed for their displacement pattern and distance travelled. In this analysis, the larvae were placed on 90 mm Petri dishes filled with embryonic medium, in groups of 13 to 22, and recorded for 2 minutes. The movements of all the larvae were analyzed using the MtrackJ plugin [39] within the ImageJ program [40]. Distances traveled (cm/1 min) were calculated for each fish.

Results

Zebrafish CARP Xa and CARP Xb proteins are similar to human CARP X

As a result of our revised gene prediction analysis within the CARP X/XI family, a total of 881 amino acid positions were improved, and six sequences were improved to completeness (Table 4). The File S1 data includes all novel sequences based on our improved gene models.

Table 4. Sequences of CARP X/XI family.

Focus sequences			
Description	**Complete protein**	**Ensembl Protein ID**	**Ensembl Transcript ID**
Homo sapiens CARP X	x	ENSP00000405388	ENST00000451037
Homo sapiens CARP XI	x	ENSP00000084798	ENST00000084798
Danio rerio CARP Xa	x	ENSDARP00000069028	ENSDART00000074540
Danio rerio CARP Xb	x	ENSDARP00000055263	ENSDART00000055264
Novel and improved sequences			
Description	**Complete protein**	**Previous Ensembl**	**Changes**
Anas platyrhynchos CARP X	x	ENSAPLP00000003254	Added 75 amino acids in the first 3 exons.
Astyanax mexicanus CARP Xa	x	ENSAMXP00000005715	Replaced 8 amino acids in the 9th exon.
Astyanax mexicanus CARP Xb	x	ENSAMXP00000001335	Added 31 amino acids in the 5th exon.
Choloepus hoffmanni CARP X	x	ENSCHOP00000007972	Added 14 amino acids in the 5th exon.
Dasypus novemcinctus CARP XI	x	ENSDNOP00000030322	Replaced 64 amino acids in 1st and 2nd exons.
Dipodomys ordii CARP X	x	ENSDORP00000010999	Added 22 residues in the 1st exon.
Dipodomys ordii CARP XI	x	ENSDORP00000009964	Replaced 68 amino acids in 6th and 7th exons.
Ficedula albicollis CARP X	x	ENSFALP00000002897	Replaced 15 amino acids in the 4th exon.
Gadus morhua CARP Xb	x	ENSGMOP00000009825	Replaced 25 amino acids in the 6th exon.
Lethenteron japonicum CARP-A	x	**Novel**	Our novel gene model.
Lethenteron japonicum CARP-B	x	**Novel**	Our novel gene model.
Loxodonta africana CARP X	x	ENSLAFP00000013325	Added 7 amino acids in the 9th exon.
Macropus eugenii CARP X	x	ENSMEUP00000011719	Added 1 amino acid in the 1st exon.
Microcebus murinus CARP X	x	ENSMICP00000008888	Replaced 2 amino acids in the 6th exon.
Otolemur garnettii CARP X	x	ENSOGAP00000004458	Replaced 25 amino acids in the 1st exon.
Pteropus vampyrus CARP X	x	ENSPVAP00000013111	Replaced 25 amino acids in the 1st exon.
Sarcophilus harrisii CARP X	x	ENSSHAP00000012943	Added 105 amino acids in the 4th, 5th, and 6th exons.
Tursiops truncatus CARP X	x	ENSTTRP00000001587	Replaced 26 amino acids in the 1st exon.

doi:10.1371/journal.pone.0134263.t004

Zebrafish and other ray-finned fishes have two *CA10* orthologs, *ca10a* and *ca10b*, as reported earlier [6]. *ca10a* is highly similar to mammalian *CA10* (90% identity to human CARP X at protein level), whereas *ca10b* is slightly more diverged, yet highly similar (75% identity between human CARP X and zebrafish CARP Xb) (Table 5). In addition, the phylogenetic branching pattern (Fig 1) and the appearance of the alignment (Fig 2) clearly support the notion that fish CARP Xa and Xb are closer to tetrapod CARP X than to CARP XI. The position of the two CARPs of lamprey (*Lethenteron*) indicates that they have duplicated from a single ancestor in the cyclostome lineage, and that the duplication to CARP X and CARP XI took place only in the jawed vertebrates.

It is notable that most vertebrates and even many insects and nematodes have two genes that code for CARP X-like acatalytic proteins, resulting from lineage-specific duplications. However, in case of birds, we could not detect even fragments of genes like *CA11* or *ca10b*, not in database searches nor in Exonerate scans of five bird genomes. In addition to *CA8*, the only gene coding for CARPs in birds is *CA10*, present as one copy per genome.

CARP X-like proteins have features of secretory proteins conserved from primitive invertebrates

A signal peptide is predicted to be present in 60 of 61 CARP X-like protein sequences by TargetP or in 59 of 61 sequences by SignalP. If we exclude the two lamprey sequences, which lack initial methionine and part of the first exon, we get predicted secretion in all sequences, with reliability classes from 1 to 3 (1 = best, 5 = worst) by TargetP and by SignalP. All tetrapod CARP X sequences, and most fish CARP Xa/Xb sequences, show signal peptide predictions with reliability class 1. The predicted signal peptide cleavage sites in human CARP X and XI, and in zebrafish CARP Xa and CARP Xb coincide with the end of the sequence coded by the first exon in each gene. No glycosyl-phosphatidylinositol anchor attachment sites were predicted for any of the sequences.

All 61 CARP protein sequences in our study possess three conserved cysteines, corresponding to the positions 60, 244, and 310 in human CARP X. In addition, there is a fourth cysteine residue (296 in human CARP X) which is conserved in CARP X in tetrapods, coelacanth (*Latimeria*), the CARPs in lamprey, and CARP Xa and Xb. However, the fourth cysteine residue is not found in CARP XI or in the invertebrate CARP X-like proteins. In addition, there are several non-conserved cysteines in the predicted signal peptide regions. The conserved cysteines C60 and C223 are predicted to be within the CA domain. Their positions in the sequence alignment, and preliminary protein model correspond approximately to the position of the conserved disulfide seen in the structures of CA IV, VI, IX, XII, and XIV, and in sequence alignments of CA XV and XVII [4], but which is absent from other, intracellular CA isoforms (Fig 3) A disulfide with a reasonable geometry could be formed easily, even though the model displaces the first cysteine by one turn of a helix relative to the position seen in other CAs.

Table 5. Comparisons of CARP X-like proteins as identity percentages between aligned protein sequences.

	Human CARP X	Human CARP XI	Zebrafish CARP Xa	Zebrafish CARP Xb
Human CARP X	100	50	90	75
Human CARP XI		100	51	47
Zebrafish CARP Xa			100	76
Zebrafish CARP Xb				100

doi:10.1371/journal.pone.0134263.t005

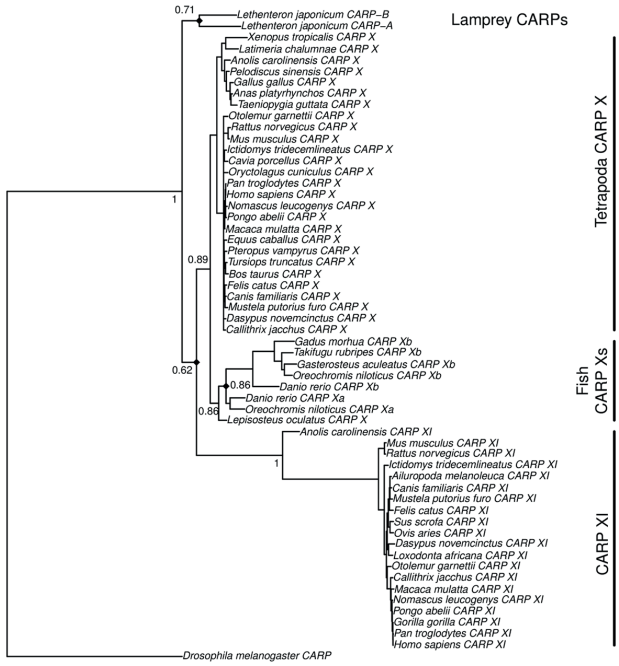

Fig 1. Bayesian phylogenetic tree of CARP sequences. Numbers at the nodes indicate posterior probabilities, and branch lengths are proportional to distances. A table of full details of the sequences is given as S1 Table.

doi:10.1371/journal.pone.0134263.g001

The third conserved cysteine (C310) occurs in the C-terminal region, which is unique to CARP X-like proteins, and for which no reliable structural template is available. The additional semi-conserved cysteine (C296), seen in CARP X/Xa/Xb but not in CARP XI, would be located near the C terminus of the CA domain. Again, it is noteworthy that the three conserved cysteines are present even in the CARP sequences of nematodes and insects (Fig 4).

Two conserved N-glycosylation motifs are seen in CARP X-like proteins, at N116 and N168 (human CARP X numbering). These positions correspond to non-conserved surface residues, which are not a part of a glycosylation motif (N—not P—S/T—not P) in any other human or zebrafish CA, except for CARP X/XI/Xa/Xb. Likewise, the positions that correspond to the adjacent S/T residues (118 and 170 in human CARP X) are conserved only in CARP X-like proteins. There is a third glycosylation site which is unique to CARP XI sequences, and another one which is unique to CARP X/Xa/Xb.

Fig 4 shows a sequence alignment of CARP X-like proteins of a diverse selection of vertebrates and invertebrates, highlighting the presence of signal peptides, three conserved cysteines, and two conserved glycosylation motifs.

Zebrafish *ca10a* and *ca10b* genes are strongly expressed in the nervous system and in developing embryos

We used RT-qPCR to study the expression of *ca10a* and *ca10b* in adult zebrafish. Expression analysis showed the presence of *ca10a* in most of the studied tissues (Fig 5A). The expression

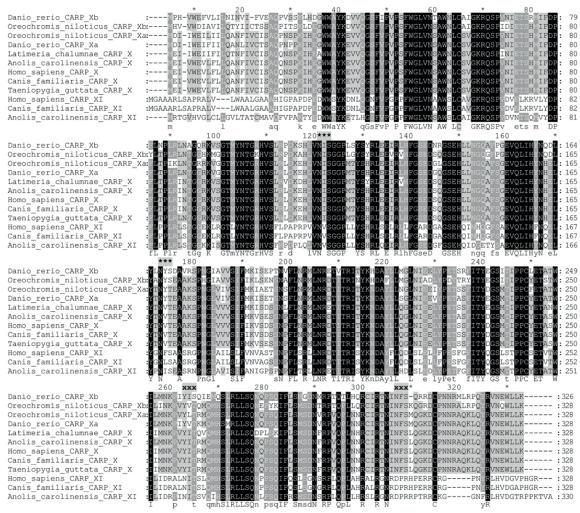

Fig 2. Multiple sequence alignment of selected CARP X-like protein sequences. Groups of three asterisks (***) above the sequences indicate conserved N-glycosylation motifs in all CARP X-like proteins, and letters 'xxx' above the sequences indicate N-glycosylation motifs which are only found in either CARP X or CARP XI sequences (NFS and NIT, respectively).

doi:10.1371/journal.pone.0134263.g002

of *ca10a* was highest in the heart, eye, and brain. In addition, *ca10a* was expressed in fins, testis, kidney, gills, intestine, ovary, spleen, skin, muscle, and swim bladder. Interestingly, no *ca10a* expression was detected in the liver (Fig 5A).

The tissue specific expression pattern of the *ca10b* gene showed differences compared to that of *ca10a* (Fig 5B). The highest expression of *ca10b* was found in the ovary, brain, and

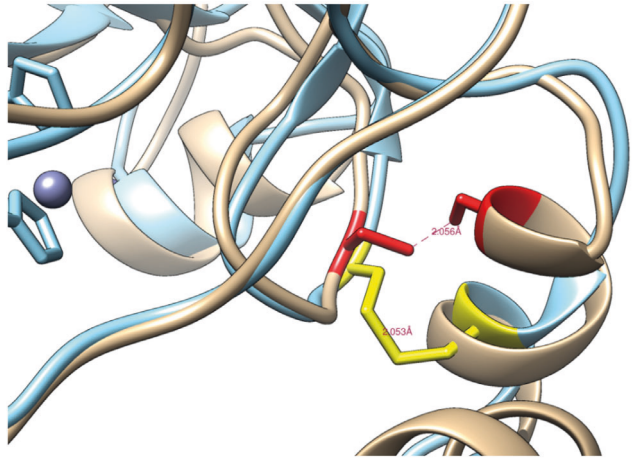

Fig 3. Preliminary model of human CARP X. The model showing a disulfide bridge between conserved cysteines C60 and C223 (marked in red).

doi:10.1371/journal.pone.0134263.g003

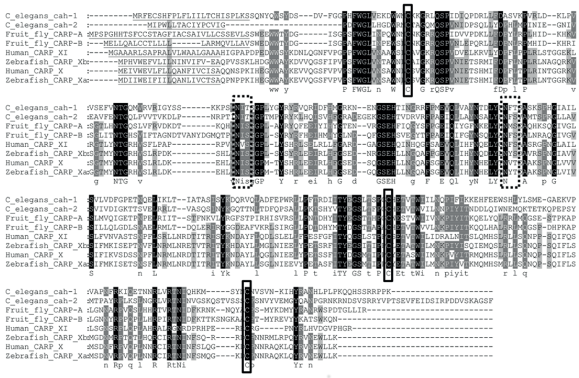

Fig 4. Sequence alignment of human, zebrafish, *C. elegans*, and *D. melanogaster* CARP X-like proteins. Dashed, broad boxes indicate conserved N-glycosylation sites, and solid, narrow boxes indicate conserved cysteines. Underlining in the N-terminal regions indicates predicted signal peptides.

doi:10.1371/journal.pone.0134263.g004

swim bladder. Expression was also observed in the fins, testis, kidney, gills, intestine, spleen, skin, heart, and eye whereas no signal for *ca10b* was found in the liver or muscle.

In addition, we used RT-qPCR to investigate the expression of *ca10a* and *ca10b* during the development of 0–168 hpf (0–7 dpf) zebrafish larvae (Fig 6). Expression of both *ca10a* and *ca10b* were highest at 96 hpf (4 hpf) and remained high thereafter. Low levels of *ca10a* and *ca10b* expression was seen at earlier time points. The expression pattern suggests that the *ca10a* gene product is required throughout embryonic development, especially after 72 hpf (3 dpf). Interestingly, *ca10b mRNA* was present at a very high level at 0 hpf, suggesting maternal origin (Fig 6B) and this is also supported by the high expression in the ovary of the adult fish (Fig 5B). The expression pattern of the *ca10b* gene suggests that this gene plays a role at the beginning of development and is required throughout embryonic development in zebrafish.

Knockdown of *ca10a* and *ca10b* genes causes developmental abnormalities in zebrafish larvae

Evolutionary conservation of *CA10*-like genes, their ubiquitous expression pattern in different tissues, and high mRNA levels during embryonic development suggest a crucial role for CARP X-like proteins in vertebrates [41]. To shed light to the biological significance of CARP X-like proteins in embryogenesis, we silenced zebrafish *ca10a* and *ca10b* genes with MOs (Fig 7A, 7B and 7C).

The translation-blocking antisense MO for *ca10a* (*ca10a*-MO1) targeted a sequence that includes the ATG start codon (from -15 to +10 nucleotides, relative to ATG) and inhibits translation of mRNA. MO2 (*ca10a*-MO2) targeted exon 8, resulting in expression of shorter length *ca10a* mRNA (Fig 7D). Both antisense MOs for the *ca10b* gene (*ca10b*-MO1 and *ca10b*-MO2) resulted in truncated *ca10b* mRNAs as shown in Fig 7E.

The 1 dpf zebrafish larvae injected with 200 μM *ca10a*-MO1 showed defects in the head, abnormal body structure, and small eyes with a delayed hatching from the chorion (Fig 8B). As the development progressed, the abnormalities became more prominent; the larvae had long tapering curved tails, curved body structure, pericardial edema, absence of swim bladder, and otolith vesicles (Fig 8B). The embryos injected with *ca10a*-MO2 showed a less severe phenotype compared with the *ca10a*-MO1 injected larvae (Fig 8D). Injection of a higher

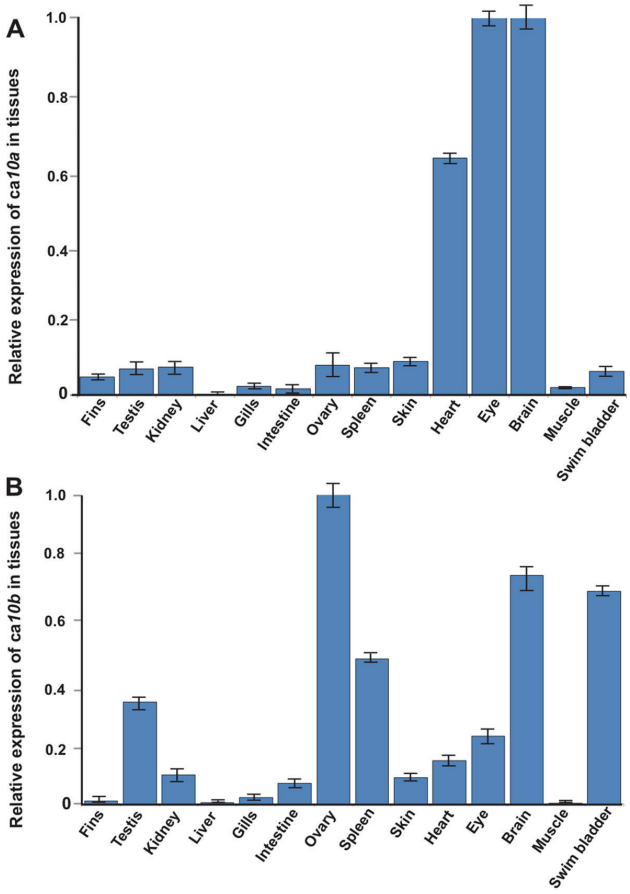

Fig 5. Expression levels of *ca10a* and *ca10b* genes in adult zebrafish tissues. A quantitative analysis of *ca10a* and *ca10b* genes was made for 14 adult zebrafish tissues using RT-qPCR. **A**, expression of *ca10a* in zebrafish tissues; **B**, expression of *ca10b* in zebrafish tissues. The values were normalized to the beta actin control according to the Pfaffl´s equation [34]. The expression of the *ca10a* gene in brain and *ca10b* in the ovary assigned a relative value of 1.

doi:10.1371/journal.pone.0134263.g005

concentration (300 μM) of *ca10a*-MO led to a more severe phenotype compared to the lower dose with higher mortality in the morphant larvae after 24 hpf (Fig 9 and Table 6). Further increase in the MO concentration (above 300 μM) had lethal effect on the larvae.

The specificities of the MOs were confirmed by analyzing the lengths of *ca10a* and *ca10b* mRNAs from the morphant embryos injected with the splice site blocking morpholinos. Analysis of *ca10a* mRNA from 5 dpf morphant fish injected with *ca10a*-MO2 (designed to knock down one exon in *ca10a* mRNA) showed two bands on the agarose gel, one corresponding to the wild type length mRNA and the other band corresponding to the *ca10a* morphant mRNA (Fig 7D). The analysis of mRNA from 5 dpf morphant zebrafish injected with *ca10b*-MO1 and *ca10b*-MO2 (both targeting different exons in *ca10b* mRNA) showed two short bands in addition to the normal length bands compared with mRNA from wild type fish (Fig 7E). The result

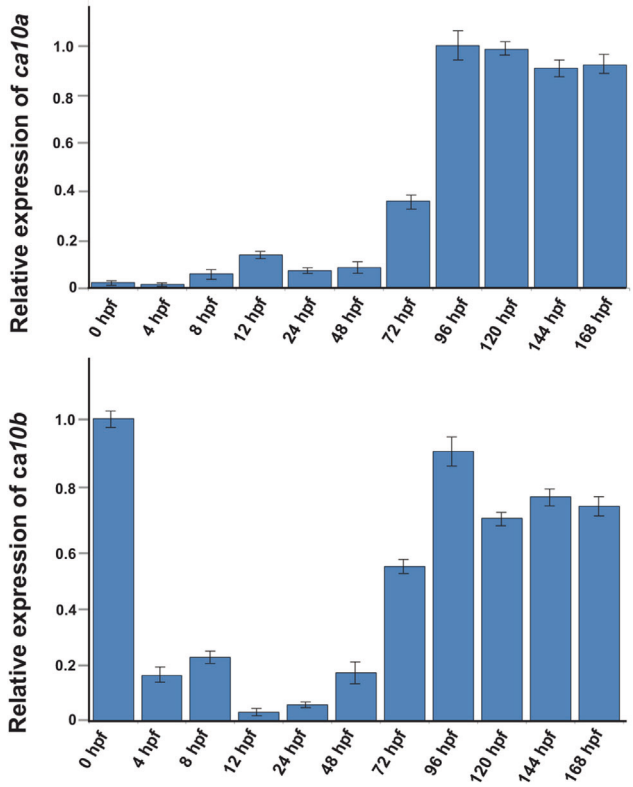

Fig 6. Expression analysis of *ca10a and ca10b* mRNAs during embryonic development. The expression levels of *ca10a and ca10b* were measured from the total mRNA isolated from the developing larvae of 0–168 hpf. **A)** Expression values of *ca10a* mRNA. **B)** Expression values of *ca10b* mRNA. The expression values were normalized to the beta actin control according to the equation of Pfaffl [34]. The expression of *ca10a* gene at 0 hpf and *ca10b* at 96 hpf assigned a relative value of 1.

doi:10.1371/journal.pone.0134263.g006

of mRNA analysis from the morphant zebrafish confirmed that the defective phenotypes observed in the *ca10a* and *ca10b* morphant fish were due to specific knock down effects of these genes by antisense MOs.

The larvae injected with 200 μM of *ca10b*-MO1 showed severe phenotypic defects as early as 12 hpf (data not shown). The *ca10b*-MO1 morphants at 1 dpf were short and the shape of the body was abnormal. The morphant larvae were very fragile and had a high mortality rate (Figs 8C and 9 and Table 6). They could not survive beyond 3 dpf nor did they hatch properly from the chorion. Injection of *ca10b*-MO2 produced a milder phenotype compared with the larvae injected with *ca10b*-MO1. The *ca10b*-MO2 morphant larvae showed abnormal body structure, smaller head and eye structure, mild pericardial edema, absence of otolith sacs, unutilized yolk sac, and curved tail (Fig 8E).

There was no significant difference between the phenotype defects and mortality rates of larvae injected with *CA*-MOs alone or in combination with *p53*-MOs (Table 6). In addition, the uninjected embryos and embryos injected with RC-MOs showed normal phenotypes and

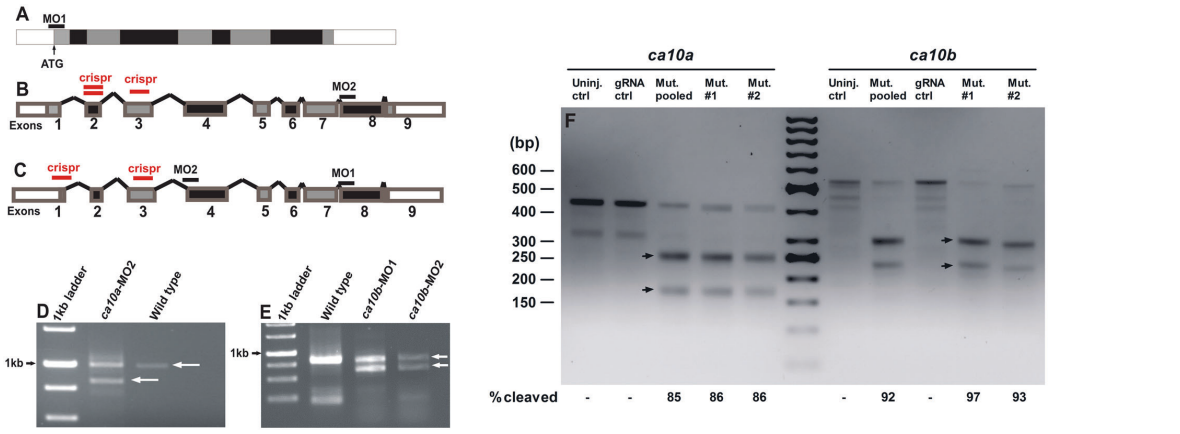

Fig 7. Silencing of *ca10a* and *ca10b* in zebrafish larvae. A) Schematic presentation of matured *ca10a* mRNA showing the site of translational blocking with MO1 at the translation start site (arrow). **B)** Schematic structure of unprocessed mRNA for *ca10a* with a target region (horizontal bar) for a splice site blocking morpholino (MO2) which knocks down the exon eight. **C)** Schematic depiction of unprocessed mRNA for *ca10b* and target sites for splice site interfering morpholinos, MO1 and MO2 (black horizontal bars) and gRNA target regions (red horizontal bars). **D)** Gel electrophoresis showing RT-PCR analysis of *ca10a* morphant mRNA injected with MO2. **E)** RT-PCR gel image of *ca10b* morphant zebrafish mRNA injected with MO1 and MO2 targeting different exons. The images show the reduction in the length of the mRNAs (Lane 2 in **D** and Lane 3 and 4 in **E)** compared with wild type mRNAs of *ca10a* and *ca10b* in wild type fish (Lane 3 in **D** and lane 2 **E**). **F)** The efficiency of the CRISPR/Cas9 mediated mutagenesis in zebrafish embryos was evaluated with a T7 endonuclease assay. For both *ca10a* and *ca10b*, uninjected and gRNA control fish are shown and as well as two individual embryos with a mutated target site and a pool of 5–10 mutated embryos. Representative cleaved PCR products of the expected sizes are shown as arrow heads. Cleavage percentage was calculated from the band intensities of each lane.

doi:10.1371/journal.pone.0134263.g007

similar survival rates (Fig 9 and Table 6). These results suggest that the phenotypic defects seen in morphant embryos injected with *ca10a* and *ca10b* MOs were most likely due to knockdown of these genes and not p53-dependent off-target effects of antisense MOs, which normally occur in 10–20% of the MO knockdown studies [42].

We validated our results of the *ca10a* and *ca10b* MO knockdown by silencing the respective genes with the CRISPR/Cas9 genome editing method [37,38]. To establish this method, we first targeted *egfp* in a transgenic zebrafish line (*fli1a:egfp*) using a previously described gRNA [37], and confirmed mutations in the target region with a T7EI assay (S2 Fig). To silence *ca10a* and *ca10b*, we initially, we designed 3 gRNAs for the *ca10a* gene and 2 gRNAs for the *ca10b* gene, each of which targeted different exons or different locations in the same exon (Fig 7B and 7C). We then compared the cutting efficiency for each gRNA and chose the most efficient gRNAs (*ca10a*-exon 3 gRNA and *ca10b*-exon 1 gRNA) for both genes based on the results of the T7EI assay (Fig 7).

Similar to the MO injected larvae, the phenotype of *ca10b* mutated larvae was severe with high mortality at 1 dpf and larvae did not survive beyond 2 dpf (Fig 8H). The *ca10a* mutated larvae showed a less severe phenotype (Fig 8G) with a lower mortality rate at 1 dpf. Larvae injected with only gRNA showed normal phenotypes compared to uninjected controls. With the T7 assay, we detected a cleavage efficiency of up to 86% for *ca10b* and up to 97% for *ca10a*. For the assay, individual mutated larvae as well as mutated larvae pooled together were analyzed (Fig 7F).

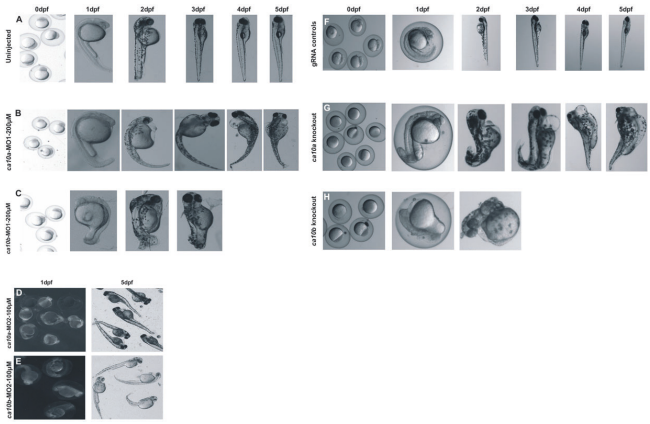

Fig 8. The *ca10a and ca10b* genes play an important role during embryonic development in zebrafish. **Left panel:** Developmental images of *ca10a* and *ca10b* morphant zebrafish injected with two different sets of antisense MOs (MO1 and MO2) over the period of 0 hpf to 5 dpf. **A)** The top row images show 0 hpf embryos and lateral views of 1–5 dpf uninjected zebrafish larvae with a normal development of organs,. **B)** *ca10a* morphant zebrafish injected with 200 μM translational blocking antisense morpholinos (MO1). **C)** Images of *ca10b* morphant zebrafish. **D)** and **E)** Images of *ca10a* and *ca10b* morphants. The images in first panel of **D** and **E** show the 1 dpf larvae with rhodamine fluorescence throughout the larvae (indicating successful MO injection) and second panel (**D** and **E**) shows the 5 dpf larvae with abnormal appearance. **Right panel:** Developmental images of *ca10a* and *ca10b* CRISPR mutated fish and gRNA controls. **F)** The top row images show 0 dpf embryos and lateral views of 1–5 dpf gRNA injected zebrafish larvae (control) with a normal development of organs. **G)** *ca10a* mutated zebrafish injected with gRNA and *cas9* mRNA targeted to exon 3 (target site shown in Fig 7B). **H)** *ca10b* mutated zebrafish injected with gRNA and *cas9* mRNA targeted to exon 1(target site shown in Fig 7C).

doi:10.1371/journal.pone.0134263.g008

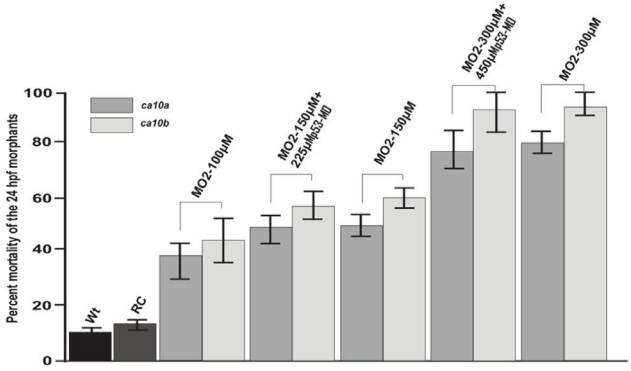

Fig 9. The percent mortality of the morphant larvae at 24 hpf. The mortality rate of *ca10a* and *ca10b* MO injected larvae was significantly higher than that of controls (P< 0.001). Larvae injected with *p53*-MOs along with *ca10a* or *ca10b* -MOs and larvae injected with *ca10a* or *ca10b* -MOs alone did not show significantly different mortality rates.

doi:10.1371/journal.pone.0134263.g009

Table 6. Phenotypes of zebrafish larvae knocked down with different concentrations of *ca10a* and *ca10b* antisense morpholinos.

ca10a/*ca10b*-MO2s (μM)	Normal	Mild	Moderate	Severe	Dead	Total
MO 300	11 (1.8)/ 9 (1.5)	16 (2.6) /7 (1.2)	46 (7.6) /37 (6.2)	70 (11.7) /73 (12.2)	457(76.2) /474(94.8)	600
MO 300 + *p53* 300	2 (0)/ 0 (0)	3 (2.0) /0 (0)	4 (9.3) /1 (0.6)	29 (19.3) /8 (5.3)	112 (74.6) /141 (94.0)	150
MO 150	22 (4.4)/ 13 (2.6)	43 (8.6) /32 (6.4)	82 (16.4) /47 (9.4)	121 (24.2) /96 (19.2)	232 (46.4) /312 (62.4)	500
MO 150 + *p53* 225	19(3.8)/ 16 (3.2)	38 (7.6) /41 (8.2)	76 (15.2) /32 (6.4)	144 (28,8) /119 (23,8)	223 (44.6) /292 (58.4)	500
MO 100	4 (2.6)/ 2 (1.3)	21 (14) /14 (9.3)	27 (18.0) /16 (10.6)	92(61.3) /51 (34)	56 (37.3)/ 67 (44.6)	150
MO 50	102(68)/92 (61.3)	27(18.3)/34 (22.6)	7(4.6)/5(3.4)	3 (2)/4(2.6)	11(7.3)/15(10)	150
RC MO	422 (84.4)	2 (0.4)	4 (0.8)	11 (2.2)	61 (12.4)	500
Uninjected	446 (89.2)	0 (0)	6 (1.2)	8 (1.6)	40 (8)	500

The phenotypic data was obtained from a minimum of three independent sets of morpholino injections with a minimum of 100–200 zebrafish embryos in each group. The *ca10a* and *ca10b* morphant larvae examined for each group is shown as percentage of total number of larvae studied at 24 hpf. Random control (RC) morpholino injections were made according to the concentration of *ca10a* and *ca10b* MO1 in each set of experiments. Larvae injected with 50 μM concentrations of either *ca10a*-MO2s or *ca10b*-MO2s had a phenotype similar to uninjected larvae but showed abnormal swim patterns (S1 and S2 movies).

doi:10.1371/journal.pone.0134263.t006

The *ca10a* and *ca10b* morphant larvae showed morphological changes in the tissues and apoptosis in the head region

The expression pattern of *ca10a* mRNA suggests that CARP Xa protein plays an important role in the brain, eye, and several other tissues. CARP Xb might play some roles in reproduction and brain functions. We studied morphological changes in the larvae injected with 200 μM *ca10a*-MO2 and *ca10b*-MO2 and compared the results with wild type larvae and larvae injected with RC-MOs. We prepared semi-thin (5–10 μm) sections of 5 dpf control larvae, larvae injected with 200 μM *ca10a*-MO2, and larvae injected with 200 μM *ca10b* -MO2 and stained them with Hematoxylin and Eosin. The morphological examination showed gross morphological changes in the head and eye regions of *ca10a* and *ca10b* morphant larvae (results not shown). Similarly, there was a clear difference between the somites of control larvae and those of the *ca10a*-MO and *ca10b*-MO injected morphant larvae.

The TUNEL assay on sections of *ca10a*-MO2 injected 5 dpf zebrafish larvae showed apoptotic cells especially in the head and eye regions (Fig 10A and 10B). Similarly, large areas of apoptotic cells were observed in the head region of 5 dpf *ca10b-MO2* morphant zebrafish larvae (Fig 10C) and weaker signals were seen in the tail region (Fig 10D). The TUNEL assay did not show any signs of apoptosis in wild-type larvae or larvae injected with RC-MOs (data not shown).

Human *CA10* and *CA11* mRNAs partially rescue the morphant phenotypes

To confirm the specificity of the phenotypes produced by antisense MOs, we co-injected the *ca10a* and *ca10b* MOs with capped human mRNAs for *CA10* and *CA11* genes. The morphant

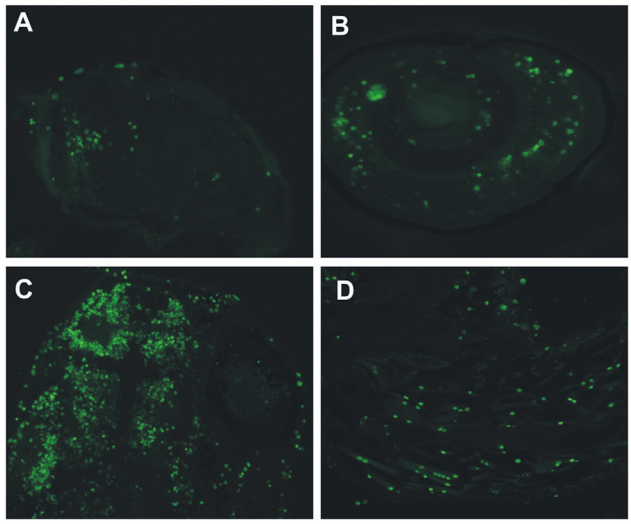

Fig 10. Knockdown of *ca10a* and *ca10b* genes leads to apoptosis in the morphant zebrafish. Results of the TUNEL assay detecting apoptotic cells in 5 dpf morphant embryos. **A)** head region of a *ca10a* morphant; **B)** eye region of a *ca10a* morphant; **C)** head region of a *ca10b* morphant; and **D)** tail regions of a *ca10b* morphant. (Original magnification 100X).

doi:10.1371/journal.pone.0134263.g010

fish injected with 80 pg of mRNA per embryo along with 300 μM antisense MOs showed observable improvement in the phenotype of morphant embryos as shown in Fig 11A–11D. The partial rescue of *ca10a* and *ca10b* morphant embryos with the injection of gene-specific human mRNAs also confirmed the specificity of the *ca10a* and *ca10b* antisense MOs used in the study.

Knockdown of *ca10a* and *ca10b* leads to abnormal movement pattern in zebrafish larvae

The expression pattern of *ca10a* and *ca10b* genes suggested that the encoded proteins play important roles in the brain. Therefore, we hypothesized that down regulation of these genes with antisense MOs may lead to changes in behavior or motor coordination, which can be investigated by monitoring the swim pattern of the morphant embryos. It is obvious that the larvae with body and tail abnormalities, induced by high concentration of *ca10a* and *ca10b* antisense morpholinos, would show abnormal swimming behavior. To see any neurological effect on movement pattern as a result of down regulation of these genes, we needed morphant larvae with no obvious phenotypic defects. To test this hypothesis, we injected the larvae with lower concentrations (100 μM) of *ca10a*-MO2 and *ca10b*-MO2. With these concentrations, the 5 dpf larvae showed normal body and tail development with no visible phenotypic defects, similar to RC-MO injected and uninjected larvae (S1–S3 Movies). In the experiment, 4 groups (uninjected, 100 μM *ca10a*-MO injected, 100 μM *ca10b*-MO injected, and RC injected embryos) of larvae were analyzed for movement patterns to observe movement of the body while swimming and traced the movement of the fish (Fig 12). Similarly, we calculated the total distance traveled for all larvae (details in the methods). Two-sample Kolmogorov-Smirnov statistical analyses were performed between each of the groups to determine if they could

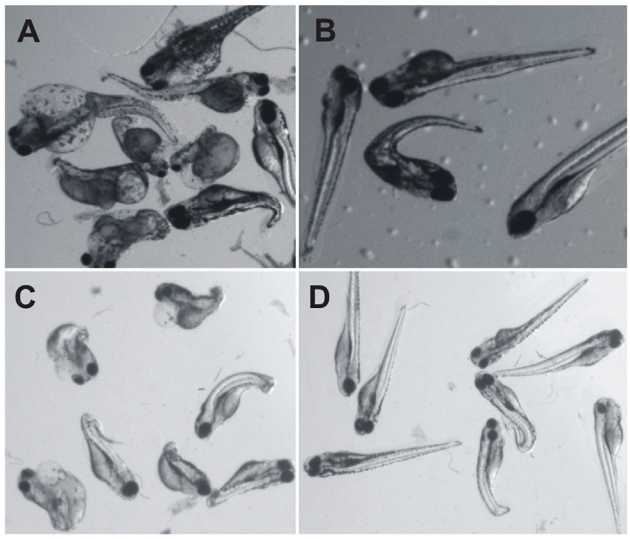

Fig 11. Partial rescue of *ca10a* and *ca10b* zebrafish morphants. A) The *ca10a* morphant (5dpf) embryos; **B)** The 5 dpf zebrafish *ca10a* morphant embryos rescued with injection of *CA10* mRNA; **C)** The *ca10b* morphant (5dpf) embryos; **D)** Partially rescued 5dpf embryos with *CA11* mRNA.

doi:10.1371/journal.pone.0134263.g011

have been drawn from the same distribution, shown in Fig 13. Both knockdown groups swam significantly smaller distances than the random control and wildtype groups. The distances of the two knockdown groups did not differ significantly. However, fish in the *ca10b* group showed a tendency towards less movement (Fig 13). The distances traveled by fish in the random control group were smaller than those of the wildtype controls. We assume that either the impact of the injection procedure or the MOs themselves account for this difference.

Analysis of the actual swim pattern revealed that the large majority of morphant larvae did not show movement during the 2 minute recording. Those that did, showed slow movements of the tail and tended to remain in the periphery of the petri dish (S2 and S3 Movies and Fig 12A and 12B). Videos obtained through microscopic viewing revealed that *ca10b* morphant larvae had difficulties in balancing the body. The 5 dpf wild type zebrafish controls showed normal swim pattern (S1 Movie, Fig 12D).

Discussion

The carbonic anhydrase related proteins (CARPs) VIII, X, and XI belong to the α-CA family and are highly conserved across all species, even more so than the enzymatically active CA isoforms [6]. The expression studies of these proteins show that CARPs are predominantly expressed in the CNS [6,10,11,44]. Spontaneously occurring mutations in CARP VIII lead to ataxia and mental retardation in humans and mice [19,20,45]. Recently, we described the function of CARP VIII in zebrafish by knocking the *ca8* gene down using antisense MOs [18]. In addition to aberrations in early embryonic development and brain development, the knockdown of *ca8* led to an ataxic movement pattern, confirming its role in motor coordination [46].

These findings and the exceptionally strong conservation of the *CA10*-like genes prompted us to study the expression of *ca10a* and *ca10b* in zebrafish. The quantitative expression analysis of the *ca10a* gene in developing larvae (0–168 hpf), using RT-qPCR, showed that *ca10a* is

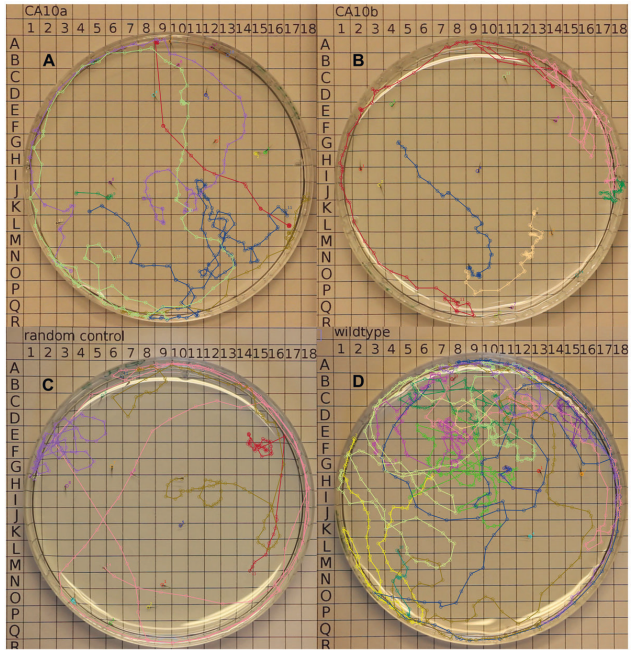

Fig 12. Displacement patterns of the morphant and control fish. Representative displacement trajectories of the movement pattern are shown for **A)** larvae injected with *ca10a*-MO2, **B)** larvae injected with *ca10b*-MO2 **C)** larvae injected with RC-MOs and, **D)** wildtype (uninjected) larvae. Groups of 13 to 22 fish were video recorded in 90mm petri dishes over a 2 minute time period. ImageJ and MtrackJ plugin were used to track the paths of all fish [39,40].

doi:10.1371/journal.pone.0134263.g012

expressed throughout the embryonic development and presents the highest level of expression between the period of 96 hpf (4dpf) to 168 hpf (7 dpf). The expression pattern of *ca10b* gene leads us to surmise that initially this gene product is at least partially of maternal origin, with the highest level of *ca10b* mRNA at 0 hpf, consistent with its highest expression in the ovaries of adult zebrafish. The level of *ca10b* mRNA decreased after 0 hpf before rising again at 48 hpf and finally achieving a very high level at 168 hpf. The expression pattern of both genes during development suggests that these genes are required for the embryonic development.

To date, there have been no systematic studies related to the expression of *CA10* and *CA11* genes during the development of a vertebrate animal. There are two studies available related to the expression analysis of CARP X and CARP XI genes during embryonic development [10,11]. In the first study, the expression was studied using RT-PCR method at four different stages of embryonic development in a murine model (E7, E11, E15, and 17) and it was shown that the signal for *CA10* appeared in the middle of gestation (E15) [11]. The signal for *CA11* was seen at an early stage of gestation and became faint as gestation progressed. In the second study, the expression patterns of *CA10* and *CA11* gene products were investigated using immunohistochemistry during five different gestational periods in the human fetal brain [10]. The signal for *CA11* gene product was seen as early as the day 84 of gestation. In contrast, the gene product for *CA10* was not observed until the 121st day of gestation. The signal for CARP X was seen on day 141 of gestation in the neural cell cortex. Both studies on developmental expression

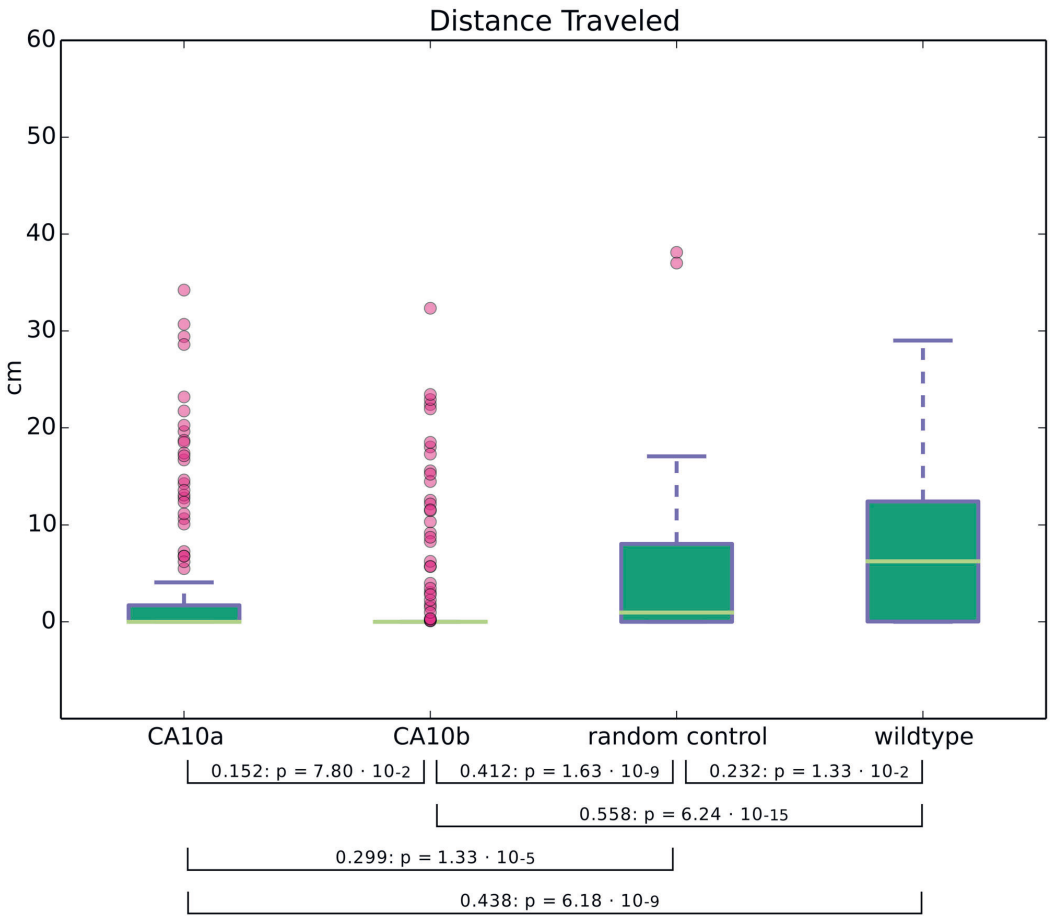

Fig 13. Knockdown of *ca10b* and *ca10b* genes results in abnormal movement pattern in morphant zebrafish larvae. The swim patterns of 5 dpf larvae injected with 100 μM antisense *ca10a*-MO2 or *ca10b*-MO2 were compared to the larvae injected with RC-MO and wildtype (uninjected) controls as described in the methods. (In addition to the swim patterns and body movement videos of 10 larvae from each group created with a Zeiss microscope for close observation as included in the supporting information). Distances traveled by 457 fish in the four groups are presented as boxplots as created with matplotlib [43]. The results of two sample Kolmogorov-Smirnov statistical analyses are included between bracket linked groups.

doi:10.1371/journal.pone.0134263.g013

suggested that *CA10* appears late in the development and *CA11* is required early in the gestation period, which are in complete agreement with our results and support our hypothesis that these genes play important roles in embryonic development in vertebrates. However, there is still a need for the systematic investigation of expression pattern of *CA10* and *CA11* genes in a mammalian model, such as mouse, during embryogenesis, at both mRNA and protein levels.

In the present study, we have completed a systematic expression analysis of *ca10a* and *ca10b* gene using RT-qPCR in a panel of 14 adult zebrafish tissues. The quantitative analysis of these genes showed that both genes are highly expressed in the brain, confirming the pattern of expression observed in mouse and human. Surprisingly, the zebrafish ovary showed very high expression of the *ca10b* gene, which has not been reported for the genes coding for CARPs in

either human or mouse. However, integrated expression data from MediSapiens In Silico Transcriptomics (http://ist.medisapiens.com/) shows a low-level expression of human *CA11* in the ovary. Interestingly, the two CARP X-like proteins in *D. melanogaster* have similar expression patterns. CARP-A is exclusively expressed in the brain, whereas CARP-B is predominantly expressed in female reproductive tissues followed by the CNS [8]. It is of interest to note that despite three different histories of duplication, two copies of CARP X-like proteins seem to have adapted to similar roles in mammals, fish, and insects: one exclusively in neural tissues, and the other additionally in ovaries and/or in early embryonic development. Neural expression is seen in *C. elegans* as well. Both CARP X-like genes, *cah-1* and *cah-2*, are expressed in several types of neurons [47]. It appears that neural expression of *CA10*-like genes has been conserved since the earliest bilaterian animals [41]. Taken together with the high level of sequence conservation, the universal and ancient history of neural expression suggests some fundamental role for CARP X-like proteins in the brain.

Even though earlier studies have recognized the presence of a signal peptide in CARP X and CARP XI [3,9,12], one later study [10] suggests cytoplasmic localization for CARP X and XI based on histochemical staining, whereas another study by the same authors [11] makes no statements of the subcellular localization. To help resolve this apparent contradiction, we also looked for other features that only have functional significance in secreted, extracellular proteins, and therefore should only be conserved in extracellular proteins: namely disulfides and N-glycosylation motifs. We confirmed that signal peptides are indeed a universal feature in all CARP X-like proteins in seemingly all animal species, including both CARP isoforms in fruit fly and *C. elegans*. Surprisingly, we also discovered a conserved pair of cysteines in nearly the same location where all enzymatically active extracellular CA isoforms have a disulfide, and confirmed by protein modelling that these cysteines could form a disulfide. The presence of a third conserved cysteine, which would be unpaired in many CARP proteins, could be a means to form dimers. In addition, we saw two conserved N-glycosylation motifs in positions which are highly variable in other CA isoforms. The disulfide cysteines and the two glycosylation motifs are found in all 61 sequences of our data set, again including both CARP isoforms in fruit fly and *C. elegans*. We take these three lines of evidence (conservation of signal peptides, disulfide cysteines, and N-glycosylation motifs) as strong evidence that CARP X, XI, Xa, Xb, and their invertebrate orthologs are all secretory proteins.

Morpholino knockdown is commonly used in zebrafish to study gene specific functions in embryonic development [48]. However, as possible off-target effects possess a major concern, MO experiments need to be validated carefully [49]. To rule out the possibility of off-target effects caused by p53 induced apoptosis [50], we co-injected the *ca10a* and *ca10b* MOs with *p53*-MOs. The co-injection of *p53*-MOs did not show any marked difference on the observed phenotype or on the mortality of the embryos, suggesting that these effects are likely not due to *p53* activation. To exclude other off-target effects, we targeted two different sites of the *ca10a* and *ca10b* genes with MOs and observed that silencing either *ca10a* or *ca10b* with MO1 and MO2 resulted in a similar phenotype between these two MOs. In addition, injection of RC MOs, with concentrations similar to *ca10a* and *ca10b* MOs, did not have any effects on the phenotype of the zebrafish embryos, also supporting gene specific silencing of *ca10a* and *ca10b*. We also showed that the abnormal phenotype of morphant zebrafish could be partially rescued by co-injection of human *CA10* and *CA11* mRNAs. Finally, we validated the results obtained from the MO knockdown of the *ca10a* and *ca10b* genes by silencing these genes using the CRISPR/Cas9 mediated mutagenesis. The phenotypes of the *ca10a* and *ca10b* mutated larvae were similar to those observed in the *ca10a* and *ca10b* morphants.

The members of CARP subfamily (CARP VIII, X and XI) are predominantly expressed in the CNS in both mouse and human, and their high level of sequence conservation suggests that

the proteins play important roles there, and missense changes at the sequence level might lead to serious phenotypic consequences. Indeed, this was the case with CARP VIII. Deletion mutations in this gene lead to ataxia and mental retardation in the mice and humans [19,20,45]. The suppression of *ca8* in zebrafish using antisense MOs led to an abnormal swim pattern and reduction in the cerebellar volume; similar to mouse and human where ataxic gait and reduced cerebellar volume are also present [18,51]. In the present study, we examined the behavioral consequences of the *ca10a* and *ca10b* morphant zebrafish larvae. The swim pattern analysis of the larvae at 120 hpf (5 dpf) showed abnormal swim pattern compared with the embryos injected with RC-MOs and uninjected embryos. This finding suggested that even the partial suppression of *ca10a* and *ca10b* genes lead to abnormal motor coordination. TUNEL assay showed neuronal cell death in the head region in the morphant fish injected with *ca10a* and *ca10b* MOs. Interestingly, the recently published report by Hsieh et al. [16] showed that the expression and localization of *CA11* is altered in a human patient with Spinocerebellar ataxia 3, transgenic mice with Machado Joseph Disease, and cultured neuronal cells with a defect in ataxin 3. In fact, all the three CARP transcripts were induced in the neuronal cells with defective ataxin 3 [16]. It has also been suggested that CARP XI, similar to CARP VIII, might interact with inositol 1,4,5-triphospate receptor 1 (ITPR1) and control the release of calcium from the intracellular reserves similar to CARP VIII [16,52], but in light of the evidence that CARP XI would be an extracellular protein, this does not seem a very likely suggestion.

Conclusions

The present work describes new data on the CARP subfamily of proteins, namely CARP Xa and CARP Xb, in embryonic development in zebrafish. Our work gives insights into the essential roles that *ca10a* and *ca10b* genes play during the embryonic development and how the lack of either of these proteins leads to abnormal motility, similar to zebrafish knocked down for *ca8*. Sequence analysis suggests that all of CARP X, Xa, Xb, XI, and their invertebrate orthologs are secretory proteins, contrary to previously accepted ideas; have a cysteine disulfide; and are potentially dimeric. To our knowledge, this is the first study to reveal that down-regulation of *ca10a* and *ca10b* genes leads to abnormal pattern of movement and also the first one to suggest that these genes are essential for early embryonic development in vertebrates. This study also introduces novel zebrafish models to investigate the mechanisms of CARP Xa and CARP Xb function.

Supporting Information

S1 Data. The data file S1 includes all novel protein and coding sequences based on our improved gene models along with known protein and coding sequences from the Ensembl database.
(FASTA)

S1 Fig. The modified gRNA design template.
(TIF)

S2 Fig. Silencing of *egfp* expression in tg(fli1a:egfp) zebrafish embryos using CRISPR/Cas9 mediated mutagenesis. A) Fluorescence microscopy was used to analyze the silencing of *egfp* in tg(*fli1a:egfp*) zebrafish embryos at 2 dpf. The un-injected control (left) and *egfp* gRNA injected control (middle) express *egfp* (green) in the vascular endothelium. The CRISPR-Cas9 mutated embryo (right) shows less fluorescence due to the disruption of the *egfp* gene. The red channel was used to detect auto-fluorescence. **B)** T7 endonuclease I (T7EI) assay was used to evaluate the *egfp* mutation efficiency in 2-day-old embryos. T7EI treated PCR products of un-

injected and *egfp* gRNA injected control fish are shown in comparison to PCR products of two individual embryos and a pooled sample of 5 *egfp* silenced embryos. The full length wild type (WT) *egfp* product (470bp) is marked with an asterix. Arrows indicate the T7E1 cleaved PCR products in the *egfp* mutated embryos.
(TIFF)

S1 Movie. The movie shows the swim pattern of wild type 5dpf zebrafish.
(MPG)

S2 Movie. The movie shows the swim pattern of *ca10a* morphant 5dpf zebrafish.
(MPG)

S3 Movie. The movie shows the swim pattern of *ca10b* morphant 5dpf zebrafish.
(MPG)

S1 Table. CARP X-like sequences from different species. The table shows the details of the sequences used in the phylogenetic tree.
(XLSX)

Acknowledgments

We thank Aulikki Lehmus for the skillful technical assistance with the experiments, Leena Mäkinen, Hannaleena Piippo, Jenna Ilomäki, Annemari Uusimäki, Matilda Martikainen, and Sanna Harjula for the morpholino injections and zebrafish experiments and Anna Oksanen and Marko Pesu for their help in establishing methodology for the CRISPR/Cas9 mediated gene silencing. The work was supported by grants from Jane & Aatos Erkko Foundation, Sigrid Juselius foundation, Finnish Cultural Foundation, Tampere Tuberculosis Foundation, and Academy of Finland.

Author Contributions

Conceived and designed the experiments: AA MT MP MO MR SP. Performed the experiments: AA MT HB CO MO AS CB PP MK. Analyzed the data: AA MT HB MO SP. Contributed reagents/materials/analysis tools: SP MR. Wrote the paper: AA MT HB MO SP.

References

1. Sly WS, Hu PY (1995) Human carbonic anhydrases and carbonic anhydrase deficiencies. Annu Rev Biochem 64: 375–401. PMID: 7574487
2. Pastorekova S, Parkkila S, Pastorek J, Supuran CT (2004) Carbonic anhydrases: current state of the art, therapeutic applications and future prospects. J Enzyme Inhib Med Chem 19: 199–229.
3. Bellingham J, Gregory-Evans K, Gregory-Evans CY (1998) Sequence and tissue expression of a novel human carbonic anhydrase-related protein, CARP-2, mapping to chromosome 19q13.3. Biochem Biophys Res Commun 253: 364–367. PMID: 9878543
4. Tolvanen ME, Ortutay C, Barker HR, Aspatwar A, Patrikainen M, et al. (2013) Analysis of evolution of carbonic anhydrases IV and XV reveals a rich history of gene duplications and a new group of isozymes. Bioorg Med Chem 21: 1503–1510. doi: 10.1016/j.bmc.2012.08.060 PMID: 23022279
5. Hewett-Emmett D, Tashian RE (1996) Functional diversity, conservation, and convergence in the evolution of the α-, β-, and γ-carbonic anhydrase gene families. Mol Phylogenet Evol 5: 50–77. PMID: 8673298
6. Aspatwar A, Tolvanen ME, Parkkila S (2010) Phylogeny and expression of carbonic anhydrase-related proteins. BMC Mol Biol 11: 25. doi: 10.1186/1471-2199-11-25 PMID: 20356370
7. Linser PJ, Smith KE, Seron TJ, Neira Oviedo M (2009) Carbonic anhydrases and anion transport in mosquito midgut pH regulation. J Exp Biol 212: 1662–1671. doi: 10.1242/jeb.028084 PMID: 19448076
8. Ortutay C, Olatubosun A, Parkkila S, M. V, Tolvanen ME, editors (2010). Hauppauge, NY: Nova Science Publishers Inc.,. pp. 145–168 p.

9. Okamoto N, Fujikawa-Adachi K, Nishimori I, Taniuchi K, Onishi S (2001) cDNA sequence of human carbonic anhydrase-related protein, CA-RP X: mRNA expressions of CA-RP X and XI in human brain. Biochim Biophys Acta 1518: 311–316. PMID: 11311946
10. Taniuchi K, Nishimori I, Takeuchi T, Fujikawa-Adachi K, Ohtsuki Y, et al. (2002) Developmental expression of carbonic anhydrase-related proteins VIII, X, and XI in the human brain. Neuroscience 112: 93–99. PMID: 12044474
11. Taniuchi K, Nishimori I, Takeuchi T, Ohtsuki Y, Onishi S (2002) cDNA cloning and developmental expression of murine carbonic anhydrase-related proteins VIII, X, and XI. Brain Res Mol Brain Res 109: 207–215. PMID: 12531530
12. Fujikawa-Adachi K, Nishimori I, Taguchi T, Yuri K, Onishi S (1999) cDNA sequence, mRNA expression, and chromosomal localization of human carbonic anhydrase-related protein, CA-RP XI. Biochim Biophys Acta 1431: 518–524. PMID: 10350627
13. Wu C, Orozco C, Boyer J, Leglise M, Goodale J, et al. (2009) BioGPS: an extensible and customizable portal for querying and organizing gene annotation resources. Genome Biol 10: R130. doi: 10.1186/gb-2009-10-11-r130 PMID: 19919682
14. Kleiderlein JJ, Nisson PE, Jessee J, Li WB, Becker KG, et al. (1998) CCG repeats in cDNAs from human brain. Hum Genet 103: 666–673. PMID: 9921901
15. Morimoto K, Nishimori I, Takeuchi T, Kohsaki T, Okamoto N, et al. (2005) Overexpression of carbonic anhydrase-related protein XI promotes proliferation and invasion of gastrointestinal stromal tumors. Virchows Arch 447: 66–73. PMID: 15942747
16. Hsieh M, Chang WH, Hsu CF, Nishimori I, Kuo CL, et al. (2013) Altered Expression of Carbonic Anhydrase-Related Protein XI in Neuronal Cells Expressing Mutant Ataxin-3. Cerebellum.
17. Lohi O, Parikka M, Ramet M (2013) The zebrafish as a model for paediatric diseases. Acta Paediatr 102: 104–110. doi: 10.1111/j.1651-2227.2012.02835.x PMID: 22924984
18. Aspatwar A, Tolvanen ME, Jokitalo E, Parikka M, Ortutay C, et al. (2013) Abnormal cerebellar development and ataxia in CARP VIII morphant zebrafish. Hum Mol Genet 22: 417–432. doi: 10.1093/hmg/dds438 PMID: 23087022
19. Kaya N, Aldhalaan H, Al-Younes B, Colak D, Shuaib T, et al. (2011) Phenotypical spectrum of cerebellar ataxia associated with a novel mutation in the CA8 gene, encoding carbonic anhydrase (CA) VIII. Am J Med Genet B Neuropsychiatr Genet 156: 826–834.
20. Turkmen S, Guo G, Garshasbi M, Hoffmann K, Alshalah AJ, et al. (2009) CA8 mutations cause a novel syndrome characterized by ataxia and mild mental retardation with predisposition to quadrupedal gait. PLoS Genet 5: e1000487. doi: 10.1371/journal.pgen.1000487 PMID: 19461874
21. Slater GS, Birney E (2005) Automated generation of heuristics for biological sequence comparison. BMC Bioinformatics 6: 31. PMID: 15713233
22. Sievers F, Wilm A, Dineen D, Gibson TJ, Karplus K, et al. (2011) Fast, scalable generation of high-quality protein multiple sequence alignments using Clustal Omega. Mol Syst Biol 7: 539. doi: 10.1038/msb.2011.75 PMID: 21988835
23. Petersen TN, Brunak S, von Heijne G, Nielsen H (2011) SignalP 4.0: discriminating signal peptides from transmembrane regions. Nat Methods 8: 785–786. doi: 10.1038/nmeth.1701 PMID: 21959131
24. Emanuelsson O, Nielsen H, Brunak S, von Heijne G (2000) Predicting subcellular localization of proteins based on their N-terminal amino acid sequence. J Mol Biol 300: 1005–1016. PMID: 10891285
25. Pierleoni A, Martelli PL, Casadio R (2008) PredGPI: a GPI-anchor predictor. BMC Bioinformatics 9: 392. doi: 10.1186/1471-2105-9-392 PMID: 18811934
26. Suyama M, Torrents D, Bork P (2006) PAL2NAL: robust conversion of protein sequence alignments into the corresponding codon alignments. Nucleic Acids Res 34: W609–612. PMID: 16845082
27. Ronquist F, Teslenko M, van der Mark P, Ayres DL, Darling A, et al. (2012) MrBayes 3.2: efficient Bayesian phylogenetic inference and model choice across a large model space. Syst Biol 61: 539–542. doi: 10.1093/sysbio/sys029 PMID: 22357727
28. Han MV, Zmasek CM (2009) PhyloXML: XML for evolutionary biology and comparative genomics. BMC Bioinformatics 10: 356. doi: 10.1186/1471-2105-10-356 PMID: 19860910
29. Paradis E, Claude J, Strimmer K (2004) APE: Analyses of Phylogenetics and Evolution in R language. Bioinformatics 20: 289–290. PMID: 14734327
30. Zhang Y (2008) I-TASSER server for protein 3D structure prediction. BMC Bioinformatics 9: 40. doi: 10.1186/1471-2105-9-40 PMID: 18215316
31. Roy A, Kucukural A, Zhang Y (2010) I-TASSER: a unified platform for automated protein structure and function prediction. Nat Protoc 5: 725–738. doi: 10.1038/nprot.2010.5 PMID: 20360767

32. Pettersen EF, Goddard TD, Huang CC, Couch GS, Greenblatt DM, et al. (2004) UCSF Chimera—a visualization system for exploratory research and analysis. J Comput Chem 25: 1605–1612. PMID: 15264254

33. Westerfield M (2000) The Zebrafish book: a guide for the laboratory use of Zebrafish (Danio Rerio). Eugene: University of Oregon.

34. Pfaffl MW (2001) A new mathematical model for relative quantification in real-time RT-PCR. Nucleic Acids Res 29: e45. PMID: 11328886

35. Krebs J (2014) CRISPR Design Tool and Protocol. figshare.

36. Altschul SF, Madden TL, Schaffer AA, Zhang J, Zhang Z, et al. (1997) Gapped BLAST and PSI-BLAST: a new generation of protein database search programs. Nucleic Acids Res 25: 3389–3402. PMID: 9254694

37. Jao LE, Wente SR, Chen W (2013) Efficient multiplex biallelic zebrafish genome editing using a CRISPR nuclease system. Proc Natl Acad Sci U S A 110: 13904–13909. doi: 10.1073/pnas.1308335110 PMID: 23918387

38. Hruscha A, Schmid B (2015) Generation of zebrafish models by CRISPR /Cas9 genome editing. Methods Mol Biol 1254: 341–350. doi: 10.1007/978-1-4939-2152-2_24 PMID: 25431076

39. Meijering E, Dzyubachyk O, Smal I (2012) Methods for cell and particle tracking. Methods Enzymol 504: 183–200. doi: 10.1016/B978-0-12-391857-4.00009-4 PMID: 22264535

40. Schneider CA, Rasband WS, Eliceiri KW (2012) NIH Image to ImageJ: 25 years of image analysis. Nat Methods 9: 671–675. PMID: 22930834

41. Aspatwar A, Tolvanen ME, Ortutay C, Parkkila S (2014) Carbonic anhydrase related proteins: molecular biology and evolution. Subcell Biochem 75: 135–156. doi: 10.1007/978-94-007-7359-2_8 PMID: 24146378

42. Ekker SC, Larson JD (2001) Morphant technology in model developmental systems. Genesis 30: 89–93. PMID: 11477681

43. Hunter JD (2007) Matplotlib is a 2D graphics package used for Python for application development, interactive scripting,and publication-quality image generation across user interfaces and operating systems. Computing in Science & Engineering 9: 90–95.

44. Nishimori I, Takeuchi T, Morimoto K, Taniuchi K, Okamoto N, et al. (2003) Expression of carbonic anhydrase-related protein VIII, X and XI in the enteric autonomic nervous system. Biomed Res 14: 70–74.

45. Jiao Y, Yan J, Zhao Y, Donahue LR, Beamer WG, et al. (2005) Carbonic anhydrase-related protein VIII deficiency is associated with a distinctive lifelong gait disorder in waddles mice. Genetics 171: 1239–1246. PMID: 16118194

46. Huang MS, Wang TK, Liu YW, Li YT, Chi TH, et al. (2014) Roles of carbonic anhydrase 8 in neuronal cells and zebrafish. Biochim Biophys Acta 1840: 2829–2842. doi: 10.1016/j.bbagen.2014.04.017 PMID: 24794067

47. Spencer WC, Zeller G, Watson JD, Henz SR, Watkins KL, et al. (2011) A spatial and temporal map of C. elegans gene expression. Genome Res 21: 325–341. doi: 10.1101/gr.114595.110 PMID: 21177967

48. Bill BR, Petzold AM, Clark KJ, Schimmenti LA, Ekker SC (2009) A primer for morpholino use in zebrafish. Zebrafish 6: 69–77. doi: 10.1089/zeb.2008.0555 PMID: 19374550

49. Eisen JS, Smith JC (2008) Controlling morpholino experiments: don't stop making antisense. Development 135: 1735–1743. doi: 10.1242/dev.001115 PMID: 18403413

50. Robu ME, Larson JD, Nasevicius A, Beiraghi S, Brenner C, et al. (2007) p53 activation by knockdown technologies. PLoS Genet 3: e78. PMID: 17530925

51. Huang M, Wang T, Liu Y, Li Y, Chi T, et al. (2014) Roles of Carbonic Anhydrase 8 in Neuronal Cells and Zebrafish. Biochimica et Biophysica Acta: In press.

52. Chen X, Tang TS, Tu H, Nelson O, Pook M, et al. (2008) Deranged calcium signaling and neurodegeneration in spinocerebellar ataxia type 3. J Neurosci 28: 12713–12724. doi: 10.1523/JNEUROSCI.3909-08.2008 PMID: 19036964

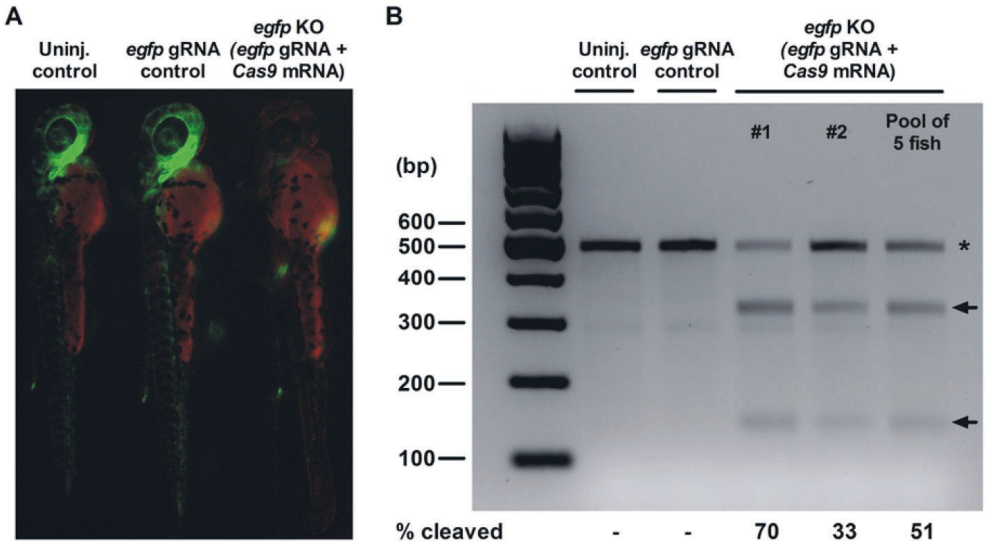

Supplementary figure 2. Silencing of egfp expression in tg(fli1a:egfp) zebrafish embryos using CRISPR/Cas9 mediated mutagenesis. A) Fluorescence microscopy was used to analyze the silencing of egfp in tg(fli1a:egfp) zebrafish embryos at 2 dpf. The un-injected control (left) and egfp gRNA injected control (middle) express egfp (green) in the vascular endothelium. The CRISPR-Cas9 mutated embryo (right) shows less fluorescence due to the disruption of the egfp gene. The red channel was used to detect auto-fluorescence. **B)** T7 endonuclease I (T7EI) assay was used to evaluate the egfp mutation efficiency in 2-day-old embryos. T7EI treated PCR products of un-injected and egfp gRNA injected control fish are shown in comparison to PCR products of two individual embryos and a pooled sample of 5 egfp silenced embryos. The full length wild type (WT) egfp product (470bp) is marked with an asterix. Arrows indicate the T7E1 cleaved PCR products in the egfp mutated embryos.

Intelectin 3 is dispensable for resistance against a mycobacterial infection in zebrafish (*Danio rerio*)

Markus J.T. Ojanen[1,2], **Meri I.E. Uusi-Mäkelä**[1], **Sanna-Kaisa E. Harjula**[1], **Anni K. Saralahti**[1], **Kaisa E. Oksanen**[1], **Niklas Kähkönen**[3], **Juha A.E. Määttä**[3], **Vesa P. Hytönen**[3], **Marko Pesu**[2,4], **Mika Rämet**[*,1,5,6,7]

Affiliations:

[1]Laboratory of Experimental Immunology, BioMediTech Institute and Faculty of Medicine and Life Sciences, University of Tampere, Tampere, Finland;

[2]Laboratory of Immunoregulation, BioMediTech Institute and Faculty of Medicine and Life Sciences, University of Tampere, Tampere, Finland;

[3]Laboratory of Protein Dynamics, BioMediTech Institute and Faculty of Medicine and Life Sciences, University of Tampere, Tampere, Finland;

[4]Department of Dermatology, Tampere University Hospital, Tampere, Finland;

[5]Department of Pediatrics, Tampere University Hospital, Tampere, Finland;

[6]Department of Children and Adolescents, Oulu University Hospital, Oulu, Finland;

[7]PEDEGO Research Unit and Medical Research Center Oulu, University of Oulu, Oulu, Finland

***Corresponding author:** Correspondence to Mika Rämet, phone: 358-50-4336276,

Email: mika.ramet@uta.fi

ABSTRACT

Tuberculosis is a multifactorial bacterial disease, which can be modeled in the zebrafish (*Danio rerio*). Abdominal cavity infection with *Mycobacterium marinum*, a close relative of *Mycobacterium tuberculosis*, leads to a granulomatous disease in adult zebrafish, which replicates the different phases of human tuberculosis, including primary infection, latency and spontaneous reactivation. Here, we have carried out a transcriptional analysis of zebrafish challenged with low-dose of *M. marinum*, and identified *intelectin 3* (*itln3*) among the highly up-regulated genes. In order to clarify the *in vivo* significance of Itln3 in immunity, we created nonsense *itln3* mutant zebrafish by CRISPR/Cas9 mutagenesis and analyzed the outcome of *M. marinum* infection in both zebrafish embryos and adult fish. The lack of functional *itln3* did not affect survival or the mycobacterial burden in the zebrafish. Furthermore, embryonic survival was not affected when another mycobacterial challenge responsive *intelectin*, *itln1*, was silenced using morpholinos either in the WT or *itln3* mutant fish. In addition, *M. marinum* infection in dexamethasone-treated adult zebrafish, which have lowered lymphocyte counts, resulted in similar bacterial burden in both WT fish and homozygous *itln3* mutants. Collectively, although *itln3* expression is induced upon *M. marinum* infection in zebrafish, it is dispensable for protective mycobacterial immune response.

INTRODUCTION

Tuberculosis is an epidemic multifactorial disease caused by *Mycobacterium tuberculosis*[1]. The susceptibility to tuberculosis depends on the *M. tuberculosis* strain and on a number of host-related factors such as environmental conditions, other underlying diseases as well as genetic variation[2-4]. Critical genes of the adaptive immunity required for the mycobacterial immune response such as *interferon gamma* (*IFNG*)[5, 6] and *interleukin 12* (*IL12*)[7, 8] were identified already in the 1980´s and 1990´s, respectively. The importance of these genes has later been verified in human tuberculosis patients[9] and by using experimental gene knockout mouse models of tuberculosis[10-13]. More recently, pattern recognition receptor (PRR) gene polymorphisms of Toll-like receptors (TLRs)[14-16] and C-type lectins[17, 18], have been associated with *M. tuberculosis* susceptibility, delineating also the central role of the innate immunity in controlling the mycobacterial infection.

Lectins are carbohydrate-binding proteins important for numerous biological processes such as intracellular glycoprotein secretion, leukocyte trafficking and in microbial recognition[19, 20]. Consequently, lectins act as recognition molecules inside cells, on the cell surface and in extracellular fluids[20]. Intelectins (ITLNs) are a distinct family of lectins, which were first identified in *Xenopus laevis*[21] and were later found in a number of chordates including human, mouse and zebrafish (*Danio rerio*)[22-25]. Although ITLN function has been linked to a number of processes such as iron absorption[26], metabolic disorders[27] as well as cancer development[28, 29], their exact biological functions are elusive. Suggesting a role for ITLNs in the immune response, *itln* gene expression is highly up-regulated upon a bacterial infection in fish [25, 30-32]. Moreover, human ITLN1 (also known as Omentin) has been shown to bind to the *Mycobacterium bovis* Bacillus Calmette-Guérin (BCG)[24], and more specifically to exocyclic 1,2-diol glycan epitopes that are expressed selectively on microbial surfaces[33].

The importance of ITLNs for immunity *in vivo*, however, is less clear. Previously, Voehringer et al., (2007) used transgenic mice with lung-specific ITLN1 and ITLN2 over-expression to study the effects of these proteins in the mouse infection models of the parasite *Nippostrongylus brasiliensis* and the *M. tuberculosis* bacterium[34]. In these settings, the authors could not detect enhanced pathogen clearance in the *Itln* transgenic mice. In contrast, a so called "natural deletion" of the *Itln2* gene has been previously associated with a higher susceptibility against the parasite *Trichinella spiralis* in a C57BL/10 mouse strain[35]. Recently, an *Itln1* knockout mouse strain was created to study inflammatory bone diseases[36]. In the aforementioned study, the lack of Itln1 was associated with a proinflammatory phenotype characterized by elevated TNF and IL6 levels in bone tissue and in serum, and was shown to result in osteoporosis[36].

The genome of the zebrafish (*Danio rerio*) was assembled for the first time in 2002 and the prevalent 11th assembly (GRCz11) is an invaluable tool for research using zebrafish as a disease model[37]. Over 70% of human genes have at least one zebrafish orthologue and for this reason, the zebrafish immune system is highly similar compared to humans[37]. In fact, most of the human immune cell populations such as T- and B-cells [38-40], neutrophils and macrophages[41], dendritic cells[42] as well as the complement system[43] and immunoglobulins[44, 45], are found in the zebrafish. Importantly, zebrafish can be modified genetically with the clustered regularly interspaced short palindromic repeats (CRISPR)/CRISPR-associated 9 (Cas9) mutagenesis[46, 47], which allows disease modeling using reverse genetics, although some genes appear difficult to target successfully[48].

A *Mycobacterium marinum* infection of zebrafish is nowadays a commonly used model for studying tuberculosis in both larvae and adult fish[49, 50]. Compared to several other tuberculosis models, the mycobacterial model of zebrafish is considered safe, cost-effective and ethical[51, 52]. More importantly, *M. marinum* is closely related to *M. tuberculosis*, and the two bacterial species have comparable pathogenic characteristics in the natural hosts; macrophage mediated intracellular multiplication as well

as the formation of granuloma structures[53-55]. The larval model enables studying specifically the innate immunity[56, 57], whereas the adult zebrafish model allows studying also components of the adaptive immune system in both an acute mycobacterial infection[58] as well as during mycobacterial latency[55, 59].

In order to identify candidate genes associated with the host response against mycobacteria, we conducted a gene expression microarray in *M. marinum* infected adult zebrafish. Here, we identified a zebrafish *ITLN* orthologue *itln3* among the genes that were most induced upon infection. In order to gain more insights into the function of ITLNs, we used CRISPR/Cas9 mutagenesis to create knockout *itln3* mutant zebrafish lines, and used the zebrafish *M. marinum* infection model to determine the *in vivo* significance of Itln3 in a mycobacterial infection.

RESULTS

Genome-wide gene expression microarray analysis of *M. marinum* infected adult zebrafish

In order to identify genes involved in the host immune response against mycobacteria, we used the zebrafish *M. marinum* infection model and conducted a genome-wide gene expression analysis using the microarray platform. To this end, we infected wild-type (WT) AB zebrafish with *M. marinum* (20 CFU; SD 6 CFU) and isolated their organ blocks (includes all the organs of the abdominal cavity) for a transcriptomic analysis at 14 days post infection (dpi). From a total of 43603 probes used in the analysis, we found 93 probes, corresponding to 70 genes, that were up-regulated and 26 probes, corresponding to 21 genes, that were down-regulated (log2 fold change > | 3 |) compared to the mock-treated (PBS) controls (Supplementary Table 1). Further evaluation of the up-regulated probes with a GOrilla gene ontology (GO) enrichment analysis[60, 61] revealed 22 enriched ($p<0.001$) processes including response to carbohydrates (GO:0009743), cholesterol homeostasis (GO:0042632) and antigen processing and presentation (GO:0019882) (Supplementary Table 2). Among the up-regulated genes we found five genes; *si:busm1-194e12.11* (*mhc2* family gene), *arachidonate 5-lipoxygenase b, tandem duplicate 3* (*alox5b.3*), *zgc:113912* (*mhc2* family gene), *CD59 molecule* (*cd59*) and *si:busm1-194e12.12* (*mhc2* family gene) with well-known immunological functions in antigen processing, inflammation and in the regulation of the complement system, respectively (Figure 1A, Supplementary Table 1). Of the 21 down-regulated genes, five were associated with the immune response; *CD58 molecule* (*cd58*), *myeloid-specific peroxidase* (*mpx*), *complement factor b-like* (*cfbl*), *immunoresponsive gene 1, like* (*irg1l*) and *si:busm1-266f07.1* (*mhc2* family gene) (Figure 1A, Supplementary Table 1). Interestingly, approximately 38% of the up-regulated probes i.e. *parvalbumin 1* (*pvalb1*), *alpha-tropomyosin* (*tpma*), *troponin I, skeletal, fast 2b, tandem duplicate 2* (*tnni2b.2*) and *myosin, heavy polypeptide 1.1* (*myhz1.1*) were related to muscle associated biological processes including muscle contraction (GO:0006936),

muscle system process (GO:0003012) and myofibril assembly (GO:0030239) (Supplementary Table 1 and 2). The GO-analysis of the down-regulated probes also showed a significant enrichment of another 22 processes including response to external biotic stimulus (GO: 0043207) and cholesterol biosynthetic process (GO:0006695) and immunological processes, such as response to other organism (GO:0051707), response to bacterium (GO:0009617) and the induction of bacterial agglutination (GO:0043152) (Supplementary Table 2).

Mycobacterial infection up-regulates *itln3* expression in both zebrafish embryos and adult fish

Previous studies in several animal models have shown the expression of the *Intelectin* (*ITLN*) gene to be induced upon a bacterial infection[25, 30, 32]. Accordingly, the expression of the zebrafish *itln3* (ENSDARG00000003523) was increased on average 3.3-fold (log2 change) upon a *M. marinum* infection in our microarray analysis (Figure 1A, Supplementary Table 1). In contrast, two other *itln* genes; *itln2* (ENSDARG00000036084) and *itln2-like* (ENSDARG00000093796) were down-regulated compared to the PBS controls (-3.5 and -3.2 log2 fold change, respectively) (Figure 1A, Supplementary Table 1), suggesting a diverse regulation of *itln* genes in the *M. marinum* infected zebrafish. Since both ENSDARG00000036084 and ENSDARG00000093796 share the same gene name, *itln2*, in Ensembl genome browser, ENSDARG00000093796 is referred to as *itln2-like* throughout the text.

To confirm the differential expression pattern of the *itln* family members in the zebrafish mycobacterial infection and to study the kinetics of the host response more carefully, we analyzed *itln1* (ENSDARG00000007534), *itln2*, *itln2-like* and *itln3* gene expression from the abdominal cavity organ blocks of *M. marinum* infected (6 CFU; SD 3 CFU) WT e46 background adult zebrafish with qPCR at 1 and 6 dpi, as well as at 4 and 9 weeks post infection (wpi) (Figure 1B-E). In line with our microarray data, *itln3* was significantly induced at 4 wpi (3.8-fold, P=0.002) and 9 wpi (5.9-fold, P=0.003) (Figure 1E), whereas *itln2* was down-regulated compared to the PBS controls both at 6 dpi

(0.3-fold, P=0.019) and 4 wpi (0.2-fold, P<0.001) (Figure 1C). No significant differences in the relative mRNA expression levels of the *itln1* (Figure 1B) or *itln2-like* (Figure 1D) genes were observed between infected and the PBS injected adult fish at any of the measured time points.

Next, we infected WT AB zebrafish embryos with mycobacteria and performed an expression analysis of the *itln* genes by qPCR. Here, *M. marinum* (39 CFU; SD 47 CFU) was microinjected into the yolk sac of the embryos and the gene expression was quantified daily between 1 and 7 dpi (Figure 1F-I). In the mycobacteria infected embryos we detected the up-regulation of both *itln1* (1.8 to 6.4-fold, P=0.008-0.016) (Figure 1F) and *itln3* (1.8 to 111.4-fold, P=0.008-0.032) (Figure 1I) starting at 2 dpi and continuing until 7 dpi, as well as the induction of *itln2* at 7 dpi (21.6-fold, P=0.008) (Figure 1G) and *itln2-like* (Figure 1H) between 4 and 7 dpi (20.7 to 76.1-fold, P=0.008-0.032) compared to the PBS controls. Also, in line with previous reports suggesting that other infectious diseases up-regulate *ITLN* expression, a significant induction of *itln3* expression (8.4-fold at 7hpi; 11.8-fold at 18hpi; 5.5-fold at 24hpi; 4.4-fold at 48hpi, P=0.002 in all comparisons) was observed in *Streptococcus pneumoniae* (T4 serotype) infected (296 CFU; SD 32 CFU) embryos (Supplementary Figure 1).

In order to understand the infection-inducible nature of the zebrafish *itln* genes at steady state, we quantified the relative mRNA levels of *itln1*, *itln2*, *itln2-like* and *itln3* in the liver, spleen, kidney and intestine of unchallenged WT e46 zebrafish by qPCR (Figure 2A-D). Here, we found that *itln2* expression was restricted to the intestine (Figure 2B), whereas *itln3* showed the highest relative expression in the liver and the highest overall expression compared to the housekeeping gene (*eukaryotic translation elongation factor 1 alpha 1, like 1; eef1a1l1*) (Figure 2D). Conversely, *itln1* was expressed in all of the studied tissues with the second highest overall expression levels (Figure 2A), while *itln2-like* was primarily expressed in the zebrafish kidney and the intestine (Figure 2C). These results are in line with a previous qPCR analysis of the *itln* gene family members in unchallenged adult zebrafish[25].

Creating *itln3* mutant zebrafish using CRISPR/Cas9 mutagenesis

The type II CRISPR/Cas system is an invaluable technology for targeted genome editing[62, 63], and to date it has been utilized in a number of model organisms. We and others have used the CRISPR/Cas9 mutagenesis method successfully in the zebrafish[46, 48, 64, 65]. Here, we used the CRISPR/Cas9 method to create zebrafish carrying nonsense *itln3* mutations for our *in vivo* studies (Figure 3). To this end, we identified a functional gRNA targeting the second exon of the *itln3* gene with an average mutagenesis efficiency of 39.5% (Figure 3A-B). After an outcross of parental mutation carriers (F0-generation) with wild-type TL zebrafish, we observed two germ-line transmitted frameshift mutations in the F1-progeny corresponding to a total loss of five base pairs (-5 bp; loss of GCATC) and to a total gain of eight base pairs (+8 bp; loss of GGAGCATC and gain of TGCTAGGTAAGTATCA) at the target loci (Figure 3C). Analyses with the Translate tool (Expasy; SIB, Swiss Institute of Bioinformatics)[66] of both the -5 bp and +8 bp mutations confirmed the disrupted reading frames from amino acids 47 and 45 onwards resulting in premature stop-codons after 79 and 71 amino acids, respectively (Figure 3C). These two different *itln3* null mutant zebrafish lines were named *itln3*^{uta145} (-5 bp mutation) and *itln3*^{uta148} (+8 bp mutation). qPCR analysis of uninjected and *M. marinum* infected (422 CFU; SD 221 CFU, 2 wpi) adult zebrafish revealed diminished *itln3* transcript levels in the homozygous *itln3*$^{uta145/uta145}$ (residual expression less than 1%, $P<0.001$) and *itln3*$^{uta148/uta148}$ mutants (residual expression less than 0.1%, $P<0.001$) compared to the WT controls (Supplementary Figure 2), suggesting that the indel-mutations lead to the nonsense-mediated RNA decay of the mutant mRNAs[67]. Furthermore, the inheritance of the mutations followed Mendelian ratios for both of the mutant lines, and the homozygous *itln3*$^{uta145/uta145}$ and *itln3*$^{uta148/uta148}$ mutants did not show any developmental defects nor phenotypical differences compared to their WT siblings (Supplementary Figure 3).

Nonsense mutation in *itln3* does not affect host resistance against *M. marinum* in zebrafish embryos

The up-regulation of the expression of the *itln3* gene in a *M. marinum* infection suggests a possible role for Itln3 in the host immunity against mycobacterial infections. To test if the resistance towards a mycobacterial infection is altered in homozygous *itln3* mutant embryos, we first infected *M. marinum* (40 CFU; SD 30 CFU) into the yolk sac of the ungenotyped F2-progeny of heterozygous *itln3*$^{uta145/+}$ and *itln3*$^{uta148/+}$ zebrafish and followed their survival until 7 dpf (Figure 4A-B). Post-experiment genotyping revealed an average survival of 47% in the *itln3*^{uta145} background embryos and 48% in the embryos with the *itln3*^{uta148} background. However, any significant differences in the survival between the homozygous and heterozygous *itln3* mutants or WT fish could not be observed in either *itln3*^{uta145} (Figure 4A) or *itln3*^{uta148} fish lines (Figure 4B) before 7 dpi (7 dpf). Next, we quantified the mycobacterial burden in the embryos that had survived by qPCR using primers for *M. marinum internal transcribed spacer* (*MMITS*)[55] (Figure 4C). The *M. marinum* quantification revealed bacterial copy number medians (log10) of 4.18 and 4.15 in 100ng of zebrafish DNA in the *itln3*^{uta145} and *itln3*^{uta145} WT groups, respectively. Comparably, heterozygous *itln3*$^{uta145/+}$ and *itln3*$^{uta148/+}$ fish had copy number medians of 4.02 and 4.22 (in 100 ng of zebrafish DNA, log10), respectively, and the homozygous *itln3*$^{uta145/uta145}$ and *itln3*$^{uta148/uta148}$ mutants 3.53 and 4.25 (in 100ng of zebrafish DNA, log10). Thus, there were no statistically significant differences in the mycobacterial burdens between the different genotypes in neither *itln3*^{uta145} nor *itln3*^{uta148} zebrafish.

The site of the bacterial injection can affect the immune response in the embryos[49]. Therefore, we next treated the ungenotyped F2-progeny of *itln3*$^{uta145/+}$ and *itln3*$^{uta148/+}$ zebrafish by injecting *M. marinum* into the blood circulation valley of 2-day-old embryos. In these fish, the *M. marinum* infection (46 CFU; SD 31 CFU) was not able to cause any mortality prior to the experimental end-point of 5 dpi (7 dpf). However, this allowed us to quantify the *M. marinum* burden in all of the infected embryos at the end-point (Figure 4D). Here, the bacterial copy number medians (log10) in 100ng of

zebrafish DNA were 3.61 (WT *itln3*^{uta145}), 3.83 (WT *itln3*^{uta148}), 3.63 (*itln3*$^{uta145/+}$), 3.77 (*itln3*$^{uta148/+}$), 3.75 (*itln3*$^{uta145/uta145}$) and 3.79 (*itln3*$^{uta148/uta148}$). Similarly to the yolk sac infection, mycobacterial quantification did not reveal any differences between the individuals of the different genotypes in either the *itln3*^{uta145} or the *itln3*^{uta148} zebrafish background. Noteworthy, we also infected the ungenotyped F2-progeny of *itln3*$^{uta145/+}$ and *itln3*$^{uta148/+}$ zebrafish with S. *pneumoniae* (serotypes 1 and T4, blood circulation valley infection at 2 dpf) and followed the survival of the fish to 5 dpi[68]. There was no difference between WT embryos and the *itln3* mutants (Supplementary Figure 1).

Deleterious mutations may lead to genetic compensation, which in turn can affect the observed phenotype in gene knockout models[69]. To address this, we used a morpholino-oligonucleotide to silence *itln1* in our *itln3* mutant zebrafish together with the yolk sac mycobacterial infection of zebrafish embryos. In order to ensure efficient termination of translation in all of the four zebrafish *itln1* (ENSDARG00000007534) transcripts, we targeted the second exon (E2) of the gene with a splice-blocking (SB) morpholino (Figure 5A). In our initial SB morpholino titration experiments, 2.8 ng of *itln1*-blocking morpholino did not reveal any adverse effects on the survival or on the phenotype of unchallenged zebrafish embryos within the first 7 dpf. However, lower WT *itln1* mRNA levels were observed in the SB morphants with residual expression of 17.1% at 4 dpi, 21.8% at 5 dpi and 33.9% at 6 dpi compared to the random control (RC) injected embryos (Figure 5B), demonstrating that this amount of the SB morpholino silences the expression of *itln1* efficiently during embryonic development. In addition, detectable *itln1* expression levels were observed in the RC morphants already at 1 dpi, whereas in the SB morpholino injected embryos *itln1* expression was evident later starting at 2 dpi based on qPCR (Figure 5B, Supplementary Figure 4). Next, we performed morpholino-*M. marinum* co-injections (20 CFU; SD 19 CFU) into the yolk sac of the un-genotyped F2-progeny of *itln3*$^{uta145/+}$ and *itln3*$^{uta148/+}$ zebrafish (Figure 5C-E) and the F3-progeny of WT *itln3*^{uta148} (13 CFU; SD 10 CFU) (Figure 5C) and followed their survival up to 7 dpi. There were few dying embryos among uninfected embryos upon RC

or *itln1* morpholino injection (Supplementary Figure 4), whereas the mortality reached 77.8%-100% in the morpholino-*M. marinum* co-injected embryos. Noteworthy, the comparison between the infected RC and SB morpholino injected WT *itln3*^{uta145} and *itln3*^{uta148} embryos did not show any differences in survival (Figure 5C). Moreover, inhibiting *itln1* expression in homozygous *itln3*$^{uta145/uta145}$ and *itln3*$^{uta148/uta148}$ mutants lead to a similar mortality compared to the corresponding heterozygous and WT siblings of the same genetic background (Figure 5D-E), indicating that the simultaneous lack of *itln1* and *itln3* functionality does not affect mycobacterial resistance in the zebrafish embryo. Consistently, we did not detect any differences in the mRNA levels of *itln1*, *itln2* and *itln2-like* between the homozygous *itln3* mutants and the WT controls either in uninjected (4 dpf) or *M. marinum* (25 CFU; SD 23 CFU, 4 dpf/4 dpi) infected embryos (Supplementary Figure 5), suggesting that there is no transcriptional compensation by the other studied intelectin gene members in the *itln3*$^{uta145/uta145}$ and *itln3*$^{uta148/uta148}$ mutant fish. Similarly, no transcriptional compensation by *itln1*, *itln2* or *itln2-like* was observed in the adult *itln3* mutant zebrafish either in steady state or upon *M. marinum* infection (Supplementary Figure 2).

Adult *itln3* mutant zebrafish have a normal immune response towards a *M. marinum* infection

In order to test the mycobacterial susceptibility of the *itln3* mutants in adult zebrafish, we performed a low-dose (48 CFU; SD 5 CFU) mycobacterial inoculation into the abdominal cavity of the fish and followed their survival for up to 24 wpi (Figure 6A-B). After the follow-up, an average of 67% of the *itln3*^{uta145} background zebrafish had survived, corresponding to 74% of the WT, 73% of the *itln3*$^{uta145/+}$ and 59% of the *itln3*$^{uta145/uta145}$ fish. In the *itln3*^{uta148} background fish, a combined survival percentage of 81% was observed (78% in the WT, 82% in the *itln3*$^{uta148/+}$ and 84% in the *itln3*$^{uta148/uta148}$ fish). Similarly to the embryonic survival experiments, no statistically significant differences in the survival between the genotypes were observed.

We and others have previously shown that the outcome of a mycobacterial infection in adult zebrafish depends not only on the host genotype but also on the infection dose. While, a so called low-dose inoculate can result in latency and a chronic disease[55], a higher dose leads to a fast progressing acute infection[58, 70]. We hypothesized that the effects caused by the lack of Itln3 could be more prominent in an infection with a higher mycobacterial dose. Consequently, we infected WT fish as well as heterozygous and homozygous *itln3* mutants from both the *itln3*^{uta145} and *itln3*^{uta148} backgrounds with a higher *M. marinum* dose (422 CFU; SD 221 CFU) and quantified the bacterial burden at 2 and 4 wpi (Figure 5C-D). In these fish, we detected *M. marinum* copy number medians (log10) of 4.19 (WT *itln3*^{uta145}), 3.76 (*itln3*$^{uta145/+}$), 4.16 (*itln3*$^{uta145/uta145}$), 3.69 (WT *itln3*^{uta148}), 3.73 (*itln3*$^{uta148/+}$) and 3.92 (*itln3*$^{uta148/uta148}$) in 100 ng of zebrafish DNA at 2 wpi and 4.72 (WT *itln3*^{uta145}), 4.36 (*itln3*$^{uta145/+}$), 4.60 (*itln3*$^{uta145/uta145}$), 4.10 (*itln3*$^{uta148/+}$) and 3.72 (*itln3*$^{uta148/uta148}$) at 4 wpi. Noteworthy, no WT *itln3*^{uta148} fish were available at 4wpi for a bacterial quantification. Altogether, these data indicate that the loss of Itln3 function is dispensable for the host resistance against abdominal cavity *M. marinum* infection in adult zebrafish.

Dexamethasone mediated lymphocyte depletion in *itln3* knockout zebrafish does not affect the survival or mycobacterial burden in a *M. marinum* infection

We have recently published a zebrafish immune-suppression model for mycobacterial reactivation using orally administered dexamethasone[59]. The dexamethasone treatment decreases the total amount of lymphocytes by an average of 36% (from a relative proportion of 19.3% to 12.4%), and consequently leads to reactivation of the *M. marinum* infection. In turn, a number of studies have suggested that Itln3 functions in microbial surveillance and therefore in the innate immunity[23, 24, 33]. In order to highlight the importance of innate immune mechanisms in the mycobacterial defense, we used the dexamethasone treatment to specifically deplete the lymphocyte population in the adult *itln3* mutation carrying zebrafish

lines *itln3*^{uta145} and *itln3*^{uta148}, and subsequently infected both WT and homozygous *itln3* mutants with *M. marinum* (47 CFU; SD 4 CFU) (Figure 7A). Expectedly, our flow cytometric analysis demonstrated a significant decrease in the lymphocyte counts of both WT *itln3*^{uta145} and *itln3*^{uta148} fish (31.5 %, P=0.002 and 23.7%, P=0.010, respectively) as well as the *itln3*$^{uta145/uta145}$ and *itln3*$^{uta148/uta148}$ mutants (31.5 % and 40.5 %, P<0.001 in both comparisons) three weeks after initiating the dexamethasone administration at 2 wpi (Figure 7B-D). In addition, neither the total cell count nor the amount of myeloid cells and blood cell precursors were affected by dexamethasone (Supplementary Figure 6). We did not detect any substantial mortality of either the *itln3*^{uta145} or the *itln3*^{uta148} mutants or WT fish during the five-week follow-up period. As is shown in the Figure 7D-E, the bacterial amounts did not differ between the groups; in 100ng of zebrafish DNA, mycobacterial copy number medians (log10) of 2.60 and 2.65 in WT *itln3*^{uta145}, 2.55 and 3.10 in *itln3*$^{uta145/uta145}$, 2.87 and 2.43 in WT *itln3*^{uta148} and 2.25 and 2.91 in *itln3*$^{uta148/uta148}$ zebrafish were observed at 2 and 4 wpi, respectively.

In conclusion, our data are in accordance with previous literature on the possible role for *itln*s in immunity, as the zebrafish *itln3* is highly induced in a mycobacterial infection. However, *M. marinum* infection experiments using both zebrafish embryos and adult fish suggest that *itln3* is dispensable for a protective mycobacterial host response. Moreover, *itln1* does not seem to compensate for the lack of functional *itln3* in the embryonic infection model. Of note, unlike has been reported for human ITLN1, we were unable to demonstrate direct binding of recombinant Itln3 to mycobacteria (or *S. pneumoniae* or *Escherichia coli*) *in vitro* (Supplementary Figure 7), which may explain the nonessential role of Itln3 for zebrafish immunity in our models.

DISCUSSION

The genetics of the host affect the outcome of a *M. tuberculosis* infection, i.e. the development of active tuberculosis[4]. Genome-wide expression analyses using microarray and RNA sequencing platforms are important for understanding complicated biological processes such as the host immune defense against pathogens. To date, a handful of transcriptome studies have been done in the zebrafish *M. marinum* infection model using microarray technology[58, 71, 72], the digital gene expression (DGE) method[73] and RNA sequencing[74-76]. Collectively, by using both zebrafish embryos and adult fish, these studies have provided important insights into the innate and adaptive host response against mycobacterial infections.

We used the adult zebrafish *M. marinum* (ATCC 927) infection model together with a zebrafish gene expression microarray to identify novel candidate genes in a mycobacterial infection. From this data, we identified a total of 91 differentially expressed genes (log2 fold change > | 3 |) that were linked to 44 enriched processes, including genes associated with the immune response. Previous studies have shown several genes of the complement system (e.g. *complement component c3b*, *c3b*; *complement component 6*, *c6*) to be up-regulated in an infection[58, 71-73, 75], whereas the expression of some complement associated genes (e.g. *complement factor b*, *cfb*; *mannose binding lectin*, *mbl*) has been shown to be reduced[71, 73]. In line with previous results, we also saw an induction of *cd59* (regulation of membrane attack complex formation) as well as reduced expression of *cfbl* (component of the C3 convertase). Conversely, although previous transcriptomic studies have shown the induction of genes that are involved in neutrophil and macrophage related functions (e.g. *mpx* and *irg1l*)[72, 75], our data indicated down-regulation of these transcripts in an infection. In summary, the aforementioned similarities and differences between these transcriptomic studies can result from a number of factors including the developmental stage of the host (embryos vs. adult fish), the time points chosen for sample collection, the different outcomes of an infection (chronic vs. acute), the use of different bacterial strains (E11,

Mma20 or ATCC 927) and doses, and they can be due to differences in the technical execution of sample preparation and analyses.

Interestingly, circa 38% of the up-regulated probes were related to muscle associated biological processes including muscle contraction (GO:0006936), muscle system process (GO:0003012) and myofibril assembly (GO:0030239). Supporting the relevance of this finding, a genome-wide expression analysis in the fruit fly *Drospohila melanogaster* identified several muscle specific genes such as *actin88F* (A*ct88F*) and *tropomycin 2* (*Tm2*) to be induced after a *Pseudomonas aeruginosa* infection[77]. Consistently, the down-regulation of muscle expressed genes (*Troponin C41C, TpnC41C*; *Glutathione S-Transferase 2, Gst2*) was later connected to an increased susceptibility to infection, suggesting an immunological role for muscle tissue[78, 79]. Although the differential expression of muscle specific genes can be indirectly linked to the immune response through the regulation of other physiological functions, as has been also suggested by Chatterjee et al., (2016)[80], both mouse and zebrafish muscle tissues have also been reported to control the expression of inflammatory cytokine genes (*Tnfa* and *Il6*) upon activation of the immune response[81, 82]. In addition, relatively recent studies in the fruit fly and zebrafish have confirmed the importance of immunological signaling pathways in the muscle in both the humoral[80] and the cellular[79] immune responses against pathogens. Further studies are required to understand the significance of muscle expressed genes also in the host response against mycobacterial infections.

Lee et al., (1997)[21] described a new carbohydrate-binding lectin family, the Intelectins, with concomitantly proposed function in the innate immunity through microbial recognition[23, 33, 83]. Two *ITLN* genes (*ITLN1* and *ITLN2*) have been identified in humans, whereas the exact number of protein coding *itln* genes in zebrafish is elusive varying between six (The Zebrafish Information Network, ZFIN) and nine annotated members (Ensembl genome browser). However, not all are expressed in significant amounts. Our genome-wide gene expression analysis showed the highest expression levels for *itln1*, *itln2, itln2-like* and *itln3* in the PBS injected fish with an average log2 expression of 9.6, 11.9, 13.0 and

10.5, respectively (the lowest average log2 expression was 6.9 for probe A_15_P113269; *ankyrin repeat and kinase domain containing 1*, *ankk1*). This was consistent with Lin et al., (2009) who reported the highest expression levels for *itln1*, *itln2* and *itln3*[25]. Since their discovery, a large number of studies have reported the induction of the expression of *ITLN* genes in different species in bacterial[25, 30-32], parasite[84-86] and viral[87] infections. In addition, although the publicly available transcriptomic data of *M. marinum* infected zebrafish embryos by Benard et al., (2016, Gene Expression Omnibus identifier: GSE76499) shows differential regulation of *itln* transcripts in this model[57], to our knowledge *itln* up-regulation in a mycobacterial infection has not previously been extensively reported in the literature. In our microarray analysis of *M. marinum* infected adult zebrafish, three of the differentially expressed genes were members of the *intelectin* family (*itln2, itln2-like* and *itln3*). The observed decrease in *itln2* expression as well as the induction of *itln3* in these fish was also later confirmed by a qPCR-based quantification of samples from a separate mycobacterial infection experiment. In line with this, a qPCR analysis of *M. marinum* infected zebrafish embryos revealed a significant induction of *itln3* expression post mycobacterial infection, a result which corresponds well with the data by Benard et al., (2016) (GSE76499)[57]. In embryos, we also observed up-regulation of *itln1*, *itln2* as well as an *itln2-like* in response to a mycobacterial infection. While *itln1* had identical induction kinetics to *itln3* with significant up-regulation starting at 2 dpi, the *itln2-like* and *itln2* genes were induced later in the infection at 4 and 7 dpi, respectively. Of note, the expression of *itln2* at 1 dpi (Figure 1G) was below the limit of detection in the qPCR. Furthermore, up-regulation of *itln3* was observed after an *S. pneumoniae* infection in zebrafish embryos, suggesting that this gene can be induced also in an immune response against pneumococcus. All in all, in this study we demonstrated the inducibility of *intelectin* genes in both a mycobacterial and a *S. pneumoniae* infection as well as the down-regulation of *itln2* and *itln2-like* transcripts after mycobacterial inoculation in adult zebrafish.

373 Transcriptomic analyzes have identified several so called classical liver-expressed acute phase
374 protein (APP) genes such as *c-reactive protein* (*crp*) and *serum amyloid a* (*saa*) also in fish species[88-90].
375 In addition, bacterial infections in rainbow trout (*Oncorhynchus mykiss*)[91], channel catfish (*Ictalurus*
376 *punctatus*)[31] as well as in zebrafish[25] have resulted in liver-specific induction of certain *itln* gene
377 members. Our mRNA expression analysis of unchallenged zebrafish confirmed the previously published
378 tissue-restricted expression pattern of zebrafish *itln* genes[25]. While *itln2* is expressed almost exclusively
379 in the intestine, the highest relative expression compared to the housekeeping gene was in the liver for
380 *itln3*. In the current study, we produced Strep-tagged® zebrafish Itln3 in a mammalian expression system
381 to study whether Itln3 could act as a potential APP in microbial recognition. Similarly to human ITLN1[33,
382 83, 92], zebrafish Itln3 was secreted into the culture media. However, although Tsuji et al., (2009) has
383 reported the ability of human ITLN1 to bind to galactofuranosyl (Galf) residues on the mycobacterial
384 cell membrane[83], recombinant Itln3 did not bind readily to *M. marinum in vitro*. Similarly, Itln3 did not
385 bind to *E. coli* or *S. pneumoniae* in our hands.
386 To our knowledge, only two *in vivo* studies on the significance of Intelectins in the host response
387 against pathogens have been conducted[34, 35]. While the lack of ITLN2 was associated with an increased
388 susceptibility toward the parasite *T. spiralis* in C57BL/10 mice[35], the over-expression of ITLN1 and
389 ITLN2 in the lungs of transgenic mice could not restrict either a *Nippostrongylus brasiliensis* or a
390 *Mycobacterium tuberculosis* infection differently from the littermate controls[34]. While genes of the innate
391 immune system can be studied autonomously in zebrafish embryos, which lack a functional adaptive
392 immunity[49], adult zebrafish have a highly similar immune system compared to humans[93].
393 Correspondingly, the embryonic *M. marinum* infection model has revealed important insights into the
394 mechanisms of the innate immunity in mycobacterial host resistance (reviewed in [49, 50]) and the adult
395 model has proven its usefulness e.g. in modelling a latent infection[55] and disease reactivation[55, 59]. In
396 order to obtain a more comprehensive view about the *in vivo* significance of ITLNs in a mycobacterial

infection, we used the *itln3* deficient zebrafish together with both the embryonic as well as the adult *M. marinum* models. In these experiments, the comparison of survival and mycobacterial burden between *itln3* mutant fish and their WT siblings did not reveal any differences in either of the mutant lines (*itln3*^{uta145} and *itln3*^{uta148}). Also, it was demonstrated that this was independent of the site or timing of the microinjection in the embryos (yolk sac at 0 dpf vs. blood circulation valley at 2 dpf). Collectively, we conclude that zebrafish *itln3* is not required for the resistance against a mycobacterial infection.

Genetic compensation is a well-known phenomenon in model organisms with experimental gene knockouts[69]. In this process, the specific function of a knockout gene can be restored by additional naturally occurring mutations or transcriptional changes in other genes[69]. Here, we report the up-regulation of *itln3* as well as another member of the *intelectin* family, *itln1*, in a *M. marinum* infection of zebrafish embryos with analogous induction kinetics. To overcome potential compensatory effects of *itln1* in our *itln3* mutants, we knocked down *itln1* by morpholinos and performed simultaneous *M. marinum* infections in the *itln3* mutant embryos. Silencing *itln1* in *itln3* mutants during a *M. marinum* infection did not reveal any differences compared to controls, demonstrating that *itln1* expression does not compensate for the lack of a functional *itln3* in a *M. marinum* infection. Moreover, our qPCR quantification of *itln1*, *itln2* and *itln2-like* in the uninjected and *M. marinum* infected zebrafish embryos as well as adult zebrafish did not reveal transcriptional compensation for *itln3* in the homozygous mutant background. Similarly, the depletion of lymphocytes in the adult zebrafish did not reveal the importance for Itln3 in the immunity against a *M. marinum* infection. All in all, our data indicate that despite being strongly induced by a mycobacterial infection, *itln3* is dispensable for the immune response against *M. marinum* both in embryonic and adult zebrafish.

METHODS

Zebrafish lines and maintenance

The zebrafish maintenance and all of the experiments were in accordance with the Finnish Act on the Protection of Animals Used for Scientific or Educational Purposes (497/2013) as well as the EU Directive on the Protection of Animals Used for Scientific Purposes (2010/63/EU). Experiments were approved by the Animal Experiment Board of Finland (permit for zebrafish maintenance: ESAVI/10079/04.10.06/2015; permits for the experiments: ESAVI/2464/04.10.07/2017, ESAVI/10823/04.10.07/2016, ESAVI/2235/04.10.07/2015 and ESAVI/11133/04.10.07/2017). WT AB fish as well as in-house CRISPR/Cas9 produced F2-generation *itln3*^{uta145} and *itln3*^{uta148} mutant zebrafish were used in the embryonic experiments, whereas three- to seven-month-old AB, *il10*^{e46}, *itln3*^{uta145} and *itln3*^{uta148} zebrafish were used in the experiments with the adult fish. Zebrafish embryos were maintained according to standard protocols in embryonic medium E3 (5 mM NaCl, 0.17 mM KCl, 0.33 mM $CaCl_2$, 0.33 mM $MgSO_4$, 0.0003 g/l methylene blue) at 28.5°C until 7 days post fertilization. Maintenance of the adult zebrafish was as follows; unchallenged fish were kept in a conventional flow through system (Aquatic Habitats, Florida, USA) with an automated light/dark cycle of 14 h/10 h and fed once a day with Gemma Micro 500 (Skretting, Stavanger, Norway) or twice with SDS 400 (Special Diets Services, Essex, UK) feed. *M. marinum* infected adults were kept in a separate flow through system (Aqua Schwarz GMbH, Göttingen, Germany) with the above-mentioned light/dark cycle and fed once a day with Gemma Micro 500 (Skretting) or SDS 400 (Special Diets Services). Infected fish were monitored daily. Humane endpoint criteria pre-defined in the animal experiment permits were applied throughout the follow-up.

Experimental *M. marinum* infections

M. marinum (ATCC 927 -strain) culture and the adult zebrafish inoculations were performed as described previously[55]. In the *M. marinum* infections of the zebrafish embryos, a total volume of 1-2 nl was microinjected either into the yolk sac (0 dpf) or into the blood circulation valley (2 dpf) by using a borosilicate capillary needle (Sutter instrument Co., California, USA), a micromanipulator (Narishige International, London UK) and a PV830 Pneumatic PicoPump (World Precision Instruments, Florida, USA). 10 mM phosphate buffered saline (PBS) with 2% polyvinylpyrrolidone-40 (PVP) (Sigma-Aldrich) and 0.3 mg/ml phenol red (Sigma-Aldrich) was used as a mycobacterial carrier solution. Prior to circulation valley injections, the 2 dpf zebrafish were anesthetized with 0.02% 3-amino benzoic acid ethyl ester (Sigma-Aldrich). Embryonic infections were visualized with a Stemi 2000 microscope (Carl Zeiss MicroImaging GmbH, Göttingen, Germany) and the survival of the embryos followed daily. Adult zebrafish were first anesthetized with 0.02% 3-amino benzoic acid ethyl ester (Sigma-Aldrich, Missouri, USA), and then injected with 5 µl of *M. marinum* in a suspension of 10 mM PBS and 0.3 mg/ml phenol red (Sigma-Aldrich, Missouri, USA) into the abdominal cavity using a 30 gauge Omnican 100 insulin needle (Braun, Melsungen, Germany). The *M. marinum* amounts from both the embryonic and adult infections were verified by plating bacterial inoculations on 7H10 agar (Becton Dickinson, New Jersey, USA) plates and counting the colony forming units (CFU) 5-days after plating.

Gene expression microarray

RNA was extracted from the zebrafish organ blocks (includes all the organs of the abdominal cavity) with TRIreagent (Molecular Research Center, Ohio, USA) following the manufacturer's protocol. Microarray procedures were carried out by the Turku Centre for Biotechnology at the Finnish Microarray and Sequencing Centre by using a Zebrafish (V3) Gene Expression Microarray, 4x44K (Agilent Technologies, California, USA). In short, 100 ng of total RNA was amplified and Cy3-labeled with Low Input Quick Amp Labeling kit, one-color (Agilent), processed using the RNA Spike-In Kit, one-color

(Agilent) and quality controlled with 2100 bioanalyzer RNA 6000 Nano kit (Agilent). Labelling and hybridization of the transcripts were done onto Agilent's 4x44K Zebrafish v3 array (Design ID 026437) using GE Hybridization Kit (Agilent). Microarrays were scanned with an Agilent scanner G2565CA using a profile AgilentHD_GX_1Color. Numerical results were obtained with Feature Extraction Software v. 10.7.3 (Agilent) with the protocol GE1_107_Sep09 and the signal intensities normalized prior further analysis. Cut-off value (log2 fold change > $\left|3\right|$) for the up- and down-regulated genes was chosen in order to obtain approximately 100 differentially expressed candidate genes for further evaluation. Gene ontology enrichment analysis was performed using GOrilla[60, 61] with two unranked lists of genes (Target list: log2 fold change > $\left|3\right|$, Background list: log2 fold change < $\left|3\right|$) using *Danio rerio* genome assembly.

qPCR

For gene expression analysis of the zebrafish embryo samples, genomic DNA (gDNA) removal and RNA isolation were performed using the RNeasy Plus Mini Kit (Qiagen, Hilden, Germany) according to the manufacturer's guidelines. Adult zebrafish RNA was extracted from the organ blocks, liver, spleen, kidney and intestine with TRIreagent (Molecular Research Center) following the associated protocol. The genomic DNA (gDNA) from the RNA samples of the adult fish was removed with RapidOut DNA Removal Kit (Thermo Fischer Scientific, Waltham, USA). RNA quality was controlled with either 1.5 % agarose Tris-acetate-EDTA (TAE) gel electrophoresis or by using Fragment Analyzer system (Advanced Analytical, Inc., Ankeny, USA) and the Standard Sensitivity RNA Analysis Kit (15 nt) (Advanced Analytical). All reverse transcriptions were done by using the SensiFAST™ cDNA synthesis kit (BioLine, London, UK), and the gene expression levels of the target genes were determined from the cDNA with quantitative PCR (qPCR) using the PowerUp™ SYBR® master mix (Thermo Fischer Scientific) and CFX96™ detection system (Bio-Rad Laboratories, California, USA). CFX Manager

490 software (v. 3.1; Bio-Rad Laboratories) was used for data analysis. Target gene expression was
491 normalized to the *eukaryotic translation elongation factor 1 alpha 1, like 1* (*eef1a1l1 or ef1a*)[94]
492 expression using the $2^{-\Delta Ct}$ method. *M. marinum* burden from the zebrafish was determined from the total
493 DNA by qPCR with *MMITS*-specific primers[55]. Embryo DNA for mycobacterial quantification was
494 isolated with standard ethanol precipitation procedure utilizing the following lysis buffer: 10 mM Tris
495 (pH 8.2), 10 mM EDTA, 200 mM NaCl, 0.5% SDS, 200 µg/ml Proteinase K (Thermo Fischer Scientific),
496 whereas TRIreagent (Molecular Research Center) was used for the adult fish DNA isolations. No reverse
497 transcriptase control samples were added to the gene expression analyses, and no template control (H_2O)
498 samples were included in all of the qPCR experiments to preclude contamination. Specificity and the
499 correct size of the qPCR products were verified by melt curve analysis and 1.5% agarose TAE gel
500 electrophoresis. Undetectable qPCR products with incorrect melt curves were given a Ct-value of 40 for
501 the gene expression analyses, and the expression was considered to be below detection. qPCR primers
502 used in the study are listed in Supplementary Table 3.
503
504 **CRISPR/Cas9 mutagenesis**
505 We have previously set-up our in-house zebrafish CRISPR/Cas9 mutagenesis method based on the
506 protocol published by Hruscha and Schmid (2015)[64, 95]. First, guide RNA (gRNA) target sequences for
507 *itln3* (ENSDARG00000003523) were designed with the CRISPR design tool (http://crispr.mit.edu/), and
508 validated with the Casellas laboratory sgRNA tool[96] and the standard nucleotide BLAST analysis[97]. *itln3*
509 exon 2 gRNA was produced by *in vitro* transcription using the MEGAshortscript T7 Transcription Kit
510 (Ambion Life Technologies, CA, USA). 2000 pg of gRNA, 330 pg of *cas9* mRNA (Sigma-Aldrich and
511 Invitrogen, California, USA) and 1.5 ng of phenol red (Sigma-Aldrich) tracer were injected into one-
512 cell-stage AB zebrafish embryos, and the success of mutagenesis was evaluated with the
513 T7 endonuclease I (T7EI)- and the heteroduplex mobility assay (HMA) from isolated DNA of 2 dpf

514 embryos[48]. Gel images were obtained with ChemiDoc™ XRS+ system (Bio-Rad Laboratories) and
515 analyzed with Image Lab software (v. 5.2; Bio-Rad Laboratories). To establish the *itln3* knockout fish
516 line, gRNA was microinjected into zebrafish embryos and the F0-generation fish grown to adulthood.
517 Individual outcrosses of the F0-zebrafish with the Tupfel long fin (TL) fish allowed us to screen for
518 germline transmitted mutations and to identify nonsense mutations of interest in the F1-progeny. The F1-
519 progeny screen was done from the tailfin DNA of the adult zebrafish with HMA followed by Sanger
520 sequencing in our institutes core-facility (MED, University of Tampere). The F1-zebrafish carrying
521 individual mutations of interest were spawn together to obtain F2-generation progeny for the
522 experiments. In the end, a total of two different *itln3* mutation (*itln3*^{uta145} and *itln3*^{uta148}) bearing zebrafish
523 lines were used in the study.
524
525 **PCR based genotyping**
526 F2-generation *itln3*^{uta145} and *itln3*^{uta148} zebrafish lines were mainly genotyped using PCR. To this end,
527 template DNA was either isolated using a standard ethanol precipitation protocol, or with a rapid tissue
528 lysis protocol[98]. Primers were designed for both the WT and the mutated sequences at the gRNA target
529 region; WT *itln3*^{uta145} F: 5'-ATGCTAGGTTGAGGAGCATC-3', mutant *itln3*^{uta145} F: 5'-
530 ATGCTAGGTTGAGGAGCTCG-3', WT *itln3*^{uta148} F: 5'-CTAGGTTGAGGAGCATCGCT-3', mutant
531 *itln3*^{uta148} R: 5'-CCGAGCTGATACTTACCTAGC-3', and amplified with the appropriate flanking
532 primer: F: 5'-GGAGCTGTCACTCCAAAGCC-3' or R: 5'-GTGGTTGATCAACCATTCAGCAC-3'.
533 To determine the genotypes of the *itln3*^{uta145} and *itln3*^{uta148} zebrafish, individual PCR reactions with both
534 WT and mutant primer pairs were prepared for each fish and 1.5% agarose TAE gel electrophoresis was
535 performed to analyze the PCR products.
536
537 **Morpholino injections**

Splice-blocking morpholino (SB) for *itln1* (5'-CTAATTCTGTACTTACTCGATTCAC-3') was designed by and ordered from GeneTools LLC, (Philomath, Oregon, USA). The targeted genomic sequence was verified from our AB and *itln3* knockout zebrafish lines by sequencing[99]. In order to ensure no adverse effects on survival or the phenotype of the morpholino injected embryos in later experiments, the oligonucleotide dosage was first titrated by using three different quantities (7.1 ng, 2.8 ng and 1.1 ng), and the survival of the embryos was observed daily until 7 dpf. The embryos were imaged using Zeiss Lumar V12 fluorescence microscope. The selected microinjection volume was set to 2 nl containing 2.8 ng of SB or random control (RC) morpholino as well as 7 mg/ml of tetramethylrhodamine dextran (Thermo Fisher Scientific) or 0.3 mg/ml phenol red tracer suspended in PBS. In the morpholino-*M. marinum* co-injections, the previously described suspension with 2% PVP was used as a mycobacterial carrier solution. All of the morpholino injections as well as morpholino and *M. marinum* co-injections were done before the 16-cell-stage of development into the yolk sac of the embryos. Similarly than in the other *M. marinum* infection experiments, the mycobacterial counts in the injections were verified by plating. Primers used for the morpholino target site sequencing were F: 5'-TGCACAGGTATTCACCATTTTATGATG-3' and R: 5'-AAGTTCTCTGCAGCTTCTTGC-3' and for the verification of the morpholino functionality as well as quantification of the WT *itln1* expression by qPCR: F: 5'-ATGATGCAGTCAGCTGGTTTTCTTCTG-3' and R: 5'-GCAGTGACCGACTCTGGAAATTCTCC-3'.

Flow cytometry

Flow cytometry for the adult zebrafish kidney cells was performed as described previously[70]. Briefly, *itln3*^{uta145} and *itln3*^{uta148} fish were euthanized with 0.04% 3-amino benzoic acid ethyl ester and their kidneys isolated and suspended in PBS supplemented with 0.5% fetal bovine serum (Sigma-Aldrich). Prior analysis, the kidney cells were filtered through a cell strainer cap with a 35 µm mesh

562 (Corning/Thermo Fisher Scientific). Relative amounts of lymphocytes, myeloid cells and blood cell
563 precursors were determined with a FACSCanto II instrument (Becton, Dickinson, New Jersey, USA) and
564 the data was analyzed with the FlowJo program (v. 7.5; Tree Star, Inc, Oregon, USA). Gating of the
565 blood cell populations is based on previous publications[59, 70, 100, 101].
566
567 **Dexamethasone mediated immunosuppression**
568 Similarly as described previously[59], 25 mg of dexamethasone (Sigma-Aldrich) was mixed with gelatin
569 (Sigma-Aldrich) and used to coat 10 g of SDS400 food (Special Diets Services). During the experiment,
570 a daily dose of 10 µg of dexamethasone (4 mg of food) was given per fish for a total of 5 weeks. A new
571 batch of dexamethasone food was prepared for usage every second week. Dexamethasone was
572 administered for a total of five weeks and the well-being of the fish monitored daily.
573
574 **Statistical analysis**
575 Sample size calculations have been described in our previous publication[100]. Statistical analyses were
576 done with the Prism v. 5.02 (GraphPad Software, California, USA). In the survival experiments a log-
577 rank (Mantel-Cox) test was used, whereas in the flow cytometry and qPCR analyses a nonparametric
578 two-tailed Mann-Whitney analysis was performed. *P* values of < 0.05 were considered significant.
579
580 **Data availability**
581 Gene expression microarray data has been submitted to Gene Expression Omnibus (GEO) repository and
582 can be found with the identifier code: GSE120552. Other generated and analyzed data is available on
583 reasonable request from the corresponding author.

584 **REFERENCES**

585 1. World Health Organization. Global Tuberculosis Report (2017).
586 http://www.who.int/tb/publications/global_report/en/.

587 2. Lerner, T. R., Borel, S. & Gutierrez, M. G. The innate immune response in human tuberculosis.
588 *Cellular Microbiology* **17**, 1277-1285 (2015).

589 3. Möller, M., de Wit, E. & Hoal, E. G. Past, present and future directions in human genetic
590 susceptibility to tuberculosis. *FEMS Immunol. Med. Microbiol.* **58**, 3-26 (2010).

591 4. Meyer, C. G. & Thye, T. Host genetic studies in adult pulmonary tuberculosis. *Semin. Immunol.* **26**,
592 445-453 (2014).

593 5. Shimokata, K., Kawachi, H., Kishimoto, H., Maeda, F. & Ito, Y. Local cellular immunity in
594 tuberculous pleurisy. *Am. Rev. Respir. Dis.* **126**, 822-824 (1982).

595 6. Onwubalili, J. K., Scott, G. M. & Robinson, J. A. Deficient immune interferon production in
596 tuberculosis. *Clin. Exp. Immunol.* **59**, 405-413 (1985).

597 7. Denis, M. Interleukin-12 (IL-12) augments cytolytic activity of natural killer cells toward
598 Mycobacterium tuberculosis-infected human monocytes. *Cell. Immunol.* **156**, 529-536 (1994).

599 8. Zhang, M. *et al*. Interleukin 12 at the site of disease in tuberculosis. *J. Clin. Invest.* **93**, 1733-1739
600 (1994).

601 9. Alcaïs, A., Fieschi, C., Abel, L. & Casanova, J. Tuberculosis in children and adults: two distinct
602 genetic diseases. *J. Exp. Med.* **202**, 1617-1621 (2005).

603 10. Flynn, J. L. *et al*. An essential role for interferon gamma in resistance to Mycobacterium
604 tuberculosis infection. *J. Exp. Med.* **178**, 2249-2254 (1993).

605 11. Cooper, A. M. *et al*. Disseminated tuberculosis in interferon gamma gene-disrupted mice. *J. Exp.*
606 *Med.* **178**, 2243-2247 (1993).

607 12. Flynn, J. L. *et al*. IL-12 increases resistance of BALB/c mice to Mycobacterium tuberculosis
608 infection. *J. Immunol.* **155**, 2515-2524 (1995).

609 13. Cooper, A. M., Magram, J., Ferrante, J. & Orme, I. M. Interleukin 12 (IL-12) is crucial to the
610 development of protective immunity in mice intravenously infected with mycobacterium tuberculosis.
611 *J. Exp. Med.* **186**, 39-45 (1997).

612 14. Dittrich, N. *et al*. Toll-like receptor 1 variations influence susceptibility and immune response to
613 Mycobacterium tuberculosis. *Tuberculosis (Edinb)* **95**, 328-335 (2015).

614 15. Stappers, M. H. T. *et al*. TLR1, TLR2, and TLR6 gene polymorphisms are associated with
615 increased susceptibility to complicated skin and skin structure infections. *J. Infect. Dis.* **210**, 311-318
616 (2014).

617 16. Qi, H. *et al*. Toll-like receptor 1(TLR1) Gene SNP rs5743618 is associated with increased risk for
618 tuberculosis in Han Chinese children. *Tuberculosis (Edinb)* **95**, 197-203 (2015).

619 17. Tanne, A. *et al*. A murine DC-SIGN homologue contributes to early host defense against
620 Mycobacterium tuberculosis. *J. Exp. Med.* **206**, 2205-2220 (2009).

621 18. Guo, Y., Liu, Y., Ban, W., Sun, Q. & Shi, G. Association of mannose-binding lectin gene
622 polymorphisms with the development of pulmonary tuberculosis in China. *BMC Infect. Dis.* **17**, 210
623 (2017).

624 19. Wesener, D. A., Dugan, A. & Kiessling, L. L. Recognition of microbial glycans by soluble human
625 lectins. *Curr. Opin. Struct. Biol.* **44**, 168-178 (2017).

626 20. Sharon, N. & Lis, H. History of lectins: from hemagglutinins to biological recognition molecules.
627 *Glycobiology* **14**, 62R (2004).

628 21. Lee, J. K. *et al*. Cloning and expression of a Xenopus laevis oocyte lectin and characterization of its
629 mRNA levels during early development. *Glycobiology* **7**, 367-372 (1997).

630 22. Yan, J. *et al*. Comparative genomic and phylogenetic analyses of the intelectin gene family:
631 implications for their origin and evolution. *Dev. Comp. Immunol.* **41**, 189-199 (2013).

632 23. Komiya, T., Tanigawa, Y. & Hirohashi, S. Cloning of the novel gene intelectin, which is expressed
633 in intestinal paneth cells in mice. *Biochem. Biophys. Res. Commun.* **251**, 759-762 (1998).

634 24. Tsuji, S. *et al*. Human intelectin is a novel soluble lectin that recognizes galactofuranose in
635 carbohydrate chains of bacterial cell wall. *J. Biol. Chem.* **276**, 23456-23463 (2001).

636 25. Lin, B. *et al*. Characterization and comparative analyses of zebrafish intelectins: highly conserved
637 sequences, diversified structures and functions. *Fish Shellfish Immunol.* **26**, 396-405 (2009).

638 26. Suzuki, Y. A., Shin, K. & Lönnerdal, B. Molecular cloning and functional expression of a human
639 intestinal lactoferrin receptor. *Biochemistry* **40**, 15771-15779 (2001).

640 27. Watanabe, T., Watanabe-Kominato, K., Takahashi, Y., Kojima, M. & Watanabe, R. Adipose
641 Tissue-Derived Omentin-1 Function and Regulation. *Compr Physiol* **7**, 765-781 (2017).

642 28. Li, D. *et al*. Intelectin 1 suppresses the growth, invasion and metastasis of neuroblastoma cells
643 through up-regulation of N-myc downstream regulated gene 2. *Mol. Cancer* **14**, 47 (2015).

644 29. Li, D. *et al*. Intelectin 1 suppresses tumor progression and is associated with improved survival in
645 gastric cancer. *Oncotarget* **6**, 16168-16182 (2015).

30. Ding, Z. *et al*. Characterization and expression analysis of an intelectin gene from Megalobrama amblycephala with excellent bacterial binding and agglutination activity. *Fish Shellfish Immunol.* **61**, 100-110 (2017).

31. Peatman, E. *et al*. Expression analysis of the acute phase response in channel catfish (Ictalurus punctatus) after infection with a Gram-negative bacterium. *Dev. Comp. Immunol.* **31**, 1183-1196 (2007).

32. Takano, T. *et al*. The two channel catfish intelectin genes exhibit highly differential patterns of tissue expression and regulation after infection with Edwardsiella ictaluri. *Dev. Comp. Immunol.* **32**, 693-705 (2008).

33. Wesener, D. A. *et al*. Recognition of microbial glycans by human intelectin-1. *Nat. Struct. Mol. Biol.* **22**, 603-610 (2015).

34. Voehringer, D. *et al*. Nippostrongylus brasiliensis: identification of intelectin-1 and -2 as Stat6-dependent genes expressed in lung and intestine during infection. *Exp. Parasitol.* **116**, 458-466 (2007).

35. Pemberton, A. D. *et al*. Innate BALB/c enteric epithelial responses to Trichinella spiralis: inducible expression of a novel goblet cell lectin, intelectin-2, and its natural deletion in C57BL/10 mice. *J. Immunol.* **173**, 1894-1901 (2004).

36. Rao, S. *et al*. Omentin-1 prevents inflammation-induced osteoporosis by downregulating the pro-inflammatory cytokines. *Bone Research* **6**, 1-12 (2018).

37. Howe, K. *et al*. The zebrafish reference genome sequence and its relationship to the human genome. *Nature* **496**, 498-503 (2013).

38. Willett, C. E., Zapata, A. G., Hopkins, N. & Steiner, L. A. Expression of zebrafish rag genes during early development identifies the thymus. *Dev. Biol.* **182**, 331-341 (1997).

39. Willett, C. E., Kawasaki, H., Amemiya, C. T., Lin, S. & Steiner, L. A. Ikaros expression as a marker for lymphoid progenitors during zebrafish development. *Dev. Dyn.* **222**, 694-698 (2001).

40. Danilova, N. & Steiner, L. A. B cells develop in the zebrafish pancreas. *Proc. Natl. Acad. Sci. U. S. A.* **99**, 13711-13716 (2002).

41. Bennett, C. M. *et al*. Myelopoiesis in the zebrafish, Danio rerio. *Blood* **98**, 643-651 (2001).

42. Lin, A. F. *et al*. The DC-SIGN of zebrafish: insights into the existence of a CD209 homologue in a lower vertebrate and its involvement in adaptive immunity. *J. Immunol.* **183**, 7398-7410 (2009).

43. Seeger, A., Mayer, W. E. & Klein, J. A complement factor B-like cDNA clone from the zebrafish (Brachydanio rerio). *Mol. Immunol.* **33**, 511-520 (1996).

44. Lam, S. H., Chua, H. L., Gong, Z., Lam, T. J. & Sin, Y. M. Development and maturation of the immune system in zebrafish, Danio rerio: a gene expression profiling, in situ hybridization and immunological study. *Dev. Comp. Immunol.* **28**, 9-28 (2004).

45. Danilova, N., Bussmann, J., Jekosch, K. & Steiner, L. A. The immunoglobulin heavy-chain locus in zebrafish: identification and expression of a previously unknown isotype, immunoglobulin Z. *Nat. Immunol.* **6**, 295-302 (2005).

46. Hwang, W. Y. *et al*. Efficient genome editing in zebrafish using a CRISPR-Cas system. *Nat. Biotechnol.* **31**, 227-229 (2013).

47. Chang, N. *et al*. Genome editing with RNA-guided Cas9 nuclease in zebrafish embryos. *Cell Res.* **23**, 465-472 (2013).

48. Uusi-Mäkelä, M. I. E. *et al*. Chromatin accessibility is associated with CRISPR-Cas9 efficiency in the zebrafish (Danio rerio). *PLoS ONE* **13**, e0196238 (2018).

49. Meijer, A. H. Protection and pathology in TB: learning from the zebrafish model. *Semin Immunopathol* **38**, 261-273 (2016).

50. Myllymäki, H., Bäuerlein, C. A. & Rämet, M. The Zebrafish Breathes New Life into the Study of Tuberculosis. *Front Immunol* **7**, 196 (2016).

51. van Leeuwen, L. M., van der Sar, Astrid M & Bitter, W. Animal models of tuberculosis: zebrafish. *Cold Spring Harbor perspectives in medicine* **5**, a018580 (2015).

52. Myllymäki, H., Niskanen, M., Oksanen, K. E. & Rämet, M. Animal models in tuberculosis research - where is the beef? *Expert Opin Drug Discov* **10**, 871-883 (2015).

53. Davis, J. M. *et al*. Real-Time Visualization of Mycobacterium-Macrophage Interactions Leading to Initiation of Granuloma Formation in Zebrafish Embryos. *Immunity* **17**, 693-702 (2002).

54. Swaim, L. E. *et al*. Mycobacterium marinum infection of adult zebrafish causes caseating granulomatous tuberculosis and is moderated by adaptive immunity. *Infect. Immun.* **74**, 6108-6117 (2006).

55. Parikka, M. *et al*. Mycobacterium marinum causes a latent infection that can be reactivated by gamma irradiation in adult zebrafish. *PLoS Pathog.* **8**, e1002944 (2012).

56. Meijer, A. H. & Spaink, H. P. Host-pathogen interactions made transparent with the zebrafish model. *Curr Drug Targets* **12**, 1000-1017 (2011).

57. Benard, E. L., Rougeot, J., Racz, P. I., Spaink, H. P. & Meijer, A. H. Transcriptomic Approaches in the Zebrafish Model for Tuberculosis-Insights Into Host- and Pathogen-specific Determinants of the Innate Immune Response. *Adv. Genet.* **95**, 217-251 (2016).

709 58. van der Sar, Astrid M, Spaink, H. P., Zakrzewska, A., Bitter, W. & Meijer, A. H. Specificity of the
710 zebrafish host transcriptome response to acute and chronic mycobacterial infection and the role of
711 innate and adaptive immune components. *Mol. Immunol.* **46**, 2317-2332 (2009).

712 59. Myllymäki, H., Niskanen, M., Luukinen, H., Parikka, M. & Rämet, M. Identification of protective
713 postexposure mycobacterial vaccine antigens using an immunosuppression-based reactivation model in
714 the zebrafish. *Dis Model Mech* **11** (2018).

715 60. Eden, E., Lipson, D., Yogev, S. & Yakhini, Z. Discovering motifs in ranked lists of DNA
716 sequences. *PLoS Comput. Biol.* **3**, e39 (2007).

717 61. Eden, E., Navon, R., Steinfeld, I., Lipson, D. & Yakhini, Z. GOrilla: a tool for discovery and
718 visualization of enriched GO terms in ranked gene lists. *BMC Bioinformatics* **10**, 48 (2009).

719 62. Jinek, M. *et al*. A programmable dual-RNA-guided DNA endonuclease in adaptive bacterial
720 immunity. *Science* **337**, 816-821 (2012).

721 63. Ran, F. A. *et al*. Genome engineering using the CRISPR-Cas9 system. *Nat Protoc* **8**, 2281-2308
722 (2013).

723 64. Aspatwar, A. *et al*. Inactivation of ca10a and ca10b Genes Leads to Abnormal Embryonic
724 Development and Alters Movement Pattern in Zebrafish. *PLoS ONE* **10**, e0134263 (2015).

725 65. Hruscha, A. *et al*. Efficient CRISPR/Cas9 genome editing with low off-target effects in zebrafish.
726 *Development* **140**, 4982-4987 (2013).

727 66. Artimo, P. *et al*. ExPASy: SIB bioinformatics resource portal. *Nucleic Acids Res.* **40**, 597 (2012).

728 67. Nickless, A., Bailis, J. M. & You, Z. Control of gene expression through the nonsense-mediated
729 RNA decay pathway. *Cell Biosci* **7**, 26 (2017).

730 68. Rounioja, S. *et al*. Defense of zebrafish embryos against Streptococcus pneumoniae infection is
731 dependent on the phagocytic activity of leukocytes. *Dev. Comp. Immunol.* **36**, 342-348 (2012).

732 69. Tautz, D. Problems and paradigms: Redundancies, development and the flow of information.
733 *BioEssays* **14**, 263-266 (1992).

734 70. Ojanen, M. J. T. *et al*. The proprotein convertase subtilisin/kexin furinA regulates zebrafish host
735 response against Mycobacterium marinum. *Infect. Immun.* **83**, 1431-1442 (2015).

736 71. Meijer, A. H. *et al*. Transcriptome profiling of adult zebrafish at the late stage of chronic
737 tuberculosis due to Mycobacterium marinum infection. *Mol. Immunol.* **42**, 1185-1203 (2005).

738 72. van der Vaart, M., Spaink, H. P. & Meijer, A. H. Pathogen recognition and activation of the innate
739 immune response in zebrafish. *Adv Hematol* **2012**, 159807 (2012).

740 73. Hegedus, Z. *et al*. Deep sequencing of the zebrafish transcriptome response to mycobacterium
741 infection. *Mol. Immunol.* **46**, 2918-2930 (2009).

742 74. Rougeot, J. *et al*. RNA sequencing of FACS-sorted immune cell populations from zebrafish
743 infection models to identify cell specific responses to intracellular pathogens. *Methods Mol. Biol.* **1197**,
744 261-274 (2014).

745 75. Benard, E. L., Rougeot, J., Racz, P. I., Spaink, H. P. & Meijer, A. H. Transcriptomic Approaches in
746 the Zebrafish Model for Tuberculosis-Insights Into Host- and Pathogen-specific Determinants of the
747 Innate Immune Response. *Adv. Genet.* **95**, 217-251 (2016).

748 76. Kenyon, A. *et al*. Active nuclear transcriptome analysis reveals inflammasome-dependent
749 mechanism for early neutrophil response to Mycobacterium marinum. *Sci Rep* **7**, 6505 (2017).

750 77. Apidianakis, Y. *et al*. Profiling early infection responses: Pseudomonas aeruginosa eludes host
751 defenses by suppressing antimicrobial peptide gene expression. *Proc. Natl. Acad. Sci. U. S. A.* **102**,
752 2573-2578 (2005).

753 78. Apidianakis, Y. *et al*. Involvement of skeletal muscle gene regulatory network in susceptibility to
754 wound infection following trauma. *PLoS ONE* **2**, e1356 (2007).

755 79. Yang, H., Kronhamn, J., Ekström, J., Korkut, G. G. & Hultmark, D. JAK/STAT signaling in
756 Drosophila muscles controls the cellular immune response against parasitoid infection. *EMBO Rep.* **16**,
757 1664-1672 (2015).

758 80. Chatterjee, A., Roy, D., Patnaik, E. & Nongthomba, U. Muscles provide protection during
759 microbial infection by activating innate immune response pathways in Drosophila and zebrafish. *Dis*
760 *Model Mech* **9**, 697-705 (2016).

761 81. Lin, S., Fan, T., Wu, J., Hui, C. & Chen, J. Immune response and inhibition of bacterial growth by
762 electrotransfer of plasmid DNA containing the antimicrobial peptide, epinecidin-1, into zebrafish
763 muscle. *Fish Shellfish Immunol.* **26**, 451-458 (2009).

764 82. Frost, R. A., Nystrom, G. J. & Lang, C. H. Lipopolysaccharide regulates proinflammatory cytokine
765 expression in mouse myoblasts and skeletal muscle. *Am. J. Physiol. Regul. Integr. Comp. Physiol.* **283**,
766 698 (2002).

767 83. Tsuji, S. *et al*. Capture of heat-killed Mycobacterium bovis bacillus Calmette-Guérin by intelectin-1
768 deposited on cell surfaces. *Glycobiology* **19**, 518-526 (2009).

769 84. French, A. T. *et al*. Up-regulation of intelectin in sheep after infection with Teladorsagia
770 circumcincta. *Int. J. Parasitol.* **38**, 467-475 (2008).

771 85. Pemberton, A. D., Knight, P. A., Wright, S. H. & Miller, H. R. P. Proteomic analysis of mouse
772 jejunal epithelium and its response to infection with the intestinal nematode, Trichinella spiralis.
773 *Proteomics* **4**, 1101-1108 (2004).

774 86. Datta, R. *et al*. Identification of novel genes in intestinal tissue that are regulated after infection
775 with an intestinal nematode parasite. *Infect. Immun.* **73**, 4025-4033 (2005).

776 87. Podok, P., Xu, L., Xu, D. & Lu, L. Different expression profiles of Interleukin 11 (IL-11),
777 Intelectin (ITLN) and Purine nucleoside phosphorylase 5a (PNP 5a) in crucian carp (Carassius auratus
778 gibelio) in response to Cyprinid herpesvirus 2 and Aeromonas hydrophila. *Fish Shellfish Immunol.* **38**,
779 65-73 (2014).

780 88. Winkelhake, J. L., Vodicnik, M. J. & Taylor, J. L. Induction in rainbow trout of an acute phase (C-
781 reactive) protein by chemicals of environmental concern. *Comp. Biochem. Physiol. C, Comp.*
782 *Pharmacol. Toxicol.* **74**, 55-58 (1983).

783 89. Kovacevic, N., Hagen, M. O., Xie, J. & Belosevic, M. The analysis of the acute phase response
784 during the course of Trypanosoma carassii infection in the goldfish (Carassius auratus L.). *Dev. Comp.*
785 *Immunol.* **53**, 112-122 (2015).

786 90. Talbot, A. T., Pottinger, T. G., Smith, T. J. & Cairns, M. T. Acute phase gene expression in
787 rainbow trout (Oncorhynchus mykiss) after exposure to a confinement stressor: A comparison of
788 pooled and individual data. *Fish Shellfish Immunol.* **27**, 309-317 (2009).

789 91. Gerwick, L., Corley-Smith, G. & Bayne, C. J. Gene transcript changes in individual rainbow trout
790 livers following an inflammatory stimulus. *Fish Shellfish Immunol.* **22**, 157-171 (2007).

791 92. Kerr, S. C. *et al*. Intelectin-1 is a prominent protein constituent of pathologic mucus associated with
792 eosinophilic airway inflammation in asthma. *Am. J. Respir. Crit. Care Med.* **189**, 1005-1007 (2014).

793 93. Renshaw, S. A. & Trede, N. S. A model 450 million years in the making: zebrafish and vertebrate
794 immunity. *Dis. Model. Mech.* **5**, 38-47 (2012).

795 94. Tang, R., Dodd, A., Lai, D., McNabb, W. C. & Love, D. R. Validation of zebrafish (Danio rerio)
796 reference genes for quantitative real-time RT-PCR normalization. *Acta Biochim. Biophys. Sin.*
797 *(Shanghai)* **39**, 384-390 (2007).

798 95. Hruscha, A. & Schmid, B. Generation of zebrafish models by CRISPR /Cas9 genome editing.
799 *Methods Mol. Biol.* **1254**, 341-350 (2015).

800 96. Krebs, J. CRISPR design tool and protocol (2015). Data retrieved: 07:16, May 19, 2015, GMT.
801 https://figshare.com/articles/CRISPR_Design_Tool/1117899.

802 97. Altschul, S. F. *et al*. Gapped BLAST and PSI-BLAST: a new generation of protein database search
803 programs. *Nucleic acids research* **25**, 3389-3402 (1997).

804 98. Meeker, N. D., Hutchinson, S. A., Ho, L. & Trede, N. S. Method for isolation of PCR-ready
805 genomic DNA from zebrafish tissues. *BioTechniques* **43**, 614 (2007).

806 99. Turpeinen, H. *et al.* Proprotein Convertase Subtilisin/Kexin Type 7 (PCSK7) Is Essential for the
807 Zebrafish Development and Bioavailability of Transforming Growth Factor beta1a (TGFbeta1a). *J.*
808 *Biol. Chem.* **288**, 36610-36623 (2013).

809 100. Harjula, S. E., Ojanen, M. J. T., Taavitsainen, S., Nykter, M. & Rämet, M. Interleukin 10 mutant
810 zebrafish have an enhanced interferon gamma response and improved survival against a
811 Mycobacterium marinum infection. *Sci Rep* **8**, 10360 (2018).

812 101. Traver, D. *et al.* Transplantation and in vivo imaging of multilineage engraftment in zebrafish
813 bloodless mutants. *Nat. Immunol.* **4**, 1238-1246 (2003).

814

ACKNOWLEDGEMENTS

This study was financially supported by the Academy of Finland (M.R., 277495, M.P. 295814 and 286477), the Sigrid Juselius Foundation (M.R.), the Jane and Aatos Erkko Foundation (M.R.), the Competitive State Research Financing of the Expert Responsibility Area of Tampere University Hospital (M.R., M.P. 9U047 and 9V049), the Competitive State Research Financing of the Expert Responsibility area of Oulu University Hospital (M.R.), the Tampere Tuberculosis Foundation (M.O., M.R., S.-K.H., M.P.), the City of Tampere Science Foundation (S.-K.H), the Väinö and Laina Kivi Foundation (M.O., S.-K.H.), the Finnish Cultural Foundation, the Central Fund (S.-K.H.), the Finnish Concordia Fund (S.-K.H.), the Orion Research Foundation sr (S.-K.H), the Maud Kuistila Memorial Foundation (M.O.), the University of Tampere Doctoral Programme in Biomedicine and Biotechnology (M.O.), the Cancer Society of Finland (M.P.) and Tays tukisäätiö (Tays Support Foundation) (M.P.).

We thank the Tampere Zebrafish Core Facility, partly funded by Biocenter Finland, for maintaining and providing the zebrafish. The use of the facilities and expertise of the Protein Technologies core facility of the University of Tampere, a member of Biocenter Finland, is also gratefully acknowledged.

We also greatly acknowledge Hannaleena Piippo, Jenna Ilomäki, Leena Mäkinen, Carina Bäuerlein, Mirja Niskanen, Juha Saarikettu, Janey Barron, Christopher Gault, Janne Kärnä, Marianne Karlsberg, Ine Herman, Anna Grönholm and Latifeh Azizi for technical assistance and Jukka Lehtiniemi for taking the adult zebrafish images. In addition we thank Henna Myllymäki, Hannu Turpeinen, Mataleena Parikka and Tero Järvinen for scientific advice and support, as well as Hannah Pratt and Helen Cooper for proof-reading this manuscript.

AUTHOR CONTRIBUTIONS

M.P., V.H. and M.R. provided materials and facilities for the research. M.O., M.U., J.M., V.H., M.P. and M.R. designed and/or directed the experiments. M.O., A.S., N.K., S.-K.H., K.O. and M.U. performed the experiments. M.O. and M.U. analyzed the data. M.O., M.U., and M.R. wrote the paper. All authors reviewed and approved the manuscript.

COMPETING INTEREST STATEMENT

The authors declare no competing interests.

FIGURE LEGENDS

Figure 1. Zebrafish *intelectin* genes are differentially expressed upon *M. marinum* infection. A) A genome-wide gene expression microarray was conducted in adult WT AB zebrafish injected with *M. marinum* (20 CFU, SD 6 CFU) (n=2) or PBS (n=3). Average numerical results (log2) for each probe in both infected fish (y-axis) and PBS controls (x-axis) are shown. Up- and down-regulated transcripts (log2 fold change $|3|$) in the organ blocks are shown in grey, and the common immunological genes are annotated. Two *itln3* probes as well as *itln2* and *itln2-like* probes are highlighted. **B-E)** The expression of zebrafish *itln* genes (*itln1*, *itln2*, *itln2-like* and *itln3*) was measured with qPCR in the organ blocks of the *M. marinum* infected (6 CFU, SD 3 CFU) and PBS injected adult WT e46 zebrafish at 1 (n=12 and n=4, respectively) and 6 dpi (n=12 and n=8, respectively) as well as 4 (n=12 and n=11, respectively) and 9 wpi (n=12 and n=10, respectively). **F-I)** The expression of *itln1*, *itln2*, *itln2-like* and *itln3* was determined with qPCR in the *M. marinum* (39 CFU, SD 47 CFU) infected WT AB embryos (n=5 at all timepoints) and in PBS injected controls (n=5 at all timepoints) at 1-7 dpi. Note the different scales of the y axes in B-I. Gene expressions were normalized to *eef1a1l1* expression and target genes were run once in the qPCR analyses. A two-tailed Mann-Whitney test was used in the statistical comparison of differences in B-I.

Figure 2. Expression of zebrafish *itln* genes in adult zebrafish tissues. Relative expression of **A)** *itln1,* **B)** *itln2*, **C)** *itln2-like* and **D)** *itln3* was measured with qPCR in the uninfected adult WT e46 zebrafish liver (n=10), spleen (n=10), kidney (n=10) and the intestine (n=10). Note the different scales of the y axes. Gene expressions were normalized to *eef1a1l1* expression and target genes were run once in the qPCR analyses.

Figure 3. Generation of *itln3*^{uta145} and *itln3*^{uta148} mutant zebrafish lines using CRISPR-Cas9 mutagenesis. A) An appropriate guide RNA (gRNA) target site was identified in the second exon of *itln3*. **B)** 2.5% agarose TAE gel electrophoresis was performed to evaluate occurrence of target site mutations in zebrafish. The *in vivo* CRISPR/Cas9 mutagenesis efficiency was estimated with the T7EI assay in the gRNA and *Cas9* mRNA injected embryos. The size of the uninjected WT control PCR product is 210 bp, whereas the PCR products of the mutated embryos are partially cleaved at the target site. The cleavage efficiency was calculated from the band intensities and the mutagenesis efficiency calculated according to following formula: % mutagenesis = 100 x (1 – (1- % of cleavage)$^{1/2}$)[63]. GeneRuler 50 bp DNA Ladder (#SM0373, Thermo Fischer Scientific) was used as a molecular weight marker (MW). Gel image is cropped to exclude portions that do not contain experimental samples. **C)** gRNA target sites were sequenced from F1-generation mutant zebrafish and two frameshift mutations (-5 bp deletion, *itln3*^{uta145} and +8bp insertion, *itln3*^{uta148}) detected, leading to truncated protein products of 79 and 71 amino acids, respectively.

Figure 4. The lack of *itln3* does not affect the survival or the mycobacterial burden of *M. marinum* infected zebrafish embryos. A-B) *M. marinum* (40 CFU, SD 30 CFU) was injected into the yolk sac of the WT (*itln3*^{uta145}) (n=31), *itln3*$^{uta145/+}$ (n=74), *itln3*$^{uta145/uta145}$ (n=22), WT (*itln3*^{uta148}) (n=19), *itln3*$^{uta148/+}$ (n=27) and *itln3*$^{uta148/uta148}$ (n=16) zebrafish embryos at 0 dpf and the survival recorded until 7 dpi. A log-rank (Mantel-Cox) test was used for the statistical comparison of differences. The data was collected from a single experiment. **C)** Mycobacterial burden was measured by qPCR from the yolk sac infected WT (*itln3*^{uta145}) (n=17), *itln3*$^{uta145/+}$ (n=32), *itln3*$^{uta145/uta145}$ (n=10), WT (*itln3*^{uta148}) (n=9), *itln3*$^{uta148/+}$ (n=15) and *itln3*$^{uta148/uta148}$ (n=7) embryos that were alive at 7 dpi. **D)** *M. marinum* (46 CFU; SD 31 CFU) was injected into the blood circulation valley of the WT (*itln3*^{uta145}) (n=29), *itln3*$^{uta145/+}$ (n=77), *itln3*$^{uta145/uta145}$ (n=36), WT (*itln3*^{uta148}) (n=31), *itln3*$^{uta148/+}$ (n=57) and *itln3*$^{uta148/uta148}$ (n=19) zebrafish

embryos at 2 dpf and the *M. marinum* burden quantified at 5 dpi. Bacterial load is represented in panels C and D as bacterial copies (log10) in 100 ng of zebrafish DNA. A two-tailed Mann-Whitney test was used in the statistical comparison of differences in C and D.

Figure 5. Morpholino mediated silencing of *iltn1* expression does not alter the survival of the WT or *itln3* knockout zebrafish in *M. marinum* infection. A) A schematic representation of the effects of the morpholino mediated silencing of *itln1*. A splice site blocking morpholino (SB) was used to prevent the normal splicing event between exon 2 and exon 3 in *itln1*. Morpholino binding to its target site leads to an alternative splicing event that deletes the start codon containing exon 2 from the transcript. Consequently, this prevents translation of the Itln1 protein. In order to quantify the relative amount of the WT *itln1* transcript, qPCR primers were designed to specifically amplify only the WT *itln1* mRNA. **B)** WT *itln1* expression was quantified with qPCR from the *itln1* SB morpholino (n=3) and random control morpholino (RC) injected zebrafish (n=3) at 1-7 dpf. Gene expression was normalized to *eef1a1l1* expression. All samples were run once as technical duplicates. **C-E)** Survival of the morpholino and *M. marinum* (20 CFU, SD 19 or 13 CFU; SD 10 CFU) co-injected embryos were followed until 7 dpi. In panel C, WT (*itln3*^{uta145} and *itln3*^{uta148}) embryos injected with either SB (n=47 and n=53, respectively) or RC morpholino (n=29 and n=54) are shown, whereas in panels D and E the *itln3*^{uta145} background (n=45-73) and *itln3*^{uta148} background embryos (n=18-35) injected with SB morpholino are depicted, respectively. Note that the SB morpholino injected WT (*itln3*^{uta145}) embryo group is shown in both C and D panels in order to simplify data representation. The data in panel C was collected from two individual experiments, whereas other data is from a single experiment. A log-rank (Mantel-Cox) test was used for the statistical comparison of differences. MO = morpholino.

Figure 6. Adult *itln3* mutant zebrafish have comparable survival and mycobacterial burden compared to WT fish upon *M. marinum* infection. A) The WT (*itln3*^{uta145}) (n=38), *iltn3*$^{uta145/+}$ (n=40), *iltn3*$^{uta145/uta145}$ (n=38) and **B)** WT (*itln3*^{uta148}) (n=38), *iltn3*$^{uta148/+}$ (n=38), *iltn3*$^{uta148/uta148}$ (n=38) zebrafish were infected with *M. marinum* (48 CFU, SD 5), and their survival followed for 24 weeks. A log-rank (Mantel-Cox) test was used for the statistical comparison of differences. The data was collected from a single experiment. **C-D)** The *itln3*^{uta145} and *itln3*^{uta148} background zebrafish were infected with *M. marinum* (422 CFU; SD 221 CFU) and bacterial burden (log10) in 100ng of zebrafish DNA determined

at 2 and 4 wpi from the organ blocks (without the kidney). Group sizes at 2 and 4 wpi, respectively, were as follows: WT (*itln3*^{uta145}) n=10, n=8; *iltn3*$^{uta145/+}$ n=12, n=12; *iltn3*$^{uta145/uta145}$ n=12, n=12; WT (*itln3*^{uta148}) n=9, n=N/A; *iltn3*$^{uta148/+}$ n=9, n=14 and *iltn3*$^{uta148/uta148}$ n=8, n=12. All samples were run once. A two-tailed Mann-Whitney test was used in the statistical comparison of differences. N/A=no fish available for analysis.

Figure 7. Dexamethasone mediated immunosuppression does not alter the survival of *itln3* deficient zebrafish in a mycobacterial infection. A) A schematic representation of the performed experiment. *M. marinum* inoculate used in the infections were 47 CFU (SD 4 CFU). **B)** Representative flow cytometry plots in WT (*itln3*^{uta148}) zebrafish at -1 wpi and 2 wpi used for quantifying lymphocyte, myeloid cell and precursor cell populations. FSC= forward scatter, SSC= side scatter. **C-D)** Lymphocyte fractions of the total cell populations for both WT and *itln3* knockout zebrafish at -1 wpi and 2 wpi. Both the *itln3*^{uta145} (n=12 in all groups) and *itln3*^{uta148} background fish (n=8 in all groups) are shown. Blood cell samples were run as technical duplicates. **E-F)** *M. marinum* burden (log10) in 100ng of zebrafish DNA were measured at 2 wpi and 4 wpi by qPCR in the infected dexamethasone treated zebrafish organ blocks (without the kidney). All bacterial quantification samples were run once. Group sizes at 2 and 4 wpi, respectively, were as follows: WT (*itln3*^{uta145}) n=9, n=8; *iltn3*$^{uta145/uta145}$ n=9, n=10; WT (*itln3*^{uta148}) n=6, n=9 and *iltn3*$^{uta148/uta148}$ n=7, n=8. A two-tailed Mann-Whitney test was used in the statistical comparison of differences.

FIGURE 1

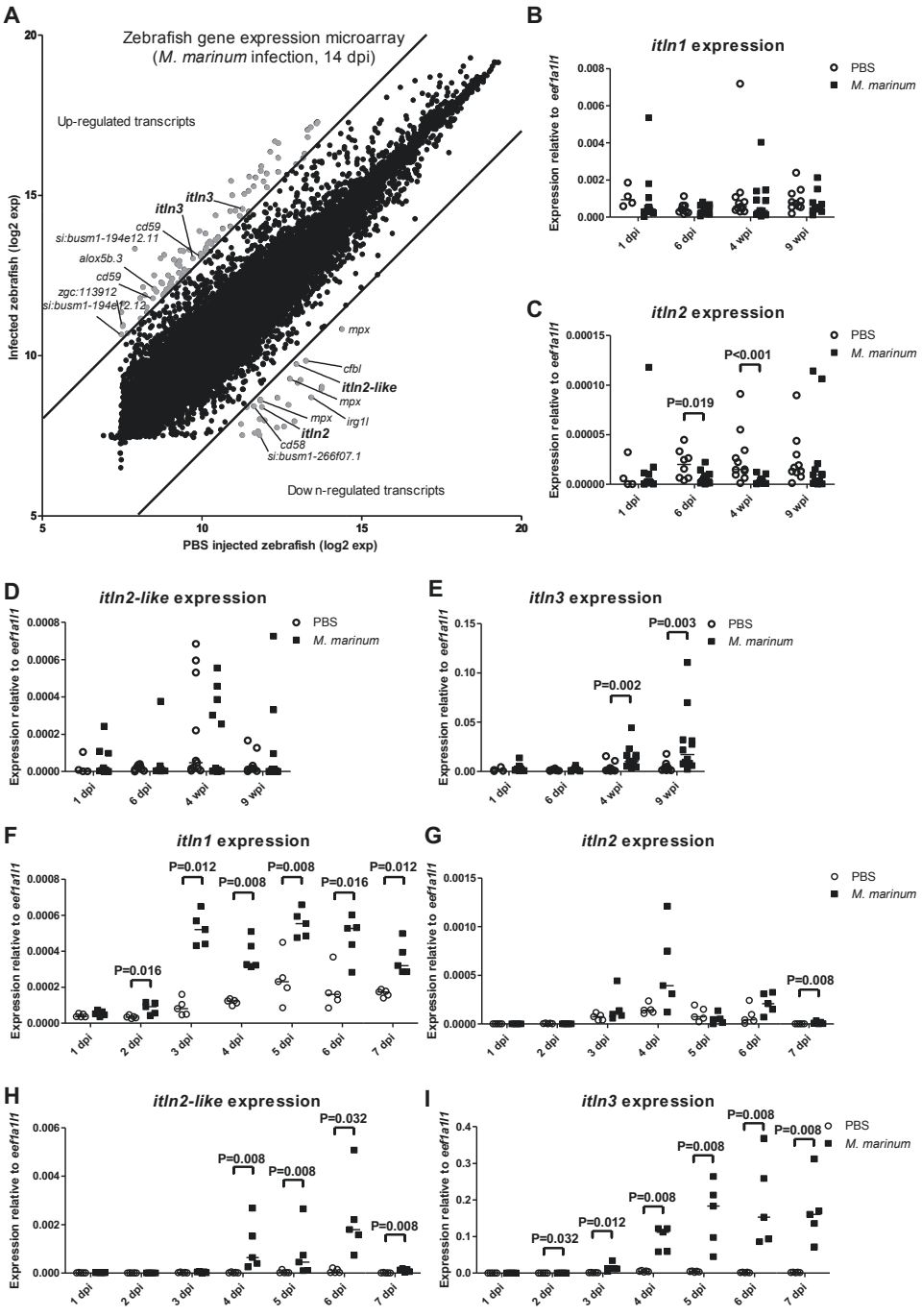
A
Zebrafish gene expression microarray
(M. marinum infection, 14 dpi)
Up-regulated transcripts
Down-regulated transcripts
Infected zebrafish (log2 exp)
PBS injected zebrafish (log2 exp)
itln3
cd59
si:busm1-194e12.11
alox5b.3
cd59
zgc:113912
si:busm1-194e12.12
mpx
cfbl
itln2-like
mpx
mpx
irg1l
itln2
cd58
si:busm1-266f07.1
B
itln1 expression
C
itln2 expression
P=0.019
P<0.001
D
itln2-like expression
E
itln3 expression
P=0.002
P=0.003
F
itln1 expression
P=0.016
P=0.012
P=0.008
P=0.008
P=0.016
P=0.012
G
itln2 expression
P=0.008
H
itln2-like expression
P=0.008
P=0.008
P=0.032
P=0.008
I
itln3 expression
P=0.032
P=0.012
P=0.008
P=0.008
P=0.008
P=0.008
PBS
M. marinum
Expression relative to eef1a1l1
1 dpi
2 dpi
3 dpi
4 dpi
5 dpi
6 dpi
7 dpi
4 wpi
9 wpi

FIGURE 2

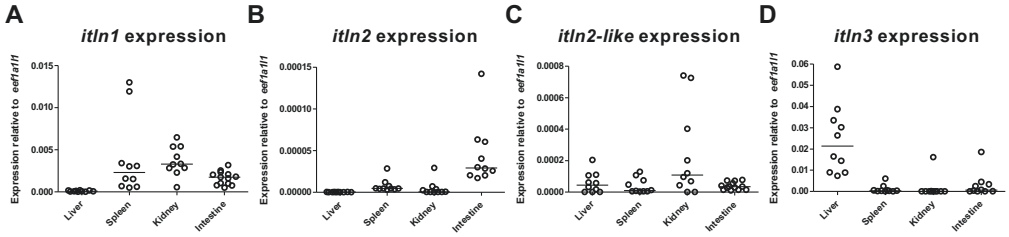

FIGURE 3

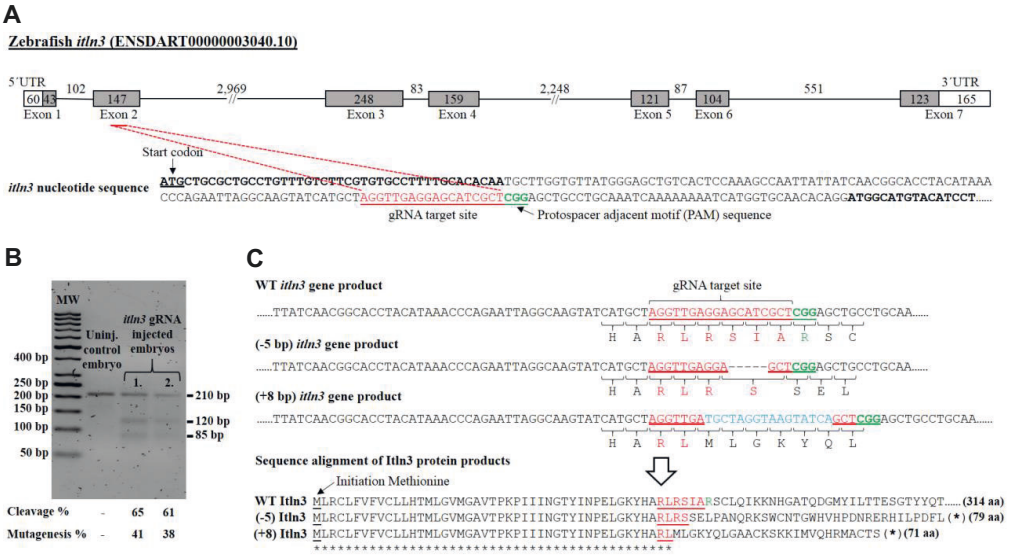

FIGURE 4

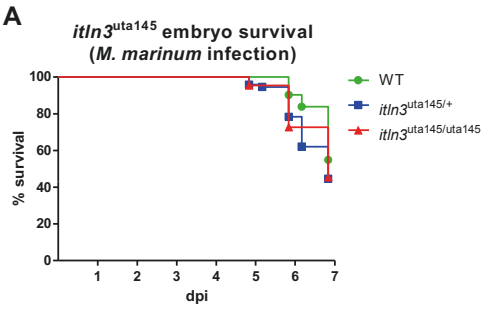
A
itln3uta145 embryo survival
(M. marinum infection)
% survival
dpi
WT
itln3uta145/+
itln3uta145/uta145

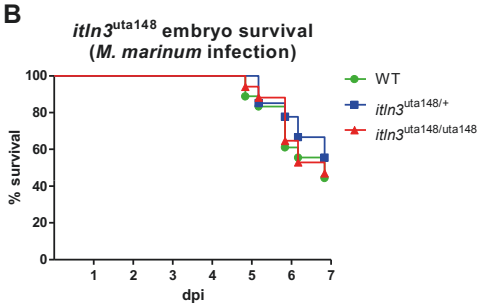
B
itln3uta148 embryo survival
(M. marinum infection)
% survival
dpi
WT
itln3uta148/+
itln3uta148/uta148

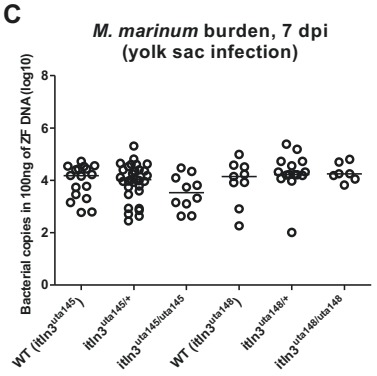
C
M. marinum burden, 7 dpi
(yolk sac infection)
Bacterial copies in 100ng of ZF DNA (log10)
WT (itln3uta145)
itln3uta145/+
itln3uta145/uta145
WT (itln3uta148)
itln3uta148/+
itln3uta148/uta148

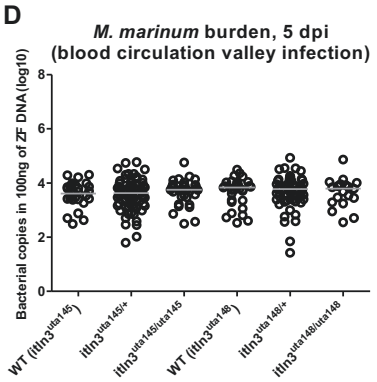
D
M. marinum burden, 5 dpi
(blood circulation valley infection)
Bacterial copies in 100ng of ZF DNA (log10)
WT (itln3uta145)
itln3uta145/+
itln3uta145/uta145
WT (itln3uta148)
itln3uta148/+
itln3uta148/uta148

FIGURE 5

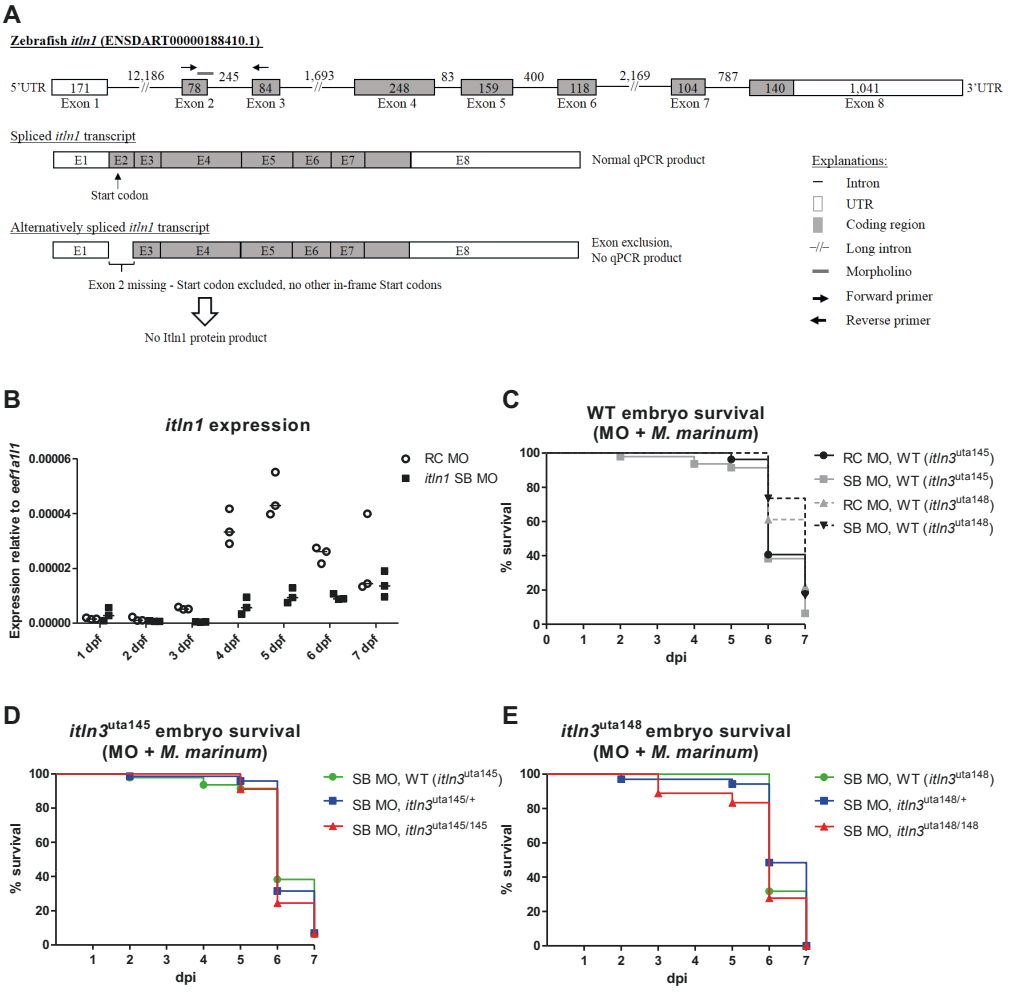
A
Zebrafish itln1 (ENSDART00000188410.1)
5'UTR
171
Exon 1
12,186
78
Exon 2
245
84
Exon 3
1,693
248
Exon 4
83
159
Exon 5
400
118
Exon 6
2,169
104
Exon 7
787
140
1,041
Exon 8
3'UTR
Spliced itln1 transcript
E1 E2 E3 E4 E5 E6 E7 E8
Start codon
Normal qPCR product
Alternatively spliced itln1 transcript
E1 E3 E4 E5 E6 E7 E8
Exon 2 missing - Start codon excluded, no other in-frame Start codons
No Itln1 protein product
Exon exclusion, No qPCR product
Explanations:
Intron
UTR
Coding region
Long intron
Morpholino
Forward primer
Reverse primer
B
itln1 expression
Expression relative to eef1a1l1
0.00006
0.00004
0.00002
0.00000
1 dpf
2 dpf
3 dpf
4 dpf
5 dpf
6 dpf
7 dpf
RC MO
itln1 SB MO
C
WT embryo survival
(MO + M. marinum)
% survival
dpi
RC MO, WT (itln3uta145)
SB MO, WT (itln3uta145)
RC MO, WT (itln3uta148)
SB MO, WT (itln3uta148)
D
itln3uta145 embryo survival
(MO + M. marinum)
% survival
dpi
SB MO, WT (itln3uta145)
SB MO, itln3uta145/+
SB MO, itln3uta145/145
E
itln3uta148 embryo survival
(MO + M. marinum)
% survival
dpi
SB MO, WT (itln3uta148)
SB MO, itln3uta148/+
SB MO, itln3uta148/148

FIGURE 6

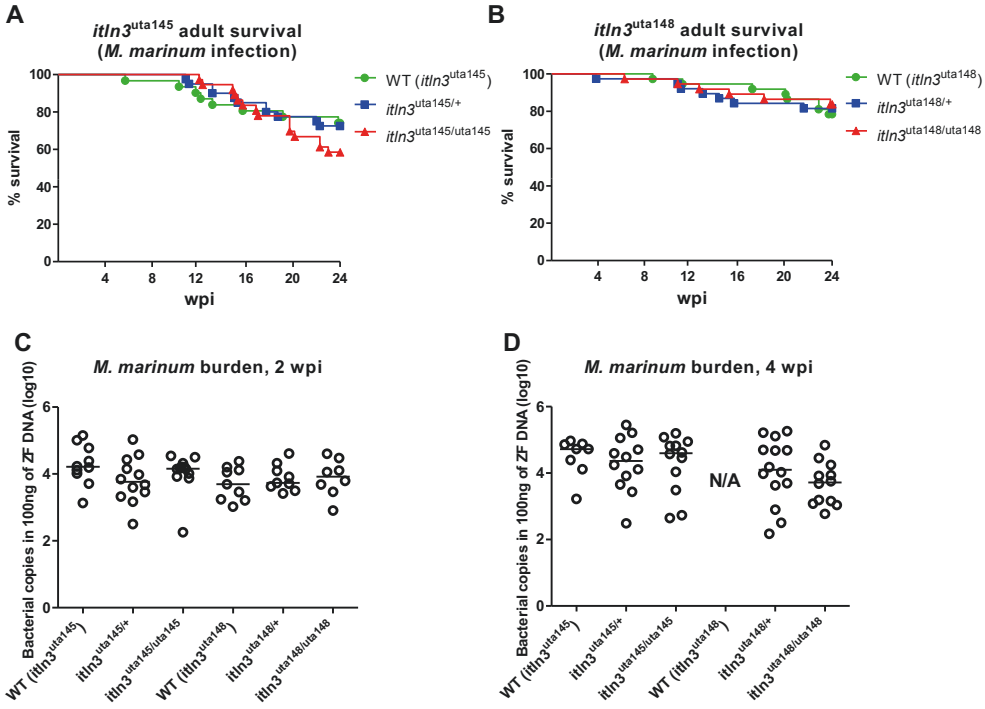
A
itln3uta145 adult survival
(M. marinum infection)
% survival
wpi
WT (itln3uta145)
itln3uta145/+
itln3uta145/uta145
B
itln3uta148 adult survival
(M. marinum infection)
% survival
wpi
WT (itln3uta148)
itln3uta148/+
itln3uta148/uta148
C
M. marinum burden, 2 wpi
Bacterial copies in 100ng of ZF DNA (log10)
WT (itln3uta145)
itln3uta145/+
itln3uta145/uta145
WT (itln3uta148)
itln3uta148/+
itln3uta148/uta148
D
M. marinum burden, 4 wpi
Bacterial copies in 100ng of ZF DNA (log10)
N/A
WT (itln3uta145)
itln3uta145/+
itln3uta145/uta145
WT (itln3uta148)
itln3uta148/+
itln3uta148/uta148

FIGURE 7

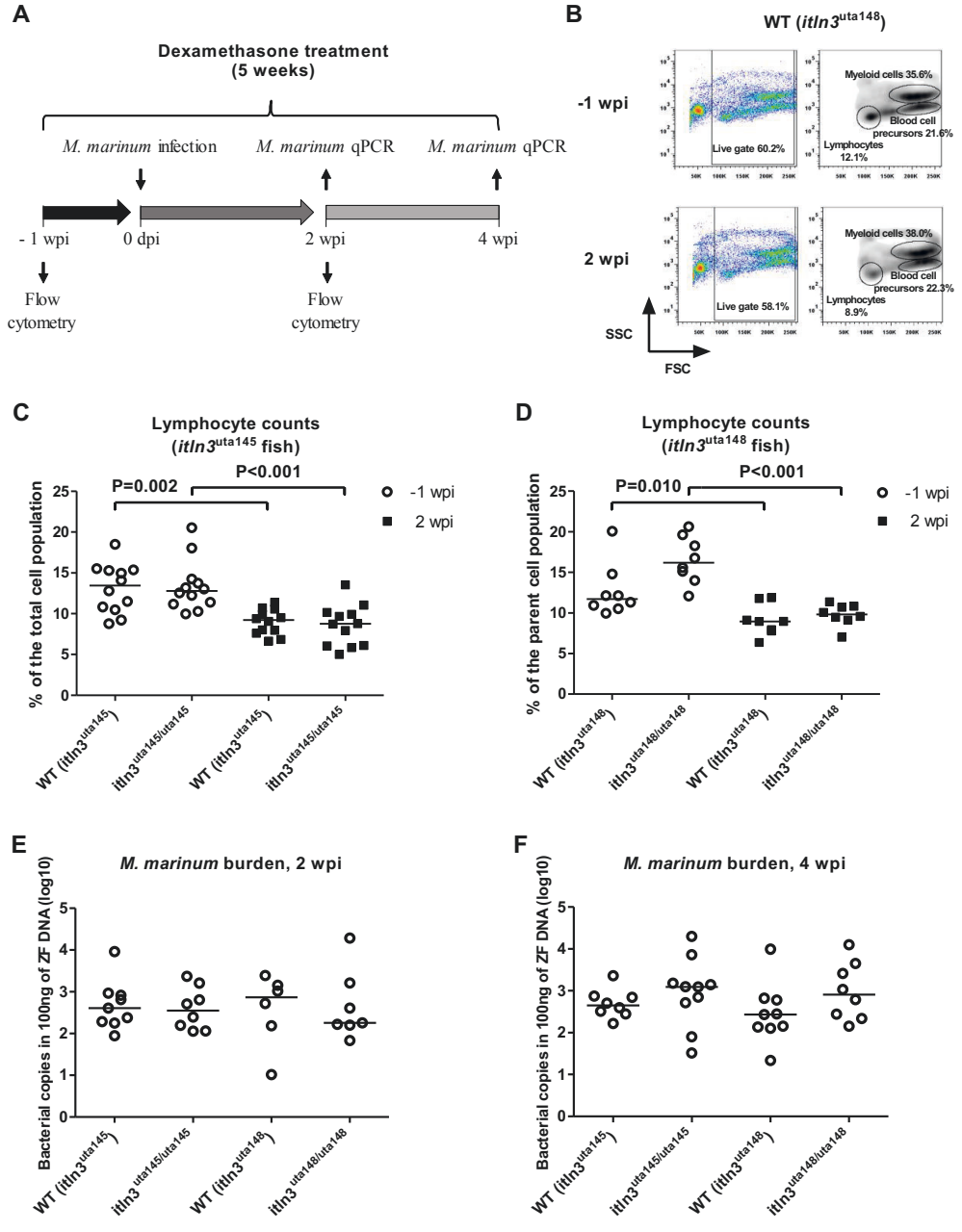
A
Dexamethasone treatment
(5 weeks)
M. marinum infection
M. marinum qPCR
M. marinum qPCR
- 1 wpi
0 dpi
2 wpi
4 wpi
Flow cytometry
Flow cytometry
B
WT (itln3uta148)
-1 wpi
Live gate 60.2%
Myeloid cells 35.6%
Blood cell precursors 21.6%
Lymphocytes 12.1%
2 wpi
Live gate 58.1%
Myeloid cells 38.0%
Blood cell precursors 22.3%
Lymphocytes 8.9%
SSC
FSC
C
Lymphocyte counts
(itln3uta145 fish)
P=0.002
P<0.001
-1 wpi
2 wpi
% of the total cell population
WT (itln3uta145)
itln3uta145/uta145
WT (itln3uta145)
itln3uta145/uta145
D
Lymphocyte counts
(itln3uta148 fish)
P=0.010
P<0.001
-1 wpi
2 wpi
% of the parent cell population
WT (itln3uta148)
itln3uta148/uta148
WT (itln3uta148)
itln3uta148/uta148
E
M. marinum burden, 2 wpi
Bacterial copies in 100ng of ZF DNA (log10)
WT (itln3uta145)
itln3uta145/uta145
WT (itln3uta148)
itln3uta148/uta148
F
M. marinum burden, 4 wpi
Bacterial copies in 100ng of ZF DNA (log10)
WT (itln3uta145)
itln3uta145/uta145
WT (itln3uta148)
itln3uta148/uta148

Supplementary information

Intelectin 3 is dispensable for resistance against a mycobacterial infection in zebrafish (*Danio rerio*)

Markus J.T. Ojanen[1,2], Meri I.E. Uusi-Mäkelä[1], Sanna-Kaisa E. Harjula[1], Anni K. Saralahti[1], Kaisa E. Oksanen[1], Niklas Kähkönen[3], Juha A.E. Määttä[3], Vesa P. Hytönen[3], Marko Pesu[2,4], Mika Rämet[*,1,5,6,7]

Affiliations:

[1]Laboratory of Experimental Immunology, BioMediTech Institute and Faculty of Medicine and Life Sciences, University of Tampere, Tampere, Finland;

[2]Laboratory of Immunoregulation, BioMediTech Institute and Faculty of Medicine and Life Sciences, University of Tampere, Tampere, Finland;

[3]Laboratory of Protein Dynamics, BioMediTech Institute and Faculty of Medicine and Life Sciences, University of Tampere, Tampere, Finland;

[4]Department of Dermatology, Tampere University Hospital, Tampere, Finland;

[5]Department of Pediatrics, Tampere University Hospital, Tampere, Finland;

[6]Department of Children and Adolescents, Oulu University Hospital, Oulu, Finland;

[7]PEDEGO Research Unit and Medical Research Center Oulu, University of Oulu, Oulu, Finland

***Corresponding author:** Correspondence to Mika Rämet, phone: 358-50-4336276, Email: mika.ramet@uta.fi

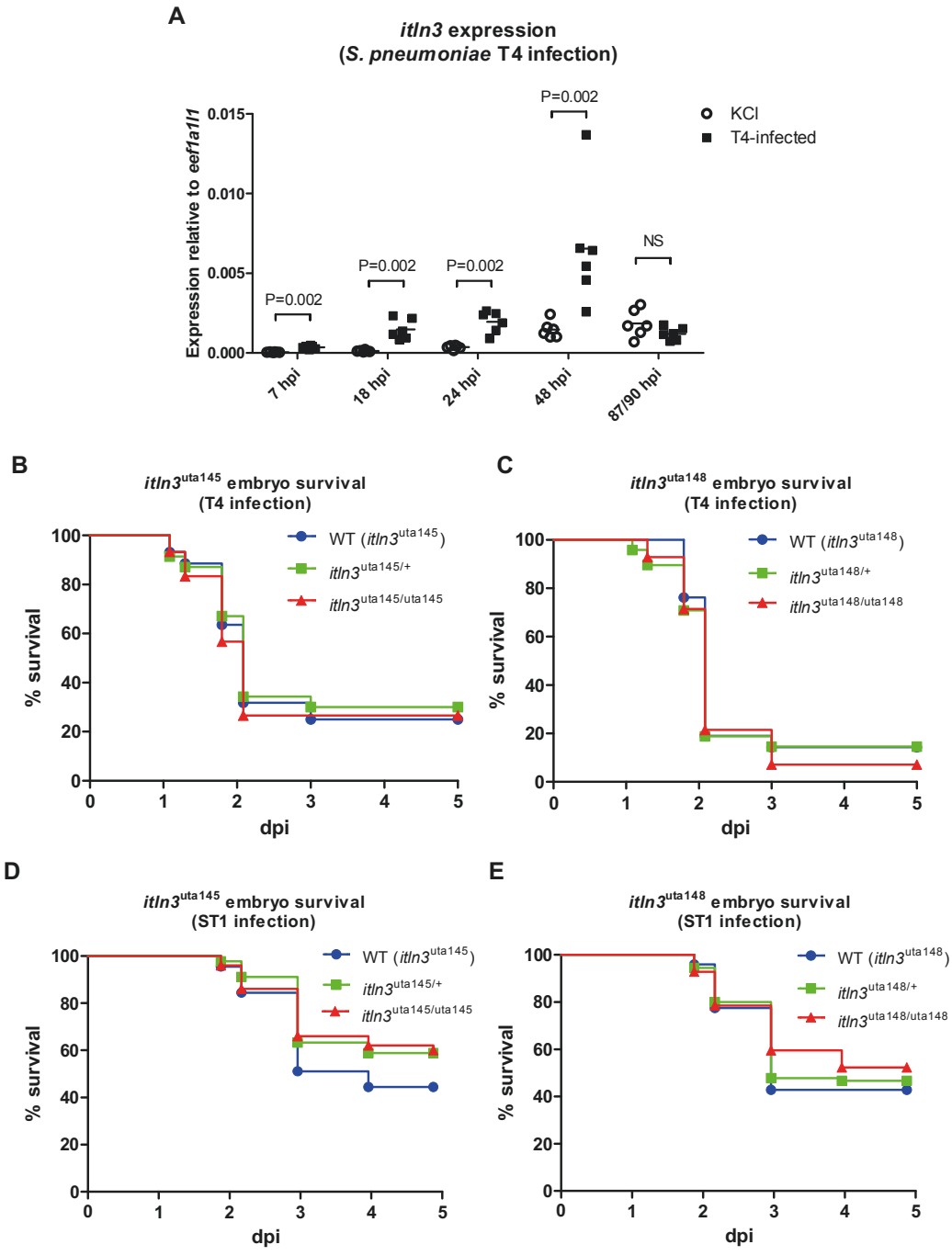
A
itln3 expression
(S. pneumoniae T4 infection)
Expression relative to eef1a1l1
0.015
0.010
0.005
0.000
P=0.002
P=0.002
P=0.002
P=0.002
NS
KCl
T4-infected
7 hpi
18 hpi
24 hpi
48 hpi
87/90 hpi
B
itln3uta145 embryo survival
(T4 infection)
% survival
dpi
WT (itln3uta145)
itln3uta145/+
itln3uta145/uta145
C
itln3uta148 embryo survival
(T4 infection)
% survival
dpi
WT (itln3uta148)
itln3uta148/+
itln3uta148/uta148
D
itln3uta145 embryo survival
(ST1 infection)
% survival
dpi
WT (itln3uta145)
itln3uta145/+
itln3uta145/uta145
E
itln3uta148 embryo survival
(ST1 infection)
% survival
dpi
WT (itln3uta148)
itln3uta148/+
itln3uta148/uta148

Supplementary Figure 1. *itln3* expression is induced in *S. pneumoniae* infected zebrafish embryos, but *itln3* is dispensable for embryo survival. A) The expression of *itln3* was measured with qPCR from zebrafish embryos infected with *S. pneumoniae* (serotype T4; 296 CFU, SD 32 CFU) 7 hpi to 90 hpi, and compared to potassium chloride (KCl) injected control fish (n=6 in both groups at all timepoints). Gene expressions were normalized to *eef1a1l1* expression. All samples were run once. A two-tailed Mann-Whitney test was used in the statistical comparison of differences. **B-C)** Both *itln3*^{uta145} (n=31-70) and *itln3*^{uta145} (n=14-48) background zebrafish embryos were infected with *S. pneumoniae* (serotype T4; 380 CFU, SD 172 CFU) and their survival followed until 5 dpi. **D-E)** The *itln3*^{uta145} (n=45-91) and *itln3*^{uta145} background (n=42-91) zebrafish embryos were infected with *S. pneumoniae* (serotype 1; 48 CFU, SD 28 CFU) and their survival followed until 5 dpi. The data was collected from a single experiment in panels B-E and a log-rank (Mantel-Cox) test was used for the statistical comparison of differences.

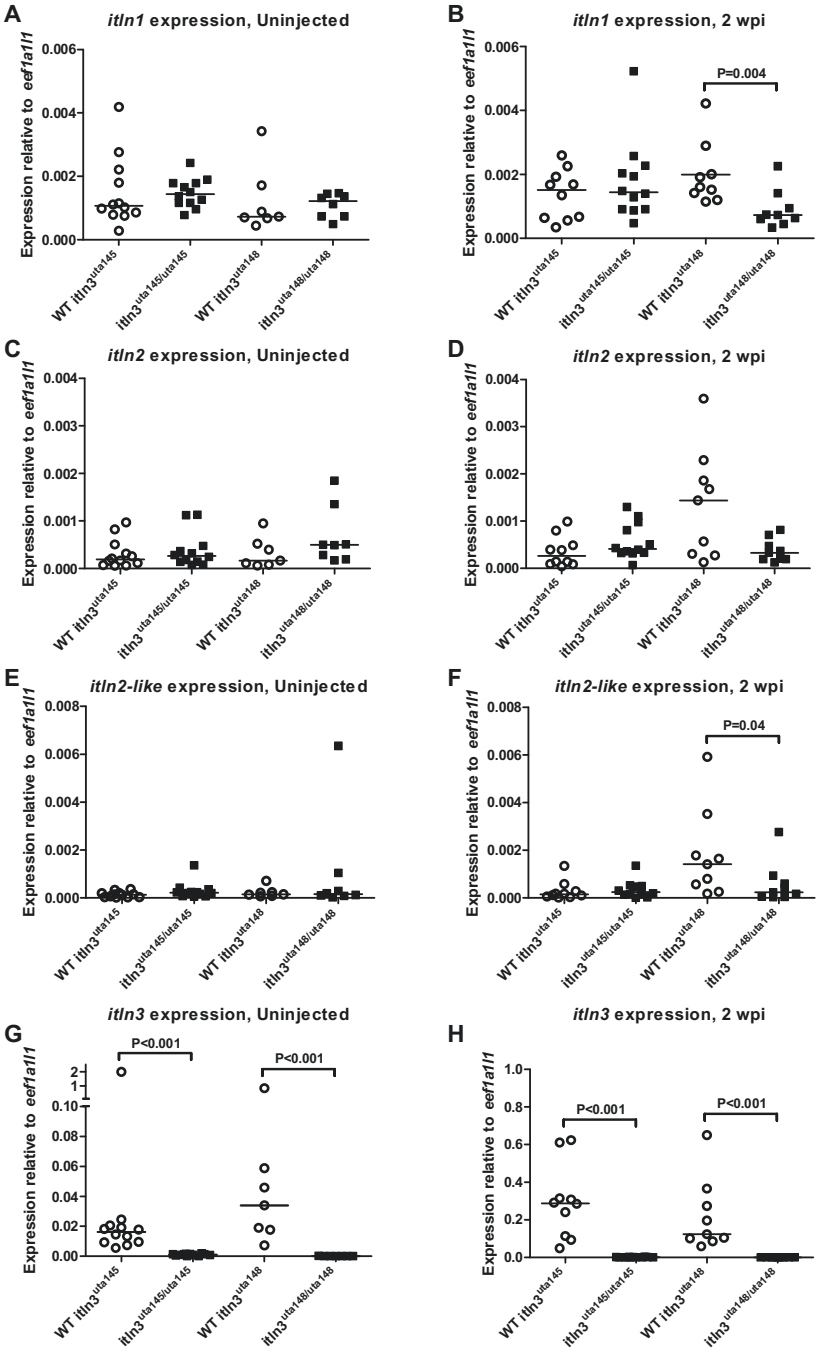
A
itln1 expression, Uninjected
Expression relative to eef1a1l1
0.006
0.004
0.002
0.000
WT itln3 uta145
itln3 uta145/uta145
WT itln3 uta148
itln3 uta148/uta148
B
itln1 expression, 2 wpi
P=0.004
C
itln2 expression, Uninjected
0.004
0.003
0.002
0.001
D
itln2 expression, 2 wpi
E
itln2-like expression, Uninjected
0.008
0.006
0.004
0.002
F
itln2-like expression, 2 wpi
P=0.04
G
itln3 expression, Uninjected
P<0.001
P<0.001
2
1
0.10
0.08
0.06
0.04
0.02
0.00
H
itln3 expression, 2 wpi
P<0.001
P<0.001
1.0
0.8
0.6
0.4
0.2
0.0

Supplementary Figure 2. Expression of zebrafish *itln* genes in uninjected and *M. marinum* infected adult *itln3*^{uta145} and *itln3*^{uta148} zebrafish. The expression of zebrafish *itln* genes (*itln1*, *itln2*, *itln2-like* and *itln3*) was measured with qPCR in the organ blocks (without the kidney) of uninjected and *M. marinum* infected (422 CFU; SD 221 CFU, 2 wpi) adult WT (*itln3*^{uta145}) (n=12 and n=10, respectively), *itln3*$^{uta145/145}$(n=12 and n=12, respectively), WT (*itln3*^{uta148}) (n=7 and n=9, respectively) and *itln3*$^{uta148/148}$ zebrafish (n=7-8 and n=9-10, respectively). Note the different scales of the y axes and the divided axis in panel G. Gene expressions were normalized to *eef1a1l1* expression. All samples were run once. A two-tailed Mann-Whitney test was used in the statistical comparison of differences.

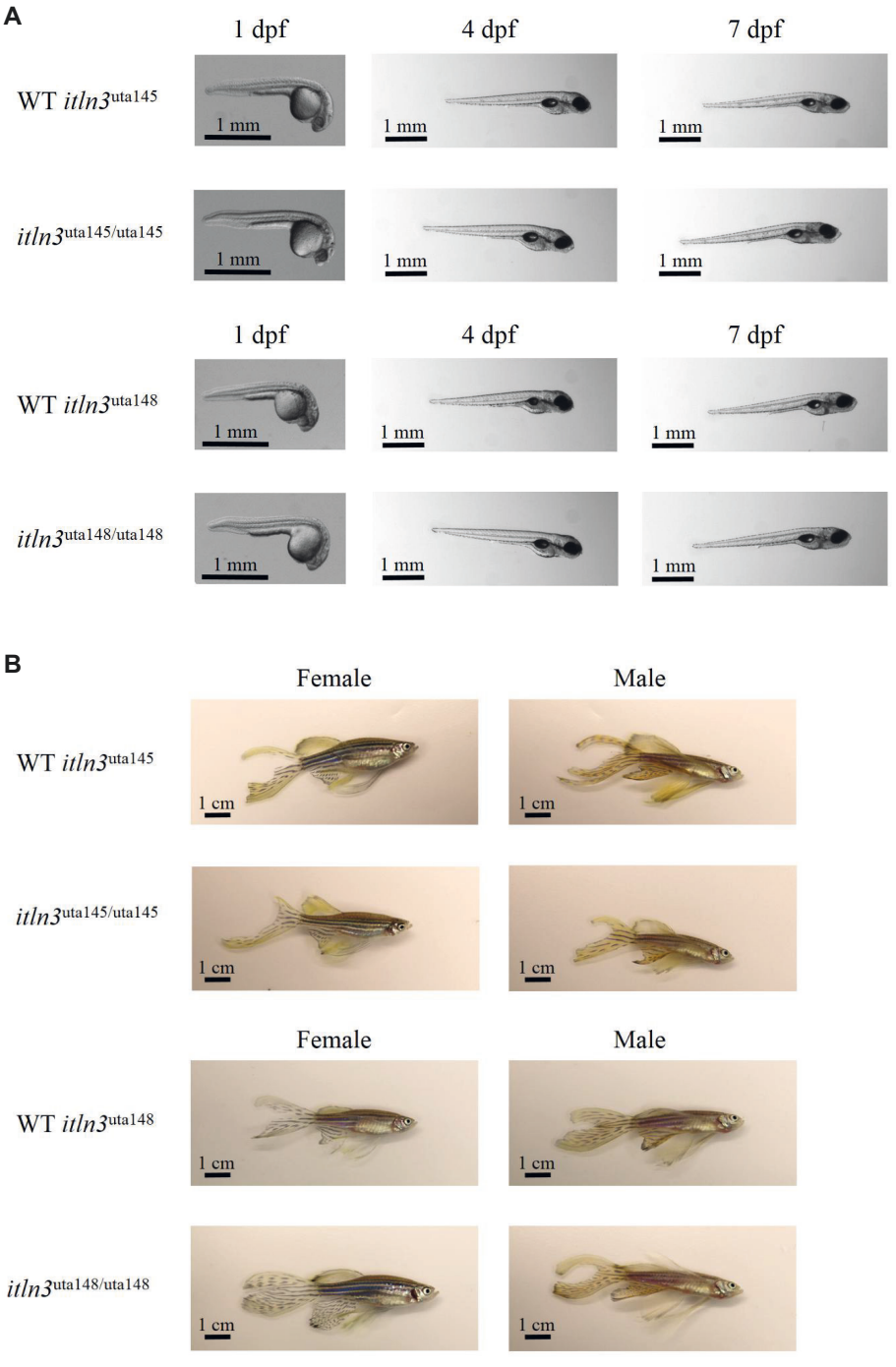
A
1 dpf
4 dpf
7 dpf
WT itln3uta145
itln3uta145/uta145
1 dpf
4 dpf
7 dpf
WT itln3uta148
itln3uta148/uta148
1 mm
B
Female
Male
WT itln3uta145
itln3uta145/uta145
Female
Male
WT itln3uta148
itln3uta148/uta148
1 cm

Supplementary Figure 3. Homozygous *itln3*$^{uta145/uta145}$ and *itln3*$^{uta148/uta148}$ mutants develop normally. A) F3-progeny of *itln3*$^{uta145/+}$ and *itln3*$^{uta148/+}$ zebrafish were imaged at 1, 4 and 7 dpf. The larvae were anesthetized for imaging with 0.02% 3-amino benzoic acid ethyl ester (Sigma-Aldrich) at 4 and 7 dpf, and the embryos collected for genotyping at 7 dpf. Representative images of *itln3*$^{uta145/145}$ and *itln3*$^{uta148/148}$ mutants as well as the corresponding WT embryos are shown. Micrographs were taken with Zeiss Lumar V12 fluorescence microscope and Axiocam MRm digital camera using a bright field exposure of 2 ms. A 23.5x-magnification was used at 1 dpf and a 15.0x-magnification at 4 and 7 dpf. **B)** 12-month-old WT (*itln3*^{uta145}), *itln3*$^{uta145/145}$, WT (*itln3*^{uta148}) and *itln3*$^{uta148/148}$ female and male zebrafish were anesthetized with 0.02% 3-amino benzoic acid ethyl ester (Sigma-Aldrich) and imaged submerged in water using Canon EOS 7D Mark II camera with an exposure time of 8 ms. Brightness was increased by 20% for all of the images in panel B using Windows Photo Viewer. All images in panels A-B were cropped to exclude unnecessary empty background from the figure.

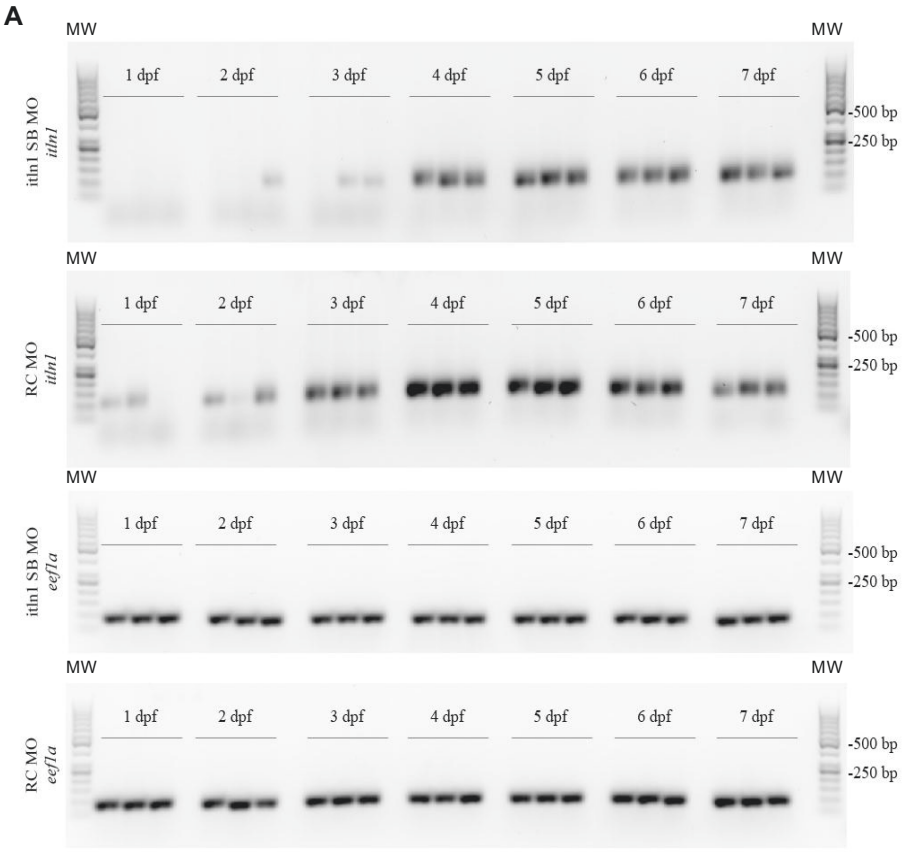
A
MW
MW
1 dpf
2 dpf
3 dpf
4 dpf
5 dpf
6 dpf
7 dpf
-500 bp
-250 bp
itln1 SB MO
itln1
RC MO
itln1
itln1 SB MO
eef1a
RC MO
eef1a
B
Embryo survival, Ungenotyped fish
(MO + PBS injection)
% survival
dpi
0
20
40
60
80
100
0
1
2
3
4
5
6
7
RC MO, itln3uta145
SB MO, itln3uta145
RC MO, itln3uta148
SB MO, itln3uta148

Supplementary Figure 4. *Itln1* splice site blocking morpholino knocks down the expression of *itln1*, but does not alter the survival of the embryos. A) The expression of *itln1* was measured with qPCR in the splice blocking morpholino (SB MO) (n=3 at all timepoints) and the random control morpholino (RC MO) (n=3 at all timepoints) injected WT AB zebrafish embryos between 0 dpf and 7 dpf (See Figure 5C). The qPCR amplified samples were run with 1.5% agarose TAE gel electrophoresis to confirm knockdown effects and to compare the intensities of the *itln1* SB MO and RC MO injected samples. GeneRuler 50 bp DNA Ladder (#SM0373, Thermo Fischer Scientific) was used as a molecular weight marker (MW). The housekeeping gene *eef1a1l1* from the same samples was also amplified and analyzed with gel electrophoresis. Images were obtained with ChemiDoc™ XRS+ system (Bio-Rad Laboratories) and analyzed with Image Lab software (v. 5.2; Bio-Rad Laboratories). Gel images are cropped to exclude portions that do not contain experimental samples. **B)** Survival of the morpholino and phosphate buffered saline (PBS) co-injected (yolk sac injection) ungenotyped embryos from both the *itln3*^{uta145} (RC, n=42; SB n=58) and *itln3*^{uta148} (RC, n=38; SB, n=72) background were followed until 7 dpi. The data was collected from a single experiment. A log-rank (Mantel-Cox) test was used for the statistical comparison of differences. RC= random control, SB= slice blocking, MO = morpholino.

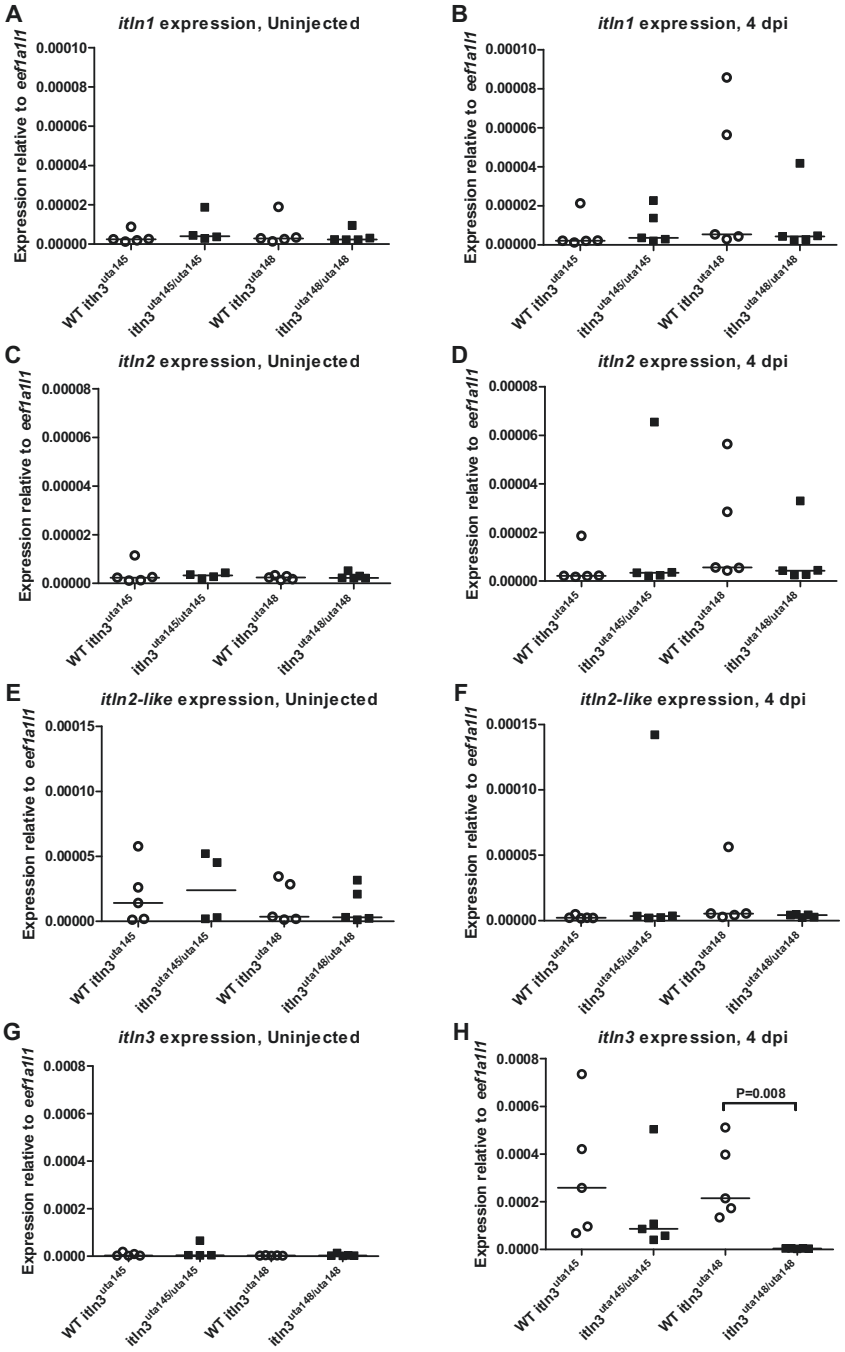
A
itln1 expression, Uninjected
B
itln1 expression, 4 dpi
C
itln2 expression, Uninjected
D
itln2 expression, 4 dpi
E
itln2-like expression, Uninjected
F
itln2-like expression, 4 dpi
G
itln3 expression, Uninjected
H
itln3 expression, 4 dpi
P=0.008
Expression relative to eef1a1l1
WT itln3uta145
itln3uta145/uta145
WT itln3uta148
itln3uta148/uta148

Supplementary Figure 5. Expression of zebrafish *itln* genes in uninjected and *M. marinum* infected *itln3*^{uta145} and *itln3*^{uta148} zebrafish embryos. The expression of zebrafish *itln* genes (*itln1*, *itln2*, *itln2-like* and *itln3*) was measured with qPCR in the uninjected (4 dpf) and *M. marinum* infected (25 CFU; SD 23 CFU, 4 dpf/ 4 dpi) WT (*itln3*^{uta145}) (n=5 in both groups), *itln3*$^{uta145/145}$(n=4 and n=5, respectively), WT (*itln3*^{uta148}) (n=5 in both groups) and *itln3*$^{uta148/148}$ zebrafish embryos (n=5 in both groups). Individual embryos were used in the *itln3*^{uta145} background samples, whereas *itln3*^{uta148} background samples were pooled from 4 to 6 embryos. Note the different scales of the y axes. Gene expressions were normalized to *eef1a1l1* expression. Target genes were run once. A two-tailed Mann-Whitney test was used in the statistical comparison of differences.

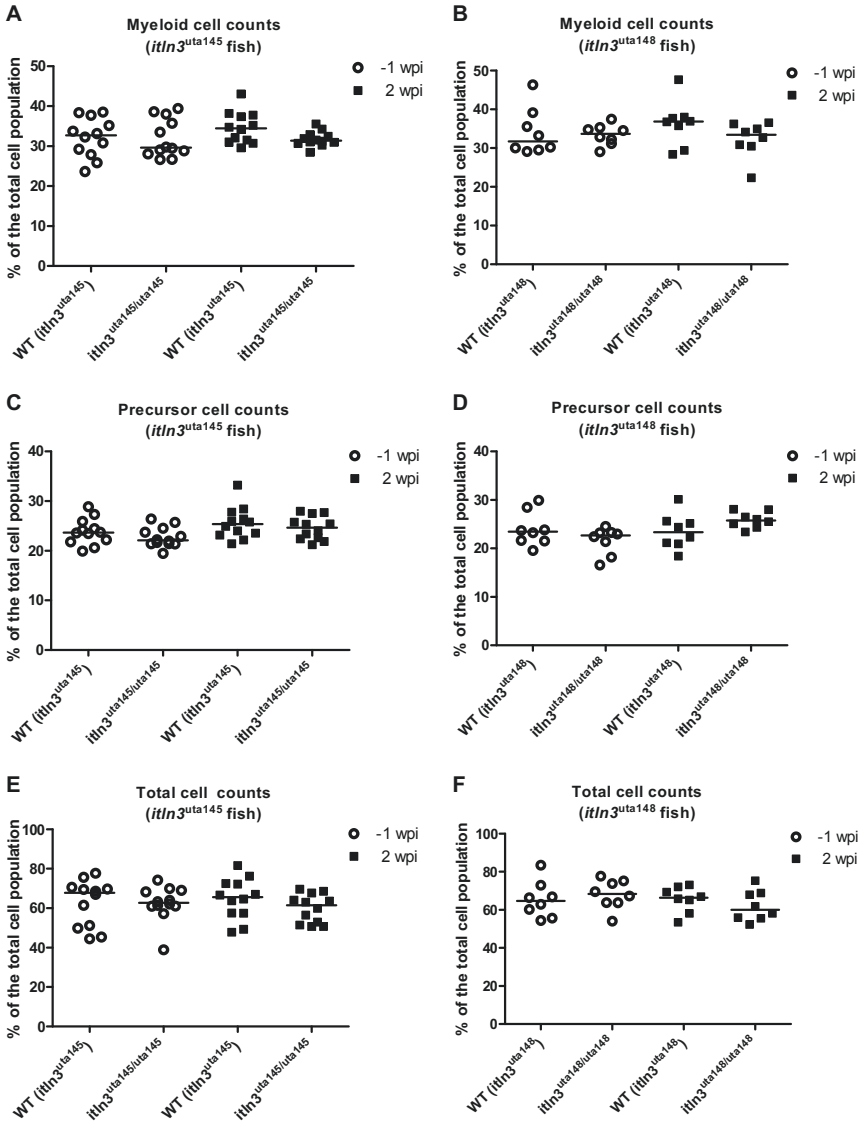

Supplementary Figure 6. Quantification of myeloid cells, precursor cells and the total cell count in the dexamethasone treated zebrafish. A-B) The fraction of myeloid cells from the total cell population for the WT (*itln3*^{uta145}) and *itln3*$^{uta145/uta145}$ as well as WT (*itln3*^{uta148}) and *itln3*$^{uta148/uta148}$ were measured with flow cytometry at -1 wpi and 2 wpi (n=12 for all of the *itln3*^{uta145} fish groups and n=8 for all of the *itln3*^{uta148} groups). Flow cytometry was used to determine also the **C-D)** precursor cell and **E-F)** the total cell counts from the same samples. Technical duplicates were run from all of the samples. A two-tailed Mann-Whitney test was used in the statistical comparison of differences.

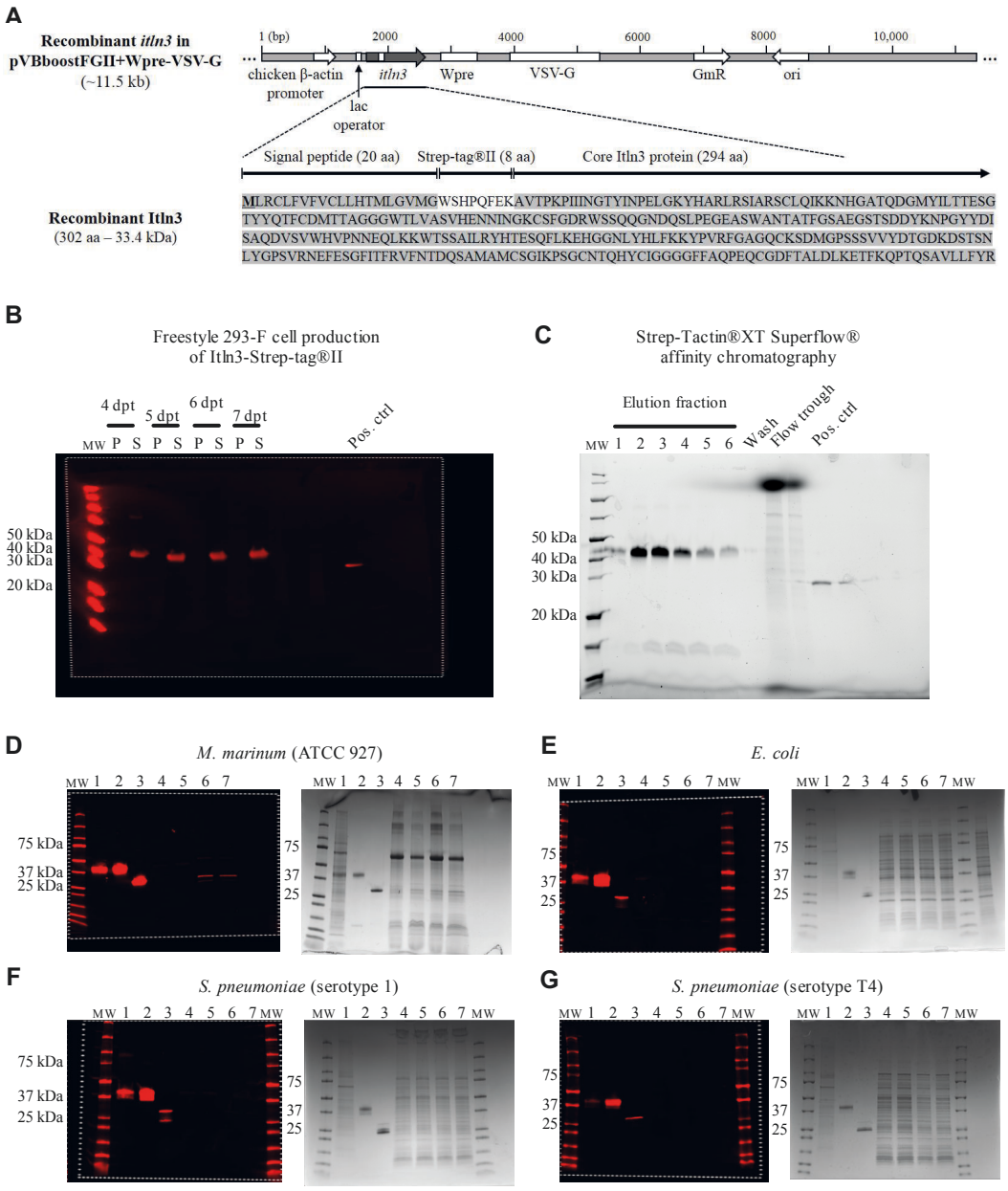

Supplementary Figure 7. Recombinant Itln3 does not bind to *M. marinum*, *S. pneumoniae* or *E. coli*. A) A schematic representation of the recombinant *itln3* cloned into pVBoostFGII+Wpre-VSV-G expression vector and of the expected 302 amino acid long Itln3-Strep-Tag®II protein product.

GmR = gentamycin resistance. ori = origin of replication. **B)** The recombinant Itln3 protein was produced in Freestyle 293-F cells, and an approximately 40 kDa product was detected with Western Blot between 4 and 7 days post transfection (dpt) in the supernatant (S) but not in the pellet (P). **C)** Following affinity chromatography with Strep-Tactin®XT Superflow® matrix, elution fractions 1-6 were run with SDS-PAGE. **D-G)** Recombinant Itln3-Strep-tag®II and GFP-Twin-Strep-tag® were incubated with either *M. marinum, E. coli* or *S. pneumoniae* (serotypes 1 and T4) in the presence (+$CaCl_2$) or absence of calcium (+EDTA). Samples were analyzed with SDS-PAGE and Strep-tagged proteins detected from blotted membrane at 700 nm using Strep-Tactin Oyster 645 conjugate. The lanes are numbered as follows; control samples: 1. 20 µl of Itln3 containing cell culture medium, 2. 1 µg of Itln3-Strep-Tag®II, 3. 1 µg of GFP-Twin-Strep-tag®, and the bacteria containing samples: 4. 7.5 µg of Itln3-Strep-Tag®II in binding buffer (+$CaCl_2$), 5. 7.5µg of Itln3-Strep-Tag®II in the absence of calcium (+EDTA), 6. 7.5µg of GFP-Twin-Strep-tag® in binding buffer (+$CaCl_2$), 7. 7.5µg of GFP-Twin-Strep-tag® in the absence of calcium (+EDTA). The PageRuler™ Unstained Broad Range Protein Ladder (#26630, Thermo Fisher Scientific) was used in panels B-C as a molecular weight marker (MW), whereas Precision Plus Protein™ Dual Xtra (#161-0377, Bio-Rad Laboratories) was used in panels D-G. White lines indicate the borders of the immunoblots. SDS-PAGE images are cropped to exclude portions that do not contain experimental samples. In panels D-G the same acquisition values for 700 nm channel have been applied.

Supplementary Table 1. Zebrafish (V3) Gene Expression Microarray, 4x44K (Agilent Technologies).

Up-regulated transcripts

Probe Name	Systematic Name	Gene Symbol	Gene Name	Average log2 Fold Change
A_15_P110361	**NM_001004534**	**si:busm1-194e12.11 (mhc2)**	**si:busm1-194e12.11 (mhc2)**	**5.43**
A_15_P269921	EH455384			4.40
A_15_P695731	ENSDART00000151988	LOC559001	fatty acid synthase-like	4.33
A_15_P541012				
A_15_P670021				
A_15_P286336	NM_001017909	zgc:112992	zgc:112992	4.24
A_15_P151116				
A_15_P772381	ENSDART00000054817	nansb	N-acetylneuraminic acid synthase b	4.11
A_15_P676036	NM_001139464	ela2	elastase 2	4.06
A_15_P437360	NM_214751	pck1	phosphoenolpyruvate carboxykinase 1 (soluble)	4.00
A_15_P661356	NM_198815	scd	stearoyl-CoA desaturase (delta-9-desaturase)	4.00
A_15_P727551				
A_15_P176621				
A_15_P170986	NM_001037420	ugt5a1	UDP glucuronosyltransferase 5 family, polypeptide A1	3.95
A_15_P117864	NM_001024408	ela3l	elastase 3 like	3.95
A_15_P623151	NM_131516	pvalb2	parvalbumin 2	3.90
A_15_P163756				
A_15_P208801	NM_001044323	zgc:152753	zgc:152753	3.88
A_15_P198561	NM_201173	cyp7a1a	cytochrome P450, family 7, subfamily A, polypeptide 1a	3.88
A_15_P100059	NM_001020482	cpa1	carboxypeptidase A1 (pancreatic)	3.84
A_15_P749196	NM_205572	pvalb1	parvalbumin 1	3.84
A_15_P106696				
A_15_P624116	NM_199605	zgc:66382	zgc:66382	3.79
A_15_P655936	NM_212783	pvalb4	parvalbumin 4	3.79
A_15_P132286				
A_15_P666139				
A_15_P209091	NM_001003737	zgc:92041	zgc:92041	3.72
A_15_P148011	NM_001076602	slc25a38a	solute carrier family 25, member 38a	3.69
A_15_P118321	NM_200212	pvalb3	parvalbumin 3	3.69
A_15_P664371				
A_15_P670531				
A_15_P104996	NM_001003423	tnni2b.2	troponin I, skeletal, fast 2b, tandem duplicate 2	3.68
A_15_P111799	NM_183070	sst1.1	somatostatin 1, tandem duplicate 1	3.66
A_15_P420075	TC425078			3.63
A_15_P162301	NM_001025180	c6ast4	six-cysteine containing astacin protease 4	3.62
A_15_P382820	NM_131105	tpma	alpha-tropomyosin	3.62
A_15_P754641				
A_15_P142756	**NM_001020578**	**alox5b.3**	**arachidonate 5-lipoxygenase**	**3.59**
A_15_P151326	NM_001003488	pkmb	pyruvate kinase, muscle, b	3.57
A_15_P674431	TC391723			3.57
A_15_P674096	NM_212618	ctrb1	chymotrypsinogen B1	3.51
A_15_P704401	ENSDART00000152233	si:ch1073-110a20.3	si:ch1073-110a20.3	3.51
A_15_P770551				
A_15_P681766	TC398257			3.49
A_15_P108203	NM_213131	mdh2	malate dehydrogenase 2, NAD (mitochondrial)	3.48
A_15_P620081	NM_200370	zgc:64043	zgc:64043	3.43
A_15_P170876	**NM_001001893**	**zgc:113912 (mhc2)**	**zgc:113912 (mhc2)**	**3.40**
A_15_P756000	NM_001004582	ctrl	chymotrypsin-like	3.35
A_15_P102930	NM_001045194	zgc:153896	zgc:153896	3.34
A_15_P728736	**NM_001159584**	**itln3**	**intelectin 3**	**3.32**
A_15_P190506				
A_15_P743431	NM_181653	tnnt3b	troponin T3b, skeletal, fast	3.31
A_15_P101676	NM_001003426	zgc:92745	zgc:92745	3.31
A_15_P488730	ENSDART00000122221	nfe2l2b	nuclear factor (erythroid-derived 2)-like 2b	3.28
A_15_P771326				
A_15_P624916	NM_001115089	myhz1.1	myosin, heavy polypeptide 1.1, skeletal muscle	3.25
A_15_P331879				
A_15_P657891				
A_15_P542682				
A_15_P665056	BC116547	myhz2	myosin, heavy polypeptide 2, fast muscle specific	3.24
A_15_P520672	NM_001003620	casq1a	calsequestrin 1a	3.24
A_15_P107326	NM_200516	zgc:66286	zgc:66286	3.23
A_15_P740921				
A_15_P764081	**ENSDART00000126737**	**cd59**	**cd59 molecule**	**3.22**
A_15_P545927				
A_15_P152786	NM_205575	tnni2a.3	troponin I, skeletal, fast 2a, tandem duplicate 3	3.22
A_15_P101653	NM_001002119	tpm2	tropomyosin 2 (beta)	3.22
A_15_P664046	AF539738	tnni2a.3	troponin I, skeletal, fast 2a, tandem duplicate 3	3.20
A_15_P729090	NM_001177498	ugt5a4	UDP glucuronosyltransferase 5 family, polypeptide A4	3.19
A_15_P657486	BC124207	wu:fc45h08	wu:fc45h08	3.19
A_15_P161846	**NM_001007206**	**si:busm1-194e12.12 (mhc2)**	**si:busm1-194e12.12 (mch2)**	**3.19**

A_15_P600272	ENSDART00000129396	LOC100536763	proline dehydrogenase 1, mitochondrial-like	3.18
A_15_P331241	NM_131619	mylz3	myosin, light polypeptide 3, skeletal muscle	3.18
A_15_P224231	NM_131563	tnnc2	troponin C type 2 (fast)	3.17
A_15_P150646	NM_001030262	plin2	perilipin 2	3.15
A_15_P107567				
A_15_P176531	NM_201009	aacs	acetoacetyl-CoA synthetase	3.15
A_15_P711187	ENSDART00000135295			3.14
A_15_P724331	NM_001110416	tnnt3b	troponin T3b, skeletal, fast	3.14
A_15_P762231	ENSDART00000151970			3.13
A_15_P133581	BC051151	muc5b	mucin 5b	3.13
A_15_P331464	NM_131188	mylpfa	myosin light chain, phosphorylatable, fast skeletal muscle	3.13
A_15_P510237				
A_15_P149696	NM_205678	myoz1a	myozenin 1a	3.10
A_15_P658631	NM_131727	sst2	somatostatin 2	3.08
A_15_P120396	NM_152982	myhz2	myosin, heavy polypeptide 2, fast muscle specific	3.07
A_15_P319166	NM_001271308	acaca	acetyl-Coenzyme A carboxylase alpha	3.07
A_15_P350165				
A_15_P106920	ENSDART00000146702	tnni2b.2	troponin I, skeletal, fast 2b, tandem duplicate 2	3.05
A_15_P661781	NM_001083827	col10a1	collagen, type X, alpha 1	3.03
A_15_P205041	NM_001076723	ugt5a2	UDP glucuronosyltransferase 5 family, polypeptide A2	3.03
A_15_P116208	NM_199271	cpa5	carboxypeptidase A5	3.02
A_15_P102410	NM_001003729	zgc:92137	zgc:92137	3.01

Down-regulated transcripts

Probe Name	Systematic Name	Gene Symbol	Gene Name	Average log2 Fold Change
A_15_P558307	ENSDART00000110325	si:ch211-160b11.4	si:ch211-160b11.4	-3.01
A_15_P163501	**NM_001098254**	**si:dkey-11f4.16 (cd58)**	**si:dkey-11f4.16 (cd58 molecule)**	**-3.20**
A_15_P114150	NM_199856	tdo2b	tryptophan 2,3-dioxygenase b	-3.21
A_15_P117407	**ENSDART00000173485.2**	**ENSDARG00000093796 (itln2-like)**	**intelectin 2 -like**	**-3.22**
A_15_P299736	EH440031			-3.35
A_15_P132151	**NM_212779**	**mpx**	**myeloid-specific peroxidase**	**-3.42**
A_15_P158486				
A_15_P637411				
A_15_P164866	ENSDART00000018062	cfbl	complement factor B-like	-3.42
A_15_P144444	**NM_001159541**	**itln2**	**intelectin 2**	**-3.47**
A_15_P628696	NM_001001730	cyp51	cytochrome P450, family 51	-3.74
A_15_P727566	NM_001089487	zgc:162608	zgc:162608	-3.76
A_15_P176481				
A_15_P181626	BC134957			-3.85
A_15_P678601	EB975183			-3.98
A_15_P365355	NM_001030096	tgm1l4	transglutaminase 1 like 4	-4.02
A_15_P631151				
A_15_P731581	TC444503			-4.10
A_15_P529217				
A_15_P163579	**NM_001007167**	**si:busm1-266f07.1 (mhc2)**	**si:busm1-266f07.1 (mhc2)**	**-4.28**
A_15_P176991	NM_001200021	LOC570474	5-hydroxyisourate hydrolase-like	-4.59
A_15_P118284	**NM_001077607**	**irg1l**	**immunoresponsive gene 1, like**	**-4.72**
A_15_P695546	EH492309	si:ch211-66i15.5	si:ch211-66i15.5	-4.73
A_15_P205021	NM_001040359	zgc:136902	zgc:136902	-4.78
A_15_P357500	TC431869			-4.78
A_15_P309606	ENSDART00000064720	tgm1	transglutaminase 1	-4.94

Supplementary Table 2. Enriched processes from gene ontology analysis.

Up-regulated transcripts vs. background list.

GO term	Description	P-value
GO:0006936	muscle contraction	3.90E-6
GO:0003012	muscle system process	5.47E-6
GO:0006941	striated muscle contraction	8.58E-6
GO:0060048	cardiac muscle contraction	4.57E-5
GO:0003009	skeletal muscle contraction	6.05E-5
GO:0006508	proteolysis	7.21E-5
GO:0061959	response to (R)-carnitine	1.65E-4
GO:0072330	monocarboxylic acid biosynthetic process	2.35E-4
GO:0019882	antigen processing and presentation	2.78E-4
GO:0060359	response to ammonium ion	3.06E-4
GO:0032787	monocarboxylic acid metabolic process	3.38E-4
GO:0044283	small molecule biosynthetic process	3.60E-4
GO:0034284	response to monosaccharide	4.90E-4
GO:0033273	response to vitamin	4.90E-4
GO:0009743	response to carbohydrate	4.90E-4
GO:0009746	response to hexose	4.90E-4
GO:0009749	response to glucose	4.90E-4
GO:0097435	supramolecular fiber organization	6.12E-4
GO:0030239	myofibril assembly	7.05E-4
GO:0055092	sterol homeostasis	7.15E-4
GO:0042632	cholesterol homeostasis	7.15E-4
GO:0014823	response to activity	9.82E-4

Down-regulated transcripts vs. background list.

GO term	Description	P-value
GO:0051707	response to other organism	1.95E-6
GO:0051704	multi-organism process	2.70E-6
GO:0043207	response to external biotic stimulus	4.13E-6
GO:0009607	response to biotic stimulus	4.83E-6
GO:0009617	response to bacterium	2.58E-5
GO: 0006695	cholesterol biosynthetic process	3.51E-5
GO:1902653	secondary alcohol biosynthetic process	3.51E-5
GO:0009605	response to external stimulus	3.56E-5
GO:0044281	small molecule metabolic process	6.15E-5
GO:0016126	sterol biosynthetic process	1.26E-4
GO:1902652	secondary alcohol metabolic process	1.76E-4
GO:0008203	cholesterol metabolic process	1.76E-4
GO:0046165	alcohol biosynthetic process	2.21E-4
GO:0016125	sterol metabolic process	3.74E-4
GO:0006694	steroid biosynthetic process	4.39E-4
GO:0006952	defense response	4.58E-4
GO:0010310	regulation of hydrogen peroxide metabolic process	6.11E-4
GO:0043152	induction of bacterial agglutination	6.11E-4
GO:0033488	cholesterol biosynthetic process via 24,25-dihydroanosterol	6.11E-4
GO:1901617	organic hydroxy compound biosynthetic process	7.06E-4
GO:0042742	defense response to bacterium	7.94E-4
GO:0008202	steroid metabolic process	8.87E-4

Supplementary Table 3. Primers used in the qPCR analyses.

Gene	Ensembl Identifier	Sequence 5´-3´	Reference
itln1	ENSDARG00000007534	F GACGACTACAAGAACCCTGG R ATCGTTGCATGTACCTATGCC	-
itln2	ENSDARG00000036084	F TATGGGAATGGCTGCCTTTC R TTTCAAGCTCATGGTTGCTG	-
itln2-like	ENSDARG00000093796	F ACTGTTCAAGAAATTCCCTGTG R ATGCCCAGTTGGTTTAGTGC	-
itln3	ENSDARG00000003523	F GTGCAACACAGGATGGCATG R TTCTGCACTGCCAAACGTAG	-
eef1a1l1 (ef1a)	ENSDARG00000020850	F CTGGAGGCCAGCTCAAACAT R ATCAAGAAGAGTAGTACCGCTAGCATTAC	(94)
mmits	-	F CACCACGAGAAACACTCCAA R ACATCCCGAAACCAACAGAG	(55)

Supplementary methods

Experimental *S. pneumoniae* infections

S. pneumoniae serotype 4 (T4, sequence type 205) as well as serotype 1 (sequence type 306) culture and infections were performed as described previously[1, 2]. In brief, *S. pneumoniae* were streaked on 5 % lamb blood agar plates (Tammer-Tutkan Maljat, Tampere, Finland) and cultured overnight. In the morning the bacteria were inoculated into 5ml Todd Hewitt broth (Becton, Dickinson and Company, New Jersey, USA) supplemented with 0.5% Todd-Hewitt yeast extract (Becton, Dickinson and Company) and cultured until OD620 ≈ 0.40. 2-day-old zebrafish embryos were anesthetized with 0.02% 3-amino benzoic acid ethyl ester (Sigma-Aldrich) and microinjected into the blood circulation valley using 2 nl of bacteria suspended in 0.2 M potassium chloride (KCl) with 7 mg/ml of tetramethylrhodamine dextran (Thermo Fisher Scientific) to visualize the injections. The survival of the embryos were monitored at least twice a day before 50 hours post infection (hpi) and at least once a day between 2 and 5 dpi. *S. pneumoniae* counts (CFU) in each of the infections were counted by plating inoculates of bacteria on 5% lamb blood agar plates overnight at 37°C with 5% CO_2.

Recombinant Itln3 production

Recombinant zebrafish *itln3* gene was initially synthetized by GeneArt (Invitrogen). AttB-sites for Gateway cloning were added with PCR using the following primers F: GGGGACAAGTTTGTACAAAAAAGCAGGCTTCACCATGCTGCGCTGCCTGTTTGTCTTCG and R: GGGGACCACTTTGTACAAGAAAGCTGGGTTTTATTAACGATAAAACAGCAGAACTG CGCTC. PCR product was Gateway cloned into a donor plasmid pDONR^{TM}211 (Thermo Fisher Scientific) and subsequently into the mammalian expression plasmid pVBboostFGII-Wpre-VSV-G[3], and gene of interest was verified by sequencing. Freestyle 293-F cells (Thermo Fisher Scientific) were

transiently transfected with 10 µg of expression plasmid using FreeStyle™ MAX Reagent (Thermo Fisher Scientific). Cells were cultured for a total of 7 days and both the cells and medium were collected for analysis and protein purification. Itln3 containing an N-terminal Strep-tag®II (Itln3-Strep-tag®II) was purified with Strep-Tactin® XT resin (IBA Life Sciences, Göttingen, Germany) using excess of biotin for elution. Purity and the molecular size of the Itln3-Strep-tag®II was analyzed by SDS-PAGE and Western blot, respectively. Briefly, the protein containing fractions were ran with SDS-PAGE (4-20% gradient gel, Bio-Rad Laboratories) or blotted from the gels on nitrocellulose membrane using Trans-Blot® Turbo™ transfer system (Bio-Rad Laboratories). SDS-PAGE gels were stained with PageBlue™ protein stain (Thermo Fisher Scientific). Immunoblot membranes were blocked in 1% BSA in 0.05% Tween TBS for 30 min at room-temperature (RT) and washed three times with 0.05% Tween TBS for 5 min. Strep-tagged proteins on the blots were detected with 2.5µg of Streptactin Oyster 645 conjugate (IBA Life Sciences, Göttingen, Germany) in 5ml of 0.05% Tween TBS and incubated for 1 h at RT. SDS-PAGE images were obtained with ChemiDoc™ XRS+ system (Bio-Rad Laboratories) and analyzed with Image Lab software (v. 5.2; Bio-Rad Laboratories), whereas blot imaging was done with the Odyssey® CLx (LI-COR Biosciences, Nebraska, USA) at 700 nm at 169 µm resolution, and the images were analyzed by using the Image Studio Lite (v. 5.2; LI-COR Biosciences).

Bacterial binding assay

M. marinum (ATCC 927) and *S. pneumoniae* (T4 and S1) were cultured as described above. *S. pneumoniae* was cultured until OD620 = 0.25 (serotype S1) or 0.35 (serotypeT4), whereas *M. marinum* was cultured until OD600 = 0.614 and 1 ml of the culture used for the bacterial binding assay. *E. coli* was inoculated from a glycerol stock into 5 ml of LB, 225 rpm 37°C. 100 µl of the culture (OD600 =1.614) was pelleted 3 min 10 000 g. Bacterial pellets were washed with 1 ml of sterile PBS, pelleted again 3 min 10 000 g and 1 ml of the protein samples added on the pellet for the bacterial binding. For

this 7.5 µg of the Itln3-Strep-tag®II or 7.5 µg of the GFP-Twin-Strep-tag® negative control protein (IBA Life Sciences) were used in either 1 ml of the binding buffer (20 mM HEPES, 150 mM NaCl, 10 mM $CaCl_2$, 0.1% BSA, 0.05% Tween-20, pH 7.4) or in the EDTA containing buffer (20 mM HEPES, 150 mM NaCl, 10 mM EDTA, 0.1% BSA, 0.05% Tween-20, pH 7.4). The samples were incubated 2 h in rotation at 4°C and washed with 1 ml of PBS as above. The samples were suspended in 30 µl of PBS, and 10 µl of 4xSDS sample buffer (0.2 M Tris-HCl pH 6.8, 8% SDS (w/v), 40% glycerol, 4% β-mercaptoethanol, 0.05 M EDTA, 0.8 mg/ml bromophenol blue) and incubated 10 min 98°C with frequent vortexing. Before loading onto the gel, samples were spinned to pellet bacterial debris and approximately 15 µl of the supernatant was run on two mini-Protean TGX-gels (Bio-Rad Laboratories, California, USA). One gel was stained over night with Page Blue™ Protein Staining Solution (Thermo Fisher Scientific) and the other gel was blotted using the Trans-Blot Turbo Transfer System (Bio-Rad Laboratories). The blot was prepared for imaging and imaged as mentioned above. 1 µg of the Itln3-Strep-tag®II, 1 µg the GFP-Twin-Strep-tag® (IBA Life Sciences) and 20 µl of the Itln3 containing medium from the cell culture were used as positive controls on the gel.

Supplementary references

1. Rounioja, S. *et al*. Defense of zebrafish embryos against Streptococcus pneumoniae infection is dependent on the phagocytic activity of leukocytes. *Dev. Comp. Immunol.* **36**, 342-348 (2012).

2. Saralahti, A. *et al*. Adult zebrafish model for pneumococcal pathogenesis. *Dev. Comp. Immunol.* **42**, 345-353 (2014).

3. Heikura, T. *et al*. Baculovirus-mediated vascular endothelial growth factor-D(ΔNΔC) gene transfer induces angiogenesis in rabbit skeletal muscle. *J Gene Med* **14**, 35-43 (2012).